

Characterisation of platelet membrane receptors in their native environment using SMALP nanodiscs

by

XUEQING WANG

A thesis submitted to the University of Birmingham for the degree of DOCTOR OF PHILOSOPHY

Institute of Cardiovascular Sciences
College of Medical and Dental Sciences
University of Birmingham
November 2022

UNIVERSITY OF
BIRMINGHAM

University of Birmingham Research Archive

e-theses repository

This unpublished thesis/dissertation is copyright of the author and/or third parties. The intellectual property rights of the author or third parties in respect of this work are as defined by The Copyright Designs and Patents Act 1988 or as modified by any successor legislation.

Any use made of information contained in this thesis/dissertation must be in accordance with that legislation and must be properly acknowledged. Further distribution or reproduction in any format is prohibited without the permission of the copyright holder.

Abstract

Platelets are small, anucleate blood cells, and their major role is in haemostasis, whereby they prevent excessive blood loss by adhesion, activation and aggregation at sites of blood vessel injury. However, they can also give rise to thrombosis, leading to myocardial infarction or ischaemic stroke, when they are activated in diseased arteries following the rupture of atherosclerotic plaques. These behaviours are dependent on the interaction between platelet membrane protein receptors and their subendothelial matrix or soluble ligands. Traditionally, membrane protein studies relied on detergent-based solubilisation methods, which remove most of the native plasma membrane lipid species and can affect protein structure and function. Recently, a novel methodology, namely styrene-maleic acid lipid particles (SMALPs), has emerged for the extraction of membrane proteins. This method utilises styrene-maleic acid co-polymers (SMA), which are amphiphilic polymer chains, to directly cut patches out of the native membrane continuum, generating SMALPs encapsulating intact membrane proteins with their surrounding lipids and partner proteins, belted by SMA, without the addition of detergent molecules in any steps. The aim of this thesis was to adopt SMALPs for the characterisation of platelet membrane protein structure and interaction partners, with a main focus on the platelet-activating collagen receptor GPVI. In transfected HEK-293T cells, GPVI was successfully purified in SMALPs together with its associated FcRγ signalling chain. Gel filtration followed by a native polyacrylamide gel electrophoresis (PAGE) method, SMA-PAGE, revealed multiple sizes of the purified GPVI/FcRγ SMALPs, suggesting the potential existence of GPVI oligomers. Importantly, GPVI/FcRγ SMALPs were functional in binding to collagen, and contained single-dispersed protein particles that could be observed under negative stain electron microscopy (EM), suggesting great potential for future investigation of GPVI stoichiometry and structure. In human platelets, the SMALP generation protocol was optimised and simplified for bench-top biochemical characterisations. This demonstrated that

membrane protein complexes could be successfully extracted into the same SMALPs, including GPVI/FcRγ and the ‘molecular scissor’ ADAM10 with its regulatory tetraspanins Tspan15. In addition, SMA-PAGE has been proved as a convenient method to investigate a wide range of platelet membrane protein interactions, by revealing the molecular weights of native protein complexes in SMALPs. Taken together, the work in this thesis suggests that SMALPs are a promising tool for the characterisation of platelet receptor structures in their native lipid bilayer and for the identification of novel membrane protein interaction partners. Such information will be valuable for the future characterisation of new antiplatelet therapeutic targets designed to prevent thrombosis with minimal effects on haemostasis.

Acknowledgements

I would like to thank my supervisor, Dr. Michael Tomlinson in School of Biosciences, for his thorough guidance throughout my whole PhD project, and especially in the first two years when I was based in his lab. Thank you for teaching me how to perform the standard experiments on molecular biology, biochemistry and cell biology, all of which I had little prior experience with, for helping me to plan, design, troubleshoot experiments and to interpret the data, and for all the scientific advice. Thanks all other members in Tomlinson lab, especially Neale and Connie, who helped me a lot during my early PhD days on everything, taught me all the basic operations in molecular coloning, flow cytometry, cell culture, Western blotting and many other techniques from scratch, led me forward on my project, and kept the lab running, and Anke and Rhiannon for the day-to-day company in the lab. Also thanks other members from different groups on Biosciences 8th floor.

I would also like to thank my other supervisor in Birmingham, Prof. Steve Watson in ICVS, for his continuous input during my PhD, both on this project and in life, and for providing me a short term technician position in his lab after the end of this three-year-long PhD project, which not only allowed me to follow up on the full-length GPVI structure determination project, but also gave me the chance to have a closer look at many others' platelet-related projects in the whole group. Thank you also to Alex S for the many useful suggestions on protein purification during my PhD, for being in every of my SSC meetings, and for working with and guiding me during my short-term position after my PhD project. Also thanks Eleyna for our discussions on SMALPs, Natalie P for chairing every SSC meeting, keeping me on track with thesis submission procedures and mentally supporting, Ying, Lourdes and Beata for helping with many protocols and running the lab, Jo for showing me how to prepare platelets, Gina and Nayandeep for the daily joy, and all other members in the Birmingham platelet group.

I would also like to thank my supervisor in Spain, Dr. Ángel García in University of Santiago de Compostela, where I spent the third year of my PhD. Thank you for the kind help with the many Spanish documents, for being very involved in my project during my time in Cimus, and for being supportive to and enthusiastic about my ideas whenever I was faced with problems. Thank you also to all other members in the platelet proteomics group—Lidia and Sara for always willing to help on Spanish documents, experiment protocols and tips on Galicia sightseeing, and my fellow PhD students Marcin, Jingnan and Delia for all the help and company. Also thanks to the people in our neighbour prion lab for the daily joy, the building

managers and technicians, especially Lucía, and all the blood donors from different labs across the building. It was a unique and valuable experience to live in a historical Spanish city, and I appreciate everybody for putting up with me not speaking Spanish.

I appreciate the help that I got from Prof. Tim Dafforn and his group members, Sarah, Naomi and Steph very much. Despite not being a member of my supervisory team, Tim has been very kind to be involved in this project when we needed, and has provided insightful advice from a SMALP expert point of view. Sarah has been guiding me through the SMALP generation protocol, showing and interpreting every step to me, Naomi has shown me her SMA-PAGE method, and Steph has kindly driven me and my samples to Warwick for negative stain EM and gave me the protocol of blue native PAGE. Besides, all three of you have put up with my constant questions and emails, and always been very kind and willing to help. Thank you also to Pooja on Biosciences 7th floor who helped me to perform some experiments during the restricted entry period to the floor in COVID time, and several other members on the floor.

I would like to acknowledge our Marie Sklodowska-Curie Innovative Training Network, Targeting Platelet Adhesion Receptors in Thrombosis (TAPAS), for funding me and my 14 fellow PhD students on our PhD projects (Marie Skłodowska-Curie grant agreement No 766118). A special thank to Caroline, the TAPAS project coordinator, who helped all of us a lot on document preparing, visa application, travel booking, keeping us on track and reminding us of document submission deadlines. It has been a lovely journey to be enrolled in this joint PhD program, to get the chance to meet the many supervisors in the top of their fields, and to present our projects frequently in each TAPAS meeting.

Finally, I would like to thank my parents for their unconditional love and support to me, without which I could never be able to finish this journey. Thank you for the financial support to me during my two-year-long MSc in Sweden prior to this PhD project, which motivated me to continue to pursue a PhD in Europe. Thank you also to my grandma, Suzhen, for your love and for putting up with me not coming back home for more than 3 years. Thanks also all my other family members and friends for your emotional support.

To my grandpa,

Tianzhou,

For his love that shined our whole extended family,

And my grandparents,

Xucheng and Sumei,

For their kindness and genuineness that influence all of us.

You will be memorised forever in our heart, and your lives will be going on with us.

Table of contents

Chapter 1 General introduction 2

1.1 Platelet biology 2

1.1.1 Overview of platelets 2

1.1.2 Platelet biogenesis (thrombopoiesis) 3

1.1.3 The role of platelets in haemostasis 6

1.1.3.1 Platelet initial adhesion to blood vessel injury site 6

1.1.3.2 Firm adhesion and platelet activation 7

1.1.3.3 Platelet spreading 7

1.1.3.4 Platelet secretion and aggregation 7

1.1.3.5 Thrombin generation and thrombi formation 8

1.1.4 The role of platelets in thrombosis 11

1.1.5 The roles of platelets beyond haemostasis and thrombosis 15

1.1.5.1 Platelets as immune cells 15

1.1.5.2 Platelets in cancer 17

1.2 Major platelet membrane receptors and platelet signalling 20

1.2.1 GPVI 23

1.2.2 CLEC-2 30

1.2.3 GPIb-IX-V complex 33

1.2.4 Platelet integrins 35

1.2.5 Platelet GPCRs 39

1.2.5.1 Protease-activated receptors (PARs) 39

1.2.5.2 $P2Y_1$ and $P2Y_{12}$ receptors 41

1.2.4.3 Other GPCRs on the human platelet surface 42

1.2.6 Tetraspanins and their partner proteins in platelets 45

1.2.7 Platelet signal transduction following activation 48

1.3 Styrene-maleic acid lipid particles (SMALPs) for studying membrane proteins 51

1.3.1 Strategies for membrane protein solubilisation 51

1.3.1.1 Detergents for membrane protein solubilisation 54

1.3.1.2 Alternative methods for membrane protein solubilisation 56

1.3.1.3 Nanodisc-based methods for membrane protein solubilisation 58

1.3.2 SMALPs are a novel strategy for the extraction and characterisation of membrane proteins....61
1.3.2.1 SMA co-polymer as the tool to extract membrane proteins....61
1.3.2.2 Alternative polymers....65
1.3.2.3 Mechanisms of SMALP formation....68
1.3.2.4 Applications of SMALPs....71
1.4 Hypothesis and aims of the thesis....75

Chapter 2 Materials and Methods....78

2.1 List of reagents....78
2.1.1 General reagents....78
2.1.2 Cell culture reagents....79
2.1.3 Antibodies....80
2.1.4 Primers used to generate GPVI isoform constructs....83
2.1.5 Kits and ready-made materials....84
2.1.6 Buffer recipes....86
2.1.7 Equipment....88
2.2 Molecular cloning....90
2.2.1 GPVIa-10xHis and GPVIb-10xHis constructs....90
2.2.2 GPVIa-Δexon5-10xHis and GPVIb-Δexon5-10xHis constructs....93
2.3 Cell culture and cell-based assays....97
2.3.1 HEK-293T cell line....97
2.3.1.1 Cell culture....97
2.3.1.2 Transient transfection with PEI....98
2.3.1.3 Cell harvesting and lysis....98
2.3.2 DT40 cell line....99
2.3.2.1 Cell culture....99
2.3.2.2 Transient transfection via electroporation for NFAT-luciferase assay....99
2.3.2.3 NFAT-luciferase assay....99
2.4 Human platelet preparation and platelet-based assays....100
2.4.1 Platelet preparation....100
2.4.2 Platelet activation....100
2.4.3 Platelet lysis....101

2.5 Platelet surface protein biotinylation assay 101
2.6 Flow cytometry 102
2.7 SMALP generation 102
2.7.1 SMALP preparation from human platelets 102
2.7.2 SMALP preparation and purification from HEK-293T cells 103
2.8 Immunoprecipitation (IP) 104
2.9 Electrophoresis, gel staining and Western blotting 105
2.9.1 SDS-PAGE 105
2.9.2 SMA-PAGE 106
2.9.3 Western blotting 106
2.9.4 Gel staining 107
2.10 Gel filtration 108
2.11 Collagen agarose binding assay 108
2.12 Negative stain electron microscopy 108
2.13 In-gel protein identification via mass spectrometry 109
2.13.1 Sample preparation for mass spectrometry 109
2.13.2 Liquid chromatography followed by tandem mass spectrometry (LC-MS/MS) 109

Chapter 3 Characterisation of GPVI-related constructs and GPVI antibodies 112

3.1 Introduction 112
3.2 Results 115
3.2.1 Generation of four GPVI-10x His expression constructs and demonstration of similar surface and whole-cell expression levels in transfected HEK-293T cells 115
3.2.2 GPVI isoforms do not show signalling differences in response to collagen 120
3.2.3 FcRγ mutant C44S signals normally 123
3.2.4 Characterisation of GPVI monoclonal antibodies' performance in Western blotting 127
3.3 Discussion 129

Chapter 4 Purification and characterisation of GPVI/FcRγ SMALPs from transfected HEK-293T cells 136

4.1 Introduction **136**
4.2 Results **139**
4.2.1 Purification of GPVI-SMALPs 139
4.2.2 Gel filtration of GPVI/FcRγ SMALPs reveals distinct populations of GPVI oligomers 142
4.2.3 GPVI-SMALPs bind collagen 144
4.2.4 The purified GPVI/FcRγ SMALPs are relatively pure 145
4.2.5 GPVI/FcRγ SMALPs show single-dispersed particles under negative stain EM 147
4.3 Discussion **149**

Chapter 5 Investigation of platelet membrane receptor interaction and stoichiometry using SMALPs **154**

5.1 Introduction **154**
5.2 Results **156**
5.2.1 Optimisation of SMALP generating methodologies for washed human platelets 156
5.2.2 GPVI/FcRγ and ADAM10/Tspan15 complexes can be preserved in SMALPs from human platelets 162
5.2.3 GPVI solubilised into detergent lysates and SMALPs has differential epitope accessibilities to anti-GPVI antibodies 164
5.2.4 GPVI SMALPs do not reveal novel phosphorylated proteins in the GPVI signalling pathway 166
5.2.5 A novel biotinylation assay, based on co-IP, does not reveal GPVI-interacting membrane proteins, but may be useful in discovering novel membrane protein interactions 168
5.2.6 A novel native PAGE method, SMA-PAGE, can be used for the investigation of platelet membrane protein interaction and stoichiometry 174
5.3 Discussion **182**

Chapter 6 General discussion **189**

6.1 Summary of results **189**
6.2 The significance of utilising SMALPs for GPVI structure and stoichiometry investigations **191**

6.3 The significance of utilising SMALPs for the investigation of platelet membrane receptor stoichiometry and interactome 196

6.4 The widening applications of SMALPs 200

6.5 Final conclusions and future remarks 207

List of Figures

Figure 1.1 Simplified illustration of platelet lineage in human. 5
Figure 1.2 Illustration of platelet generation, platelet activation and thrombosis formation... 10
Figure 1.3 Components of the coagulation pathways. 14
Figure 1.4 Illustration of several major platelet membrane receptors and several signal transduction pathways. 22
Figure 1.5 GPVI structures in the literature. 26
Figure 1.6 Rap1 regulation pathways. 50
Figure 1.7 Timescale of membrane protein solubilisation method development. 53
Figure 1.8 Generation of SMALPs. 64
Figure 1.9 Chemical formulas of polymers that can be used to generate lipid nanodiscs. 67
Figure 1.10 Proposed mechanisms of SMALP formation. 70
Figure 3.1 Schematic representation and sequence alignment of the four GPVI isoforms with 10x His tags 116
Figure 3.2 Generation of GPVIa-10xHis and GPVIb-10xHis constructs. 117
Figure 3.3 Generation of GPVIa-Δexon5-10xHis and GPVIb-Δexon5-10xHis constructs. . 117
Figure 3.4 The four GPVI-10xHis constructs have comparable surface and whole cell expression levels when transiently transfected into HEK-293T cells. 119
Figure 3.5 The four GPVI-10xHis constructs have similar downstream signalling shown by an NFAT-luciferase reporter assay in DT40 B cells. 122
Figure 3.6 Sequence alignment of FcRγ in different species. 124
Figure 3.7 Wild-type and FcRγ C44S mutant have similar GPVI signalling and surface expression levels in DT40 B cells. 126
Figure 3.8 Characterisation of anti-GPVI monoclonal antibodies for Western blotting. 128
Figure 4.1 Experimental procedures for generating and purifying GPVI SMALPs from transfected HEK-293T cells. 140
Figure 4.2 Purification of GPVIa-His SMALPs. 141
Figure 4.3 Gel filtration of GPVI/FcRγ SMALPs reveals distinct populations of GPVI oligomers 143
Figure 4.4 GPVI SMALPs bind collagen. 144
Figure 4.5 The purified GPVI/FcRγ SMALPs are relatively pure. 146
Figure 4.6 Representative negative stain electron microscopy images of GPVI SMALPs showed single-dispersed, protein-like particles. 147

Figure 4.7 2D class averages from particles picked from negative stain electron microscope images. 148
Figure 5.1 Platelet membrane proteins can be solubilised by SMALP 30010P. 158
Figure 5.2 Whole cell SMALPs from human platelets yield hyper-phosphorylated proteins that are independent of CRP activation. 159
Figure 5.3 Influence of different buffer conditions on platelet protein tyrosine phosphorylation..... 160
Figure 5.4 Whole cell lysates and whole cell SMALPs from human platelets presented similar band patterns on p-Tyr Western blot, when using the optimised SMALP buffer B containing 150 mM NaCl. 161
Figure 5.5 SMALPs isolated from human platelets preserve GPVI/FcRγ and ADAM10/Tspan15 complexes. 163
Figure 5.6 GPVI mAbs immunoprecipitate GPVI in detergent lysates and in SMALPs with different efficiencies. 165
Figure 5.7 GPVI IPs on GPVI SMALPs from human platelets did not reveal novel phosphorylated proteins in the GPVI signalling pathway. 167
Figure 5.8 Experimental procedures of the co-IP assay on biotinylated SMALPs from human platelets. 171
Figure 5.9 A novel co-IP assay based on biotin-streptavidin interaction is useful in confirming membrane protein interactions and for the potential discovery of novel protein interactions. 172
Figure 5.10 Immunoprecipitation of GPVI SMALPs from human platelets does not reveal novel GPVI-interacting membrane proteins. 173
Figure 5.11 SMA-PAGE on human platelet SMALPs followed by Western blotting revealed the molecular weights of protein complexes. 181

List of Tables

Table 1.1 Several GPCRs that express on platelets, their ligands and coupled G proteins 44
Table 1.2 Several G proteins and their downstream signalling pathways in platelets.....44
Table 2.1 General reagents 78
Table 2.2 Cell culture reagents 79
Table 2.3 Primary antibodies used in the thesis.....80
Table 2.4 Secondary antibodies used in the thesis.....82
Table 2.5 Primers used to generate GPVI isoform constructs 83
Table 2.6 Kits and ready-made materials used in the thesis 84
Table 2.7 Buffers used in the thesis and their recipes.....86
Table 2.8 Equipment used in the thesis 88
Table 2.9 Components used to add 10xHis tags to GPVIa and GPVIb.....90
Table 2.10 PCR reaction to add 10xHis tags to GPVIa and GPVIb.....90
Table 2.11 Components used to digest GPVIa-10xHis or GPVIb-10xHis.....91
Table 2.12 Components used for ligation of GPVIa-10xHis or GPVIb-10xHis with pEF6.C vector.....91
Table 2.13 Components used for colony PCR.....92
Table 2.14 PCR reaction on colonies to check inserts in colonies 92
Table 2.15 Components used to clone the piece of cDNA before exon5 94
Table 2.16 PCR reaction to clone the piece of cDNA before exon5 94
Table 2.17 Components used to clone the piece of cDNA after exon5 94
Table 2.18 PCR reaction to clone the piece of cDNA after exon5 95
Table 2.19 Components used to join the pieces of cDNA before and after exon5 together....95
Table 2.20 PCR reaction to join the pieces of cDNA before and after exon5 together.....95
Table 2.21 Components used to digest GPVIa-Δexon5-10xHis or GPVIb-Δexon5-10xHis ..96
Table 2.22 Components used for ligation of GPVIa-Δexon5-10xHis or GPVIb-Δexon5-10xHis with pEF6.C vector.....96
Table 2.23 Materials used for PEI-transfection of HEK-293T cells in different sizes of culturing plates.....98
Table 2.24 Agonists used for platelet activation.....101

Abbreviations

ADAM10	A Disintegrin and Metalloproteinase 10
ADP	Adenosine diphosphate
APC	Antigen-presenting cell
ATP	Adenosine triphosphate
BRET	Bioluminescence resonance energy transfer
Btk	Bruton's tyrosine kinase
CCL5	Chemokine (C-C motif) ligand 5
CD	Cluster of differentiation
CLEC-2	C-type lectin-like receptor 2
CMC	Critical micellar concentration
Co-IP	Co-immunoprecipitation
COX	Cyclooxygenase
CRP	Collagen-related peptides
CRP-XL	Cross-linked collagen-related peptide
Cryo-EM	Cryogenic electron microscopy
CV	Column volume
CVX	Convulxin
CXCL1	Chemokine (C-X-C motif) ligand 1
DAG	Diacylglycerol
DAPT	Dual-antiplatelet therapy
DIBMA	Diisobutylene-maleic acid co-polymer
DIBMALPs	Diisobutylene maleic acid lipid particles
EM	Electron microscopy
ELISA	Enzyme-linked immunosorbent assay
Fab	Fragment antigen-binding
Fc	Fragment crystallisable
FcRγ	Fc receptor γ chain
FRET	Förster resonance energy transfer
Gads	Grb2-related adaptor protein
GPCR	G protein-coupled receptors
GPIb-IX-V	Glycoprotein Ib-IX-V

GPO	Gly-Pro-Hyp motif
GPVI	Glycoprotein VI
Grb2	Growth-factor-receptor-bound protein 2
HEK	Human embryonic kidney
HIV	Human immunodeficiency virus
HSCs	Haematopoietic stem cells
ICAM-1	Intercellular adhesion molecule 1
IgSF	Immunoglobulin superfamily
IL	Interleukin
IMS	Invaginated membrane system
IP	Immunoprecipitation
IP_3	Inositol 1,4,5-trisphosphate
ITAM	Immunoreceptor tyrosine-based activation motif
kDa	Kilodalton
LAT	Linker of activated T cells
LPS	Lipopolysaccharide
LSCs	Lymphoid stem cells
mAb	Monoclonal antibody
MHC I	Major histocompatibility complex I
MSCs	Myeloid stem cells
MSP	Membrane scaffold protein
NET	Neutrophil extracellular trap
NFAT	Nuclear factor of activated T cells
NK cells	Natural killer cells
NMR	Nuclear magnetic resonance
NO	Nitric oxide
NTA	Nitriloacetic acid
OCS	Open canalicular system
PAR	Proteanase-activated receptors
PE	Pulmonary embolism
PF4	Platelet factor 4
PGI_2	Prostacyclin
PI3K	Phosphoinositide 3-kinase

PIP_2	Phosphatidylinositol bisphosphate
PKA/B/C/G	Protein kinaseA/B/C/G
PLCβ/γ	Phospholipase C
pLGICs	Pentameric ligand-gated ion channels
PMA	Polymethacrylate
PS	Phosphatidylserine
pTyr	Phosphorylated tyrosine
RAFT	Reversible addition fragmentation chain transfer
SDS-PAGE	Sodium dodecyl sulfate–polyacrylamide gel electrophoresis
SFK	Src family kinase
SH2	Src homology 2
SLP-76	SH2-domain-containing leukocyte protein of 76 kDa
SMA	Styrene maleic acid co-polymer
SMAd-A	Styrene maleimide-amine co-polymer
SMA-EA	SMA-ethanol amine co-polymer
SMALPs	SMA lipid particles
SMAnh	Styrene maleic anhydride co-polymer
SMA-QA	Styrene maleimide quaternary ammonium co-polymer
SMI	Styrene-maleimide co-polymer
SMILPs	SMI lipid particles
SPR	Surface Plasmon Resonance
Syk	Spleen tyrosine kinase
TF	Tissue factor
TLR	Toll-like Receptor
TM	Transmembrane
TP	Thromboxane A_2 receptor
TPO	Thrombopoietin
T_XA_2	Thromboxane A_2
VCAM-1	Vascular cell adhesion protein 1
VTE	Venous thromboembolism
vWF	von Willebrand factor
WT	Wild type

CHAPTER 1

General introduction

Chapter 1 General introduction

1.1 Platelet biology

1.1.1 Overview of platelets

Platelets are small, anucleate cell fragments existing in blood circulation. Platelets are around 2-5 μm in diameter and are the second most abundant blood cells, only less than erythrocytes (red blood cells). With a canonical role of stopping bleeding at the sites of blood vessel injury—the procedure of haemostasis, platelets are also termed thrombocytes. Beside this, platelets also process many other roles beyond haemostasis, including atherogenesis, immune responses such as inflammation, angiogenesis, and wound healing (Badimon et al., 2012; Golebiewska & Poole, 2015; van der Meijden & Heemskerk, 2019).

Most of the roles of platelets are dependent on platelet activation. In normal, intact blood vessels, platelets exist in their resting state with a discoid shape; both the size and the shape cause platelets to be pushed close to vessel endothelium in the blood flow, which help them to accumulate and respond quickly in the event of vessel injury (Hartwig, 2013). Upon stimulation, usually when the endothelium layer is broken, the resting platelets are activated by a variety of agonists. Activated platelets change their shape, become flattened and develop feeler-like bulges, all of which increase their surface area towards the broken endothelium layer and therefore help platelets to exert their haemostasis function (Thomas, 2019). Activated platelets also express specific surface receptor proteins and secrete molecules in the further steps of haemostasis (Yun et al., 2016). Most of the changes from resting to activated platelets are due to cytoskeleton protein reorganisation, granule secretion and increasing of platelet surface area via the open canalicular system (OCS). The OCS is the major source of platelet membrane extension, and is connected to platelet plasma membrane; in resting states, the OCS is mostly

reserved inside platelets, and its connection with the plasma membrane generates small openings on the platelet outer surface (Selvadurai & Hamilton, 2018).

1.1.2 Platelet biogenesis (thrombopoiesis)

The biogenesis of platelets starts from haematopoietic stem cells (HSCs) which are located in the bone marrow and are subjected to self-renewal (Machlus & Italiano, 2013). HSCs differentiate into myeloid stem cells (MSCs), which further develop into megakaryocytes, erythrocytes, neutrophils and monocytes, and lymphoid stem cells (LSCs), the latter of which further develop into natural killer cells (NK cells), T cells and B cells (Figure 1.1). Megakaryocytes are the precursors of platelets, and the formation of platelets happens in sinusoidal blood vessels (Stegner et al., 2017; Tavassoli & Aoki, 1989).

Once formed, the megakaryocytes undergo maturation, which is mediated by thrombopoietin (TPO), a cytokine synthesised in the liver (Hitchcock & Kaushansky, 2014; Kato et al., 1995; Kelemen et al., 1958). TPO binds its receptor, c-Mpl on the megakaryocyte surface, initiating downstream signalling pathways that promote platelet generation (Bartley et al., 1994; de Sauvage et al., 1994). It was initially believed that the binding of TPO induces c-Mpl dimerisation which leads to activation of the downstream pathways; however, it is recently proposed that c-Mpl forms inactive dimers in its resting state, and TPO binding changes the conformation of these dimers, especially in their cytoplasmic tails, inducing signal transduction (Kuter, 2019). TPO induces megakaryocyte endomitosis and the subsequent increase of their ploidy. Meanwhile, the amount and size of megakaryocytes are also increased following TPO activation (Kuter et al., 1994). The invaginated membrane system (IMS) is formed during megakaryocyte maturation; the IMS distributes throughout the cytoplasm and serves as a reservoir of membrane for future platelet production (Eckly et al., 2014; Schulze et al., 2006).

It is during megakaryocyte maturation that the proteins needed to be packed into platelets are synthesised and the cytoskeleton is reorganised (Machlus & Italiano, 2019). The latter induces pseudopods which stay connected to the megakaryocyte surface, while protruding into the blood flow through the space between adjacent endothelial cells that line the sinusoidal blood vessels. The formation of these pseudopods, termed proplatelets, is regulated by multiple cytoskeletal proteins such as microtubules, actin and motor protein dynein (Bender et al., 2015; Italiano et al., 1999; Tanenbaum et al., 2013). Proteins and other cellular contents to be presented in platelets are trafficked from the central area of megakaryocytes into proplatelets, while the nucleus is not (McArthur et al., 2018; Richardson et al., 2005). The shear rate in blood flow sheds proplatelets out of mature megakaryocytes, generating preplatelets into the circulation (Thon et al., 2010). Preplatelets are barbell-shaped fragments without a nucleus; they are larger than platelets and will further divide into the final platelets (Machlus & Italiano, 2019).

Platelet count in healthy human beings is 1.5-4.5 x 10^6 /mL of blood (Daly, 2011). A higher count is termed thrombocytosis, while a lower count is termed thrombocytopenia. Platelet turnover time is around 7-10 days (Siegel et al., 1989), and platelet clearance is mediated by a few proteins on its surface, including β-galactosidase which gets exposed on aged, desialylated platelets and can be recognised by hepatocytes and macrophages, and platelet receptors GPIb and integrin αIIbβ3 which can be recognised by autoantibodies in a process called opsonization (Quach et al., 2018).

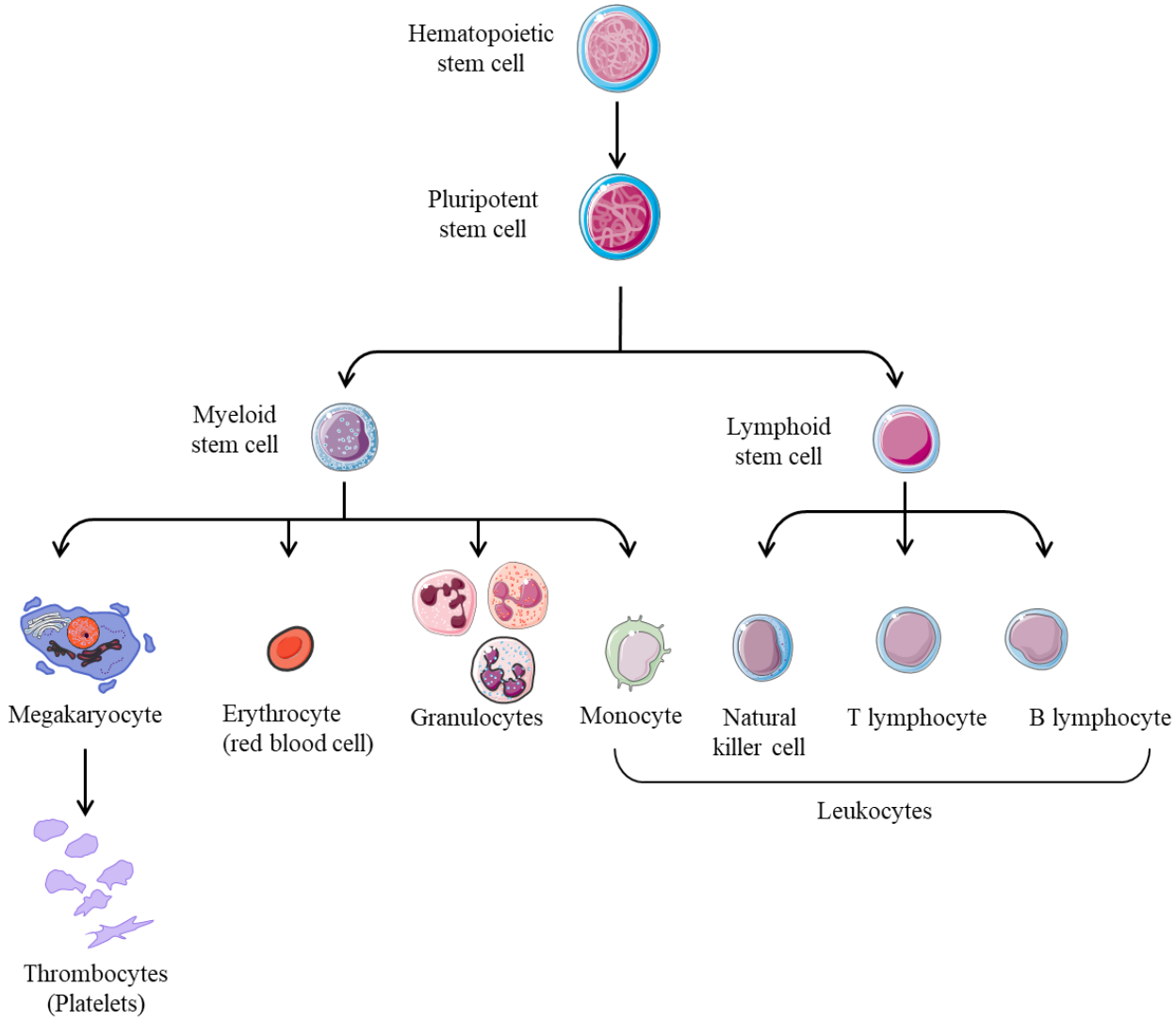


Figure 1.1 Simplified illustration of platelet lineage in human.

Haematopoietic stem cells (HSCs) differentiate into pluripotent stem cells, which further differentiate into myeloid stem cells and lymphoid stem cells. Myeloid stem cells are the precursor of megakaryocytes, which further develop into platelets through a series of stages including burst-forming unit (BFU) megakaryocytes and colony-forming unit (CFU) megakaryocytes (not shown). Platelets are derived from proplatelets, the protrusions on megakaryocytes, that can be shed by blood flow shear stress, and their shapes change following agonist activation, a procedure mediated by cytoskeleton reorganisation. Myeloid stem cells are also the precursor of erythrocytes, granulocytes and monocytes; the other lineage, where the pluripotent stem cells differentiate into lymphoid stem cells and further into natural killer cells, T lymphocytes and B lymphocytes, is termed lymphopoiesis. Images are partly adapted from Servier Medical Art, licensed under a Creative Commons Attribution 3.0 Unported License (https://creativecommons.org/licenses/by/3.0/).

1.1.3 The role of platelets in haemostasis

Platelets are the major cells in blood flow to react to vascular injury and to stop excessive bleeding that would otherwise follow. They achieve this via interactions with various ligands on the subendothelial matrix that only come into contact with the interior contents of blood vessels in an injury condition. The formation of such interactions leads to platelet adhesion to the injury site, a series of intracellular signalling events that activate platelets and induce platelet shape change, release of soluble mediators to further activate nearby platelets and aggregate them together, the involvement of the coagulation pathway, and finally the formation of stable thrombi (Brass et al., 2019; Hou et al., 2015). This whole haemostasis process involves numerous molecules in platelets, including but not limited to the surface-expressed receptors, intracellular signalling nodes, and granule contents. In this section, the haemostasis process will be divided into five progressive steps, following the classic haemostasis model. Note that some of the molecular interactions can happen in multiple steps and have effects at different stages of thrombi formation. Some of the key molecules involved, especially major membrane receptors, will be discussed further in section 1.2.

1.1.3.1 Platelet initial adhesion to blood vessel injury site

In an intact blood vessel environment, platelets circulate in a resting or quiescent state. At this stage, they are discoid shaped, and their activation is suppressed by endothelial cell-derived inhibitory factors, including nitric oxide (NO), prostacyclin (PGI_2) and an endothelial surface protein, CD39 (Brass et al., 2019). At the site of vascular injury, platelets get into contact with the components of subendothelial matrix, notably fibrous collagen, and von Willebrand factor (vWF) which is a soluble glycoprotein (Xu et al., 2016). vWF binds to the collagen fibres, and, upon the high shear rate generated by the blood flow, its A1 domain gets exposed, providing the binding site for GPIb, a platelet membrane receptor (Clemetson, 2012). The interaction between GPIb and vWF, though unstable and reversible, slows down platelets in circulation

and helps form the initial platelet adhesion monolayer, enabling further interaction and molecular signalling events to follow (Hou et al., 2015).

1.1.3.2 Firm adhesion and platelet activation

The initial adhesion and rolling of platelets, mediated by GPIb-vWF interaction, is stabilised by the major collagen receptor, glycoprotein VI (GPVI). The GPVI-collagen interaction produces signal transduction through Fc receptor γ (FcRγ) that initiates a downstream signalling pathway involving extensive phosphorylation events, leading to intracellular Ca^{2+} concentration increase, and subsequent "inside-out" activation of integrins (Rayes et al., 2019). Integrin α2β1 is also a receptor for collagen, while integrin αIIbβ3 interacts with fibrin(ogen) and vWF (Haining et al., 2019). Together, these receptor-ligand interactions facilitate firm adhesion of platelets at the injury site.

1.1.3.3 Platelet spreading

The activation of platelets also leads to cytoskeleton reorganisation, which is triggered by the "outside-in" signalling of αIIbβ3. This reorganisation starts from the formation of protrusions called filopodia/pseudopodia, followed by the formation of lamellipodia (Durrant et al., 2017). Platelets become flattened towards the injury surface, with increased surface area which is in part due to exocytosis of platelet granules (Smith, 2018). Thus, more firm adhesion is formed between the platelet surface and the subendothelial matrix, and blood loss is further restrained (Brass et al., 2019).

1.1.3.4 Platelet secretion and aggregation

Activated, spread platelets further undergo degranulation processes, which mainly involves α- and dense-granules. α-granule contents include some large proteins, including vWF and fibrinogen, which bind αIIbβ3 from nearby platelets, and thus recruit more platelets to the injury site and trigger their activation (Flaumenhaft & Sharda, 2019). Dense-granules release

ADP, which activates platelets via two types of G protein coupled receptors (GPCRs), $P2Y_1$ and $P2Y_{12}$, leading to intracellular Ca^{2+} concentration increase and subsequent integrin activation (Cattaneo, 2019a). In addition, activated platelets also secrete thromboxane A_2 (T_XA_2) that interacts with T_XA_2 receptor (TP), which is also a GPCR (Offermanns, 2006). ADP and T_XA_2 work in synergy to activate platelets from circulation (Offermanns, 2006).

1.1.3.5 Thrombin generation and thrombi formation

The activated platelets accumulating at the injury site expose phosphatidylserine, and provide the surface for procoagulant enzyme complexes to form (Hou et al., 2015). This involves proteins in the coagulation cascade, mainly factor Xa and Va (see also section 1.1.4), which cleave prothrombin to thrombin. The generated thrombin plays two important roles in this step: cleavage of fibrinogen to fibrin which forms an insoluble mesh network, and activation of platelets through another group of GPCRs, protease-activated receptors (PARs) (Colman, 2006; Offermanns, 2006). Fibrin interacts with αIIbβ3 and thus holds a stable thrombus together with the platelets attached to it (Bledzka et al., 2019). More recently, the collagen receptor GPVI has also been shown to bind fibrinogen and fibrin (Mammadova-Bach et al., 2015), thus can also contribute to this final step of thrombus formation. The PARs involved in this process are PAR1 and PAR4 in human platelets, and PAR1 and PAR3 in mouse platelets. The formed thrombus further undergoes clot contraction, especially in its core region which is more compact and contains more fully activated platelets in comparison to the shell region (Kim et al., 2017). Such clot contraction reinforces haemostasis at the injury site, and prevents dissociation of a formed thrombus from the vascular wall, which might occlude the blood vessel (Lam et al., 2011).

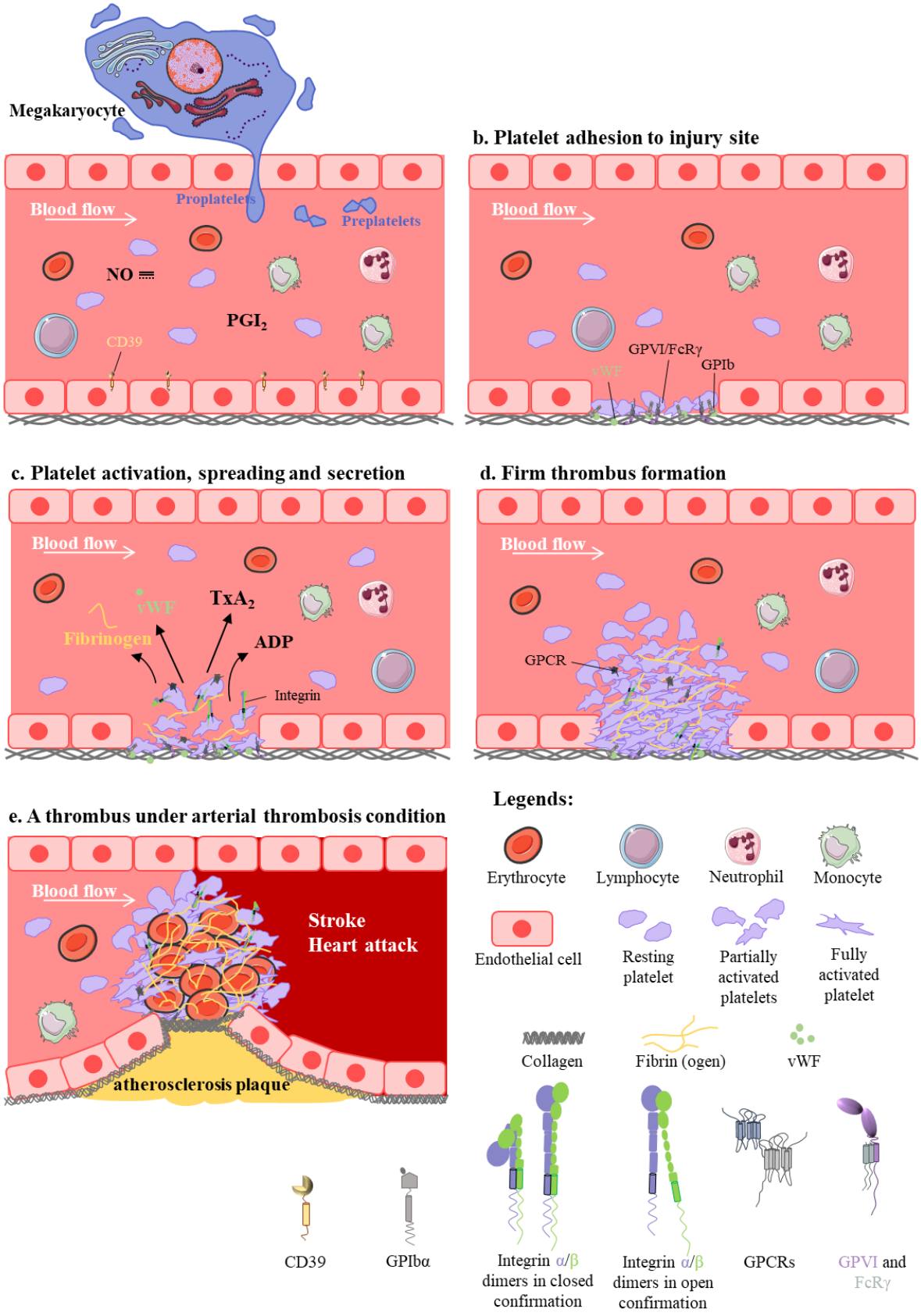

a. Platelet generation from megakaryocytes and resting platelets in blood flow
Megakaryocyte
Blood flow
Proplatelets
Preplatelets
NO
PGI2
CD39
b. Platelet adhesion to injury site
Blood flow
GPVI/FcRγ
GPIb
vWF
c. Platelet activation, spreading and secretion
Blood flow
vWF
Fibrinogen
TxA2
ADP
Integrin
d. Firm thrombus formation
Blood flow
GPCR
e. A thrombus under arterial thrombosis condition
Blood flow
Stroke
Heart attack
atherosclerosis plaque
Legends:
Erythrocyte
Lymphocyte
Neutrophil
Monocyte
Endothelial cell
Resting platelet
Partially activated platelets
Fully activated platelet
Collagen
Fibrin (ogen)
vWF
CD39
GPIbα
Integrin α/β dimers in closed confirmation
Integrin α/β dimers in open confirmation
GPCRs
GPVI and FcRγ

Figure 1.2 Illustration of platelet generation, platelet activation and thrombosis formation.

(a) Platelets are generated from protrusions of megakaryocytes, termed proplatelets, which are shed by blood flow shear stress, forming preplatelets in blood flow. Preplatelets further divide into platelets. Platelets are maintained in their resting state in intact blood vessels, due to the existence of NO and PGI_2 in blood flow, and CD39 which is expressed on the surface of endothelial cells. (b) Upon blood vessel injury, inner vessel components are exposed to subendothelial matrix, which contains rich collagen fibres and vWF attaching to them. Platelets adhere to subendothelial matrix initially via vWF binding GPIbα, and the adhesion is reinforced by GPVI binding collagen. (c) GPVI binding collagen activates platelets, initiating downstream signalling events which ultimately leads to cytoskeleton reorganisation, integrin activation and degranulation. During these procedures, activated platelets change their shapes, become spread, secrete various molecules including fibrinogen, vWF, TxA_2 and ADP, thus recruit more nearby resting platelets and activate them. Activated integrin αIIbβ3 binds fibrin(ogen) and vWF, facilitating thrombus growth. (d) Activated platelets serve as the surface for procoagulant enzyme complexes to form, which cleave prothrombin to thrombin (not shown). Thrombin further activates platelets through its receptors, and cleaves fibrinogen to insoluble fibrin fibre meshes. Activated integrin αIIbβ3 binds fibrin meshes and facilitates firm thrombus formation; GPVI also contributes to fibrin binding. (e) Example of a thrombus under arterial thrombosis condition. The rupture of an atherosclerotic plaque generates a different environment from that at the site of blood vessel injury, including higher amount of collagen and inflammatory cytokines. An arterial thrombosis contains richer amounts of fibrin and erythrocytes, and can potentially block blood flow, causing serious health conditions such as stroke and heart attack. Images of megakaryocyte organelles, erythrocytes, lymphocytes, neutrophils and monocytes are adapted from Servier Medical Art, licensed under a Creative Commons Attribution 3.0 Unported License (https://creativecommons.org/licenses/by/3.0/).

1.1.4 The role of platelets in thrombosis

Apart from haemostasis, platelets also play a crucial role in thrombosis. Thrombosis happens in a disease context when the thrombus blocks the blood flow. There are two different types of thrombosis: arterial thrombosis and venous thrombosis. As the names suggest, the difference between these two types is mainly due to the site where thrombosis happens. Arterial thrombosis occurs in arteries, where the shear flow is high, and the thrombus usually develops at atherosclerotic plaque rupture regions where the endothelium is damaged and platelets are exposed to subendothelial matrix. Arterial thrombi can block major arteries, causing severe conditions such as myocardial ischemia, heart attack and stroke (Previtali et al., 2011). In contrast, venous thrombosis occurs in veins, where the shear flow is low, and the thrombus forms in intact blood vessels. This is promoted by the activation of endothelium, which induces leukocyte and platelet attachment; the attached leukocytes become activated and express TF, which initiates the coagulation pathway and thus promote thrombus generation (Koupenova et al., 2017). With the low shear rate in veins, the anti-coagulant effect of the endothelium is nearly abolished (Mackman, 2012). Venous thrombi are richer in erythrocytes and fibrin, and are not adherent to the endothelium as tightly, thus they are more prone to detach and cause distant vessel occlusive diseases such as venous thromboembolism (VTE) and pulmonary embolism (PE) (Koupenova et al., 2017).

Importantly, thrombosis and haemostasis share very similar molecular mechanisms. The differences between these two conditions mainly attribute to the environment where the thrombi are formed, or, in other words, the conditions when thrombus formation happens (Brass et al., 2019). Thrombosis typically happens when the blood vessel is already narrowed under pathological conditions. For example, arterial thrombosis happens at the site of a ruptured atherosclerosis plaque, which has a higher collagen content than a normal wound, and contains molecules that don’t normally appear in a healthy condition, including inflammatory

cytokines. Meanwhile, the thrombosis site usually doesn't encounter a sufficient loss of blood vessel contents and the subsequent pressure drop as in the case of blood vessel injury. Thus, the composition of a thrombotic thrombus and a haemostatic thrombus has differences. For example, a thrombotic thrombus contains more erythrocytes, which are trapped in the fibrin mesh (Brass et al., 2019).

The coagulation system contributes greatly to both haemostasis and thrombosis, and more to venous thrombosis. The coagulation system includes a series of soluble serine proteases and their co-factors. The system consists of extrinsic, intrinsic and common pathways (Figure 1.3). The extrinsic pathway is initiated by tissue factor (TF) binding to FVII, through which FVII is transformed to its active form, FVIIa. TF is expressed on subendothelial cells and cells outside of the blood vessel (Mackman, 2004), thus its exposure to blood flow only happens in the case of blood vessel injury, which accounts for the name "extrinsic". The intrinsic pathway contains FXI and FIX. FXI is present on activated platelets and can be activated into FXIa; the latter then activates FIX to FIXa in the presence of FVIII (Colman, 2006). The TF-FVIIa and FIXa-FVIII complex can both activate FX to FXa, which associates with FV to form prothrombinase, cleaving prothrombin to thrombin. Thrombin is an important component in the thrombus formation procedure by playing several roles. It cleaves soluble fibrinogen to fibrin, both of which bind to integrin αIIbβ3 on platelets, with fibrin forming meshes that hold activated platelets together to generate the stable thrombi, through αIIbβ3 binding (Colman, 2006). Thrombin is also the ligand for PARs; upon binding, thrombin cleaves PARs, releasing a short peptide from the N-terminal and exposing a new N-terminal sequence, which binds back to the cleaved PARs and induces activation of PAR-binding G proteins (see also section 1.2.4.1) (Han et al., 2019). This initiates downstream signalling pathways that lead to intracellular Ca^{2+} concentration increasing and platelet activation. FX activation in the existence of FV, together with prothrombin cleavage to thrombin, and fibrinogen cleavage to fibrin, are termed as the

common pathway in the coagulation system. The generated thrombin can in turn activate FXI to FXIa, forming positive feedback to the intrinsic pathway (Colman, 2006).

Platelets interact with the coagulation pathway in several aspects, which contributes to both haemostasis and thrombosis. The phospholipids on the outer surface of the resting platelet membrane lack charge, therefore do not provide binding sites for the pro-enzymes and active forms of proteases in the coagulation pathway. Upon platelet activation, phosphatidylserine, an anionic phospholipid, gets exposed to the outer surface, which can form interactions with positively charged coagulation factors and serves as the reaction surface for the coagulation pathway, including FX activation by extrinsic and intrinsic pathways, FXI activation and the subsequent FIX activation by FXIa, and the cleavage of prothrombin to thrombin (Smith & Morrissey, 2019; Zwaal et al., 1998). Furthermore, thrombin generated by the coagulation pathway plays important roles in platelet activation and aggregation, as discussed before.

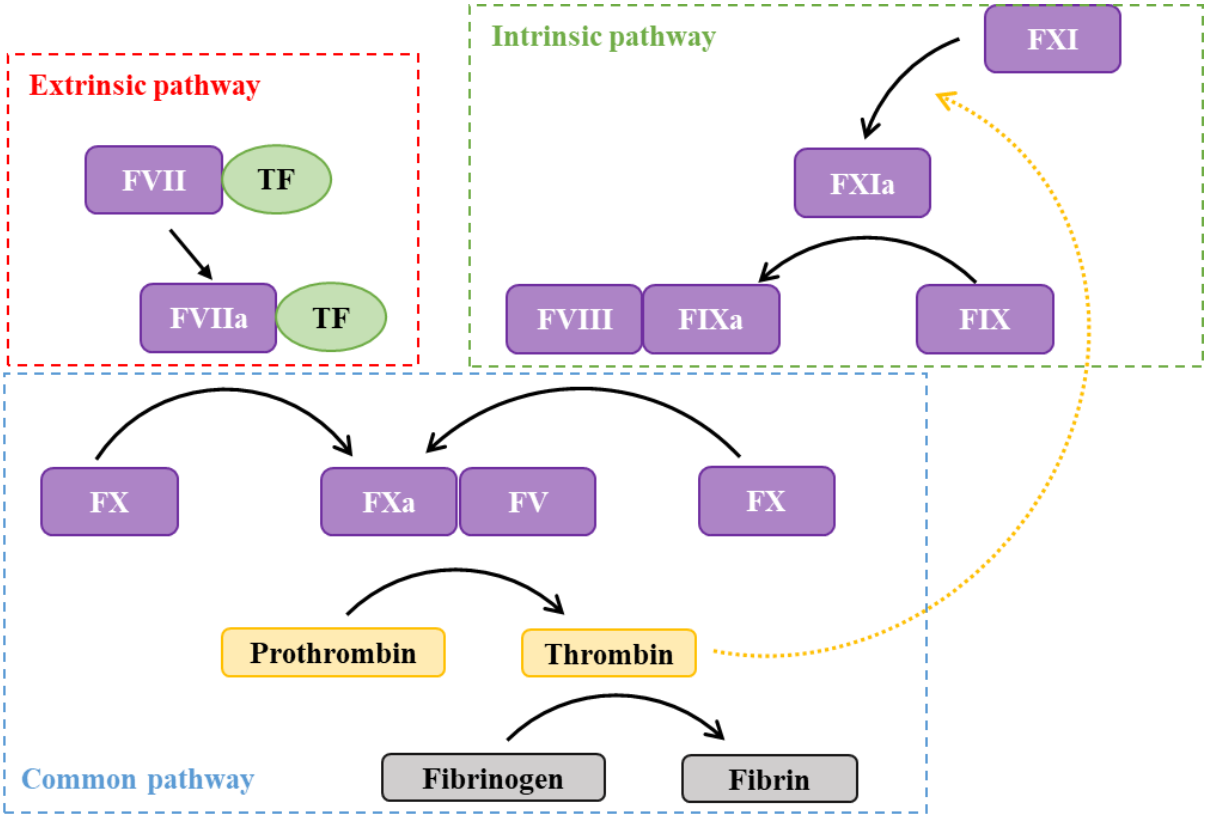


Figure 1.3 Components of the coagulation pathways.

The coagulation system consists of extrinsic, intrinsic and common pathways. The extrinsic pathway is initiated by tissue factor (TF) binding to FVII, which activates FVII to its active form, FVIIa. The intrinsic pathway includes FXI activation to FXIa, which activates FIX to FIXa in the presence of FVIII. Both TF-FVIIa and FIXa-FVIII complex can activate FX to FXa, which initiates the common pathway. FXa forms complex with FV, and the complex serves as a prothrombinase, cleaving prothrombin to thrombin. Thrombin further cleaves fibrinogen to fibrin, facilitating firm thrombus formation. Thrombin also activates FXI to FXIa on the surface of active platelets, acting as a positive feedback to the coagulation system.

1.1.5 The roles of platelets beyond haemostasis and thrombosis

Apart from their canonical roles in haemostasis and thrombosis, platelets also play significant roles in many other important physiological processes, such as immune response, inflammation, and several diseases including cancer (Morrell et al., 2014). These effects are achieved by several mechanisms. Firstly, the formation of haemostatic thrombi can serve as a physical barrier to pathogens that may otherwise come into blood vessels at injury sites. Secondly, platelets store numerous molecules with immune functions in their granules, including cytokines, chemokines and cell surface adhesion molecules, which play essential roles in exerting immune responses and mediating platelet interactions with other immune cells (Li et al., 2012). This section will focus on platelets' roles in immune responses and in cancer.

1.1.5.1 Platelets as immune cells

Platelets have been recognised as immune cells for a long time, as evidenced by their expression of molecules with known immune functions. They express several members of the Toll-like Receptors (TLRs), which constitute a family of single transmembrane proteins playing key roles in the innate immune system (Aslam et al., 2006; Morrell et al., 2014). Platelet TLRs include TLR1, TLR2, TLR4, TLR6, TLR8, and TLR9 (Aslam et al., 2006). TLR4 can recognise lipopolysaccharide (LPS) from gram-negative bacteria (Andonegui et al., 2005; Morrell et al., 2014), and LPS-stimulated platelet activation further induces platelet-neutrophil interaction, promoting neutrophil degranulation and the formation of neutrophil extracellular traps (NETs) (Clark et al., 2007). NETs are mesh structures of DNA and can trap and kill microbes due to their proteolytic activities (Clark et al., 2007; Vorobjeva & Chernyak, 2020). Platelet activation via TLR4-LPS has important therapeutic implications, as sepsis-induced thrombocytopenia caused by gram-negative bacterial infection has been a considerable clinical problem, and the NETs promoted through TLR4-activated platelets can kill the bacteria (Andonegui et al., 2005). Apart from TLR4, other members in the TLR family can also activate

platelets; for example, TLR2 has been shown to interact with *Streptococcus pneumoniae* (Keane et al., 2010). Platelets also express interleukins (ILs), which are cytokines with pro-inflammatory functions (Li et al., 2012). IL-1β from platelets has been shown to contribute to the acute phase response (Aggrey et al., 2013) and thus participates in the early stage in the immune system's response to infection. Platelet IL-1α has been reported to activate cerebrovascular endothelial cells by inducing the expression of adhesion molecules, ICAM-1 and VCAM-1, and by increasing the release of chemokine CXCL1 (Thornton et al., 2010), therefore may contribute to the progression of neurological diseases. In addition, platelets express major histocompatibility complex class I (MHC I) and can function as antigen-presenting cells (APCs) (Chapman et al., 2012).

Platelets have been shown to interact with many other immune cells, in both innate and adaptive immune systems (Li et al., 2012). Co-culture of platelets and monocytes showed that monocyte differentiation into macrophages can be promoted by platelets (Kaneider et al., 2003), and this effect has been further shown to be dependent on cytokines such as IL-1β and chemokines such as platelet factor 4 (PF4) and CCL5 (Ali et al., 2015; Gear & Camerini, 2003). Platelets also facilitate neutrophil function by binding to neutrophils and contributing to NET formation via TLR4, as discussed before (Clark et al., 2007). Thrombin-activated platelets induce dendritic cell activation (Kaneider et al., 2003). Moreover, platelets modulate T cell and B cell activities; many of these modulation events are related to platelet-expressed CD40L (Henn et al., 1998), which binds CD40 on APCs and therefore initiates immune responses. For example, an early study showed that platelet CD40L can augment $CD8^+$ T cell responses and induce B cell isotype switching (Elzey et al., 2003). Platelets can also modulate the adaptive immune system via secreted molecules. The platelet-specific chemokine, PF4, has been shown to stimulate the proliferation of human $CD4^+$ $CD25^+$ regulatory T cells but inhibit the proliferation of $CD4^+$ $CD25^-$ T cells which are non-regulatory (C. Y. Liu et al., 2005). The $CD4^+$ $CD25^+$ regulatory

T cells downregulate T cell responses to both foreign and self-antigens; therefore, by inhibiting their proliferation, platelets can play important roles in modulating different T cell populations.

Taking together, not only do platelets play important roles in haemostasis, but also in immune responses. Platelets can act as immune cells themselves and facilitate the functions of other immune cells, and this is achieved by the expression of immune effector proteins on the platelet surface and granule-released molecules upon platelet activation. Because of these immune functions, platelets are associated with many diseases, including malaria, sepsis, HIV, arthritis and atherosclerosis (Ali et al., 2015; Li et al., 2012). Although the roles of platelets in these diseases and the underlying molecular mechanisms are still under investigation, it is clear that they are an important component of the immune system.

1.1.5.2 Platelets in cancer

Platelets are also involved in cancer progression. Tumoral cells can activate platelets, and the subsequent formation of thrombi further complicate cancer treatments. This can be achieved by several mechanisms. Cancer cells have been shown to secrete numerous molecules that can activate platelets, including thrombin, T_XA_2 and ADP (Palacios-Acedo et al., 2019). Thrombin activates platelets through platelet activated receptors (PARs) while also cleaves fibrinogen to fibrin, which further stabilises the thrombus (sections 1.1.3.5 and 1.2.5.1). T_XA_2 and ADP also activate platelets through their corresponding receptors, TP and $P2Y_{1/12}$. In addition, tissue factor (TF) has been shown to express on cancer cells from different types of cancers including cervical cancer, breast cancer, pancreatic cancer and melanoma (Cocco et al., 2011; Han et al., 2014; Thaler et al., 2013; Zhao et al., 2013). TF is one of the major players in the coagulation pathway (section 1.1.4), thus its expression further promotes thrombus formation. In turn, activated platelets express and secrete molecules that can mediate cancer cell growth and metastasis. Activated platelets express P-selectin and active integrins on their surface, which mediate platelet-cancer cell interaction (Menter et al., 2014; Schlesinger, 2018). Such interaction can not only protect cancer

cells from natural killer (NK) cells, but also facilitates cancer-endothelial and cancer-leucocyte interactions (Palacios-Acedo et al., 2019). Activated platelets also secrete transforming growth factor beta (TGF-β) and vascular endothelial growth factor (VEGF) from their α-granules, and ADP and serotonin from their dense granules, all of which can promote tumour growth. For example, TGF-β can impact the granule mobilization of NK cells, thus protecting cancer cells from NK-cell-mediated cytolysis (Nieswandt et al., 1999); it also contributes to neutrophil transformation to a pro-tumorigenic phenotype (Olsson & Cedervall, 2018; Palacios-Acedo et al., 2019). Active serotonin production has been shown to link to poor prognosis in breast cancer patients (Leoncikas et al., 2016). Endothelial P2Y receptors, the receptors for ADP, once activated, can promote cancer cell invasion and metastasis (Ballerini et al., 2018; Li et al., 2013; Schumacher et al., 2013). Interestingly, platelet-derived microparticles can transfer micro-RNA into human and mouse tumours, which inhibited the growth of lung and colon carcinoma ectopic tumours, adding in multiple layers of platelet regulation to cancer (Michael et al., 2017).

In addition to promoting cancer cell growth, platelets can serve as a shield on cancer cells, protecting the latter from being attacked by immune cells and from blood shear forces. This is achieved by the interaction between adhesion molecules on platelets and cancer cells, as described above. Such platelet-cancer cell aggregation has been shown to protect the membrane damage of A2780 ovarian cancer cells in an *ex vivo* viscometer setting (Egan et al., 2014), while can also help to stabilise cancer cell interaction with the endothelial cell layer (Palacios-Acedo et al., 2019). Platelets also facilitate angiogenesis, and the separation of blood and lymphatic vessels, which aid cancer metastasis (Olsson & Cedervall, 2018).

GPVI, the receptor of focus in this thesis, has been shown to facilitate cancer metastasis. GPVI$^{-/-}$ mice injected with Lewis lung carcinoma or melanoma cell lines showed an approximately 50% reduction in observable tumour loci, in comparison to WT mice, suggesting that GPVI promotes cancer metastasis (Jain et al., 2009). More recently, the genetic deficiency of GPVI in mice showed

decreased metastasis of breast and colon cancer cells, and galectin-3 was identified as the major receptor for GPVI on cancer cells using gene knock-out methods (Mammadova-Bach et al., 2020). Podoplanin, the endogenous ligand for another platelet receptor, CLEC-2, which shares a similar immunoreceptor tyrosine-based activation motif (ITAM)-based signalling pathway to GPVI, expresses at the invasive front of many types of tumour cells, and was shown to promote the spreading, migration and invasion of cancer cells (Rayes et al., 2019; Wicki & Christofori, 2007). Blocking of podoplanin on cancer cells inhibited cancer progression, and the podoplanin/CLEC-2 axis facilitates cancer spreading and growth by promoting an immunosuppressed microenvironment (Agrawal et al., 2015; Sasaki et al., 2018).

1.2 Major platelet membrane receptors and platelet signalling

As described in the last section, many functions of platelets are dependent on platelet surface receptors, through their interactions with ligands that locate inside or outside the vasculature, mechanistic activation by, for example, shear rate change, and conformational change. In this section, several major receptors on platelets, including two of the ITAM receptors (GPVI and CLEC-2), the GPIb-IX-V complex, platelet integrins and platelet GPCRs, as well as a family of regulatory proteins, tetraspanins, are briefly described, with focuses on their structures, physiological functions and therapeutic implications. Finally, platelet signalling events downstream of these receptors are also introduced. A schematic of the mentioned receptors and several intracellular signalling pathways is illustrated (Figure 1.4).

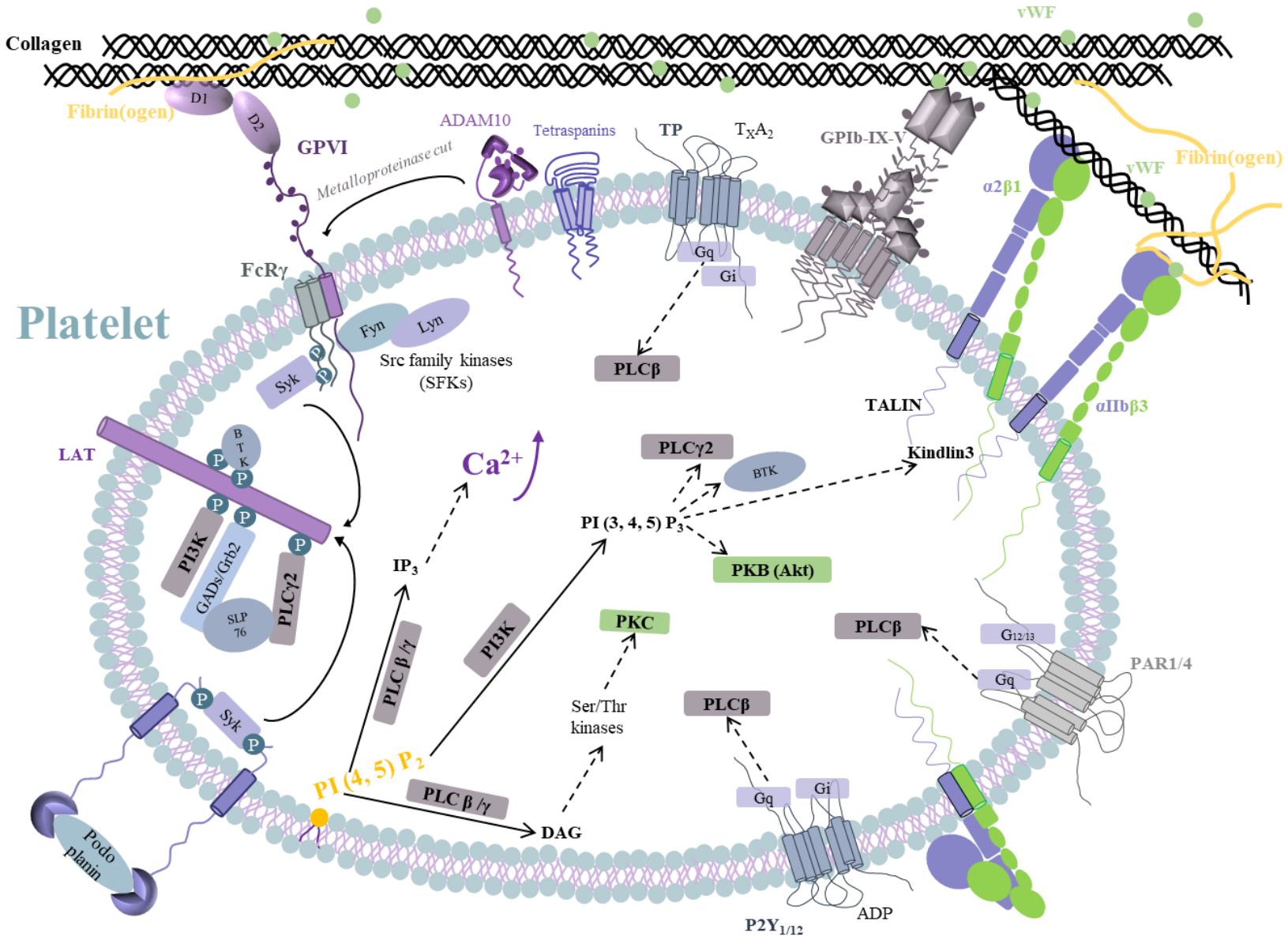

Collagen
vWF
Fibrin(ogen)
D1
D2
GPVI
ADAM10
Tetraspanins
TP
T_XA_2
GPIb-IX-V
α2β1
vWF
Fibrin(ogen)
Metalloproteinase cut
FcRγ
Platelet
Gq
Gi
Fyn
Lyn
Src family kinases
(SFKs)
Syk
PLCβ
TALIN
αIIbβ3
LAT
B
T
K
PLCγ2
BTK
Kindlin3
Ca^{2+}
PI3K
GADs/Grb2
SLP
76
PLCγ2
IP_3
PI (3, 4, 5) P_3
PKB (Akt)
PKC
PLCβ
$G_{12/13}$
PAR1/4
Gq
PLC β /γ
PI3K
Ser/Thr
kinases
PLCβ
Syk
PI (4, 5) P_2
PLC β /γ
DAG
Gq
Gi
Podo
planin
ADP
$P2Y_{1/12}$

Figure 1.4 Illustration of several major platelet membrane receptors and several signal transduction pathways.

Platelet tethering to ECM is initiated by GPIbα binding vWF in collagen fibres. GPVI then binds to collagen and initiates the downstream signalling pathway of ITAM receptors, highlighted by the LAT signalosome. The LAT signalosome integrates and activates several adaptor proteins and kinases, and recruits phospholipase C gamma 2 (PLCγ2) and phosphoinositide 3-kinase (PI3K). PLCγ2 hydrolyses phosphatidylinositol-4,5-bisphosphate ($PI(4,5)P_2$) to inositol 1,4,5-trisphosphate (IP_3) and diacylglycerol (DAG), which induces platelet intracellular Ca^{2+} concentration increase and PKC signalling, respectively. PI3K phosphorylates $PI(4,5)P_2$ to $PI(3,4,5)P_3$, whose effector proteins include PLCγ2, tyrosine kinases, Kindlin3, and Akt. Kindlin3 facilitates the separation of integrin tails, which is important for integrin inside-out signal transduction. Integrins are then transformed into high-affinity states, bind to extracellular ligands and initiate outside-in signalling. Platelet GPCRs also contribute substantially to platelet activation and signalling transduction procedures, with different downstream G proteins. Regulators of secondary messengers are showed in grey rectangles, while signal integrators are showed in green rectangles. Platelet inhibitory receptors and their pathways are omitted in the figure.

1.2.1 GPVI

GPVI is the major platelet receptor for collagen, and is exclusively expressed on platelets and megakaryocytes. It is a type-I membrane protein, composing of two immunoglobulin superfamily (IgSF) domains in the N-terminal (termed D1 and D2) followed by one heavily O-glycosylated stalk region in the extracellular side, a single transmembrane helix, and a 51-amino-acid long intracellular C-terminal region. The copy number is 3,000-4,000 GPVI molecules per platelet in human (Rayes et al., 2019). GPVI has 339 amino acids, and the numerous O-glycosylation sites in the extracellular stalk region contribute substantially to its molecular weight of 62 kDa. It also has an N-glycosylation site on the D1 domain. In the membrane, GPVI forms a complex with two Fc receptor γ (FcRγ) chains, through which the downstream signalling pathway is initiated. FcRγ is also a single transmembrane protein, composed of a short, four-amino acid N-terminal extracellular region, followed by the transmembrane helix and a C-terminal tail. FcRγ forms a disulphide-bound homodimer of ~18 kDa. GPVI and FcRγ interact via a salt bridge in their transmembrane regions (Zheng et al., 2001).

As described in section 1.1.3, GPVI interaction with subendothelial collagen contributes markedly to platelet activation, and GPVI interaction to fibrin(ogen) may contribute to thrombus stabilisation in the later stage. GPVI initiates its downstream signalling pathway through FcRγ, which contains the immunoreceptor tyrosine-based activation motif (ITAM) (Reth, 1989) with two series of YxxL (where Y is tyrosine, L is leucine and x is any other amino acid) separated by seven amino acids. Agonist binding induces phosphorylation of the two tyrosines in FcRγ ITAMs, and this is achieved by Src family kinases (SFKs), mainly Lyn and Fyn (Figure 1.4). SFKs are in close proximity with the GPVI tail region, regardless of GPVI activation status, and can therefore quickly respond upon agonist binding to GPVI. Following this, the phosphorylated ITAMs provide docking sites for the tyrosine kinase Syk.

The binding of Syk to an FcRγ ITAM is mediated by its tandem SH2 domains, which further induces Syk activation through auto-phosphorylation and SFK activities (Haining et al., 2019; Poole et al., 1997; Senis et al., 2014). Activated Syk further phosphorylates multiple sites in the cytoplasmic part of Linker of Activated T-cells (LAT), a transmembrane scaffold protein, and this recruits a series of kinases, adaptor and effector proteins to LAT. This complex of proteins, comprising adaptor proteins SLP-76, Gads and Grb2, and Tec family kinases such as Btk, forms a LAT signalosome, which further recruits phospholipase C gamma 2 (PLCγ2) and phosphoinositide 3-kinase (PI3K) to LAT (Figure 1.4). PLCγ2 and PI3K are two of the central players in platelet signalling and they act on phosphatidylinositol bisphosphate (PIP_2) (Section 1.2.6). Both the enzymes facilitate a series of reactions that ultimately lead to cytoskeleton reorganisation and integrin activation.

Structurally, it has been shown that GPVI binds to the typical Gly-Pro-Hyp (GPO) motifs on collagen, where Hyp is hydroxyproline, a unique amino acid in collagen. The GPO repeat is unique to GPVI binding (Feitsma et al., 2022; Knight et al., 1999). A synthetic peptide, collagen-related peptide (CRP) (Asselin et al., 1997; Morton et al., 1995), consisting of the sequence $GCO(GPO)_{10}GCOG$, mimics the triple helix structure of collagen, and, once cross-linked (termed CRP-XL), can induce potent, GPVI-specific platelet activation. The structures of GPVI extracellular IgSF domains, with and without CRP binding, have been solved by X-ray crystallography (Feitsma et al., 2022; Horii et al., 2006) (Figure 1.4A and B), showing back-to-back dimers of two GPVI (D1 and D2 domains only), with the interaction interface being on the D2 domains. The amino acids in the CRP-binding site have been mapped (Feitsma et al., 2022). The crystal structure of GPVI binding one inhibitory nanobody, Nb2, has also been solved recently, using a D1 and D2 GPVI-Fc construct (dimer) (Slater et al., 2021) (Figure 1.4C). This GPVI-Nb2 structure shows a domain-swapped GPVI dimer (Figure 1.5C); a C-C' hinge has been shown to be crucial for domain swapping, and when this hinge was deleted, the

resulted mutant could not induce collagen- or CRP- mediated GPVI signalling in an NFAT-luciferase reporter assay, supporting the functional relevance of the domain-swapped dimer. However, domain swapping was not revealed in the two aforementioned dimeric structures (Figure 1.4A and B), and the C-C' hinge may play other roles in signalling, for example allosteric modulation. Full-length GPVI/FcRγ structures are required to test the validity of existing dimer structures. The Nb2 binding site is close to but not overlapping with the proposed CRP-binding region, suggesting that Nb2 may inhibit CRP binding through a combination of allosteric modulation and steric clash effects.

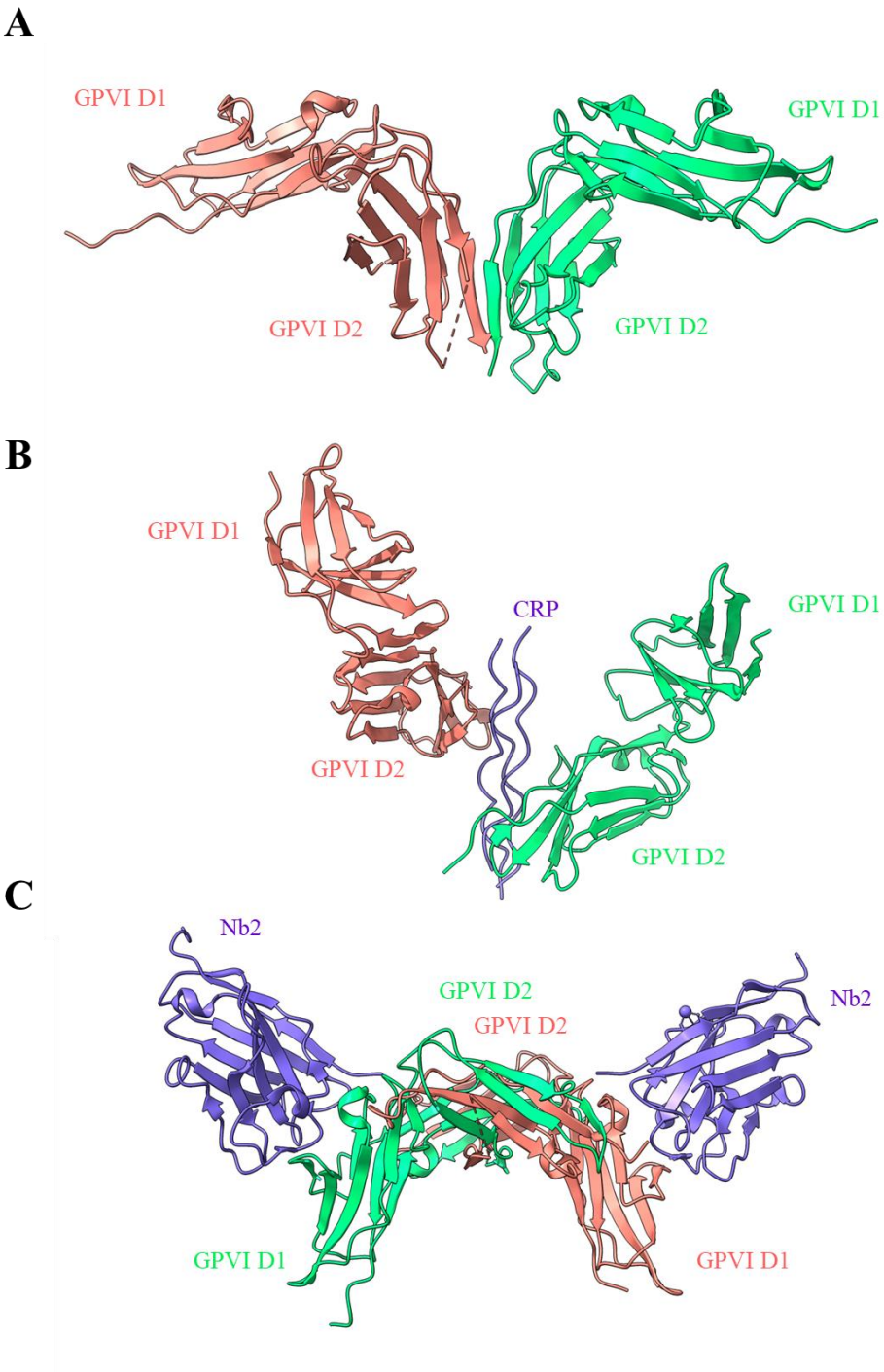


Figure 1.5 GPVI structures in the literature.

(A) GPVI IgSF domains form back-to-back dimers, with the interface between two D2 domains (PDB ID: 2GI7). (B) GPVI IgSF domains bind to CRP via D1 domain (PDB ID: 5OU8). (C) D1 and D2 GPVI-Fc construct with an inhibitory nanobody, Nb2, binding D1. GPVI shows a domain-swapped structure in the D2 domains (PDB ID: 7NMU). Domain swapping refers to the exchange of identical domains between the two individual proteins in a homodimer. In all these structures, GPVI D1 and D2 domains are coloured in pink or green, with the same colour indicating that they from the same molecules, and the ligands (CRP or Nb2) are coloured in purple.

Apart from collagen, which is the physiologically significant ligand, GPVI has also been shown to be the receptor for several other ligands (Gawaz, 2018). GPVI supported platelet tethering and stable adhesion to fibrin under flow, as shown by real-time video microscopy experiments that an anti-GPVI Fab, 9O12, significantly reduced platelet adhesion to fibrin under both low and high shear flow rate (Mammadova-Bach et al., 2015). Since this first evidence that GPVI binds fibrin, several groups have shown that fibrinogen, fibrin and D-dimer (the product of plasmin lysis on fibrin) all bind GPVI, using methods including ELISA, surface plasmon resonance (SPR), platelet spreading, lumi-aggregometry (Ebrahim et al., 2018; Mangin et al., 2018; Onselaer et al., 2017; Xu et al., 2021). A more recent study, using different types of fibrin including endogenous fibrinogen in plasma (plasma fibrin) and a TF-coated surface with whole blood flowing (blood fibrin), in comparison to isolated or recombinant fibrinogen, however, showed that inhibition of GPVI or GPVI signalling did not significantly reduce platelet coverage on plasma fibrin and blood fibrin, suggesting that GPVI may not function as an active fibrin receptor in physiologically relevant conditions (Zhang et al., 2020). There have also been studies showing that recombinant GPVI-Fc binds fibronectin by *in vitro* coated ELISA plates (Bultmann et al., 2010), and vitronectin by ELISA and flow chamber (Schonberger et al., 2012). Laminin was also identified as the ligand for GPVI, as platelets from GPVI-deficient mice had impaired spreading on laminin, and laminin-induced platelet protein phosphorylation was dependent on GPVI (Inoue et al., 2006). In contrast to GPVI–collagen interaction, the functional consequences of other GPVI ligands are poorly understood, and collagen is still by far the most physiologically important ligand. Exogenously, several snake venom toxins have also been shown to bind GPVI, with the most well-documented being convulxin (CVX) (Clark, Damaskinaki, et al., 2021). CVX is a potent platelet activator with an effective dose (ED50) of only 200 pM (Niedergang et al., 2000), and has therefore been widely used in platelet studies; its multivalent structure indicates that it has the potential to bind up to eight individual GPVI

molecules (Horii et al., 2009), which may explain the strong downstream signalling responses it induces.

It was assumed in the last decade that the dimer represents an active conformation of GPVI which is essential for its signalling. Dimer-specific antibodies indicate a unique conformation of GPVI dimer, in comparison to the monomer (Jung et al., 2012; Jung et al., 2009; Loyau et al., 2012). Collagen was shown to bind specifically to recombinant dimeric but not monomeric GPVI, as initially shown by the fact that recombinant dimeric extracellular domains of GPVI (GPVI-Fc), but not the monomeric GPVI extracellular domain, inhibited platelet aggregation by collagen and bound to fibrous collagen in ELISA and SPR experiments (Miura et al., 2002). However, there are several findings that challenged the "dimer-specific conformation" idea. The newly identified ligands, fibrinogen and fibrin, have been shown to bind both monomeric and dimeric GPVI (Slater et al., 2018; Xu et al., 2021). Collagen has also been shown to be capable of binding monomeric GPVI in SPR (Onselaer et al., 2017) and ELISA (Xu et al., 2021), although with lower affinity to dimeric GPVI. The recent crystal structure showed CRP binding to the D1 domain, which is distant from the dimer interaction site at D2 in the first GPVI structure. Moreover, D2-deficient GPVI was able to signal in response to collagen in a transfected cell line (Clark, Neagoe, et al., 2021). Interestingly, the recent domain-swap crystal structure did favour the unique conformation of GPVI dimer, and the deletion of the C-C' hinge which is crucial to the domain swap rendered GPVI unresponsive to collagen.

It is now accepted that GPVI exists as a mixture of monomers and dimers on the surface of transfected cell lines, and at least partially as dimers on resting platelets. In cell lines, it has been shown by fluorescence correlation spectroscopy that GPVI, when expressed in transfected HEK293T cells, displayed an oligomerisation state in between CD86 which is monomeric and CD28 which is a disulphide-linked homodimer (Clark, Neagoe, et al., 2021). In human platelets, this has been shown by Förster resonance energy transfer (FRET), where platelet GPVI

molecules were probed by antibodies labelled with donor fluorophore alone, or by antibodies labelled with donor and acceptor fluorophores; the measurement of mean fluorescence intensity (MFI) showed the existence of GPVI dimers on resting platelets, and that GPVI dimerisation did not significantly increase upon CRP simulation (Clark, Neagoe, et al., 2021). The amplified signalling events are then dependent on formation of large oligomeric clusters of GPVI from the previously produced GPVI dimers. GPVI clustering events have been visualised by imaging studies where real-time GPVI dimers were observed to cluster on different immobilized collagenous substrates, including CRP-XL and different types of collagen (Poulter et al., 2017). The multimeric characteristic of GPVI ligands also supports the idea that ligand-binding induces GPVI clustering (Clark, Damaskinaki, et al., 2021), and therefore the amplification of downstream signalling.

Mice with GPVI depleted by an anti-GPVI monoclonal antibody (mAb), JAQ1, displayed abolished responses to collagen and CRP, but the tail bleeding time was only moderately increased; these mice were protected from lethal thromboembolism (Nieswandt, Schulte, et al., 2001). In a GPVI-null mice model, the platelets failed to respond to fibrillar collagen or the snake venom protein convulxin, which is GPVI's agonist, but no severe bleeding tendency was observed by tail bleeding time measurements (Kato et al., 2003). Similarly, in another genetically modified GPVI-deficient mice model, the platelets did not respond to fibrillar collagen or CRP, but responded normally to other platelet agonists such as ADP, and platelet adhesion to fibrillar collagen under both static and dynamic conditions was dramatically reduced; importantly, these GPVI-deficient mice were protected against lethal thromboembolism, and showed similar tail bleeding time in comparison to wild type mice (Lockyer et al., 2006). GPVI was also shown to protect formation of occlusive thrombi in mice models with $FeCl_3$ or mechanical injury (Bender et al., 2011). These results suggest that GPVI may be a promising antithrombotic target. In human, a missense mutation in exon 6 of the *Gp6*

gene, which generates soluble GPVI without the transmembrane region, rendering no GPVI expression on the surface of their platelets, has been identified from Chile, with an estimated number of ~4,000 individuals being homozygous (*Gp6*$^{-/-}$) (Matus et al., 2013; Nagy et al., 2020). The *Gp6*$^{-/-}$ platelets showed abolished aggregation to collagen, CVX and CRP, and abolished spreading on surfaces coated with collagen and vWF, but unaltered adhesion under flow on collagen and non-collagen surfaces (Matus et al., 2013; Nagy et al., 2020). Established targeting strategies towards GPVI include utilising soluble forms of GPVI to bind the endogenous ligands, and utilising GPVI-binding reagents such as GPVI nanobodies and the Fab fragment of GPVI antibodies, and small molecule inhibitors binding GPVI or their downstream signalling proteins (Harbi et al., 2021). For example, Revacept, the recombinant GPVI-Fc (Schupke et al., 2019), is already in Phase II trials for symptomatic carotid artery stenosis ("Revacept in Symptomatic Carotid Stenosis,"). ACT017, a humanised Fab against GPVI (Lebozec et al., 2017), significantly inhibited platelet aggregation in primate studies without bleeding side effects, and is now in Phase I trial (Voors-Pette et al., 2019). Inhibitors for Btk, a tyrosine kinase downstream of GPVI signalling that activates PLCγ2, are also under development (Harbi et al., 2021).

1.2.2 CLEC-2

C-type lectin-like receptor 2 (CLEC-2) is another ITAM receptor of platelets, and it has been shown to play roles in several non-classical functions of platelets. It is expressed on platelets with a copy number of 2,000–4,000 in human, and also on megakaryocytes and dendritic cells (Haining et al., 2019; Rayes et al., 2019). CLEC-2 is a type-II transmembrane protein, with a C-terminal extracellular domain that consists of a Ca^{2+}-dependent (C-type) lectin-like domain, a transmembrane helix and a short cytoplasmic tail in the N-terminal. The C-type lectin-like domain of CLEC-2 lacks the Ca^{2+} binding residues but preserves all other characteristics (Watson et al., 2007; Zelensky & Gready, 2005). The stalk region, located between C-type

lectin-like domain and the transmembrane region (Watson & O'Callaghan, 2005), has been suggested to play an important role in CLEC-2 dimerisation (Watson et al., 2007). This dimerization is important for CLEC-2 function, as it only contains a hem-ITAM motif (YxxL) in its cytoplasmic tail, and the initiation of its downstream signalling, through activated Syk kinases, requires the two SH2 domains of Syk each binding a phosphorylated YxxL motif (Haining et al., 2019). The rest of the downstream signalling events are similar to those of GPVI, with PLCγ2 being the important final effector. However, CLEC-2 signalling has been shown to depend more on secondary mediators, ADP and TxA_2, and cytoskeleton remodelling (Pollitt et al., 2010). The reason for this difference between CLEC-2 and GPVI signalling is unclear, and might be that Syk and SFK act simultaneously on CLEC-2 hemITAM phosphorylation (Haining et al., 2019).

Podoplanin, a transmembrane protein, is the first identified and best characterised endogenous ligand of CLEC-2; it does not express in the blood vasculature, but expresses widely on different cell types including kidney podocytes, lymphatic endothelial cells, fibroblastic reticular cells of lymphoid organs, and lung epithelial cells (Astarita et al., 2012; Rayes et al., 2019). As a result, the role of CLEC-2 in the canonical haemostasis model has not been well documented; instead, CLEC-2 participates in several non-classical functions of platelets. CLEC-2 deficient mice displayed blood and lymphatic vessel mixing, and perinatal mortality (Rayes et al., 2019; Suzuki-Inoue et al., 2010; Uhrin et al., 2010). CLEC-2 on dendritic cells was also shown to regulate lymph node expansion through its interaction with podoplanin; in this process, CLEC-2-clustered podoplanin disrupted the actomyosin contractility that was induced by podoplanin interaction with Rho proteins and kinases (Acton et al., 2014). Mouse platelets treated with an anti-CLEC-2 antibody, which displayed complete loss of CLEC-2, adhered normally under flow, but showed severely defective subsequent aggregate formation both *in vitro* and *in vivo*, suggesting the role of CLEC-2 in platelet adhesion (May et al., 2009);

in a more recent study from the same group, the knock-in mouse model with a signalling-dead CLEC-2 (hem-ITAM tyrosine mutated) phenocopied the blood-lymphatic mixing and lethality of CLEC-2 knock-out mice but did not show any thrombotic defect (Haining, Cherpokova, et al., 2017). These studies demonstrated the possible contribution of CLEC-2 as an adhesion molecule in stabilising thrombi. CLEC-2 has also been shown to regulate lung development through its interaction with podoplanin (Tsukiji et al., 2018). Moreover, platelet CLEC-2 can engage podoplanin in disease scenarios. In a mouse model of systemic *Salmonella typhimurium* infection, thrombosis was triggered by inflammation, due to the increasing number of podoplanin-expressing monocytes, and depletion of platelet CLEC-2 inhibited thrombus formation (Hitchcock et al., 2015). More recently, a second endogenous ligand of CLEC-2, hemin, which is an oxidised version of heme, has been identified, as hemin-induced platelet activation was abolished by recombinant human CLEC-2-Fc fusion protein (Bourne et al., 2021; Martin et al., 2021). The detailed molecular interactions between CLEC-2 and hemin, and the binding difference between high and low concentration of hemin to CLEC-2, need to be further investigated. Exogenously, the snake C-type lectin, rhodocytin, has been shown to activate CLEC-2 (Fuller et al., 2007; Suzuki-Inoue et al., 2006). Both podoplanin and rhodocytin bind distally from the canonical binding site of C-type proteins, and they have one overlapping binding site, as shown by crystal structures (Nagae et al., 2014).

Similar to GPVI, CLEC-2 has been shown to exist as a mixture of monomer and dimer on resting platelets (Hughes et al., 2010; Martin et al., 2021). Also similar to GPVI, CLEC-2 forms larger-order clusters upon agonist stimulation, as shown by platelets binding artificial lipid bilayers containing mobile podoplanin (Pollitt et al., 2014). In addition, homophilic CLEC-2 interaction between adjacent cells has also been proposed, as shown by SPR that recombinant CLEC-2 in the flow and on the surface bound each other, by platelet spreading on a CLEC-2-coated surface which was attenuated in CLEC-2 deficient platelets, and by binding of soluble

recombinant CLEC-2 to platelets which was also attenuated in CLEC-2 deficient platelets (Suzuki-Inoue et al., 2010). This homophilic association of CLEC-2 facilitates thrombus formation (Suzuki-Inoue et al., 2010).

1.2.3 GPIb-IX-V complex

The GPIb-IX-V complex was first discovered in the 1970s, when the absence of this complex was found to be the cause of Bernard-Soulier syndrome, a rare bleeding disorder with the symptoms of enlarged platelets, thrombocytopenia and increased bleeding time (Jenkins et al., 1976; Nurden & Caen, 1975). GPIb-IX-V mediates platelet rolling and tethering at sites of vascular damage, and is the second most abundant receptor on platelets, with a copy number of 25,000-30,000 (Li, 2019; Zeiler et al., 2014). The complex comprises four transmembrane proteins, GPIbα, GPIbβ, GPIX and GPV, with molecular weights of approximately 135 kDa, 26 kDa, 20 kDa and 85 kDa, respectively (Li, 2019; Li & Emsley, 2013; Luo et al., 2007; Mo et al., 2012). The largest component, GPIbα, contains the largest extracellular domain in the complex, with a ligand-binding domain that is rich in leucine, followed by the sialomucin region that is rich in serine and threonine, is heavily O-glycosylated and contains two N-glycosylation sites, followed by a mechanosensory domain, which precedes the transmembrane helix and the cytoplasmic domain (Li, 2019). The GPIbα extracellular region can be shed by the metalloproteinase ADAM17 at the mechanosensory domainMSD (Bergmeier et al., 2004). This cleavage releases a soluble fragment called glycocalicin, which circulates in the normal plasma (Beer et al., 1994; Fox, 1994), and has been used as a marker for certain diseases as it reflects platelet damage and possibly dysfunction (Beer et al., 1994). GPIbα interacts with GPIbβ through disulphide bonds to form GPIb; GPIbβ further associate with GPIX and GPV via non-covalent bonds, with the association with GPV being weaker (Li & Emsley, 2013). The cytoplasmic tails of neither of these proteins have defined structural domains (Li, 2019).

The stoichiometry of GPIb-GPV-GPIX complex has been of debate. GPIbα and GPIbβ, originally discovered as a 1:1 complex (Berndt et al., 1985; Du et al., 1987; Phillips & Agin, 1977), have been shown later to form a 1:2 (GPIbα: GPIbβ) complex, as demonstrated from the existence of two extracellular cysteines located near the GPIbβ transmembrane region that can both form disulphide bonds with GPIbα transmembrane region (Luo et al., 2007), and the four-helix-bundle organisation of the transmembrane helices with one from GPIbα, two from GPIbβ and the other one from GPIX (Luo & Li, 2008). The stoichiometry between the GPIb-IX complex and GPV, on the other hand, is less well-defined, partly because of the lack of GPV structural data, and the relatively loose association between GPV and the GPIb-IX complex. It has been suggested that GPIb-IX may form a complex with GPV via diffusion on the plasma membrane, and GPIb-IX can also form complexes with other membrane proteins, such as GPVI (Arthur et al., 2005) and FcγRIIA (Sullam et al., 1998), via similar behaviours (Li & Emsley, 2013). The most well-accepted stoichiometry of the whole complex, up until now, is GPIbα: GPIbβ: GPIX: GPV=1:2:1:1 (Burkhart et al., 2012), although this model requires confirmation via structural studies, and there have also been suggestions that GPIb-IX and GPV form a complex with 2:1 ratio (Li et al., 1995).

GPIb-IX-V is the receptor for many ligands, including vWF, α-thrombin and collagen, and several other receptors including integrin αMβ2 (Mac-1) and P-selectin (Andrews et al., 2003). vWF binding GPIb-IX-V is the important initial step of platelet adhesion to the blood vessel injury site and is important in inducing the downstream signalling of GPIb. α-thrombin binds the ligand-binding domain of GPIbα with high affinity (Zarpellon et al., 2011); this binding facilitates thrombin binding to PAR receptors (see section 1.2.5.1) (De Candia et al., 2001), and may also directly induce GPIb-IX-V downstream signalling (Ramakrishnan et al., 2001). Collagen is currently the only known ligand for GPIb-IX-V that doesn't bind GPIbα; instead it binds the extracellular domain of GPV (Kimmerlin et al., 2022; Li, 2019). GPIb-IX-V binding

to the counter receptors helps regulate platelet interaction with other cells, including leukocytes, endothelial cells and other activated platelets (Andrews et al., 2003). Apart from extracellular binding, the cytoplasmic tails of GPIb-IX-V interact with cytoplasmic components including signalling protein 14-3-3ζ (Du et al., 1994), filamin A (Nakamura et al., 2006) and calmodulin (Andrews et al., 2001). Furthermore, the juxtamembrane sequence of GPIbβ cytoplasmic region is rich in basic residues and thus may interact with negatively charged lipids in the plasma membrane (Li, 2019).

The GPIb-V-IX complex is primarily a receptor for platelet adhesion and tethering, with relatively minimal roles in signalling. The signalling pathways from vWF binding GPIb-IX-V to integrin αIIbβ3 activation are not entirely clear, although several mechanisms have been identified, including SFK mediation, PLCγ2, PI3K-Akt and PKG pathway (Yin, Liu, et al., 2008; Yin, Stojanovic, et al., 2008). vWF binding to GPIb-IX-V also leads to the secretion of secondary mediators, ADP and TxA_2, which further recruit and activate nearby platelets (J. Liu et al., 2005). The αIIbβ3 activation leads to subsequent platelet activation, platelet secretion, platelet binding vWF and fibrinogen, and thrombus growth/stabilisation.

1.2.4 Platelet integrins

Integrins are transmembrane proteins whose main role is mediating cell-cell and cell-ECM adhesion, and they also facilitate signal transduction across the membrane (Mezu-Ndubuisi & Maheshwari, 2021). Each integrin is a heterodimer composed of one α chain and one β chain; each chain contains a large extracellular domain, a transmembrane helix and the cytosolic region, and the two chains are non-covalently bound to each other. In total, there are 18 types of α chains and 8 types of β chains in mammals, and their combination generates 24 different integrin heterodimers in human (Takada et al., 2007; Telser, 2002).

αIIbβ3 is the most highly expressed integrin on platelets, and it is an exclusive platelet protein. It is also the most expressed membrane protein on platelets, with a copy number of 80,000-100,000 per platelet, representing 3% of the total platelet protein amount and around 17% of the mass of platelet membrane proteins (Phillips et al., 1988; Stouffer & Smyth, 2003). αIIbβ3 is the most important mediator of platelet aggregation—when platelets are activated by the agonists of other receptors, including ITAM receptors, GPIb-IX-V complex and GPCRs, the signalling pathways induced by these activated receptors lead to cytoskeleton reorganisation, which brings about the conformational changes of αIIbβ3, thus inducing its inside-out signalling. The inside-out signalling changes αIIbβ3 conformation and the activated heterodimer has a higher affinity to its extracellular ligands (Bledzka et al., 2019). Of note in these ligands are fibrinogen and its cleavage product, fibrin, which forms a mesh that stabilises platelet aggregates in the last stages of thrombus formation, and vWF, which is secreted by activated platelets (Plow et al., 2000). αIIbβ3 binding these ligands serves as the molecular basis for the activated platelets to recruit nearby platelets from blood circulation and activate them, therefore is the basis for thrombus growth.

Activation of αIIbβ3 is largely dependent on cytoskeleton protein TALIN binding the cytoplasmic regions of the two integrin chains (Das et al., 2014; Shattil et al., 2010). In its resting state, the intracellular tails of αIIb chain and β3 chain interact with each other, and the whole heterodimer is in a "folded" state, with extracellular regions bent over one side and having relatively low affinity for the extracellular ligands (Figure 1.4). Platelet agonists including collagen, TxA_2, thrombin and ADP, which bind other platelet receptors, activate phospholipase β and γ isoforms (PLCβ and PLCγ), which are enzymes that induce platelet cytosolic Ca^{2+} concentration increase and catalyse diacylglycerol (DAG) generation. Agonist binding can also activate phosphoinositide 3-kinases (PI3Ks). These signalling events converge in TALIN binding to the αIIbβ3 tail, which is mediated by Kindlin3, one of the

effector proteins downstream of the PI3K pathway (Bledzka et al., 2019; Malinin et al., 2009). TALIN binding separates αIIb and β3 tails, which further leads to the disruption of interactions between transmembrane helices. Following these, the extracellular regions of αIIb and β3 also move away from each other, resulting in an active heterodimer that is mainly connected by the headpieces—the β-propeller from αIIb and A-domain from β3. This complex serves as the binding domain for most of the ligands (Xiao et al., 2004; Xiong et al., 2001). The transition from resting to active states in αIIbβ3 extracellular regions involves extensive movement of different domains and metal ion participation (Raborn et al., 2011). Ligand binding brings about outside-in signalling events via αIIbβ3, which further supports platelet spreading and clot retraction (Lee et al., 2019), via small GTPases RAC1 and RHOA.

Lack of αIIbβ3 expression on platelets, or defects in αIIbβ3 structure by mutation or aberrant splicing, lead to an autosomal recessive disease called Glanzmann thrombasthenia (Cattaneo, 2003). The phenotype of Glanzmann's patients is characterised by severe mucocutaneous bleeding and bleeding after trauma, surgery or postpartum (Cattaneo, 2003; Kannan et al., 2009; Siddiq et al., 2011). Platelet aggregation by all agonists in Glanzmann's patients is absent or severely defective, and clot retraction is also impaired; in some severe cases of Glanzmann's, the platelet α granules lack fibrinogen, as the αIIbβ3-dependent uptake from plasma is impaired (Cattaneo, 2019b; Cattaneo et al., 1992; Harrison et al., 1989). Numerous therapeutic agents targeting αIIbβ3 have been developed, including antibodies and antibody fragments, peptides and non-peptide inhibitors; some of them can be taken orally, while others are administrated intravenously (Huang et al., 2019). Three therapeutic agents, including abciximab, which is the Fab fragment of an anti-β3 antibody, and two small molecule inhibitors, eptifibatide and tirofiban, have been approved for clinical use. Abciximab was shown to prevent ischemic cardiac complications in certain patients (Stoffer, 2022). Tirofiban and eptifibatide were introduced into clinical practice more recently, have been approved for the treatment of

unstable angina and angioplasty, and were developed for the treatment of acute coronary syndrome, where they served as a bridge strategy for revascularisation (Huang et al., 2019). As αIIbβ3 is where several major receptors' signalling events converge, the inhibition of it can easily induce the overall platelet dysfuntion and subsequent bleeding complications (De Luca et al., 2015). Therefore, novel therapies, including targeting the αIIbβ3 outside-in signalling pathways to preserve the first wave of the haemostasis processes, and using small molecules to specifically inhibit fibrinogen binding without causing overall conformational change of the integrin, have been developed (Law et al., 1999; Li et al., 2014; Liu et al., 2018).

Platelets also express five other integrins, αvβ3, α2β1, α5β1, α6β1, and αLβ2 (Clemetson & Clemetson, 2019; Zeiler et al., 2014). α2β1 is the receptor for collagen, with a copy number of ~4,000 (Clemetson & Clemetson, 2019). α2β1 binding collagen may facilitate platelet adhesion to the injury site in the initial haemostasis steps, and can also bring platelets closer to collagen fibres, facilitating collagen binding to GPVI and the initiation of its downstream pathways (Bledzka et al., 2019; Santoro et al., 1991). α2 or β1 null mice displayed normal bleeding time and normal adhesion to collagen; the β1-deficient platelets also aggregated normally to equine tendon collagen, but did not aggregate to soluble collagen (J. Chen et al., 2002; Grenache et al., 2003; Nieswandt, Brakebusch, et al., 2001). α6β1 is the laminin receptor on platelets with an expression level of 11,500 per platelet (Burkhart et al., 2012). Platelet-specific α6β1-depleted mice failed to adhere to several types of laminins, had decreased arterial thrombosis but retained normal tail bleeding time, suggesting this receptor as a potential drug target (Schaff et al., 2013). α5β1 is a receptor for fibronectin on platelets; it also plays a supplementary role in platelet adhesion and platelet activation mediated by sCD40L (Piotrowicz et al., 1988; Simic et al., 2017; Varga-Szabo et al., 2008). αvβ3 has a copy number of only several hundreds per platelet, but it mediates platelet adhesion to osteopontin and vitronectin *in vitro* (Bennett et al., 1997). αvβ3 also has a copy number of several hundreds per platelet, and its function on

platelets is not totally clear; it mediates platelet adhesion to osteopontin *in vitro*, as shown by the blockage of platelet adhesion to surface-coated osteopontin by anti-αvβ3 but not anti-αIIbβ3 antibodies in a solid phase assay (Bennett et al., 1997). αvβ3 is a receptor for vitronectin in other cells types (Pytela et al., 1985). Platelet-specific β2-null mice have a shorter lifespan and do not localise to the inflammation site (Guo & Piguet, 1998); however, αLβ2 was only detected on activated but not resting platelets, and was not detected by proteomic or transcriptomic studies, thus it is possible that this integrin is transferred to activated platelets by vesicles from other cells (Clemetson & Clemetson, 2019).

1.2.5 Platelet GPCRs

GPCRs are present broadly on different cell types, with the solved structures occupying >30% of the total number of membrane protein structures, and approximately two thirds of clinically approved drugs target GPCRs. They are also expressed on platelets and play important roles in platelet activation.

1.2.5.1 Protease-activated receptors (PARs)

Protease-activated receptors (PARs) were first identified as the platelet receptors for thrombin, a robust agonist for platelets, when PAR1 was cloned in 1991 (Vu et al., 1991). Human platelets express PAR1 and PAR4. Thrombin binds its recognition sites at the N-terminus (located extracellularly) of PARs, cuts at arginine 41 for PAR1 and arginine 47 for PAR4, releasing a new N-terminus that can bind to PAR itself, thus inducing receptor conformation change which leads to G protein activation and initiates downstream signalling pathways (Han et al., 2019).

The signalling events downstream of PAR1 and PAR4 share the $G_{\alpha q}$ pathway which involves the generation of inositol 1,4,5-trisphosphate (IP_3) and DAG, leading to the increase of intracellular Ca^{2+} level and PKC activation, and the $G_{\alpha 12/13}$ pathway which involves RhoA activation and RhoGEF regulation. Despite the similarity in the downstream signalling

pathways, PAR1 and PAR4 play different roles in response to thrombin: PAR1 acts as the low-concentration-thrombin receptor, responding to lower concentration of thrombin and initiating a quick but transient signal, while PAR4 senses higher concentration of thrombin, inducing a sustained, irreversible signal that leads to potent activation of platelets and the formation of a thrombus (Han et al., 2019; Offermanns, 2006).

Interactions between the same or different PARs have been reported, where each PAR as part of a homo- or hetero-dimer modulates the activation and signalling events of the other. For example, PAR4 cleavage efficiency by thrombin was greatly increased when it is expressed together with PAR1, and this can be diminished by mutations of residues at the PAR1-PAR4 binding interface (Arachiche et al., 2013; Leger et al., 2006; Nieman, 2008). Homodimers of PAR4 have also been reported, which helps in maintaining PAR4 response to its agonists (de la Fuente et al., 2012; Edelstein et al., 2014). PAR4 has also been shown to interact with other GPCRs, e.g. $P2Y_{12}$, the functional significance of which is yet to be defined (Khan et al., 2014).

Small molecule drugs targeting PAR1 or PAR4 has been developed, with several of them already on the market or in clinical trials. Vorapaxar, a PAR1 antagonist, approved by the FDA in 2014, can reduce further cardiovascular risk of patients with history of myocardial infarction or peripheral artery disease (Baker et al., 2014); however, due to the increasing risk of intracranial hemorrhage in patients with prior ischemic stroke history, Vorapaxar has been suggested to be discontinued in such patients (Morrow et al., 2013; Tantry et al., 2020). Despite the challenge of developing selective antagonists to PAR4 over PAR1, at least two highly selective compounds to PAR4 have entered clinical trails (Wilson et al., 2018; Wong et al., 2017), with one of them, BMS-986120, showing the capacity of reducing arterial thrombus size with decreased risk of bleeding in comparison to clopidogrel (Wilson et al., 2018). As PAR4 serves as the high-concentration thrombin receptor in platelets, selective PAR4

antagonists could potentially bypass the bleeding side effects as the activation of PAR1 can still be preserved (Han & Nieman, 2018).

1.2.5.2 $P2Y_1$ and $P2Y_{12}$ receptors

Adenosine diphosphate (ADP), though a relatively weak agonist of platelet activation, can amplify the responses of platelets to other agonists (Cattaneo, 2005), and stabilise platelet aggregation (Cattaneo et al., 1990; Trumel et al., 1999). $P2Y_1$ and $P2Y_{12}$ are two important ADP receptors on platelets.

$P2Y_1$, a 42 kDa protein, was detected and identified as an ADP and ATP receptor (with ADP being the agonist and ATP the antagonist) in 1997 (Leon et al., 1997). ADP coupling to this receptor initiates Gq-mediated signalling pathways, including PLCβ activation followed by IP_3 formation, cytosol Ca^{2+} level increase, and Rap1 activation from GDP-bound form to GTP-bound form. Rap1 activation leads to integrin αIIbβ3 activation via TALIN and Kindlin3. $P2Y_1$ and its downstream signalling pathways are responsible for ADP-induced platelet shape change and reversible aggregation (Cattaneo, 2019a). In addition, $P2Y_1$ plays a role in collagen-induced aggregation (Fabre et al., 1999), chemokine-induced platelet activation (Clemetson et al., 2000), and vWF and GPIbα dependent platelet activation under flow (Turner et al., 2001). Although not directly involved in thrombin receptor signalling pathways, the interplay between $P2Y_1$ and PAR receptors may reinforce the response of both receptors (Cattaneo, 2019a; Kim et al., 2002). $P2Y_1$ exists as a mixture of monomers and dimers on the platelet surface, and the percentage of dimers increases upon its agonist stimulation (Jacobson et al., 2011). Apart from existing on the platelet surface, $P2Y_1$ was shown to exist inside platelets—on the membrane of α granules and in the open canalicular system (Nurden et al., 2003). Several small molecule antagonists of $P2Y_1$ have been developed; however, none of these molecules have been taken to clinical trial stages (da Silva Ferreira et al., 2019).

$P2Y_{12}$ is also activated by ADP and inhibited by ATP. Activation of $P2Y_{12}$ initiates Gαi-mediated signalling pathways, which inhibit the activity of adenylyl cyclase to catalyse cAMP production (Mills, 1996). Apart from that, ADP activation of $P2Y_{12}$ leads to PI3K activation (Dangelmaier et al., 2001), which contributes to platelet activation and aggregation mediated by αIIbβ3. Similar to $P2Y_1$, $P2Y_{12}$ is also expressed both on the surface and in the cytoplasm of platelets, and the intracellular $P2Y_{12}$ comes to the surface upon platelet activation (Haberstock-Debic et al., 2011). $P2Y_{12}$ is an established anti-thrombotic drug target, with many inhibitor drugs routinely used in the clinic, for example, clopidogrel and ticagrelor, both can be used together with aspirin. The use of aspirin in combination with a $P2Y_{12}$ inhibitor is the standard treatment for heart attack patients (see also section 1.2.5.3). Many other $P2Y_{12}$ inhibitors are also in clinical uses or pre-clinical trials. Despite some existing limitations including the bleeding side effect, like many other anti-platelet drugs, $P2Y_{12}$ inhibitors remain the major component of anti-platelet therapies, making $P2Y_{12}$ an important target (Cattaneo, 2019a).

1.2.4.3 Other GPCRs on the human platelet surface

Platelets also express a wide range of other GPCRs. T_XA_2 receptors (TPs) are the only type of thromboxane receptors in platelets, and they couple with multiple G proteins to induce signal transduction. Platelet TPs have been shown to largely locate in lipid rafts, and raft disruption can inhibit T_XA_2-induced Ca^{2+} increase and nucleotide release. TPs couple to both Gq and $G_{12/13}$ (Offermanns et al., 1994; Shenker et al., 1991). The "gold standard" anti-platelet drug for arterial thrombosis, aspirin, which has been in clinic for over 100 years, is an indirect inhibitor of TPs (Schror, 1997). Aspirin inhibits platelet function by acetylating the platelet cyclooxygenase (COX-1) and thus blocking the substrate catalytic site of the enzyme. COX-1 catalyses platelet-dependent T_XA_2 synthesis, which is irreversibly inhibited by aspirin (Patrono, 2019; Schror, 1997). Aspirin is also commonly used in the dual-antiplatelet therapy (DAPT)

together with one of the $P2Y_{12}$ inhibitors, normally clopidogrel, ticagrelor or prasugrel (Degrauwe et al., 2017). Another GPCR, the adrenergic receptor, α_{2A}, can interact with epinephrine, and it couples with both Gi and Gz. Adenosine receptor $A_{2A}R$ is a Gs-coupled GPCR that inhibits platelet activation upon binding adenosine (Offermanns, 2006). Platelets also express several prostacyclin receptors, including PGI_2 receptor—IP, which is the major inhibitory prostaglandin receptor on platelets, PGE_2 receptor which is an activating receptor, and PGD_2 receptor (Cattaneo, 2019a).

Table 1.1 Several GPCRs that express on platelets, their ligands and coupled G proteins

GPCRs	Ligands	G proteins that coupled with GPCR	Notes
PAR1	Thrombin	Gq, $G12_{/13,}$ Gi	PAR1 interaction with Gi needs further information
PAR4	Thrombin	Gq, $G_{12/13}$	
TPα/β	TxA_2	Gi, Gq, $G_{12/13}$	
$P2Y_1$	ADP	Gq	
$P2Y_{12}$	ADP	Gi	
α_{2A}	Epinephrine	Gi	
IP	prostacyclin	Gs	
$A_{2A}R$	adenosine	Gs	

Table 1.2 Several G proteins and their downstream signalling pathways in platelets

G proteins	Downstream cellular responses and signalling pathways
Gq	PLC activation
$G_{12/13}$	RHO-GEF/RHOA activation
Gi	AC inhibition by Giα, PI3K phosphorylation by Giβγ
Gs	AC activation

1.2.6 Tetraspanins and their partner proteins in platelets

Tetraspanins are a family of transmembrane proteins that are expressed in a wide range of organisms, from multicellular fungi to plants and to animals (Hemler, 2005; Protty et al., 2009). Their main recognised function is to form complexes with certain other transmembrane proteins, which are called partner proteins, and thus regulate partner proteins' expression, trafficking, membrane localisation and lateral diffusion (Termini & Gillette, 2017). Moreover, tetraspanins are known as "molecular organisers", as they form unique tetraspanin microdomains that enrich several tetraspanins and specific partner proteins, thus compartmenting the continuum of lipid membrane and helping localise specific membrane proteins for their function (Charrin et al., 2014). As the name suggests, tetraspanins possess four transmembrane helices; they also share two extracellular loops—the large extracellular domain and the small extracellular loop (Seigneuret et al., 2001; Skaar et al., 2015), and intracellular N- and C- terminals. The first crystal structure of a tetraspanin (CD81) showed that the four transmembrane helices group into two two-helix bundles, connected by the large extracellular domain (Zimmerman et al., 2016). The two bundles converge in the cytoplasmic side, making the whole protein a cone-like structure. The intramembrane pocket features a cholesterol molecule. Molecular dynamics simulations further showed that this cholesterol molecule helps lock CD81 in a "closed" conformation where the large extracellular domain is a "cap" over the intramembrane pocket, whereas CD81 without this cholesterol favoured an "open" conformation where the large extracellular domain is flipped upwards, leaving the intramembrane pocket open to the extracellular environment. While CD81 has more recently been shown to exist in this extended conformation when in complex with its partner CD19, which is an important co-receptor for B cell receptor signalling (Susa et al., 2021), there is no evidence yet for dynamic, cholesterol-regulated conformational changes in CD81 or any other tetraspanin.

There are 33 tetraspanins expressed in human, and many of them are expressed in platelets, including CD9, CD63, CD151, Tspan9, Tspan15, Tspan32 and Tspan33 (Lewandrowski et al., 2009). CD9 is the most highly expressed tetraspanin in human platelets (Boucheix et al., 1991), and the second most highly expressed protein of all, with a copy number of ~50,000 (Protty et al., 2009). However, the role of CD9 in platelets and the partner(s) it interacts with remain unclear; the CD9-knockout mouse has no substantial platelet phenotype and the main phenotype of the mice is an infertility in females due to impaired sperm/egg fusion (Mangin et al., 2009). Tspan9 was identified as a novel platelet tetraspanin in 2009 (Protty et al., 2009) and has a copy number of ~2,800. Its expression in platelets and megakaryocytes is considerably higher than in most other cells. Tspan9 knockout mice were reported to have no obvious phenotype, but GPVI-activated platelets had partially impaired platelet activation and GPVI lateral diffusion was reduced by 50% (Haining, Matthews, et al., 2017). Although Tspan9 was reported to interact with GPVI (Haining, Matthews, et al., 2017; Protty et al., 2009), it remains unclear whether this is a robust interaction or how Tspan9 affects GPVI mechanistically. CD151 has an expression level of ~3,000 in human platelets and CD151-knockout mice have a mild bleeding phenotype and impaired platelet aggregation to a variety of ligands, and impaired spreading and clot retraction (Lau et al., 2004). These phenotypes were attributed to CD151 interaction with and regulation of αIIbβ3, but the interaction was only shown by co-immunoprecipitation in weak detergents (Lau et al., 2004) and it remains unclear how a relatively weakly expressed tetraspanin could directly regulate a much more highly expressed integrin. In other cell types, CD151 is well known to partner with laminin-binding integrins and to regulate their clustering and signalling; indeed, human patients lacking CD151 have a skin blistering phenotype consistent with impaired laminin-binding integrin function on epithelial cells (Karamatic Crew et al., 2004). CD63, a surface marker for platelet activation, is a lysosomal membrane protein and only comes to the platelet plasma membrane

upon activation. Its role on platelets is unclear, because CD63-knockout mice have no platelet phenotype (Schroder et al., 2009); CD63's role on other cell types is also unclear.

A subgroup of six tetraspanins, Tspan5, Tspan10, Tspan14, Tspan15, Tspan17 and Tspan33, termed TspanC8s due to the conservation of 8 cysteines in their large extracellular domains, can all form complexes with a metalloprotease, a disintegrin and metalloproteinase 10 (ADAM10). ADAM10 is a ubiquitously expressed transmembrane protease, has over 100 substrates, and functions by cleaving the extracellular domain of its substrate transmembrane proteins in a process termed shedding (Harrison et al., 2021; Koo et al., 2022). Its best-known substrates are the cell fate regulatory Notch proteins and amyloid precursor protein (APP) which is involved in Alzheimer's disease (Harrison et al., 2021). ADAM10-knockout mice are embryonic lethal due to a lack of Notch cleavage and subsequent signalling and activation of transcription (Hartmann et al., 2002). ADAM10 over-expression in the brain is protective in a mouse Alzheimer's model, because APP cleavage by ADAM10 reduces the build-up of pathogenic amyloid β peptides that derive from APP (Postina et al., 2004). ADAM10 also sheds GPVI to release a soluble fragment of GPVI extracellular domain, which is a marker of platelet activation and has elevated levels in several thrombosis-related diseases (Bender et al., 2010; Gardiner et al., 2004; Gardiner et al., 2007; Harrison et al., 2021; Koo et al., 2022; Matthews et al., 2017; Pallini et al., 2021). However, the functional role of GPVI shedding remains unclear, because platelet-specific ADAM10-knockout mice have no platelet phenotype, apart from reduced GPVI shedding (Bender et al., 2010). Recently, ADAM10 substrate specificity has been shown to be regulated by its interacting TspanC8 (Jouannet et al., 2016; Lipper et al., 2022; Matthews et al., 2018; Reyat et al., 2017). Human platelets express three TspanC8s, Tspan14, 15 and 33, of which Tspan15/ADAM10 and Tspan33/ADAM10 have been shown to shed GPVI (Koo et al., 2022; Matthews, 2018). Understanding ADAM10

substrate specificity via TspanC8s may help to develop tetraspanins as novel therapeutic targets, avoiding the toxic effects of targeting ADAM10 due to its ubiquitous expression.

1.2.7 Platelet signal transduction following activation

Platelet receptors respond to extracellular stimuli and transduce biochemical signals inside platelets which ultimately lead to platelet activation or inhibition. Several signalling transduction molecules and events are shared by major receptors. Depending on their orders of action in platelet activation, they can be roughly divided into second messengers, signal integrators and cellular responses (Lee et al., 2019) (Figure 1.4).

Platelet second messengers, including Ca^{2+}, DAG and cyclic nucleotides, and the effector molecules, phospholipases (PLCs), phosphoinositide 3-kinases (PI3K), which catalyse the generation of these second messengers, act following receptor activation. Central to secondary messenger activities is the phosphatidylinositol-4,5-bisphosphate ($PI(4,5)P_2$). Two major reactions of $PI(4,5)P_2$ exist in platelets: it can be hydrolysed to IP_3 and DAG via the catalysation of PLCs, or be phosphorylated by PI3K into phosphatidylinositol 3,4,5-trisphosphate ($PI(3,4,5)P_3$). IP_3 diffuses in the cytosol and binds IP_3 receptors on intracellular Ca^{2+} stores, leading to intracellular Ca^{2+} concentration increase, while DAG is associated with the plasma membrane and activates Ser/Thr kinases of the protein kinase C (PKC) (Heemskerk et al., 2001). PLCs are downstream of many activating receptors and there are two types of PLCs in platelets, PLCβ and PLCγ. PLCβ isoforms are downstream of GPCRs coupled with Gq, while PLCγ isoforms are activated by tyrosine kinase cascade signalling which is downstream of (hem)ITAM receptor (GPVI, CLEC-2 and FcγRIIA) signalling (Guidetti et al., 2009; Lian et al., 2005; Suzuki-Inoue et al., 2003). $PI(3,4,5)P_3$, generated through the PI3K-mediated pathway, binds PH-domain containing proteins in platelets, including PLCγ2, tyrosine kinases Btk and Tec, and Kindlin3 (Lee et al., 2019). Cyclic nucleotides, cAMP and cGMP, are

inhibitory secondary mediators in platelets. Their generation is evoked by PGI_2 and NO, and their effectors are protein kinase A and G (PKA and PKG) (Lee et al., 2019).

The effects of second messengers converge on signal integrators, including kinases PKC/A/G and Rap1 signalling. PKCs are effectors of Ca^{2+} and DAG, and the majority of PKC isoforms are activating integrators. Different isoforms of PKCs have distinct roles. PKCα and PKCβ are classical PKCs; they act downstream of PLCβ and PLCγ, and they can also induce platelet granule secretion (Gilio et al., 2010; Konopatskaya et al., 2009). PKA and PKG, on the other hand, are inhibitory integrators in platelets. They are activated by cAMP and cGMP, respectively, and subsequently phosphorylate several proteins at different phases of platelet activation, for example, TP and IP_3 receptor (Antl et al., 2007; Beck et al., 2014; Tertyshnikova et al., 1998). PKA/G also restrict cytoskeleton dynamics by phosphorylating actin binding proteins such as VASP (Lee et al., 2019). The small GTPase Rap1 is an important "molecular switch" between GDP- and GTP-bound states (Figure 1.6). Rap1 together with adapter proteins, TALIN and Kindlin3, are parts of the αIIbβ3 activation complex. The transition from Rap1-GDP to Rap1-GTP is regulated by guanine nucleotide exchange factors (GEFs) and GTPase activating proteins (GAPs) (Stefanini et al., 2009). The major GEF in platelets is calcium-and DAG-regulated guanine exchange factor-1 (CalDAG-GEFI); as the name suggests, CalDAG-GEFI is activated by Ca^{2+} and DAG release following PLC activation (Burkhart et al., 2012; Crittenden et al., 2004; Eto et al., 2002). The major GAP in human platelets is Ras P21 protein activator 3 (RASA3), which is inhibited by the PI3K pathway (Burkhart et al., 2012; Stefanini et al., 2015).

Platelet signalling events ultimately converges in several cellular responses: cytoskeleton reorganisation, granule secretion and αIIbβ3 activation. Cytoskeletal reorganisation mediates platelet shape changes and spreading. Granule secretion generate ligands for platelet receptors including ADP, TxA_2, fibrinogen and vWF, which helps to recruit and activate more nearby

platelets and therefore thrombi growth. αIIbβ3 "inside-out" activation transforms the receptor to its high-affinity state for its ligands, and subsequent "outside-in" signalling events.

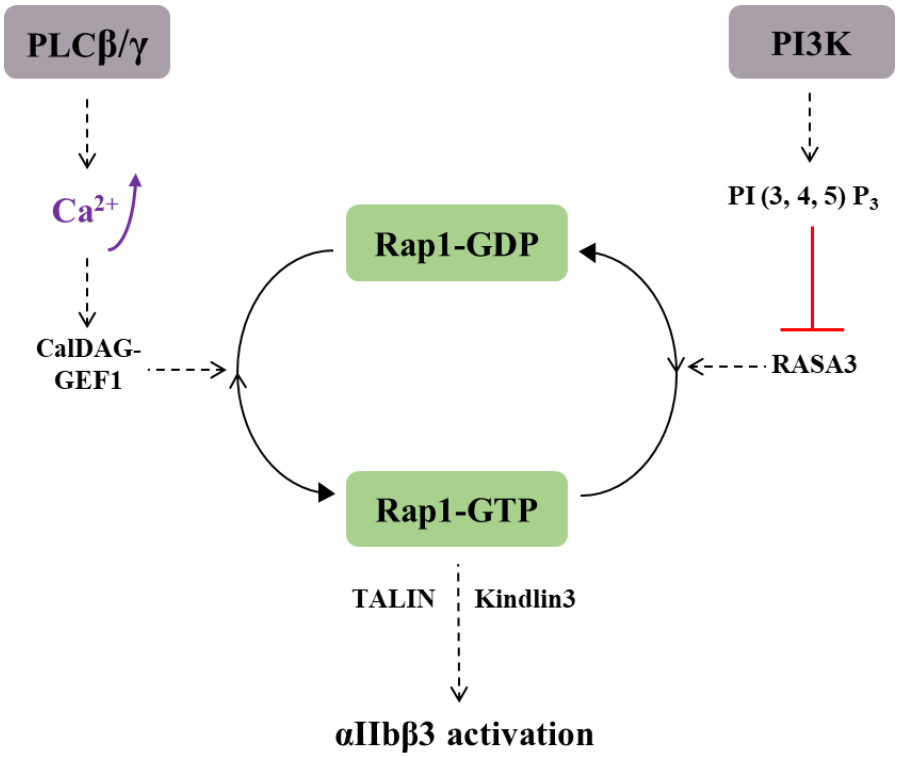


Figure 1.6 Rap1 regulation pathways.

The small GTPase Rap1 is an important "molecular switch" which circulates between GDP- and GTP-bound states. Guanine nucleotide exchange factors (GEFs) exchange GDP to GTP, while GTPase activating proteins (GAPs) mediate GTP hydrolysis and turn Rap1-GTP back to Rap1-GDP. In human platelets, the major GEF is calcium and diacylglycerol-regulated guanine nucleotide exchange factor I (CalDAG-GEF1), which is activated in respond to platelet cytoplasmic Ca^{2+} concentration increase that is triggered by PLC-mediated IP_3 generation. The major GAP in human platelets is Ras P21 protein activator 3 (RASA3), which is inhibited by PI (3, 4, 5) P_3 generated through PI3K pathway. Together, the activation of CalDAG-GEF1 and the inhibition of RASA3 lead to Rap1 activation to the GTP-bound form, which, together with its adaptor proteins, TALIN and Kindlin3, activates integrin αIIbβ3, inducing integrin outside-in signalling events.

1.3 Styrene-maleic acid lipid particles (SMALPs) for studying membrane proteins

1.3.1 Strategies for membrane protein solubilisation

Many of the proteins of interest in this work are embedded in platelet membranes serving as receptors, or associated with, either directly or through other mediators, to membrane-embedded proteins. This makes membrane proteins challenging to study, since their extraction from the native lipid bilayer environment typically removes native lipids and can impair their structure, function, and interaction with other proteins and lipids (Krishnarjuna & Ramamoorthy, 2022). Due to these limitations, structural studies of membrane proteins have long lagged behind those of soluble proteins (Lee et al., 2016).

Over the years of membrane protein solubilisation, researchers have developed different amphiphilic molecules as tools to extract membrane proteins (Figure 1.7). In these studies, the amphiphilic molecules play an essential role in disrupting the cell membrane continuum and dissolve individual or complexed membrane proteins into aqueous solutions. This is achieved by replacing the native membrane environment with these amphiphilic molecules, which can happen either at almost the exact interface between the transmembrane surfaces and the lipid acyl tails or to some distance from the protein-lipid interface, i.e. preserving the adjacent membrane environment.

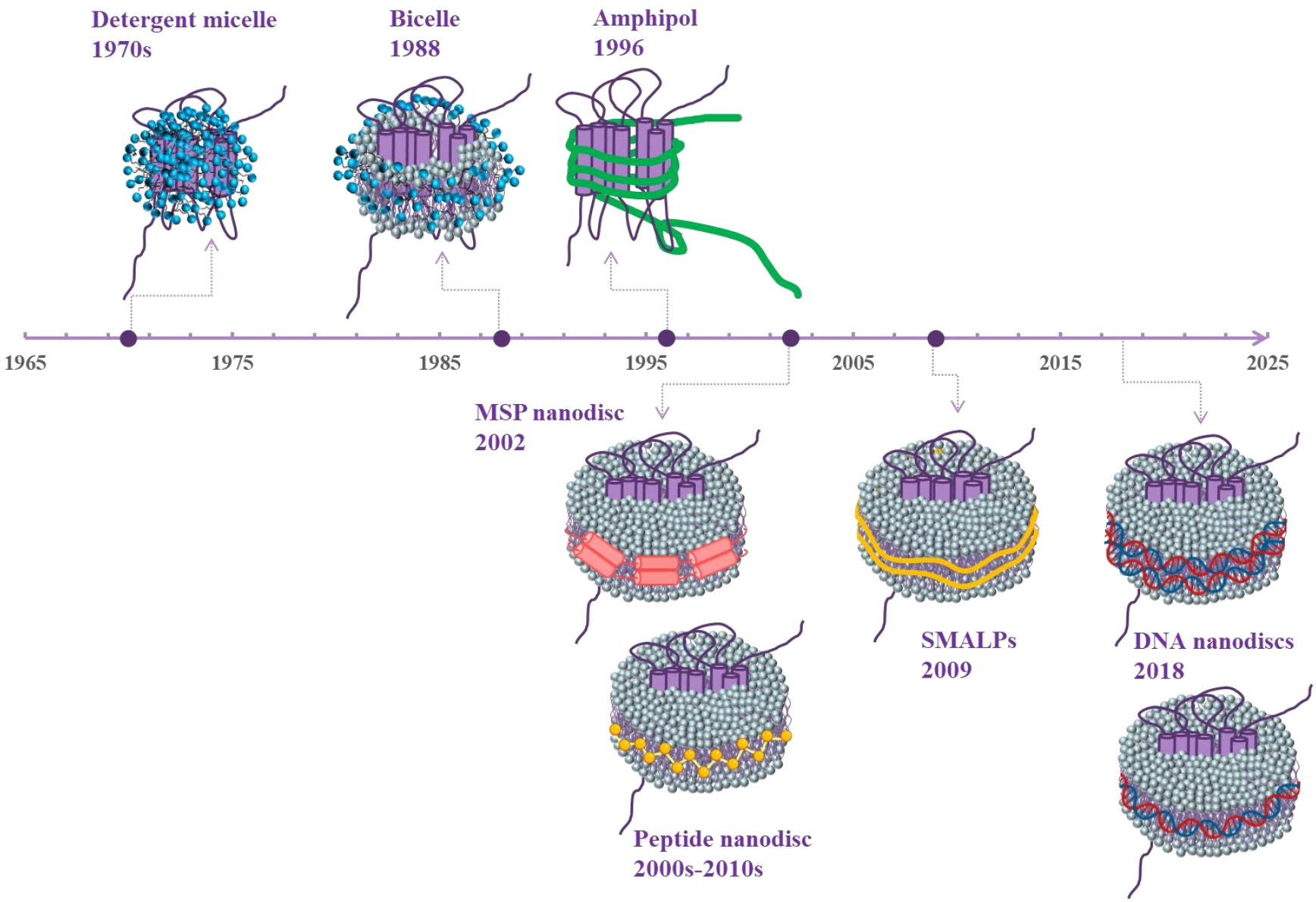

Detergent micelle
1970s
Bicelle
1988
Amphipol
1996
1965
1975
1985
1995
2005
2015
2025
MSP nanodisc
2002
SMALPs
2009
DNA nanodiscs
2018
Peptide nanodisc
2000s-2010s

Figure 1.7 Timescale of membrane protein solubilisation method development.

Detergents (head groups in blue) were used for membrane protein solubilisation since 1970s. Bicelles (detergent head groups in blue, membrane lipid head groups in light green) were developed in 1988. Amphiphols (in green lines) were developed in 1996. Nanodisc-based methods come out since the 21st century, with membrane scanffold proteins (MSPs, in red) and peptides (in orange) developed for nanodiscs in the early 00s, SMALPs and alternative polymer-based nanodiscs (polymers in orange lines) firstly developed since 2009, and DNA-based nanodiscs (DNA chains in blue and red) firstly described in 2018.

1.3.1.1 Detergents for membrane protein solubilisation

Detergents have been adapted as a common tool for membrane protein isolation since the 1970s (Helenius & Simons, 1975). They are small, amphiphilic molecules comprising of hydrophilic head groups and hydrophobic tails. Under low concentration, they exist as monomers in solution, but when the concentration reaches the critical micellar concentration, the excess of these monomers can spontaneously aggregate into micelles. Above the critical micellar concentration, the increase of detergent concentration no longer elevates monomer amount in solution, but instead contributes to the formation of more micelles (Brown et al., 1989).

A typical single molecule of detergent has a larger head group than the single hydrophobic tail, resulting in a cone shape of the whole molecule. In comparison, phospholipids in biological membranes normally posess two hydrophobic tails attached to the head group, thus they have a cylinder shape. Therefore, accumulation of detergent molecules generates micelles, with their large head groups facing outside (i.e. to the aqueous solution) and the thin tails intertwined inside the sphere and forming hydrophobic interactions. In contrast, biological phospholipids tend to form a planar bilayer structure.

When detergents are mixed with cell membrane fractions, the membrane can be fragmented and membrane proteins extracted into detergent micelles, generating protein-detergent complexes which are dispersed in the aqueous solution (Moraes et al., 2014). The hydrophobic surfaces of the membrane proteins are buried inside the micelles and interact with detergent tails by a hydrophobic effect, while the head groups of the detergent enable solubilisation. Two models of the solubilisation procedures have been inferred: the membrane proteins are incorporated into pre-established micelles, or the detergent monomers invade into the space between lipid molecules in the bilayer membrane and gradually replace them (Kleinschmidt et al., 1999; le Maire et al., 2000; Le Maire et al., 1983; Moller & le Maire, 1993). The generated membrane protein/micelle complex can be applied to downstream biochemical/biophysical

characterisations, for example electrophoresis, size exclusion chromatography, immunoprecipitation, circular dichroism, analytical ultracentrifugation, small-angle scattering techniques (SAXS or SANS), and can be used for protein structure determination via X-ray crystallography, cryogenic electron microscopy (cryo-EM) and/or nuclear magnetic resonance (NMR).

The physical and chemical properties of membrane proteins/micelles complexes depend on the proteins, the detergents of choice, and the environmental characteristics such as the overexpression system, the components of the solution and the temperature. Depending on the proteins and downstream applications, different combination of proteins/detergents are desired in different studies, and sometimes a mixture of several detergents is needed. Many different types of detergents have been developed over the years, and they can be generally divided into ionic, non-ionic and zwitterionic, with diverse chemical structures and solubilisation behaviours (Barniol-Xicota & Verhelst, 2020; le Maire et al., 2000). The size and formula of the detergent affect the aggregation number (the average number of detergent molecules per micelle) and the size of micelles (Garavito & Ferguson-Miller, 2001). As effective in solubilising membrane as detergents are, and despite the fact that they have made a remarkable contribution to our understanding of many important membrane proteins (Dorr et al., 2016), they have several significant drawbacks (Chipot et al., 2018; Krishnarjuna & Ramamoorthy, 2022). Firstly, detergent micelles are a poor resemblance to the phospholipid bilayer. The tails surrounding and interacting with the transmembrane region of proteins are highly disordered, unlike the interior of biological membranes which contains orderly arranged alkyl chains (Dawaliby et al., 2016). The spherical shape and highly curved surface of micelles fail to provide the lateral pressure in biological membranes, which could be important to keep membrane protein structure integrity and facilitate their function (van den Brink-van der Laan et al., 2004; Zoghbi et al., 2016). Secondly, the micelle solution is a vastly dynamic

environment, with monomers in solution and monomers lining the micelle surface undergoing constant interchange with each other (Krishnarjuna & Ramamoorthy, 2022). This can expose part of the protein transmembrane regions into aqueous solution, which may further impair their structure and stability, and such exposure can happen at various times in the whole protein extraction and purification processes. It is also important to maintain all the follow-up solutions with sufficient concentration of the detergents (above the critical micellar concentration) used for protein extraction, so that the formed protein/micelle won't fall apart. Thirdly, detergents strip away the interacting molecules of a target membrane protein, including their surrounding lipids and other proteins (Lee, 2003; Malia & Wagner, 2007). These molecules may be important for stabilising protein structure and maintaining their function. Moreover, in studies aiming to discover novel protein-protein and protein-lipid interactions, this information is largely lost for detergent-extracted membrane proteins (Gunsel & Hagn, 2022); due to the dynamic properties of the formed micelles, they may marge together or separate into different micelles, along with their encapsulated membrane proteins, thus generating false-positive and false-negative results for protein-protein interaction studies. Finally, as already mentioned, different detergents/membrane proteins display distinct biochemical/biophysical properties, and the screening process to search for the best combination and condition for the desired application is usually tedious and expensive (Arachea et al., 2012; Gutmann et al., 2007; Hardy et al., 2018; Sjostrand et al., 2017). Therefore, over the years, alternative methods using other reagents for membrane protein extraction have been explored.

1.3.1.2 Alternative methods for membrane protein solubilisation

As many of the drawbacks of detergent micelles are due to the direct contact between detergent tails and membrane proteins and the disorder of these tails, it is a logical effort to retain the protein transmembrane region in a lipid bilayer. This has been achieved by the development of bicelles, which are a mixture of membrane protein, lipids and detergents, where the membrane

protein is immediately surrounded by a lipid bilayer, and the outline of this lipid bilayer is surrounded by detergent molecules, so the whole particle is soluble in aqueous solution (Figure 1.7). The concept of bicelles was firstly described in 1988 (Ram & Prestegard, 1988). Bicelles are generated by mixing lipids and detergents in a certain ratio during membrane protein extraction; the types of lipids and detergents and their ratio need to be carefully selected for the best extraction efficiency (Durr et al., 2013; Prosser et al., 1998). Apart from being able to preserve protein structure integrity, bicelles have the extra advantage of being easily aligned in the magnetic fields of NMR studies (Prosser et al., 1998).

Amphipols are amphiphilic polymers that have been applied to membrane protein extraction since 1996 (Tribet et al., 1996). The idea is to develop amphiphilic reagents which have such high affinities to the transmembrane parts of proteins that they can directly interact and wrap around the transmembrane proteins, and they can achieve this without having to exist above a certain concentration, unlike detergents which have to be above their critical micellar concentration to take effect in protein solubilising (Popot et al., 2011). Amphipols are composed of hydrophilic backbones and hydrophobic sidechains. These sidechains serve as interacting anchors with the encapsulated proteins, and they are densely arranged on the backbone, such that no loops of the backbone can be formed (this is preferred by many biophysical characterisations). Many different amphiphilic polymers have been developed as amphipols since the first one, A8–35 (Tribet et al., 1996). There have been a large number of successful cases where membrane proteins were solubilised into protein/amphipol complexes, for example, several GPCRs, diacylglycerolkinase (DAGK), and nicotinic acetylcholine receptors (nAChRs) (Dahmane et al., 2009; Nasarre et al., 2010; Popot et al., 2011). While some of these membrane proteins remain fully active and are more stable than in detergent micelles, others have shown impaired conformational changes between different functional states (Popot et al., 2011). This can be attributed to the fact that amphipol binding restricts

membrane protein movement, which can both prevent denaturation and hamper native conformational transitions. As polymers, amphipols are chemically sensitive to cations in solution, and low pH; they are also unable to perturb the biological membrane by themselves, meaning that the membrane proteins need to be firstly solubilised by detergents before adding in amphipols (Popot et al., 2003).

The solubilised membrane proteins can be reconstituted into model membrane systems, such as liposomes for delivering the proteins to specific systems, and artificial lipid bilayers for membrane diffusion kinetics and protein interaction/signalling studies. Nevertheless, the lipid composition and compartmentalisation can be systematically controlled in these model membrane systems (Dorr et al., 2014). Limitations include that the artificial bilayers are unsuitable for solution-based characterisation methods, and the large size of liposomes make them not applicable to many spectroscopic techniques due to light scattering (Dorr et al., 2016).

1.3.1.3 Nanodisc-based methods for membrane protein solubilisation

Nanodiscs are a new generation of membrane protein solubilisation methodology. The concept was firstly created in 2002, when the sequence of apolipoprotein A-I was engineered to be able to spontaneously form disc-like nanoparticles when co-incubated with synthetic phospholipids (Bayburt et al., 2002). These engineered proteins are termed membrane scaffold proteins (MSPs), and have a helical structure with two of them stacking on each other to create a belt around discs with a size of ~10 nm. MSPs have controllable sizes and secondary structures, and the encapsulated disc contains membrane proteins surrounded by a lipid bilayer. Membrane proteins are firstly solubilised by detergents, then incubated together with MSP and phospholipids in an appropriate ratio, during which time the MSP nanodiscs are formed with the membrane proteins inside. The ratio of different components (MSPs, phospholipids and encapsulated proteins) highly impacts the oligomerisation status of the inserted proteins (Nath, Atkins, et al., 2007). MSP-belted nanodiscs can also be generated from cell-free protein

expression systems, in which case detergents are not required (Proverbio et al., 2013). The lipid species to be added in MSP nanodiscs can be selected according to the preference of the encapsulated membrane protein. Numerous membrane proteins have been successfully incorporated and characterised using MSP-nanodiscs, including microsomal cytochrome P450 (CYP) and GPCRs, and ligand-binding studies on many of these proteins have generated valuable information on their pharmacological profiles (Lavington & Watts, 2020; Leitz et al., 2006; Nath, Grinkova, et al., 2007).

More recently, another type of lipid-binding protein, saposin A, has been shown to form nanodiscs encapsulating lipids and proteins (Frauenfeld et al., 2016). Saposins have been shown to bind lipid membrane, transport lipids and form lipid complexes (Bruhn, 2005; Olmeda et al., 2013; Popovic et al., 2012), and several structures of saposin proteins have been reported (Ahn et al., 2003; Popovic et al., 2012; Rossmann et al., 2008). Membrane proteins are firstly extracted into detergent solutions, then incubated together with phospholipids and saposin A to form saposin-lipoprotein (Salipro) nanoparticles, which are similar in size to MSPs (Frauenfeld et al., 2016). The number of membrane protein structures solved in saposin nanodiscs is increasing, with several of these proteins being roton-activated chloride channel ASOR (Wang et al., 2022), α3β4 nicotinic receptor in its ligand-binding states (Gharpure et al., 2019), and muscle nicotinic receptor in both resting and desensitised states (Rahman et al., 2022). In addition, a new pipeline to generate saposin nanodiscs, direct membrane extraction (DirectMX), has been developed, which can extract membrane proteins from crude cell membranes into saposin nanodiscs in one step (Lloris-Garcera et al., 2020). Although DirectMX has been shown to be suitable for SPR and cryo-EM analysis (Drulyte et al., 2023), this method still needs to incubate the crude membranes with detergent solution, because detergents can increase membrane fluidity (Lloris-Garcera et al., 2020) and activate saposin A by inducing its conformational change (Chien et al., 2017).

Several peptides have also been developed as nanodisc belt reagents for membrane protein solubilisation, for example lipopeptides which comprise an amphipathic α-helix with hydrophobic and hydrophilic sides in the same helix (Prive, 2009), lipid-like peptides (Corin et al., 2011), stabilizing engineered β-strand peptides (Tao et al., 2013), dimeric peptides with rigid or flexible linkers (Larsen et al., 2016), and amphipathic bi-helical peptides (Carlson et al., 2018). A few drawbacks of the MSP-belted, saposin-belted, and other peptide-belted nanodiscs include that detergents and additional phospholipids still need to be added to the system in most cases, that the ratio of MSP / target protein / phospholipid / detergents needs to be optimised, and that the existence of scaffold proteins or other peptides may interfere with certain downstream characterisation of the encapsulated proteins.

Other nanodisc systems, without using proteins or peptides as the belts, have been established. Using amphiphilic polymer chains, styrene maleic acid co-polymer (SMA), as the belt, SMA lipid particles (SMALPs) have been developed recently (Knowles et al., 2009; Lee et al., 2016). Like the MSP nanodiscs, SMALPs consist of membrane proteins encapsulated in a lipid bilayer, belted by the ring of SMA, which enables solubilisation of SMALPs in aqueous solution. Notably, SMALPs are by far the only method to directly extract membrane proteins from their native lipid bilayer environment without any need of additional detergents or synthetic lipids. A detailed description on SMALPs and their applications will follow in section 1.3.2, and the SMALP generating process is illustrated in Figure 1.8.

Recently, a novel type of nanodisc, the DNA-encircled lipid nanodiscs, have been described (Iric, 2020; Iric et al., 2018). DNA origami, designed to form rings with desired chemical modifications, can be precisely programmed with regards to their size, shape and positions of functionalisation. Alkylation has been performed on the interim of the DNA rings to increase their hydrophobicity, and this has led to spontaneous lipid bilayer formation inside the DNA ring when phospholipids are added. A new version of DNA rings, the “double-decked” DNA

ring, has also been developed so that the height of the rings (~4 nm) better matches the thickness of the lipid bilayer. As for the opportunities to incorporate membrane proteins into these DNA-encircled lipid nanodiscs, CCR5, a member of the GPCR family, has been engineered to contain a DNA label, and the DNA rings encircling the lipid bilayer have also been designed to contain protruding sequences that are complementary to the DNA tag on the protein to be inserted (Iric, 2020). Although the final result of membrane proteins encapsulated in DNA-nanodiscs using the above method has not been reported yet, coarse-grained simulation has shown the stability of DNA-nanodiscs when the DNA ring contains protruding dodecyl alkyl groups (Iric, 2020). The technique is still in its infancy, but has shown the potential as a new membrane protein solubilisation strategy.

1.3.2 SMALPs are a novel strategy for the extraction and characterisation of membrane proteins

1.3.2.1 SMA co-polymer as the tool to extract membrane proteins

SMA is the co-polymer of styrene and maleic acid, which are the hydrophobic and hydrophilic parts, respectively. SMA is synthesised by hydrolysis of the anhydride units of its precursor polymer, styrene maleic anhydride (SMAnh). Both SMA and SMAnh are widely used polymers in industry such as being additives to plastics for enhanced thermal performance (Dorr et al., 2016; Klumperman, 2010). In life sciences, SMA has been used as a drug delivery system due to its amphiphilic property (Simon et al., 2018). For example, doxorubicin, an anti-cancer reagent, can be constructed in SMA micelles due to the hydrophobic effect with the styrene moieties; the resulted SMA–Dox showed enhanced bio-availability and less cytotoxicity compared to the free form of the drug (Greish et al., 2004). Pirarubicin, an improved version of doxorubicin, can also be encapsulated into SMA micelles, and these micelles showed improved survival rate in a murine liver metastasis model and inhibition of liver metastases (Daruwalla et al., 2010). More recently, SMA has been shown to interact with

phospholipids and can form discs with phospholipids inside. The capability of SMA to solubilise membrane proteins from intact biological lipid bilayers into disc-like structures, SMALPs, with a diameter of ~10 nm, was firstly described in 2009 (Knowles et al., 2009). Since then, SMALPs have been applied to a wide range of membrane proteins and have been proven useful in their structural and functional studies.

SMAnh polymer is synthesised by radical reaction, where monomers are added into the end of the polymer chain and the chain is elongated in this way. As the end of styrene can incorporate both styrene (S) and maleic anhydride (MAnh), but the end of maleic anhydride can only incorporate styrene, the minimum ratio of S:MAnh in the synthesised SMAnh is 1:1 (Alfrey & Lavin, 1945; Dorr et al., 2016; Hill et al., 1985). The serial composition along the SMAnh is largely uncontrollable, although the overall S:MAnh ratio can be regulated by controlling the original amount of the two monomers (Klumperman, 2010). Strategies have been applied to better control the monomer arrangement along the polymer chain, for more homogenous polymers. For example, living radical polymerization methods have been applied to SMAnh synthesis, including reversible addition fragmentation chain transfer (RAFT)-mediated polymerisation. This uses two blocks of short polymer chains, one with almost precisely alternative S and MAnh, while another is poly-S, to generate a more precisely controlled overall microstructure of SMAnh polymer (Craig et al., 2016; Klumperman, 2010). SMAnh is further hydrolysed to form the final product, SMA, by increasing buffer pH (Lee et al., 2016). The functional relevance of SMA microstructure on their application in SMALPs is still under investigation.

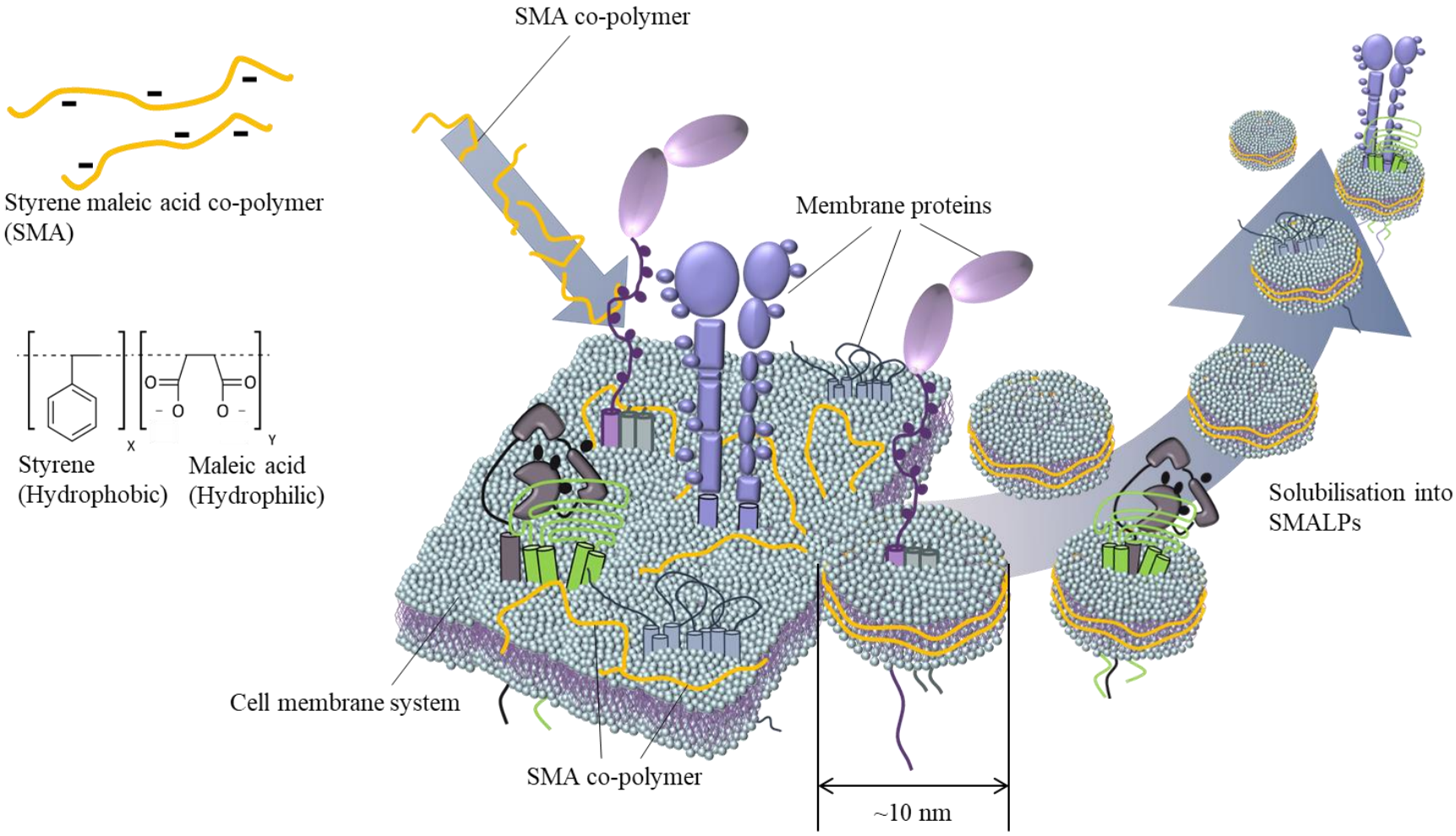

SMA co-polymer
Styrene maleic acid co-polymer
(SMA)
Membrane proteins
Styrene
(Hydrophobic)
Maleic acid
(Hydrophilic)
Solubilisation into
SMALPs
Cell membrane system
SMA co-polymer
~10 nm

Figure 1.8 Generation of SMALPs.

When amphiphilic SMA polymer chains are mixed with cell membranes, they can insert themselves into the membrane and cut out membrane fractions like a cookie cutter. SMA cut out and form SMALPs in a non-selective manner of membrane components, i.e. not in favour of solubilising certain lipids or proteins.

1.3.2.2 Alternative polymers

Despite the advantages of using SMA to generate SMALPs, several limitations regarding SMA chemistry remain. Due to the existence of two carboxyl groups with pKa values being 6 and 10, respectively, the charge status of SMA is largely dependent on buffer pH. If pH is below 6, SMA will possess no negative charge on its maleic acid moieties and the hydrophobic effect provided by the styrene moieties will take dominance (Banerjee et al., 2012; Dorr et al., 2016). The polymer will then precipitate from aqueous solution, into aggregates that are maintained by styrene groups (Scheidelaar et al., 2016). In addition, the two carboxyl groups can chelate divalent cations such as Mg^{2+} and Ca^{2+}, when their concentration in solution is higher than 5 mM, and the chelated product is also insoluble (Lee et al., 2016; Morrison et al., 2016). With regards to the S group, the aromatic ring interacts with encapsulated phospholipids, which can restrict lipid movement and disorder their acyl chains; it also interferes with UV absorbance at 280 nm and thus can interfere with protein concentrations measurement (Ball et al., 2021; Tonge & Tighe, 2001). Based on these drawbacks, other amphiphilic polymers have been developed recently, and have been applied to isolate membrane proteins directly into nanodiscs.

Diisobutylene maleic acid copolymer (DIBMA) replaces the styrene moieties with diisobutylene which interfere less with the lipid acyl chains. DIBMA also has the advantage of not interfering with protein concentration measurement via ultraviolent light, as it doesn't have the aromatic ring which is the main source of absorbance at 280 nm (Ball et al., 2021). DIBMA forms larger lipid nanodiscs (DIBMALPs) than SMALPs, with a diameter of ~25 nm (Gulamhussein et al., 2020). DIBMA is a promising tool to study large membrane proteins and protein complexes, and has been shown to allow native conformational changes of the encapsulated protein, but it is also harder to solubilise native membranes than with SMA (Grime et al., 2021; Gulamhussein et al., 2020).

With regards to the maleic acid moiety that accounts for low tolerance to acidic pH and divalent cations, modifications have been made to this, generating several derivatives including styrene maleimide copolymer (SMI), SMA-ethanol amine copolymer (SMA-EA), SMA-amine copolymer (SMAd-A), and styrene maleimide quaternary ammonium copolymer (SMA-QA) (Hall et al., 2018; Ravula et al., 2018; Ravula, Hardin, et al., 2017; Ravula, Ramadugu, et al., 2017). They can all tolerate acid pH, with SMI and SMAd-A having an opposite pH tolerance window to SMA (SMI: pH 5-7.8, SMAd-A: pH 3-6), and the other two having wider windows (SMA-EA: pH 5-10, SMA-QA: pH 2.5-10). These polymers can also tolerate higher divalent cation concentrations, with SMA-QA and SMAd-A being able to form stable nanodiscs with the concentrations of Mg^{2+} or Ca^{2+} as high as 200 mM. Moreover, SMI, SMAd-A and SMA-QA are positively charged polymers, thus can be a good replacement for the negatively charged SMA and SMA-EA in certain circumstances, for example when the encapsulated protein has large, positively charged extracellular domains. Oppositely charged protein domains and polymers can interact with each other and the protein structural integrity can be disrupted (Krishnarjuna & Ramamoorthy, 2022). Although less well characterised than SMA, these derivative polymers offer a powerful toolbox for screening studies to explore the best solubilising polymer for the proteins of interest, and they have all been made commercially available in the last few years.

Polymethacrylate (PMA) is another amphiphilic copolymer that can be used to form and serve as the belt for lipid nanodiscs (Yasuhara et al., 2017). With completely different composition of both hydrophobic and hydrophilic moieties from SMA, PMA is more tolerant to low pH and higher concentration of Mg^{2+} or Ca^{2+}, and has no aromatic rings to disrupt lipid acyl chains or interrupt with protein concentration determination. The use of PMA to isolate membrane proteins into nanodiscs is still in an early stage; however, there have been examples of

membrane proteins successfully isolated and characterised in PMA-lipid nanodiscs, e.g. amylin and neurotensin receptor 1 (Lavington & Watts, 2021; Yasuhara et al., 2017).

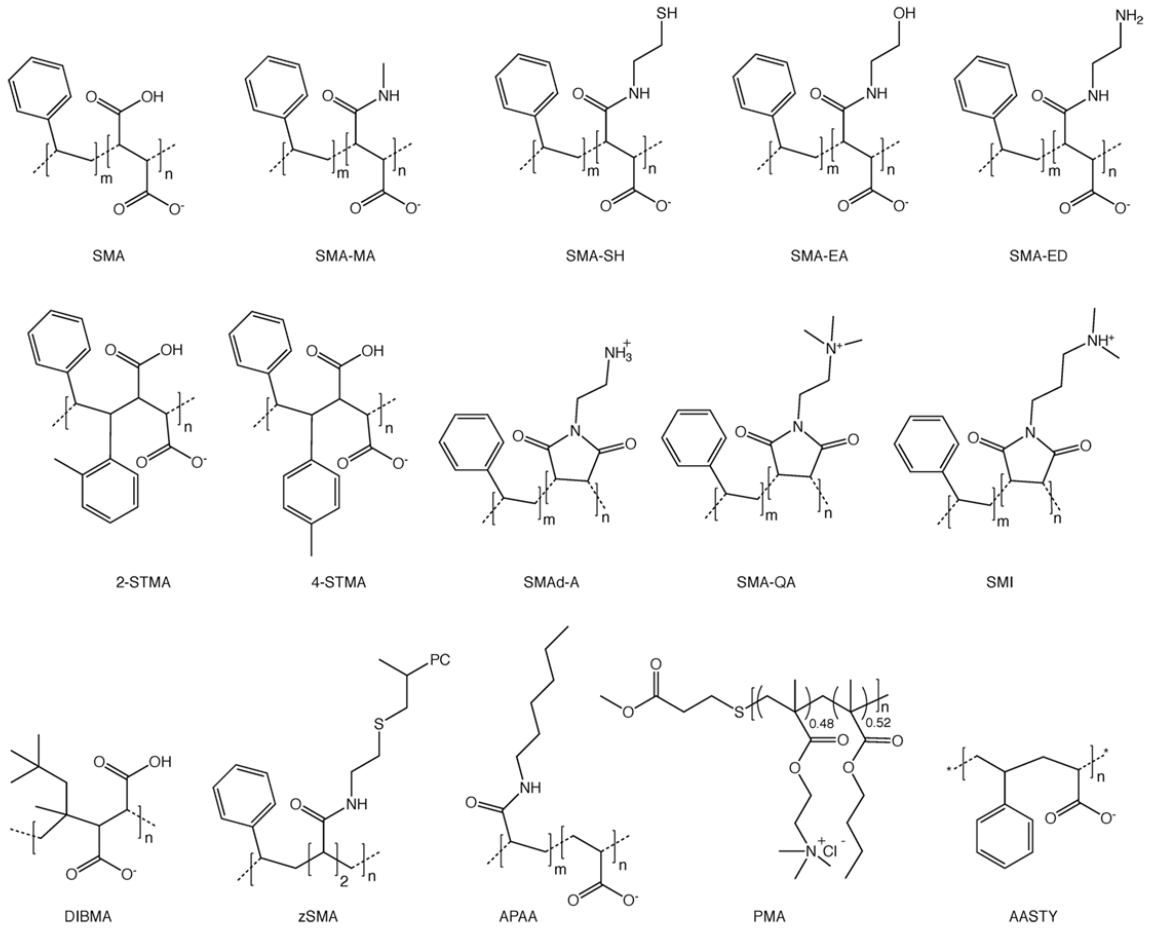


Figure 1.9 Chemical formulas of polymers that can be used to generate lipid nanodiscs.

SMA, styrene-maleic acid co-polymer. SMA-MA, SMA-amine co-polymer. SMA-SH, SMA-thiol co-polymer. SMA-EA, SMA-ethanol amine co-polymer. SMA-ED, SMA-ethylenediamine co-polymer. 2-STMA, 2-methyl-stilbene–maleic acid co-polymer. 4-STMA, 4-methyl-stilbene–maleic acid co-polymer. SMAd-A, styrene maleimide-amine co-polymer. SMA-amine co-polymer. SMA-QA, styrene maleimide quaternary ammonium co-polymer. SMI, styrene-maleimide co-polymer. DIBMA, diisobutylene-maleic acid co-polymer. zSMA, zwitterionic styrene-maleic acid co-polymer. APAA, alkyl polyacrylic acid. PMA, polymethacrylate. AASTY, styrene-acrylic co-polymer. Figure adopted from https://www.smalp.net/ with permission.

1.3.2.3 Mechanisms of SMALP formation

The precise mechanisms and molecular interactions underlying the formation of SMALPs and other polymer-encircled nanodiscs are still largely unclear. However, models describing these processes have been developed, mainly by means of computational simulation. In these models, membrane solubilisation by SMA or other polymers can be roughly divided into three stages: absorption of polymers to lipid bilayer surface, lipid bilayer disruption by the polymers, and formation of nanodiscs (Figure 1.10).

In the first step, the polymers adhere to the outer side of lipid bilayers. Although this step is against the energy gradient, the hydrophobic interaction between polymer hydrophobic groups and the lipid acyl groups serves as the driving force for polymer binding membrane (Jamshad, Grimard, et al., 2015; Krishnarjuna & Ramamoorthy, 2022). Therefore, both lipid and polymer types can strongly impact this process. The more anionic lipid head groups are, the longer the lipid tail groups are, and the more tightly packed the lipids are, the harder and slower this membrane binding process is (Orekhov et al., 2022; Scheidelaar et al., 2015). This is because the anionic lipids have increased repulsive forces towards negatively charged polymers (here the focus is on the most commonly applied polymers, which are mostly negatively charged, but in case of the positively charged polymers as mentioned in section 1.3.2.2, the effect of anionic lipids should be opposite), and the longer lipid tails and tightly packed lipids make the penetration of polymer hydrophobic moieties through the membrane harder (Krishnarjuna & Ramamoorthy, 2022).

The membrane-bound polymers then disrupt the membrane continuity, which has been proposed to be achieved by two means: pore-forming and lipid extraction (Orekhov et al., 2019) (Figure 1.10). In the pore-forming model, small, water-filled pores on the lipid membrane appear after polymer binding, where the rims of these pores are stabilised by polymers. Due to the self-aggregation property of the polymers, the formed pores have the tendency to merge,

leading to larger, water-filled pores. This model was firstly observed in a coarse-grain simulation study, then confirmed by surface acoustic wave resonance sensing and microscopy studies (Bjornestad et al., 2021; Caparotta et al., 2021; Orwick Rydmark et al., 2019; Xue et al., 2018). The formation of the final polymer-belted nanodiscs, from the polymer-rimmed, water-filling pores on the continuous lipid bilayer, have not been achieved in course-grain simulation due to technical limitations, but they have been shown to be the thermodynamically preferred end state (Xue et al., 2018). The lipid extraction model, on the other hand, proposes that the membrane-bound polymers pull their interacting lipids out of the bilayer continuum. Importantly, these two models do not contradict each other, as the mode of action depends on the relative composition of the hydrophobic and hydrophilic monomers: in another course-grain-based study on SMA, the system underwent the pore-forming route when S:MA was 2:1, while adopting the lipid extraction route when S:MA was 3:1 (Orekhov et al., 2022; Orekhov et al., 2019). It was pointed out that when three or more styrenes are in a row, the lipid extraction motion is preferred (Orekhov et al., 2022). This could also be the case for other polymers. The two modes of action can happen at the same time at different sites in the same reaction, as the monomer arrangement of SMA varies along the polymer chain.

Lipids encapsulated in the formed nanodiscs preserve their dynamic properties, though these are constrained by the polymer belt to a certain degree. The formed nanodiscs can undergo lipid exchange upon collision with each other, and the isomerization of azolipids in SMALPs has also shown to be preserved (Cuevas Arenas et al., 2017; Dominguez Pardo et al., 2019). However, studies based on electron paramagnetic resonance and differential scanning calorimetric measurements have shown that DMPC lipids in polymer-nanodiscs have broader main melting transition, different water accessibility in the bilayer, plus additional constraints, in comparison to DMPC in liposomes (Hoffmann et al., 2021). It has also been shown that lipids in DIBMALPs are less constrained than those in SMALPs (Colbasevici et al., 2020).

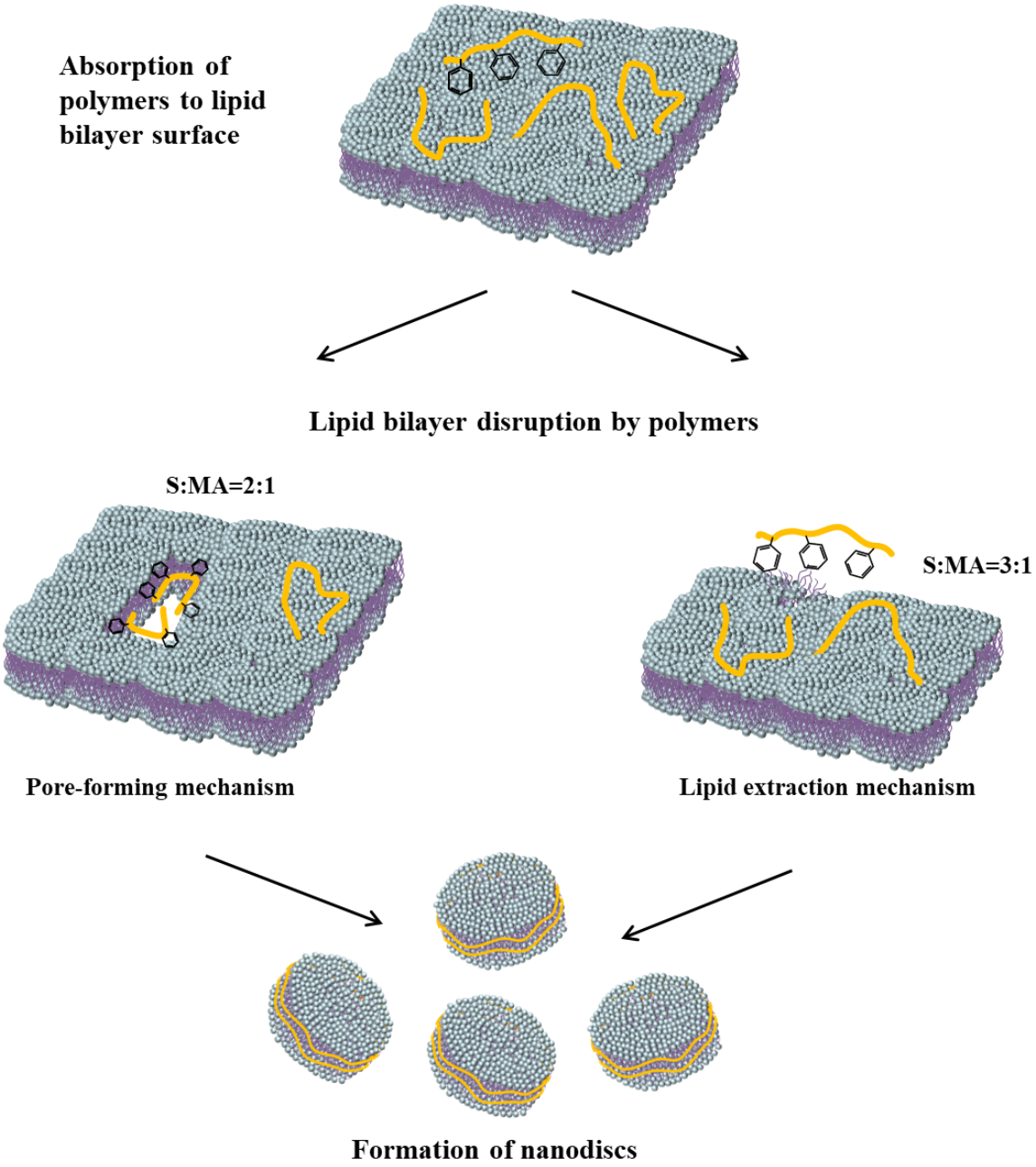


Figure 1.10 Proposed mechanisms of SMALP formation.

Membrane solubilisation by SMA or other polymers can be roughly divided into three stages: absorption of polymers to lipid bilayer surface, lipid bilayer disruption by the polymers, and formation of nanodiscs. Two potential mechanisms of lipid bilayer disruption have been proposed when SMA polymer is incubated together with membrane. When the S:MA ratio is 2:1, SMA is proposed to form water-filled pores, with the rim of the pores stabilised by the polymer chains. When S:MA ratio is 3:1, SMA is proposed to pull lipid molecules out of the membrane continuum, based on the hydrophobic effect between lipid acyl chains and the benzene rings from SMA. Although complete destruction of bilayer and formation of nanodiscs (SMALPs) have not been fully described, numerous experiments have confirmed their disc shape, the existence of polymer belt, and their sizes.

1.3.2.4 Applications of SMALPs

Numerous membrane proteins have been successfully solubilised and characterised using SMALPs or nanodiscs belted by other polymers, and both the number of characterised proteins and the characterising methodologies are rapidly emerging. SMALPs are stable over freeze-thaw cycles, and once formed, no extra SMA polymers are needed in the downstream buffers, unlike in the case of detergents where their concentration usually needs to be above the critical micellar concentration in all the buffers (Jamshad, Charlton, et al., 2015; Pollock et al., 2018; Wheatley et al., 2016). Not only are SMALPs readily amendable to a variety of widely used biophysical and biochemical characterisations, including circular dichroism (Ayub et al., 2020; Gulamhussein et al., 2020; Knowles et al., 2009), dynamic light scattering (Craig et al., 2016; Gulamhussein et al., 2020; Harding et al., 2019), SAXS and SANS (Brady et al., 2019; Jamshad, Grimard, et al., 2015), flow cytometry (Luna et al., 2018), immunoprecipitation and antibody binding (Desrames et al., 2020), but also they can be used in advanced techniques such as native mass spectrometry for oligomerisation status analysation (Hellwig et al., 2018), SPR for ligand screening (Cao et al., 2022), NMR for protein and lipid characterisation studies (Park et al., 2020; Radoicic et al., 2018), mass spectrometry for lipid analysis (Teo et al., 2019), X-ray crystallography (Broecker et al., 2017) and cryo-EM for structure determination (Krishnarjuna & Ramamoorthy, 2022; Kumar et al., 2021; Sun et al., 2018; Sun & Gennis, 2019; Yu et al., 2021).

SMALPs have been used to solve membrane protein structures with high-resolution and in their native states, i.e. in their native conformation and/or with important binding partners including lipids and other proteins. For example, several structures of the proteins from pentameric ligand-gated ion channels (pLGICs) have been solved in SMALPs. These include the *Erwinia* ligand-gated ion channel (ELIC), whose cryo-EM structure was solved in SMALPs to 2.5 Å in its unliganded state. The same study also showed evidence of the existence of two

types of tightly binding phospholipids, namely diacylated phospholipid and tetra-acylated cardiolipin, both corresponding to the bacterial membrane environment (Kumar et al., 2021). Another study solved the cryo-EM structures of another ion channel in the same superfamily, glycine receptor GlyR, in both SMALPs and reconstituted MSP-nanodiscs. This study showed that MSP-nanodisc reconstitution may shift the conformational equilibrium of the channels, while SMALPs preserved their native conformational states, and the structure of GlyR open state in SMALPs corresponds better to experimental data than a previously solved, open-state GlyR structure from detergent micelles. In addition, SMALP-encapsulated GlyR showed for the first time the partial agonist-binding, closed state of the receptor (Yu et al., 2021). Alternative complex III (ACIII) is another transmembrane protein whose structure has been solved in SMALPs to 3.4 Å, in complex with another enzyme, cyt aa_3. With 48 transmembrane helices, this is by far the largest membrane protein encapsulated in SMALPs, and the radius of the transmembrane region cross-section reached 13 nm. The structure also showed that two of the subunits of ACIII are anchored to the lipid bilayer, and that cyt aa_3 adopted conformational changes when in complex with ACIII, indicating the importance of supercomplex formation (Sun et al., 2018). The bacterial-expressed, multidrug efflux transporter AcrB has also been isolated into SMALPs and structurally characterised (Qiu et al., 2018). The 3.2 Å structure of trimeric AcrB, with each protomer in a different state, was solved together with well-packed lipid molecules both inside the central cavity and outside as the belt. 31 lipid molecules were distinguished, and the details of lipid-protein interaction were mapped. The study also showed that the structure of a mutant AcrB in SMALPs, AcrB D407A with the mutation at one of the putative proton-relay residues, is very similar to that of WT AcrB, which is in contrast with the previous transmembrane-largely collapsed D407A structure in detergent micelles (Su et al., 2006), suggesting a supporting and restraining function of the native lipid bilayer.

Apart from structure determination, SMALPs also have many other applications. Many studies have determined specific lipids surrounding membrane proteins in SMALPs, and lipidomics analysis using thin-layer chromatography, mass spectrometry and/or NMR are emerging. A lipidomics study comparing extracted phospholipids from SMALPs containing three bacterial membrane proteins, ZipA, FtsA and PgpB, showed that individual proteins associate preferentially with a subset of lipids (Teo et al., 2019). SMALPs can be used to preserve the native conformation of the encapsulated proteins; for example, a conformation-dependent Rhesus D (RhD) antibody could detect RhD in SMALPs isolated from RhD^+ donors, indicating that at least one important comformation of RhD epitope was preserved in SMALPs from erythrocyte membrane (Desrames et al., 2020). This offers exciting opportunities of using SMALPs for allo-antibody screening and binding studies on erythrocytes (Desrames et al., 2020). SMALPs can also be used to preserve native membrane protein complexes that would otherwise be lost in detergent micelles, for example a metabolon containing dhurrin and all the enzymes that catalyze its formation (Laursen et al., 2016), the bacterial holo-translocon containing SecYEG–SecDF–YajC–YidC proteins (Komar et al., 2016), and the different oligomeric states of K^+ importer A (KimA) (Hellwig et al., 2018).

The application of SMALPs and other types of polymer-belted nanodiscs has been extremely useful to study a number of membrane protein families. For example, GPCRs are highly dynamic receptors, with a large number of family members and a wide range of agonists, partial agonists, antagonists and allosteric modulators. Even phospholipids have been shown to allosterically modulate GPCR conformations. These modulators have been shown to stabilise certain conformations of their target GPCRs, and their binding can favour and/or inhibit the initiation of different downstream signalling pathways of GPCRs, mainly through G-protein binding behaviours. As a result, GPCRs adopt a collection of conformations in physiologically relevant conditions, and detergent extraction methods typically destroy these native

conformations, resulting in unstable GPCRs and hampering ligand screening. Strategies such as mutagenesis and using engineered G proteins were helpful for stabilising GPCRs in structural studies (Garcia-Nafria et al., 2018), but also constrained the conformational dynamics. Several GPCRs, including $A_{2A}R$ and rhodopsin, have been extracted into SMALPs, SMI lipid particles (SMILPs) and/or DIBMA lipid particles (DIBMALPs), and their conformational changes upon ligand binding have been observed (Grime et al., 2020; Grime et al., 2021; Hall et al., 2018; Szundi et al., 2021). Polymer-based nanodiscs may therefore revolutionise the fields of GPCR structure and function. Research into the similarly dynamic pLGIC family could also benefit from these nanodiscs. In addition, the study of tetraspanins, a family of membrane proteins with major functions in forming complexes with other membrane proteins, may also benefit greatly from SMALPs and relevant nanodiscs, as these nanodiscs could potentially facilitate the discovery of novel partner membrane proteins of tetraspanins.

1.4 Hypothesis and aims of the thesis

GPVI, as the major receptor for collagen and initiating downstream signalling upon ligand binding that ultimately leads to platelet activation, plays major role in thrombosis and a relatively minor role in haemostasis. Therefore, it is a promising anti-thrombosis drug target. Understanding the structural details of GPVI is important for the interpretation of its drug binding behaviours and for designing new drugs. In addition, the ligand-binding and signalling behaviours of GPVI, as well as of other platelet surface receptors, could be dependent on the micro-environment, including surrounding lipids and other membrane proteins. However, our current understanding of both the structural conformation of GPVI, and the spatial arrangement of GPVI in relation to other proteins on the platelet surface, is only rudimentary. In particular, the published crystal structures of GPVI only contain its IgSF domains (Feitsma et al., 2022; Horii et al., 2006; Slater et al., 2021), with the information of its glycosylated stalk, the transmembrane region, the cytoplasmic region, and the interaction with its signalling chain, FcRγ, completely absent. There have been controversies whether the GPVI dimer represents a unique, functionally active form of this receptor, or just the increased avidity to its ligands (Clark, 2020; Clark, Neagoe, et al., 2021; Slater et al., 2018); the regions other than the IgSF domains may play important roles in refining the conformational arrangement of GPVI, and help to explain the controversies in GPVI's dimerisation mode including the interacting interfaces as revealed by the existing GPVI structures. Moreover, mapping the configuration of GPVI, and other major platelet receptors, with regards to their spatial proximity with other membrane proteins, is crucial to understand how their structures and functions are regulated, yet this information is usually missing in the current attempts to isolate platelet membrane protein assemblies using detergent-based methods, which can generate artefacts in protein-protein interaction identification. The hypothesis in this thesis, therefore, is that SMALPs can preserve the native conformation and micro-environment of GPVI and other platelet receptors,

thus the isolation of platelet surface receptors into SMALPs can generate useful information on GPVI structure, and the stoichiometry and interaction of platelet receptors. The aims of this thesis are:

1. To isolate and purify GPVI and FcRγ into SMALPs, from a transfected HEK-293T cells, and characterise these GPVI/FcRγ SMALPs with biochemical and biophysical methods.

2. To isolate SMALPs from native human platelets, characterise these SMALPs to check their ability for preserving native membrane protein complexes, and utilise them for the investigation of platelet membrane protein interaction and stoichiometry.

CHAPTER 2

Materials and methods

Chapter 2 Materials and Methods

2.1 List of reagents

2.1.1 General reagents

Table 2.1 General reagents

Chemical name	Supplier
Acrylamide, 30%	Geneflow
AEBSF	ThermoFisher Scientific
Ampicillin	Sigma-Aldrich
Aprotinin	Sigma-Aldrich
Bovine serum albumin (BSA)	Sigma-Aldrich or Thermo Fisher Scientific
Brij97	Sigma-Aldrich
Coomassie blue R-250	ThermoFisher Scientific
CRP-XL	CambCol Laboratories
Dimethyl sulfoxide (DMSO)	ThermoFisher Scientific
Dipotassium phosphate (K_2HPO_4)	Sigma-Aldrich
Dithiothreitol (DTT)	Sigma-Aldrich
Ethylene glycol-bis(β-aminoethyl ether)-N,N,N′,N′-tetraacetic acid (EGTA)	Sigma-Aldrich
Ethylenediaminetetraacetic acid (EDTA)	Sigma-Aldrich
Glucose	Sigma-Aldrich
Glycerol	ThermoFisher Scientific
Glycine	ThermoFisher Scientific
Horm collagen	Nycomed
Imidazole	Sigma-Aldrich
Integrilin	Sigma-Aldrich
Ionomycin	Sigma-Aldrich
L-arginine	ThermoFisher Scientific
Leupeptin	Enzo Life Sciences AG

Luciferin	MP Biomedicals
Magnesium chloride ($MgCl_2$)	ThermoFisher Scientific
Monopotassium phosphate (KH_2PO_4)	ThermoFisher Scientific
Nonidet-40 (lgepal/NP-40)	ThermoFisher Scientific
Pepstatin	Sigma-Aldrich
Prostacyclin (PGI_2)	Cayman Chemical Company
Sodium azide	ThermoFisher Scientific
Sodium chloride (NaCl)	ThermoFisher Scientific
Sodium citrate	Sigma-Aldrich
Sodium dodecyl sulfate (SDS)	ThermoFisher Scientific
Sodium orthovanadate (Na_3VO_4)	Sigma-Aldrich
Streptavidin Protein, DyLight™ 800	ThermoFisher Scientific
Tetramethylethylenediamine (TEMED)	Sigma-Aldrich
Tris	ThermoFisher Scientific
TritonX-100	ThermoFisher Scientific and Sigma-Aldrich
Tween-20	ThermoFisher Scientific

2.1.2 Cell culture reagents

Table 2.2 Cell culture reagents

Reagent	**Source**
Dulbecco's Modified Eagle Medium (DMEM)	Sigma-Aldrich
Fetal bovine serum (FBS)	Gibco
L-Glutamine	Sigma-Aldrich
Opti-MEM serum-free media	Gibco
Penicillin/Streptomycin	Sigma-Aldrich
Phosphate Buffered Saline (PBS)	Sigma-Aldrich
Polyethylenimine (PEI)	Sigma-Aldrich
Roswell Park Memorial Institute medium (RPMI)	Sigma-Aldrich

Trypsin-EDTA solution	Sigma-Aldrich
β-mercaptoethanol (50 mM)	ThermoFisher Scientific

2.1.3 Antibodies

Table 2.3 Primary antibodies used in the thesis

Antigen	Antibody name	Supplier	Host species	Application
ADAM10	11G2	Abcam	Mouse	Immunoprecipitation Western blotting (0.5 ug/mL)
CD151	11B1	From Leonie Ashman lab, University of Adelaide, Australia (Fitter et al., 1995; Sincock et al., 1997)	Mouse	Western blotting
CD36	D8L9T	Cell Signalling Technology	Rabbit	Western blotting
CD9	C9-BB	Described previously (Berditchevski et al., 1996)	Mouse	Western blotting (1:20 from tissue culture supernatant)
CD9	1AA2	From Leonie Ashman lab, University of Adelaide, Australia (Sincock et al., 1997)	Mouse	Immunoprecipitation
CLEC-2	AYP2	From Steve Watson lab, University of Birmingham (Gitz et al., 2014; May et al., 2009)	Mouse	Western blotting
FcRγ	06-727	Sigma-Aldrich	Rabbit	Western blotting, 1:2000
FcRγ	9E1	Abcam	Rabbit	Western blotting, 1:1000

GPIbα	WM23	From Bernhard Nieswandt lab, University of Würzburg (Berndt et al., 1985)	Mouse	Western blotting (0.5 μg/mL)
GPVI	336E2	From Bernhard Nieswandt lab, University of Würzburg	Mouse	Immunoprecipitation Western blotting (0.5 μg/mL)
GPVI	338E5	From Bernhard Nieswandt lab, University of Würzburg	Mouse	Immunoprecipitation Western blotting (0.5 μg/mL)
GPVI	338E7	From Bernhard Nieswandt lab, University of Würzburg	Mouse	Immunoprecipitation Western blotting (0.5 μg/mL)
GPVI	11A7	From Elizabeth Gardiner lab, Australian National University (Al-Tamimi et al., 2009)	Mouse	Western blotting (0.5 μg/mL)
GPVI	313A10	From Bernhard Nieswandt lab, University of Würzburg	Mouse	Immunoprecipitation Western blotting (0.5 μg/mL)
GPVI	322D10	From Bernhard Nieswandt lab, University of Würzburg	Mouse	Immunoprecipitation Western blotting (0.5 μg/mL)
GPVI	336A9	From Bernhard Nieswandt lab, University of Würzburg	Mouse	Immunoprecipitation Western blotting (0.5 μg/mL)
GPVI	HY101	eBioscience	Mouse	Immunoprecipitation
GPVI	JAQ1	From Bernhard Nieswandt lab, University of Würzburg (Nieswandt et al., 2000)	Mouse	Immunoprecipitation Western blotting (0.5 ug/mL)
Integrin α6	4F10	Abcam	Mouse	Western blotting

Integrin αIIb	H-160	Santa Cruz	Rabbit	Western blotting (1:500)
Mouse IgG1	MOPC-21	Sigma-Aldrich	Mouse	Immunoprecipitation and flow cytometry
Mouse IgG1	P3.6.2.8.1 (Kappa Isotype)	ThermoFisher Scientific	Mouse	Immunoprecipitation
Pear-1	AF4527	R&D Systems	Goat	Western blotting
p-Tyr	4G10	Merck Millipore	Mouse	Western blotting (1:1000)
Tspan15	1C12	From Michael Tomlinson lab, University of Birmingham (Koo et al., 2020)	Mouse	Immunoprecipitation
Tspan15	4A4	From Michael Tomlinson lab, University of Birmingham (Koo et al., 2020)	Mouse	Immunoprecipitation
Tspan15	NBP1-92540	Novus Biologicals	Rabbit	Western blotting (1:500)
Tspan9		From Michael Tomlinson lab, University of Birmingham (Protty et al., 2009)	Rabbit	Western blotting (1:200)

Table 2.4 Secondary antibodies used in the thesis

Antibody name	**Catalogue no.**	**Supplier**	**Application and concentration**
Donkey anti-Goat IgG (H+L)	A15999	ThermoFisher Scientific	Western blotting (1: 10, 000)

Secondary Antibody, HRP			
Goat anti-Mouse IgG (H+L) Secondary Antibody, HRP	31430	ThermoFisher Scientific	Western blotting (1: 10, 000)
Goat anti-mouse IgG IRDye 680RD	925-68070	LI-COR Biosciences	Western blotting (1: 10, 000)
Goat anti-mouse IgG IRDye 800CW	925-32210	LI-COR Biosciences	Western blotting (1: 10, 000)
Goat anti-Rabbit IgG (H+L) Secondary Antibody, HRP	31460	ThermoFisher Scientific	Western blotting (1: 10, 000)
Goat anti-rabbit IgG IRDye 680RD	925-68071	LI-COR Biosciences	Western blotting (1: 10, 000)
Goat anti-rabbit IgG IRDye 800CW	925-32211	LI-COR Biosciences	Western blotting (1: 10, 000)
Sheep anti-mouse IgG FITC	F2883	Sigma-Aldrich	Flow cytometry (1: 100)

2.1.4 Primers used to generate GPVI isoform constructs

Table 2.5 Primers used to generate GPVI isoform constructs

Primers	**Recognition sequence**	**Sequences**
MT4150	GPVI, reverse (after 10x His tag and notI restriction site)	GATCAGCCTCGACTGTGCCT
MT5147	GPVI, forward (for pEF6/myc-His C)	CAAGCCTCAGACAGTGGTTC

MT5435	GPVI, forward (for pcDNA3)	TAGTAGGATCCACCATGTCTCCATCCCCGAC
MT5686	GPVI, reverse (with 10xHis tag)	TAGTAGGCGGCCGCTCAGTGGTGGTGATGATG GTGATGGTGGTGGTGTGAACATAACCCGCGGC TGTG
MT5695	GPVI cDNA piece after exon5, forward	CCCTGGAGCTTGTGGTCACAGAATTCTCAGAAG CCACCGC
MT5696	GPVI cDNA piece before exon5, reverse	GCGGTGGCTTCTGAGAATTCTGTGACCACAAGC TCCAGGG

2.1.5 Kits and ready-made materials

Table 2.6 Kits and ready-made materials used in the thesis

Ready-made materials	**Supplier**
10 x T4 DNA ligase buffer	New England Biolabs
10x cutsmart buffer	New England Biolabs
2x REDTaq® ReadyMix™ PCR Reaction Mix	Sigma-Aldrich
4–15% Mini-PROTEAN® TGX™ Precast Protein Gels, 12-well	Bio-Rad
4–20% Mini-PROTEAN® TGX™ Precast Protein Gels, 15-well	Bio-Rad
5x HF buffer	New England Biolabs
BamHI restriction enzyme	New England Biolabs
BlueEasy Pre-Stained Protein Ladder, (6.5 – 270kDa)	Geneflow
BlueSafe	Nzytech
BLUeye Pre-Stained Protein Ladder, 10-245 kDa	Geneflow
Collagen agarose	Sigma-Aldrich
cOmplete™, Mini Protease Inhibitor Cocktail	Sigma-Aldrich
E. coli DH5α competent cells	Merck

EZ-Link™ Sulfo-NHS-LC-Biotin	ThermoFisher Scientific
GeneJET Plasmid Miniprep Kit	ThermoFisher Scientific
GenElute™ HP Plasmid Midiprep Kit	Sigma-Aldrich
Immobilon®-FL PVDF membrane	Merck Millipore
Immobilon®-P PVDF membrane	Merck Millipore
NativeMark™ Unstained Protein Standard	ThermoFisher Scientific
NativePAGE™ Novex™3 to 12%, Bis-Tris, 1.0 mm, Mini Protein Gel, 10-well	ThermoFisher Scientific
NativePAGE™ Novex™4 to 16%, Bis-Tris, 1.0 mm, Mini Protein Gel, 15-well	ThermoFisher Scientific
NativePAGE™ Sample Buffer (4X)	ThermoFisher Scientific
NotI restriction enzyme	New England Biolabs
Novex™ WedgeWell™ 4 to 12%, Tris-Glycine, 1.0 mm, Mini Protein Gel, 10-well	ThermoFisher Scientific
Novex™ WedgeWell™ 4 to 12%, Tris-Glycine, 1.0 mm, Mini Protein Gel, 15-well	ThermoFisher Scientific
Novex™ WedgeWell™ 4 to 20%, Tris-Glycine, 1.0 mm, Mini Protein Gel, 10-well	ThermoFisher Scientific
NuPage MES running buffer	ThermoFisher Scientific
NuPage MOPC running buffer	ThermoFisher Scientific
NuPAGE Novex 4-12% Bis-Tris Protein Gels, 1.0 mm, 10 well	ThermoFisher Scientific
NuPAGE Novex 4-12% Bis-Tris Protein Gels, 1.0 mm, 15 well	ThermoFisher Scientific
NuPAGE Novex 4-12% Bis-Tris Protein Gels, 1.0mm, 12 well	ThermoFisher Scientific
NuPAGE Novex 4-12% Bis-Tris Protein Gels, 1.5 mm, 10 well	ThermoFisher Scientific
NuPAGE Novex 4-12% Bis-Tris Protein Gels, 1.5 mm, 15 well	ThermoFisher Scientific
NuPAGE™ LDS Sample Buffer (4X)	ThermoFisher Scientific
NuPAGE™ Sample Reducing Agent (10X)	ThermoFisher Scientific

PageRuler™ Prestained Protein Ladder, 10 to 180 kDa	ThermoFisher Scientific
Phusion polymerase	New England Biolabs
Pierce™ ECL Western blotting	ThermoFisher Scientific
Pierce™ Silver Stain Kit	ThermoFisher Scientific
Protease inhibitor cocktail	Sigma-Aldrich
Protein A/G PLUS-Agarose	Santa Cruz
Protein G-sepharose beads	Generon
ProteoSilver™ Plus Silver Stain Kit	Sigma-Aldrich
QIAquick Gel Extraction Kit	QIAGEN
QIAquick PCR purification kit	QIAGEN
Slide-A-Lyzer™ MINI Dialysis Devices, 3.5K MWCO	ThermoFisher Scientific
SMALP 30010P (new name SMALP 200)	Orbiscope B.V.
Super Ni-NTA Affinity resin	Generon
Super optimal broth with catabolite repression (S.O.C) medium	ThermoFisher Scientific
SYBR safe DNA gel stain	ThermoFisher Scientific
T4 DNA ligase	New England Biolab
Vivaspin 10 kDa MWCO spin concentrator	GE Healthcare

2.1.6 Buffer recipes

Table 2.7 Buffers used in the thesis and their recipes

Buffer	**Components**
1 M potassium phosphate buffer	0.9 M K_2HPO_4, 0.09 M KH_2PO_4, pH=7.8
1% Brij97 lysis buffer	1% Brij97, 10 mM Tris pH=7.5, 150 mM NaCl, 1 mM $CaCl_2$, 1 mM $MgCl_2$, 0.02% NaN_3
1% NP-40 lysis buffer	1% NP-40, 10 mM Tris, 150 mM NaCl, 1 mM EGTA, 1 mM EDTA, pH=7.5
1% Triton X-100 lysis buffer	1% Triton X-100, 10 mM Tris pH=7.5, 150 mM NaCl, 1 mM EDTA, 0.02% NaN_3

2 x non-reduced sample buffer	100 mM Tris pH=6.8, 4% (w/v) sodium dodecyl sulphate (SDS), 20% glycerol, 0.02% (w/v) Bromophenol blue
2 x Reduced sample buffer	100 mM Tris pH=6.8, 4% (w/v) sodium dodecyl sulphate (SDS), 20% glycerol, 5 % β-mercaptoethanol, 0.02% (w/v) Bromophenol blue
4 x SMA-PAGE sample buffer	20 mM Tris pH=8, 50% (v/v) glycerol, 0.08 mg/mL bromophenol blue
5 x non-reduced sample buffer	125 mM Tris pH=6.8, 10% (w/v) sodium dodecyl sulphate (SDS), 50% glycerol, 0.05% (w/v) Bromophenol blue
5 x Reduced sample buffer	125 mM Tris pH=6.8, 10% (w/v) sodium dodecyl sulphate (SDS), 50% glycerol, 4 % β-mercaptoethanol, 0.05% (w/v) Bromophenol blue
Acid/citrate/dextrose (ACD)	97 mM sodium citrate, 111 mM glucose and 71 mM citric acid
Coomassie blue staining solution	50% methanol, 10% acetic acid, 0.05% w/v Coomassie Blue R250
Coomassie destaining solution	30% methanol, 7% acetic acid
FACS buffer	0.2% BSA, 0.02% NaN_3 in PBS
FACS fix buffer	1 % formaldehyde, 2% FBS in PBS
Luciferase assay buffer	200 mM potassium phosphate buffer, 20 mM $MgCl_2$, 10 mM ATP
Luciferase harvest buffer	200 mM potassium phosphate buffer, 10% Triton X-100, 1 mM DTT
Luciferin solution	20 mM luciferin in dH_2O
Modified SMALP solution B	50 mM Tris, 150 mM NaCl, 10 % glycerol, where Tris is diluted 1:10 from 500 mM Tris solution (pH=8)
Modified Tyrode's buffer	134 mM NaCl, 0.34 mM Na_2HPO_4, 2.9 mM KCl, 12 mM $NaHCO_3$, 20 mM HEPES, 1 mM $MgCl_2$, pH=7.3
SDS-PAGE running buffer	25 mM Tris, 192 mM glycine, 0.1% SDS

SMALP solution A	50 mM Tris, 2 mM EDTA, 5 % glycerol, where Tris is diluted 1:10 from 500 mM Tris solution (pH=8)
SMALP solution B	50 mM Tris, 500 mM NaCl, 10 % glycerol, where Tris is diluted 1:10 from 500 mM Tris solution (pH=8)
SMA-PAGE running buffer	25 mM Tris, 192 mM glycine
TAE buffer	40 mM Tris, 20 mM glacial acetic acid, 1 mM EDTA
TBS	20 mM Tris, 137 mM NaCl, pH=7.6
TBST	20 mM Tris, 137 mM NaCl, 0.1% Tween-20, pH=7.6
TBST with high salt	20 mM Tris, 500 mM NaCl, 0.1% Tween-20, pH=7.6
Transfer buffer	25 mM Tris, 192 mM Glycine, 20 % methanol

2.1.7 Equipment

Table 2.8 Equipment used in the thesis

Equipment name	**Supplier**
Accuri C6 flow cytometer	BD Biosciences
ÄKTA pure	Cytiva
Avanti C6	Avanti Polar Lipids
Avestin EmulsiFlex-C3 High Pressure Homogenizer	Biopharma Group Limited
Beckman Optima XL-90 ultracentrifuge	Beckman Coulter
FACS Calibur flow cytometer	BD Biosciences
JA-25.50 fixed-angle rotor	Beckman Coulter
Mini-PROTEAN® Tetra Cell	Bio-Rad Laboratories
Odyssey infrared imaging system	LI-COR Biosciences
Superdex 200 increase 10/300 GL prepacked column	Cytiva
SW 60 Ti Swinging-Bucket Rotor	Beckman Coulter
Type 70 Ti Fixed-Angle Titanium Rotor	Beckman Coulter
Type 70.1 Ti Fixed-Angle Titanium Rotor	Beckman Coulter

XCell II™ Blot Module	ThermoFisher Scientific
XCell SureLock Mini-Cell Electrophoresis System	ThermoFisher Scientific

2.2 Molecular cloning

2.2.1 GPVIa-10xHis and GPVIb-10xHis constructs

Human GPVIa-10xHis and GPVIb-10xHis were generated by PCR from pcDNA3-human GPVIa-myc and GPVIb-myc vectors (Tomlinson Lab, unpublished) with primers MT5435 and MT5686 (Figure 3.1 and Table 2.7). Materials were mixed as indicated in Table 2.9 and the PCR reaction performed as indicated in Table 2.10.

Table 2.9 Components used to add 10xHis tags to GPVIa and GPVIb

Components	Amount (µL)
5x HF buffer	10
10 mM dNTPs	1
Forward primer—MT5435 (2 µM)	5
Reverse primer—MT5686 (2 µM)	5
pcDNA3-human GPVIa or GPVIb (5 ng/µL)	2
Phusion polymerase enzyme	0.5
dH_2O (to 50 µL)	27.5

Table 2.10 PCR reaction to add 10xHis tags to GPVIa and GPVIb

Steps	Temperature (°C)	Time (s)	Notes
Initial denaturation	98	30	
Denaturation	98	10	Cycle 30 times
Annealing	66	30	
Extension	72	20	
Final extension	72	300	
Cooling	4	∞	

After the PCR reaction, products were checked on TAE-agarose gels. A QIAquick PCR purification kit (QIAGEN) was used to purify and concentrate the PCR products according to the manufacturer's instructions.

Digestion was done by incubating DNA with restriction enzymes (NotI and BamHI) at 37 °C for 2 h, with the components indicated in Table 2.11.

Table 2.11 Components used to digest GPVIa-10xHis or GPVIb-10xHis

	GPVIa-10xHis or GPVIb-10xHis PCR products	**pEF6/myc-His C vector**
10x cutsmart buffer	2.5 μL	2 μL
NotI	1 μL	1 μL
BamHI	1 μL	1 μL
DNA	19 μL	2 μL (1 μg/μL)
dH_2O	1.5 μL	14 μL

The digestion products were gel purified in TAE-agarose gels; the bands of correct sizes were cut out and the DNA inside was purified using a QIAquick gel extraction kit (QIAGEN) according to the manufacturer's instructions.

Ligation was then done by incubating the mixture of digested genes and digested vector, at 16 °C overnight, with the components and their amounts indicated in Table 2.12. The ratio of the inserted gene and the vector was estimated to be 3:1 in molar terms.

Table 2.12 Components used for ligation of GPVIa-10xHis or GPVIb-10xHis with pEF6.C vector

	GPVIa-10xHis	**GPVIb-10xHis**	**Vector-only Control**
10 x T4 DNA ligase buffer	1 μL	1 μL	1 μL

Vector (50 ng)	0.53 μL	0.53 μL	0.53 μL
GPVI-10xHis (28 ng)	2.19 μL	1.16 μL	0 μL
T4 DNA ligase	1 μL	1 μL	1 μL
dH_2O	Up to 10 μL	Up to 10 μL	Up to 10 μL

The ligated products were transformed into *E. coli* DH5α competent cells. Briefly, 2 μL of ligation mix was added into 50 μL of competent cells, and the mixture was incubated on ice for 30 min. The mixture was then heat shocked at 42 °C for 45 s, and incubated back on ice for 2 min. After that, 500 μL of SOC medium was added to the mixture, and the culture was incubated in a shaking incubator at 37 °C for 1 h. Transformation was done by spreading the culture on LB-ampicillin plates, and incubating the plates at 37 °C overnight. The next day, single colonies were picked out, and inserts checked by PCR, with the materials and conditions detailed at Table 2.13 and Table 2.14, respectively.

Table 2.13 Components used for colony PCR

Components	**Amount (μL)**
2x REDTaq® ReadyMix™ PCR Reaction Mix	12.5
Forward primer (MT5147, 2 μM)	2.5
Reverse primer (MT4150, 2 μM)	2.5
Templates	5
dH_2O	2.5

Table 2.14 PCR reaction on colonies to check inserts in colonies

Steps	**Temperature (°C)**	**Time (s)**	**Notes**
Initial denaturation	95	300	
Denaturation	95	30	Cycle 35 times
Annealing	55	30	
Extension	72	30	

Final extension	72	300

The colony PCR products were then run on TAE-agarose gels to check for the band size of inserts. The colonies with the correct band sizes were cultured in 4 mL of LB buffer with ampicillin for ~8 h (day culture), then the culture amplified in 100 mL of LB buffer with 100 µg/mL ampicillin overnight. Both the day culture and the overnight culture were performed at 37 °C in a shaking incubator. The overnight culture was collected and subjected to a Miniprep kit (Thermo Fisher) or a Midiprep kit (QIAGEN) according to manufacturers' instructions. The products were sequenced by Source BioScience (Nottingham, UK), and the sequencing results were aligned to the required sequences using Clustal Omega (https://www.ebi.ac.uk/Tools/msa/clustalo/) with default settings.

2.2.2 GPVIa-Δexon5-10xHis and GPVIb-Δexon5-10xHis constructs

GPVIa-Δexon5-10xHis and GPVIb-Δexon5-10xHis were cloned from pEF6/myc-His C vector containing GPVIa-10xHis and GPVIb-10xHis, respectively, which were generated from section 2.2.1. The regions of cDNA before and after exon5 in each GPVI isoform were PCR-amplified from the His-tagged-GPVI-containing pEF6 vectors, with the sequences of the primers detailed in Table 2.5. These were designed with overlapping sequences to allow the resulting PCR productsto be joined together in a second PCR reaction. Materials and the reaction condition for the first PCR reactions are detailed in Table 2.15 and Table 2.16, respectively. Materials and the reaction condition for the PCR reaction to get the fractions after exon5 were detailed in Table 2.17 and Table 2.18, respectively. The products from these PCR reactions were confirmed to be of correct sizes by electrophoresis on TAE-agarose gel, and purified using QIAquick PCR purification kit (QIAGEN) following manufacturer's instructions.

Table 2.15 Components used to clone the piece of cDNA before exon5

Components	Amount (µL)
5xHF buffer	10
dNTPs (10 mM)	1
MT5147 (2 µM)	12.5
MT5696 (2 µM)	12.5
Starting Material (GPVI a/b –His, 5 ng/uL)	2
Phusion polymerase enzyme	0.5
dH_2O	11.5

Table 2.16 PCR reaction to clone the piece of cDNA before exon5

Steps	Temperature (°C)	Time (s)	Notes
Initial denaturation	98	30	
Denaturation	98	10	Cycle 30 times
Annealing	65.5	30	
Extension	72	20	
Final extension	72	300	
Cooling	4	∞	

Table 2.17 Components used to clone the piece of cDNA after exon5

Components	Amount (µL)
5xHF buffer	10
dNTPs (10 mM)	1
MT5695 (2 µM)	12.5
MT4150 (2 µM)	12.5
Starting Material (GPVI a/b -His, 5 ng/µL)	2
Phusion polymerase enzyme	0.5
dH_2O	11.5
Total	50

Table 2.18 PCR reaction to clone the piece of cDNA after exon5

Steps	Temperature (°C)	Time (s)	Notes
Initial denaturation	98	30	
Denaturation	98	10	Cycle 30 times
Annealing	69	30	
Extension	72	20	
Final extension	72	300	
Cooling	4	∞	

The purified products were then mixed and subjected to the second round of PCR reaction, for them to be joined together, with the materials and PCR reaction condition detailed in Table 2.19 and Table 2.20, respectively. The correct band size was confirmed by running the product on a TAE-agarose gel, and the product was purified using QIAquick PCR purification kit (QIAGEN) following the manufacturer's instructions.

Table 2.19 Components used to join the pieces of cDNA before and after exon5 together

Components	Amount
5xHF buffer	10 μL
dNTPs (10 mM)	1 μL
MT5147 (2 μM)	12.5 μL
MT4150 (2 μM)	12.5 μL
Starting Material 1 (GPVIa or GPVIb fraction before exon5)	50 ng
Starting Material 2 (GPVIa or GPVIb fraction after exon5)	50 ng
Phusion polymerase enzyme	0.5 μL
dH_2O	Up to 50 μL

Table 2.20 PCR reaction to join the pieces of cDNA before and after exon5 together

Steps	Temperature (°C)	Time (s)	Notes
Initial denaturation	98	30	
Denaturation	98	10	Cycle 30 times
Annealing	63.6	30	
Extension	72	20	
Final extension	72	300	
Cooling	4	∞	

The products were then digested at 37 °C for 2 h with the materials detailed in Table 2.21.

Table 2.21 Components used to digest GPVIa-Δexon5-10xHis or GPVIb-Δexon5-10xHis

	GPVIa-Δexon5-10xHis	GPVIb-Δexon5-10xHis
10x cutsmart buffer	2.5 μL	2.5 μL
NotI	1 μL	1 μL
BamHI	1 μL	1 μL
DNA	24 μL	24 μL
dH_2O	Up to 30 μL	Up to 30 μL

The digestion products were gel purified in TAE-agarose gels; the bands of correct sizes were cut out and the DNA inside was purified using a QIAquick gel extraction kit (QIAGEN) according to the manufacturer's instructions.

Ligation was then done by incubating the mixture of digested genes and digested vector (generated in section 2.2.1), at 16 °C overnight, with the components and their amounts indicated in Table 2.22. The ratio of the inserted gene and the vector was estimated to be 3:1 in molar terms.

Table 2.22 Components used for ligation of GPVIa-Δexon5-10xHis or GPVIb-Δexon5-10xHis with pEF6.C vector

	GPVIa-Δexon5-10xHis	GPVIb-Δexon5-10xHis	Vector-only Control
10 x T4 DNA ligase buffer	1 µL	1 µL	1 µL
Vector (50 ng)	0.53 µL	0.53 µL	0.53 µL
GPVI- Δexon5-10xHis (28 ng)	2 µL	3.6 µL	0 µL
T4 DNA ligase	1 µL	1 µL	1 µL
dH_2O	Up to 10 µL	Up to 10 µL	Up to 10 µL

Transformation, colony PCR to check for successful ligation, and the subsequent miniprep or midiprep were performed as described in section 2.2.1. The products were sequenced by Source BioScience (Nottingham, UK), and the sequencing results were aligned to the required sequences using Clustal Omega (https://www.ebi.ac.uk/Tools/msa/clustalo/) with default settings.

2.3 Cell culture and cell-based assays

2.3.1 HEK-293T cell line

2.3.1.1 Cell culture

Human embryonic kidney (HEK)-293T cells with ADAM10 knocked out (Koo et al., 2020) were cultured in Dulbecco's Modified Eagle Medium (DMEM) supplemented with 10% fetal bovine serum (FBS), 4 mM L-glutamine, 100 U/ml penicillin and 100 µg/mL streptomycin. Cells were grown in plates and incubated in a humidified incubator at 37 °C with 5% CO_2.

Cell passage was done at least once a week when the cells reached confluency, by gently removing the medium without disrupting the cell layer, briefly washing the cells with PBS, then detaching the adherent cell layer with a 2-min trypsin incubation at 37 °C with 5% CO_2,

followed by adding in fresh DMEM with supplements (4:1 v/v ratio to trypsin), then diluting to fresh DMEM with supplements in a fresh plate.

2.3.1.2 Transient transfection with PEI

HEK-293T cells were seeded to fresh plates with certain amounts (Table 2.23) on the day before transfection. On the day of transfection, DNA was added to Optimem serum-free medium, followed by PEI, with the indicated amounts (Table 2.23). The mixture was gently vortexed and left for 10 minutes at room temperature to allow DNA/PEI complexes to form. The DNA/PEI was then gently added to the cells and mixed well in the plate.

Table 2.23 Materials used for PEI-transfection of HEK-293T cells in different sizes of culturing plates

Plate size	Cells plated	Media volume	Opti-mem	DNA	PEI
6-well	3×10^5	2 mL	100 µL	1 µg	4 µL
6 cm	1×10^6	3 mL	300 µL	3 µg	12 µL
10 cm	3×10^6	10 mL	1 mL	9 µg	36 µL
15 cm	6×10^6	20 mL	2 mL	18 µg	72 µL

2.3.1.3 Cell harvesting and lysis

Cell collection was done on the second day post transfection. The medium was aspirated and cells scraped into PBS. The collected cells were spun down at 3,000 xg for 5 min in a bench-top centrifuge, and lysed for 30 min on ice in lysis buffer with protease inhibitors. The debris was removed from cell lysate by centrifuging at 21,000 xg for 10 min at 4 °C. The supernatant was collected.

2.3.2 DT40 cell line

2.3.2.1 Cell culture

The DT40 chicken B cell line was cultured in Roswell Park Memorial Institute Medium (RPMI) supplemented with 10% fetal bovine serum (FBS), 4 mM L-glutamine, 100 U/ml penicillin, 100 μg/mL streptomycin and 50 μM β2-mercaptoethanol. Cells were grown in flasks and incubated in a humidified incubator at 37 °C with 5% CO_2. Cell density was maintained under 1 x 10^6 /mL.

2.3.2.2 Transient transfection via electroporation for NFAT-luciferase assay

Approximately 24 hours before transfection, cells were counted and adjusted to 2 x 10^5 /mL. On the day of transfection, cells were at a density of 5 x 10^5 /mL – 10 x 10^5 /mL, and were washed in RPMI (without supplements) and resuspended in RPMI to 3.75 x 10^7 /mL. For each transfection, 1.5 x 10^7 cells, 20 μg NFAT-luciferase reporter (Tomlinson et al., 2007), and equal amounts of GPVI and FcRγ constructs (0.25 μg for each unless otherwise stated; constructs were from Tomlinson lab collection (Tomlinson et al., 2007) or generated from section 2.2) was used. Cells and DNA were mixed well in a 0.4 cm cuvette, left for 10 minutes, electroporated at 350V and 500 μF, and left for a further 5-10 minutes. The transfected cells were then removed from cuvettes and incubated for 24 h in 8 mL medium in 6-well plates.

2.3.2.3 NFAT-luciferase assay

NFAT-luciferase assay was performed as previously described (Tomlinson et al., 2007; Tomlinson et al., 2004). Briefly, transfected cells were cultured at 37 °C for 16 h, then centrifuged down and resuspended in supplemented RPMI medium to 2 x 10^6 /mL. Cells were stimulated with 5 μg/mL Horm collagen (unless a different concentration was stated), for 6 h at 37 °C and with 5% CO_2. The negative controls used an equal volume of medium without collagen. Positive controls were stimulated with PMA (50 ng/ml) and ionomycin (1 μM). The

cells were then lysed in 1% TritonX-100 lysis buffer and mixed with luciferase assay buffer. Luciferin was injected into the samples at a final concentration of 4 mM, and the luciferase activity was measured by the intensity of emitted light via a luminometer.

2.4 Human platelet preparation and platelet-based assays

2.4.1 Platelet preparation

Human platelets were prepared from freshly drawn blood by the Watson protocol as previously described (Asazuma et al., 2000; Pallini et al., 2021). Blood was drawn into 10% (v/v) sodium citrate as anticoagulant, and 10% of ACD (warmed to 37°C) was added in. Platelet rich plasma (PRP) was obtained by centrifuging at 200 xg, room temperature, for 20 min. The supernatant was collected, and platelets were separated from platelet poor plasma (PPP) by centrifuging at 1,000 xg, room temperature, for 10 min, in the presence of 0.1 μg/mL prostacyclin (PGI_2) added to inhibit platelet activation. The platelet pellet was resuspended in 1 mL of modified Tyrode's buffer (pH=7.3) with 0.9 g/L glucose and containing 150 μL of ACD, and diluted to a final volume of 28 mL by adding approximately 24 mL of modified Tyrode's buffer containing 3 mL ACD. Platelets were counted using a Coulter Counter, and centrifuged again at 1,000 xg, room temperature, for 10 min, in the presence of 0.1 μg/mL PGI_2. The washed platelets were then resuspended in modified Tyrode's buffer to the desired platelet concentration, and rested for 30 min at room temperature before downstream assays.

2.4.2 Platelet activation

Platelets were resuspended in modified Tyrode's buffer to a concentration of 8 x 10^8 /mL. Integrilin was added to this platelet resuspension to a final concentration of 9 μM, gently mixed and incubated with platelets for 10 min at room temperature, to inhibit αIIbβ3-mediated platelet aggregation. After that, platelets were warmed in a 37 °C water bath for 4 min, and the agonist was added as indicated in Table 2.24. During agonist incubation, the tubes containing platelets

were inverted every 30 s to ensure mixing. The activated platelets were then lysed directly in 2x lysis buffer, or centrifuged down at room temperature (10,000 xg for 1 min, or 1,000 xg for 5 min, as indicated) and resuspended in another buffer, depending on the downstream assays.

Table 2.24 Agonists used for platelet activation

Agonist name	Target	Concentration	Incubation time	Incubation temperature	Platelet concentration during activation
CRP-XL	GPVI	3 μg/mL	90 s	37 °C	8×10^8 /mL
Rhodocytin	CLEC-2	200 nM	5 min	37 °C	8×10^8 /mL

2.4.3 Platelet lysis

Platelet lysis was done by adding 2x lysis buffer into platelet resuspension or by adding 1x lysis buffer onto platelet pellets, as indicated. Lysis buffer was supplemented with protease inhibitors and phosphatase inhibitor, or with the protease inhibitor cocktail. Platelets were mixed thoroughly in lysis buffer by vortexing, and lysis was done by incubation on ice for 30 min. The debris was removed from cell lysates by centrifuging at 21,000 xg for 10 min at 4 °C. The supernatant was collected.

2.5 Platelet surface protein biotinylation assay

Platelets prepared as stated in section 2.4.1 were resuspended at 5×10^8 /mL in modified Tyrode's buffer, with 1 mg/mL EZ-Link® Sulfo-NHS-LC-Biotin (ThermoFisher Scientific). This Sulfo-NHS-LC-Biotin reacts with primary amine groups, thus labelling lysine residues and primary amines at the N-terminus of proteins. This is achieved by the crosslinking of NHS ester with primary amines, forming a stable conjugate via amide bond. Sulfo-NHS-LC-Biotin is membrane impermeable, thus labelling only cell surface proteins on their extracellular side. Biotinylation of membrane proteins was done by incubation at room temperature with agitation

for 30 min, and was quenched by addition of 100 mM glycine. Biotinylated platelets were spun down in the presence of 0.1 μg/mL PGI_2 at 1,000 xg for 6 min at room temperature, and resuspended into the desired buffer for SMALP generation.

2.6 Flow cytometry

Approximately 5 x 10^5 cells were used per measurement. Cells were pelleted for 5 min at 270 xg and the supernatant was aspirated. 50 μL of primary antibody, in a concentration of 10 μg/mL in FACS buffer, was added onto the cells, mixed gently, and incubated with the cells for 20-30 min on ice. The primary antibody was then washed off by adding 1 mL FACS buffer, gently mixing, and centrifugation for 5 mins at 270 xg. The supernatant was aspirated. 50 μL FITC-conjugated anti-mouse antibody, diluted in FACS buffer, was added onto and incubated with the cells for 20-30 min on ice in dark. Finally, 500 μL FACS buffer was added, and cells directly subjected to FACS analysis or fixed in FACS fix buffer prior to FACS analysis. Data was collected by a FACS Calibur flow cytometer and analysed with CellQuest Pro (section 3.2), or collected by an Accuri C6 flow cytometer and analysed with BD Accuri C6 Software (section 3.3). Cells were gated by size and granularity, and 2,500-10,000 gated events were collected per sample.

2.7 SMALP generation

2.7.1 SMALP preparation from human platelets

Platelets were resuspended to 4 x 10^8 /mL or 5 x 10^8 /mL in modified SMALP solution B (50 mM Tris diluted 1:10 from pH=8, 150 mM NaCl, 10% glycerol v/v), or the original SMALP solution B with 500 mM NaCl if indicated. cOmplete ™ Mini Protease Inhibitor Cocktail was added to the SMALP solution prior to platelet resuspension. The resuspension was homogenised with a dounce homogeniser, then the homogenised sample was incubated with 2.5% (wt/vol) of SMALP 30010P (1 g/mL) for at least 2 h at room temperature for membrane

proteins to be solubilised into SMALPs. The un-SMALPed material was removed by ultracentrifugation at 100,000 xg at 4 °C for 1 h. The supernatant containing SMALPs was used directly for experiments or preserved at -20 °C until usage. Where indicated, NaCl was supplemented to 500 mM in the final solution containing SMALPs, to minimise the potential SMALP aggregation in low salt concentration.

2.7.2 SMALP preparation and purification from HEK-293T cells

100 15-cm plates of adherent HEK-293T cells (ADAM10 knock-out) (Koo et al., 2020) were transfected with equal amounts of pEF6-GPVIa-10xHis (generated in section 2.2.1) and pEF6-FcRγ (Tomlinson et al., 2007), harvested and preserved at -80 °C until use. Approximately 8 mL of cells were collected. On the day of SMALP generation, cells were defrosted on ice, resuspended in 50 mL SMALP solution A with one tablet of cOmplete ™ Mini Protease Inhibitor Cocktail, and homogenised with a dounce homogeniser. The homogenised cells were passed through a C3 machine for four rounds, with air supply being around 40 psi, and the actual pressure on cells being 10-15,000 psi for the cells to be burst and further homogenised. Membrane was separated from cell debris by centrifuging at 8,200 xg in a Beckman JA-25.50 fixed-angle rotor for 30 min at 4 °C. The supernatant was collected and membrane pelleted from it by ultracentrifugation at 100,000 xg for 1 h at 4 °C. The pelleted membrane was resuspended in SMALP solution B to 40 mg/mL and homogenised with dounce homogeniser. SMALP 30010P (Orbiscope) was added to the membrane resuspension to a 2.5% (wt (g)/vol (mL)), and incubated at room temperature for 2 h. Un-SMALPed material was removed by ultracentrifugation at 100,000 xg for 1 h at 4 °C, and SMALPs in solution were incubated with 5 mL of Ni-NTA beads (50% slurry) at room temperature for 48 h to maximise binding. As the un-SMALPed pellet still looked oily, potentially due to insufficient SMA solubilisation, it was collected and re-SMALPed by resuspending to 40 mg/mL in SMALP solution B with 2.5%

SMALP 30010P in the same manner as described. This 2nd round of SMALPs were incubated with 3 mL of Ni-NTA beads (50% slurry) at room temperature for 24 h.

His-tag purification was done in a gravity column. Briefly, the Ni-bead-SMALP mixture from the two rounds of SMALPs were combined into one column, resulting in 8 mL of 50%-slurry beads (4 mL of dried beads). Beads were washed in one column volume (CV) of SMALP solution B twice, in one CV of SMALP solution B with 10 mM imidazole once, in one CV of SMALP solution B with 20 mM imidazole once, followed by four times of 1.5 mL elution with 500 mM imidazole in SMALP solution B. Samples in each step were collected and loaded on SDS-PAGE. The eluates were then combined (4 mL in total), dialysed in 3.5 kDa MWCO mini dialysis devices (ThermoFisher Scientific), concentrated by a Vivaspin 5000MWCO concentrator at 3,000 xg, 4 °C to 500 µL, and subjected to gel filtration (section 2.10).

2.8 Immunoprecipitation (IP)

750 µL-1.3 mL of whole-cell lysate or whole-cell SMALPs in solution was used per IP. 0.8 x 10^8-5 x 10^8 platelets were used per IP, depending on the platelet count of each donor. The samples were pre-cleared by incubating with 20 µL of Protein A/G PLUS-Agarose (50 % slurry) beads at 4 ºC for 60-90 min with rotation. The mixture was then spun down at 21,000 xg and the supernatant was collected. 1-5 µg of antibody was added to the pre-cleared samples, as indicated in each individual experiment, and the mixture was incubated overnight with rotation at 4 ºC. On the next day, a new 20 µL of Protein A/G PLUS-Agarose beads was briefly washed in corresponding buffer, the washed beads were added to the antibody/lysate or antibody/SMALP mixture, and the whole mixture was incubated with rotation at 4 ºC for 1 h. The beads were spun down at 2,500-3,000 xg and washed four times. Each wash was done by resuspending the beads in 1 mL of ice-cold buffer, vortexing for 10 s, spinning down and aspirating the supernatant. The supernatant was preserved if indicated. Each spin in the washes

was done on a bench-top centrifuge at 2,500-3,000 xg for 30 s at 4 ºC. In the final wash, ~50 µL of supernatant was reserved, the beads were briefly re-centrifuged in the same manner, and the supernatant was aspirated to get rid of as much liquid as possible. In SMALP solution with 150 mM NaCl, the NaCl concentration was supplemented to 500 mM if indicated, to minimise the potential SMALP aggregation. Where indicated, the beads were added into lysates or SMALPs at the same time with the antibody, and the mixture was rotated at 4 ºC overnight before subjected to the aforementioned washing steps.

Alternatively, the antibody was firstly incubated with 20 µL of protein G-sepharose beads (50 % slurry) overnight at 4 °C with rotation, in corresponding buffer (lysis buffer or SMALPs in solution). The next day, the antibody-bound G-sepharose beads were washed twice, added to whole-cell lysate or whole-cell SMALP solution, and the mixture incubated for 90 min at 4 °C with rotation. The G-sepharose beads were then washed four times in the same manner as stated above.

2.9 Electrophoresis, gel staining and Western blotting

2.9.1 SDS-PAGE

Cell lysates in detergent buffer or SMALPs in solution were mixed with 2x, 4x or 5x homemade Laemmli sample buffer or NuPAGE™ LDS sample buffer, in either non-reduced or reduced conditions, as indicated in each experiment. For IPs, 50 µL of 2x sample buffer was applied per 10 µL of washed beads (“dry beads”). Samples in Laemmli sample buffer were boiled at 95.2 °C for 5 min for the proteins to be denatured and coated with SDS, while samples in NuPAGE™ LDS sample buffer were boiled at 70 °C for 10 min. The boiled samples were loaded into polyacrylamide gels. The handmade gels have fixed percentages of polyacrylamide (6% to 15%) in the resolving part, and 4% or 5% of polyacrylamide in the stacking part; for

precast gels, NuPAGE™ 4 -12% gels were used. Electrophoresis was done in the XCell SureLock™ Mini-Cell system.

2.9.2 SMA-PAGE

SMALPs in solution were mixed with 4x Native sample buffer (Thermo Fisher) and loaded onto native gels without being boiled. For handmade native gels, no SDS was added into the gel or the running buffer. No stacking gel was used, i.e. the comb was directly inserted into the resolving gel, as the slight acidic pH in stacking gel may render SMA insoluble in aqueous solution and thus destroy the disc structure of SMALPs. Electrophoresis was done in the XCell SureLock™ Mini-Cell system.

2.9.3 Western blotting

The gel was removed from the cassette after electrophoresis. For SDS-PAGE, the gel was briefly soaked in transfer buffer before transferring. Transferring was done in an XCell II™ Blot Module, onto Immobilon®-FL PVDF membrane (for fluorescence-conjugated antibodies) or Immobilon®-P PVDF membrane (for HRP-conjugated antibodies), at 4 °C, 200 mA for 2 h, or 4 °C, 35 V for 1 h. Alternatively, transferring was done in the same module at room temperature, 30 V for 90 min. Blocking was done in either 5% milk powder in TBS, or 3% BSA in TBST, for 1 h at room temperature, or overnight at 4 °C; for streptavidin blotting and phosphotyrosine blotting, blocking was always done in 3% BSA in TBST, as the milk contains phosphoproteins and biotin. The membrane was briefly washed twice in TBST if blocked with milk. Primary antibody probing was done in 3% BSA in TBST (with 0.1% NaN_3) with desired antibody concentration, typically overnight at 4 °C, or with desired duration and temperature of the antibody. Primary antibody was washed off three times in TBST, 10 min each wash, at room temperature. Secondary antibody probing was done in 3% BSA in TBST (with 0.1% NaN_3) with desired antibody concentration, for 2 h at room temperature. If using TBST for

secondary antibody probing, the incubation was done for 1 h at room temperature. Streptavidin probing was done in 3% BSA in TBST for 1 h at room temperature. Secondary antibody was washed off three times in TBST, 10 min each wash, at room temperature. Alternatively, membrane washes after antibody incubation were done in TBST with high salt to remove unspecific background. For SMA-PAGE, the gel was soaked in SDS-PAGE running buffer for 10 min at room temperature with agitation, for the protein surfaces to be coated with SDS to facilitate transferring, then briefly soaked in transfer buffer before transferring to PVDF membrane. Blocking was done in 5% BSA in TBST (with 0.1% NaN_3) with 25 mM L-arginine to remove unspecific binding. The rest of the protocol was the same as that for Western blotting of SDS-PAGE.

For membrane imaging, if using IRDye-conjugated antibody or IRDye-conjugated streptavidin, the membrane was dried with filter paper and scanned on the LI-COR Odyssey Infrared Imaging System; if using HRP-conjugated antibody, the membrane was incubated with Pierce™ ECL Western blotting substrate following the manufacturer's instructions and imaged on films, and the films were then developed and fixed.

2.9.4 Gel staining

Gels were removed from the cassette after electrophoresis. For Coomassie staining, the gel was briefly washed in H_2O, stained in homemade Coomassie blue R-250 staining solution prewarmed at 40 °C, for a few hours until the whole gel was stained blue, and destained in destaining solution. Alternatively, the gel was incubated in BlueSafe protein stain (Nzytech) at room temperature until the desired band intensity was achieved. Silver stain was performed with Pierce™ Silver Stain Kit following the manufacturer's instructions.

2.10 Gel filtration

Eluted SMALPs from HEK-293T cells were combined, dialysed, and concentrated to approximately 500 µL, as described in section 2.7.2. Gel filtration was done on ÄKTA pure with S200 increase 10/300 column (Cytiva). The column was washed with dH_2O and equilibrated in SMALP solution B overnight. SMALP solution B was loaded during gel filtration, and 500 µL fractions were collected.

2.11 Collagen agarose binding assay

Collagen agarose (Sigma-Aldrich) was washed in SMALP solution B, and resuspended to a 50% slurry. 20 µL of slurry was added to 1 mL of SMALPs in solution. Incubation was done at room temperature with rotation for 90 min. After that, the supernatant was preserved, and beads washed three times. Each wash was done by adding in 1 mL of SMALP solution B, vortexing for 10 s and spinning down at 2,655 xg for 20 s. In the final wash, ~50 µL of supernatant was reserved, the beads were briefly re-centrifuged and the supernatant was aspirated to remove as much supernatant as possible. 50 µL of 2x Laemmli sample buffer was applied per 10 µL of washed beads. Samples in Laemmli sample buffer were boiled at 95.2 °C for 5 min, and subjected to SDS-PAGE.

2.12 Negative stain electron microscopy

Negative stain electron microscopy (EM) was kindly performed by Dr. Saskia Bakker from Advanced Bioimaging, University of Warwick. Briefly, GPVI SMALP samples were applied to a glow-discharged, carbon/formvar coated grid (EM Resolutions) and stained with 2% uranyl acetate for 1 minute. Grids were imaged using the JEOL 2100Plus (JEOL, Japan) with Gatan OneView camera (Gatan/Ametek, USA) at 40,000 magnification. Averages were produced using Relion (Zivanov et al., 2018).

2.13 In-gel protein identification via mass spectrometry

2.13.1 Sample preparation for mass spectrometry

Mass spectrometry sample preparation was kindly performed by Dr. Norman Day from the Advanced Mass Spectrometry Facility, University of Birmingham. The samples were destained and digested by the Robo3000 system. Briefly, silver-stained gel was washed in ultrapure dH_2O, and the bands were excised. Gel pieces was destained with acetonitrile followed by 100 mM ammonium bicarbonate with repetition. Destained gel pieces were dried and rehydrated in 100 mM ammonium bicarbonate. Reduction was done by incubation with 10 mM DTT at 60 °C for 15 min. Alkylation was done by incubation with 50 mM iodoacetamide and 100 mM ammonium bicarbonate at room temperature for 45 min in the dark. The gel pieces were washed and dried again. Trypsin digestion was performed at room temperature for 20 min with agitation, then diluted with 100 mM ammonium bicarbonate for neutralisation and incubated overnight at 37 °C. For peptide extraction, the gel pieces were firstly extracted by 2% acetonitrile with 0.1% formic acid, for 30 min at room temperature with agitation, then subjected to the 2nd round of extraction by 40% acetonitrile with 0.1% formic acid, for 30 min at room temperature with agitation. The supernatant from the two rounds of extraction was pooled, dried, and re-suspended in 2% acetonitrile with 0.1% formic acid for subsequent LC-MS/MS analysis.

2.13.2 Liquid chromatography followed by tandem mass spectrometry (LC-MS/MS)

Liquid chromatography and tandem mass spectrometry (LC-MS/MS) were kindly performed by Dr. Jinglei Yu from the Advanced Mass Spectrometry Facility, University of Birmingham. The UltiMate® 3000 HPLC series (Dionex, Sunnyvale, CA USA) was used for peptide concentration and separation. Samples were trapped on uPrecolumn Cartridge, Acclaim PepMap 100 C18, 5 µm, 100 A 300 µm i.d. x 5 mm (Dionex, Sunnyvale, CA USA) and separated in Nano Series™ Standard Columns 75 µm i.d. x 15 cm, packed with C18

PepMap100, 3 µm, 100 Å (Dionex, Sunnyvale, CA USA). The gradient used was from 3.2% to 44% solvent B (0.1% formic acid in acetonitrile) for 30 min. Peptides were eluted directly (~ 350 nL min^{-1}) via a Triversa Nanomate nanospray source (Advion Biosciences, NY) into a QExactive HF (QEHF) mass spectrometer (Thermo Fisher Scientific). The data-dependent scanning acquisition was controlled by Xcalibur 4.0 software. The mass spectrometer alternated between a full FT-MS scan (m/z 360 – 1600) and subsequent high energy collision dissociation MS/MS scans of the 20 most abundant ions. Survey scans were acquired in the QEHF with a resolution of 120,000 at m/z 200 and automatic gain control 3 x 10^6. Precursor ions were fragmented in high energy collision dissociation MS/MS with resolution set up at 15,000 and a normalized collision energy of 28. Automatic gain control target for high energy collision dissociation MS/MS was 1 x 10^5. The width of the precursor isolation window was 1.2 m/z and only multiply-charged precursor ions were selected for MS/MS. Spectra were acquired for 56 min with dynamic exclusion time of 20 s.

The MS and MS/MS scans were searched against the Uniprot database using Proteome Discoverer 2.2 (ThermoFisher Scientific). Variable modifications were deamidation (N and Q), oxidation (M) and phosphorylation (S, T and Y). The precursor mass tolerance was 10 ppm and the MS/MS mass tolerance was 0.02 Da. Two missed cleavages were allowed and were accepted as a real hit proteins with at least two high confidence peptides.

CHAPTER 3

Characterisation of GPVI-related constructs and GPVI antibodies

Chapter 3 Characterisation of GPVI-related constructs and GPVI antibodies

3.1 Introduction

Before generating and characterising SMALPs from different sources of cells, one must have a good understanding of the reagents used. For the transfection system, where recombinant GPVI and its associated protein, FcRγ, need to be over-expressed in the first place, it is important to decide which isoform of protein to transfect, and to examine whether there are any functionally significant mutants which could be interesting to compare. Meanwhile, for the biochemical assays that are to be performed in this thesis, antibodies are a useful tool and play essential roles in, for example, isolating, purifying and identifying the proteins of interest. Due to the relatively low abundance of commercial monoclonal antibodies against GPVI, and the fact that our collaborator Professor Bernhard Nieswandt in the University of Wurzburg, Germany, has recently generated several human GPVI monoclonal antibodies which have yet to be fully characterised, an aim of this chapter was to characterise these GPVI antibodies for their performance in Western blotting.

In human GPVI, polymorphic variants in nine amino acids have been identified so far, with different frequencies among populations (Perrella et al., 2021; Watkins et al., 2006). Among them, there are two major allelic isoforms, namely GPVIa and GPVIb, different from each other in 5 amino acids (Figure 3.1), with GPVIa counting for 85% and GPVIb 13% of haplotypes (Nurden, 2019). Controversial results regarding the expression levels and function of these two allelic isoforms have been shown by different groups. For example, the bb genotype was initially reported to be correlated with significantly lower surface and whole cell GPVI expression level, less platelet activation and aggregation, and lower tyrosine phosphorylation in response to CRP-XL, thus the bb population may be more prone to bleeding

(Joutsi-Korhonen et al., 2003). However, the effect on surface expression that the b haplotype has was later calculated to account for only 15.5% of the variation of GPVI surface expression, reported by the same group (Jones et al., 2007). In addition, Trifiro et al. showed no difference in ligand binding capacity between GPVIa and GPVIb, but the two haplotypes differed in their ability to bind calmodulin and Src family kinases in their intracellular region. The L317 in GPVIb had increased binding to calmodulin compared to Q317 in GPVIa, and N322 in GPVIb accounted for a decreased binding to Fyn and Lyn compared to H322 in GPVIa (Trifiro et al., 2009). GPVI polymorphisms have also been reported to have clinical significance, with GPVIb linked to severe bleeding in patients with type I von Willebrand disease (VWD) (Kunicki et al., 2004). In the early GPVI cloning studies (Clemetson et al., 1999; Ezumi et al., 2000; Jandrot-Perrus et al., 2000), three isoforms of GPVI were cloned, which included the canonical sequence of GPVI, an exon5 deleted variant (Δexon5) and a longer variant of 620 amino acids which lacks the transmembrane region. The expression and functional aspects of the latter two isoforms remain poorly investigated.

FcRγ has a cysteine residue (C44) at the junction of the transmembrane and cytoplasmic region, which can potentially be palmitoylated. Palmitoylation is a lipid modification that is important for the localisation and function of certain other proteins (Schlesinger et al., 1980; Smotrys & Linder, 2004), but this has not been investigated for FcRγ. Therefore, a final aim of this chapter was to characterise GPVI/FcRγ expression and signalling in a C44S mutant of FcRγ.

The aims of this chapter are:

1. To generate and characterise various GPVI and FcRγ expression constructs, to select the best candidates for the transfection work in the next chapters.

2. To characterise GPVI monoclonal antibodies on their performance in Western blotting, select those with the best performance and utilise them for biochemistry studies in the later chapters.

3.2 Results

3.2.1 Generation of four GPVI-10x His expression constructs and demonstration of similar surface and whole-cell expression levels in transfected HEK-293T cells

Expression constructs for GPVIa and GPVIb, wild-type or Δexon5, were generated using PCR strategies (Figures 3.2 and 3.3). To characterise their expression, the four GPVI constructs were transiently transfected into the HEK-293T cell line, which does not express endogenous GPVI. Flow cytometry with a GPVI mAb showed that all four GPVI constructs had comparable surface expression levels, as judged by relative geometric mean fluorescence intensity (gMFI) of transfected cells and percentage of cells transfected (Figure 3.4A). Western blotting showed that all four GPVI constructs had comparable whole-cell expression levels (Figure 3.4B).

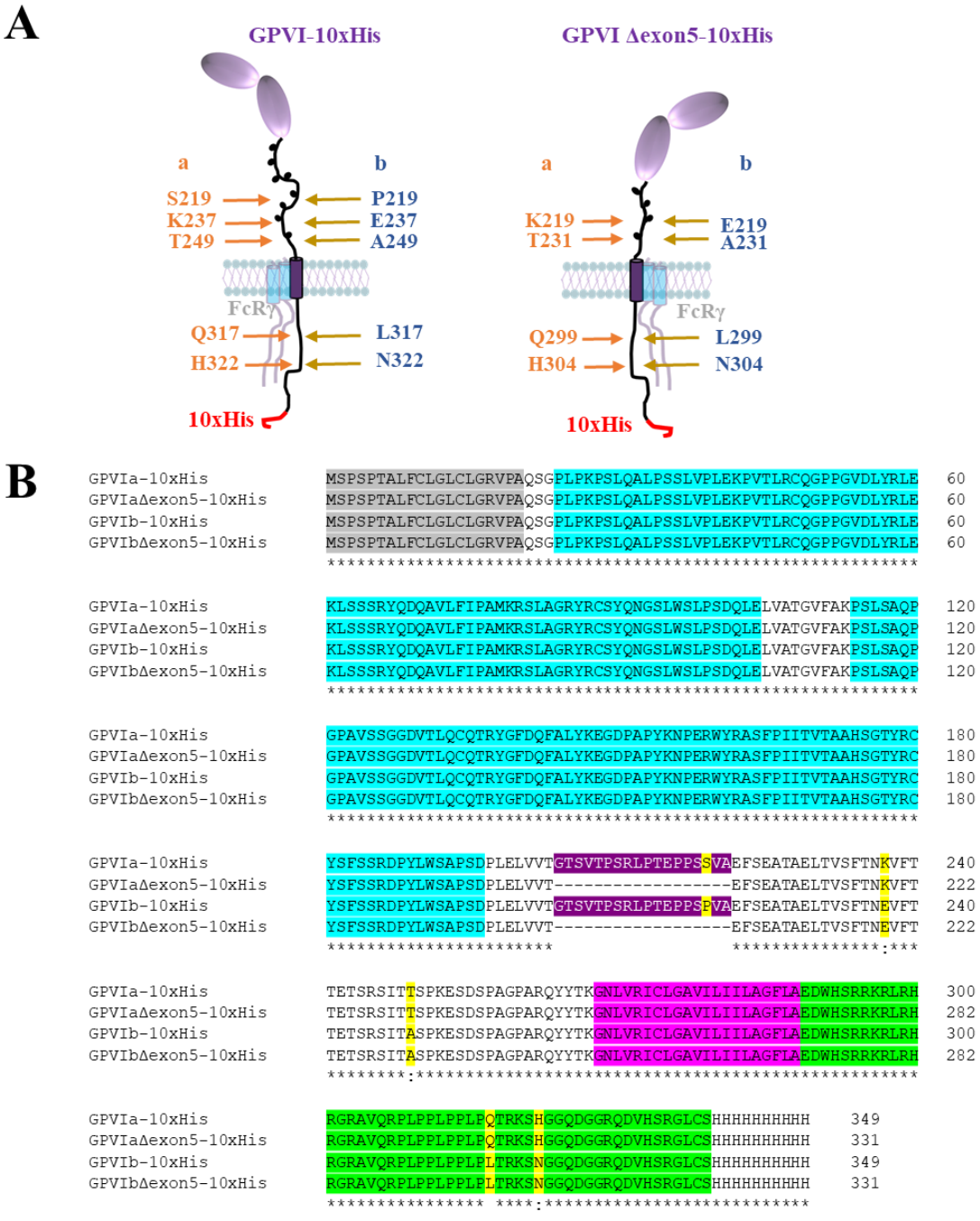


Figure 3.1 Schematic representation and sequence alignment of the four GPVI isoforms with 10x His tags.

(A) The cartoon illustration of GPVI structures, with the different amino acids in allelic isoforms a and b labelled. (B) Sequence alignment of the four constructs of GPVI. The signal sequences are highlighted in grey, two IgSF domains in the extracellular region are highlighted in light blue, exon5 is highlighted in dark purple, the transmembrane region is highlighted in light purple, the intracellular region highlighted in light green, and the different amino acids between allelic isoforms are highlighted in yellow.

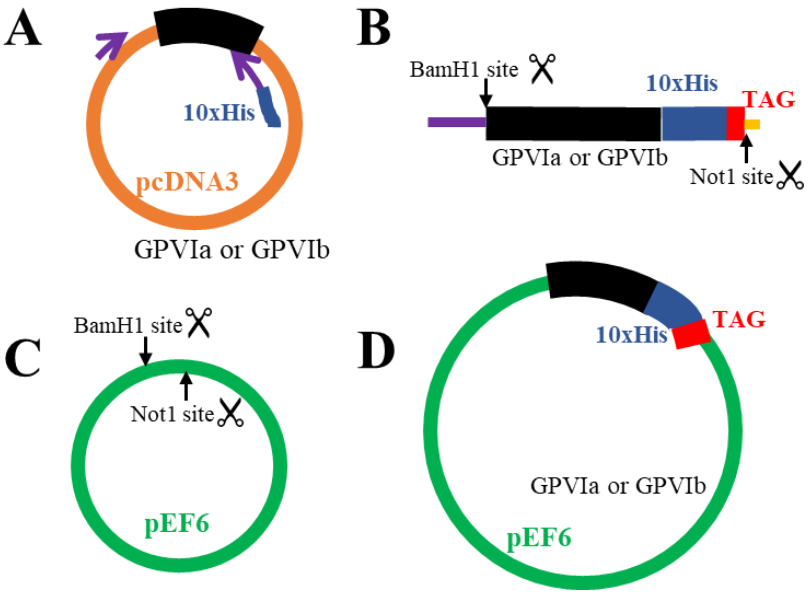


Figure 3.2 Generation of GPVIa-10xHis and GPVIb-10xHis constructs.

GPVI was PCR-amplified from pcDNA3-GPVI vectors and 10xHis-tag added via primers (A), digested by two restriction enzymes to generate sticky ends (B), ligated into pEF6 vector (C) which was digested by the same two restriction enzymes (D).

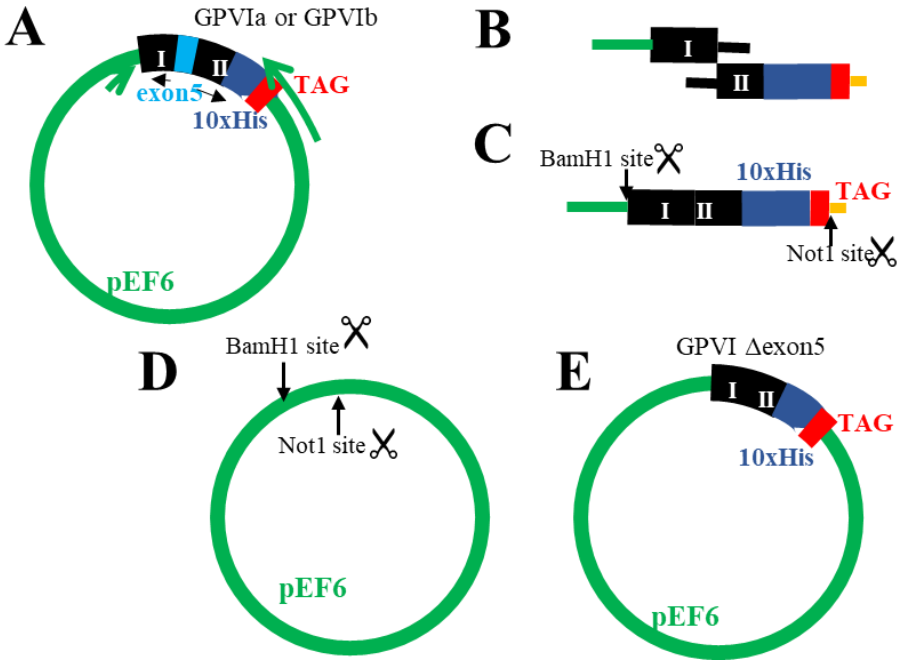


Figure 3.3 Generation of GPVIa-Δexon5-10xHis and GPVIb-Δexon5-10xHis constructs.

The fractions before and after exon5 in each GPVI isoform were PCR-amplified from the His-tagged-GPVI-containing pEF6 vectors (A) generated in Figure 3.1, with the primers designed to create overlapping ends. This allowed them to be joined together in a second PCR reaction (B). The resulting PCR product (GPVI-Δexon5) and empty pEF6 were digested with the same two restriction enzymes (C and D), and GPVI-Δexon5 ligated into pEF6 (E).

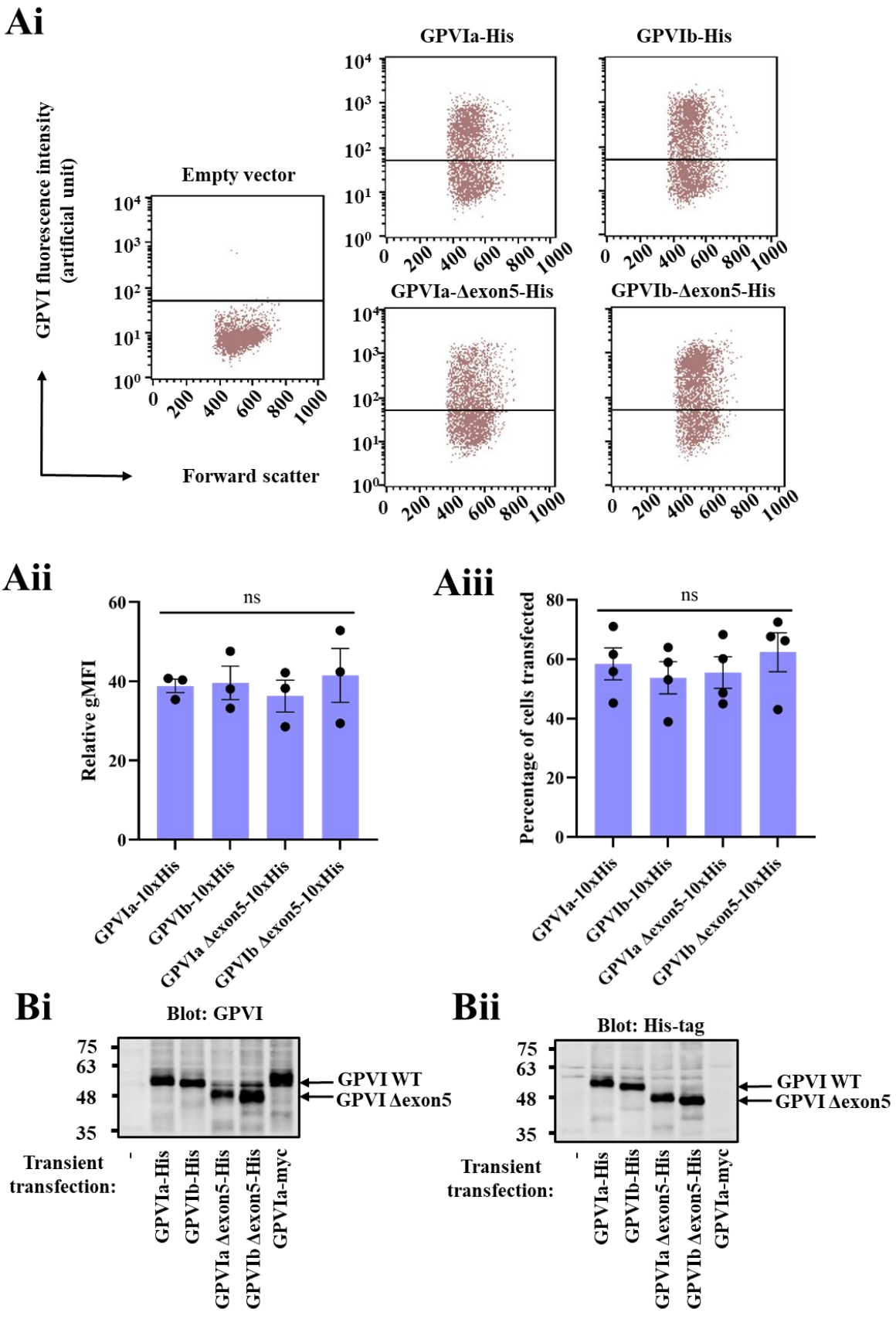

Ai
GPVIa-His
GPVIb-His
Empty vector
GPVIa-Δexon5-His
GPVIb-Δexon5-His
GPVI fluorescence intensity (artificial unit)
Forward scatter
Aii
Relative gMFI
ns
GPVIa-10xHis
GPVIb-10xHis
GPVIa Δexon5-10xHis
GPVIb Δexon5-10xHis
Aiii
Percentage of cells transfected
ns
GPVIa-10xHis
GPVIb-10xHis
GPVIa Δexon5-10xHis
GPVIb Δexon5-10xHis
Bi
Blot: GPVI
GPVI WT
GPVI Δexon5
Transient transfection:
-
GPVIa-His
GPVIb-His
GPVIa Δexon5-His
GPVIb Δexon5-His
GPVIa-myc
Bii
Blot: His-tag
GPVI WT
GPVI Δexon5
Transient transfection:
-
GPVIa-His
GPVIb-His
GPVIa Δexon5-His
GPVIb Δexon5-His
GPVIa-myc

Figure 3.4 The four GPVI-10xHis constructs have comparable surface and whole cell expression levels when transiently transfected into HEK-293T cells.

(Ai) HEK-293T cells were transiently transfected with empty vector control or the indicated His-tagged GPVI and FcRγ expression constructs, and cell surface GPVI was detected by flow cytometry with GPVI monoclonal antibody HY101 followed by FITC-conjugated anti-mouse secondary antibody. The plots shown are representative of four independent experiments. (Aii) Relative GPVI expression was quantified by dividing the geometric mean of fluorescence intensity (gMFI) of the GPVI-transfected by the gMFI of the empty vector negative control. (Aiii) The percentage of transfected cells was quantified. Error bars represent the standard error of the mean. (B) Transfected cells from panel A were lysed in 1% Triton X-100 lysis buffer and lysates subjected to Western blotting with (Bi) anti-GPVI antibody 11A7 and (Bii) anti-His antibody. The blots shown are representative of two independent experiments.

3.2.2 GPVI isoforms do not show signalling differences in response to collagen

To evaluate the four GPVI constructs for their ability to initiate downstream signalling in response to collagen, an NFAT-luciferase transcriptional reporter assay was applied, which has previously been used to measure GPVI signalling (Tomlinson et al., 2007). DT40, a chicken B-cell cell line, was transfected with 0.25 μg of the expression constructs of interest (one of the four GPVI-10x His constructs, myc-tagged GPVIa or GPVIb as positive control, or a mixture of two His-tagged GPVI constructs), 0.25 μg of FcRγ, and 20 μg of an NFAT-luciferase reporter construct per 1.5 x 10^7 cells. The negative control cells were transfected with empty vector and NFAT-luciferase reporter construct. Collagen-induced NFAT activation was similar for all four isoforms of 10xHis-tagged GPVI (Figure 3.5A), and they expressed at similar levels on the cell surface (Figure 3.5B). These data suggest no major signalling differences between GPVIa, GPVIb and Δexon5 variants, and this is the first such characterisation of the latter. However, a caveat is the cell line system used, and experiments in platelets would be needed to confirm this finding in future.

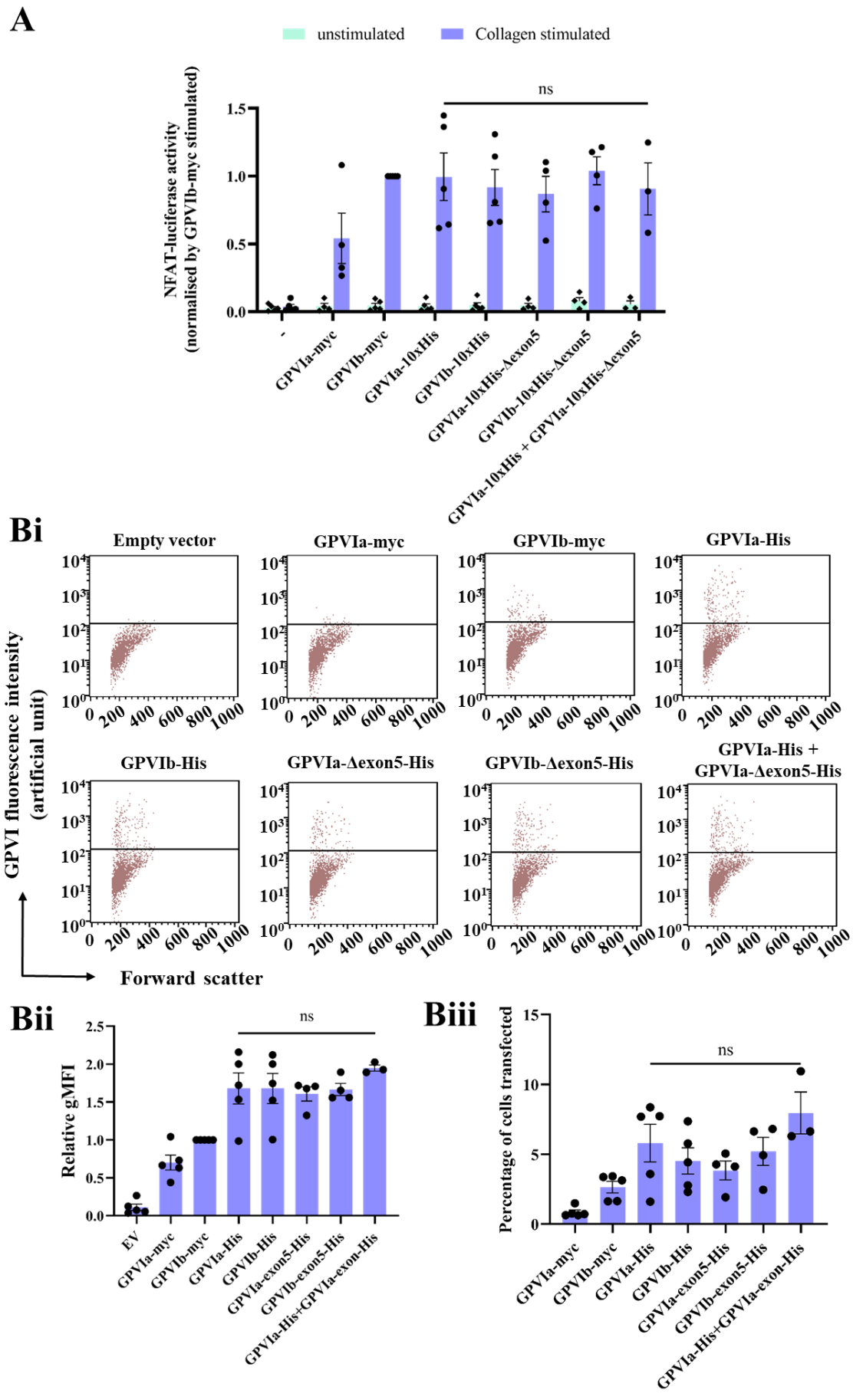

A
unstimulated
Collagen stimulated
NFAT-luciferase activity
(normalised by GPVIb-myc stimulated)
ns
1.5
1.0
0.5
0.0
-
GPVIa-myc
GPVIb-myc
GPVIa-10xHis
GPVIb-10xHis
GPVIa-10xHis-Δexon5
GPVIb-10xHis-Δexon5
GPVIa-10xHis + GPVIa-10xHis-Δexon5
Bi
Empty vector
GPVIa-myc
GPVIb-myc
GPVIa-His
GPVIb-His
GPVIa-Δexon5-His
GPVIb-Δexon5-His
GPVIa-His +
GPVIa-Δexon5-His
GPVI fluorescence intensity
(artificial unit)
Forward scatter
Bii
Relative gMFI
ns
2.5
2.0
1.5
1.0
0.5
0.0
EV
GPVIa-myc
GPVIb-myc
GPVIa-His
GPVIb-His
GPVIa-exon5-His
GPVIb-exon5-His
GPVIa-His+GPVIa-exon-His
Biii
Percentage of cells transfected
ns
15
10
5
0
GPVIa-myc
GPVIb-myc
GPVIa-His
GPVIb-His
GPVIa-exon5-His
GPVIb-exon5-His
GPVIa-His+GPVIa-exon-His

Figure 3.5 The four GPVI-10xHis constructs have similar downstream signalling shown by an NFAT-luciferase reporter assay in DT40 B cells.

(A) DT40 cells were transfected with NFAT-luciferase reporter, the indicated GPVI isoform and FcRγ, stimulated with 5 ug/mL of Horm collagen, then subjected to luciferase reporter assay. The luminometer readout of unstimulated or collagen-stimulated was presented after being normalised by the readout of collagen-stimulated, GPVIb-myc transfected cells. Error bars represent the standard error of the mean from five independent experiments. (Bi) GPVI surface expression was measured by flow cytometry, with GPVI monoclonal antibody HY101 followed by FITC-conjugated anti-mouse antibody. The plots shown are representative from six independent experiments. (Bii) Relative GPVI expression was quantified by dividing the geometric mean of fluorescence intensity (gMFI) of the GPVI-transfected cells by the gMFI of the empty vector negative control. Error bars represent the standard error of the mean from four independent experiments. (Biii) The transfection rate was quantified. Error bars represent the standard error of the mean from five independent experiments. EV, empty vector. WT, wild type.

3.2.3 FcRγ mutant C44S signals normally

After the comparison of GPVI-His constructs, two different FcRγ constructs were also evaluated. In wild type FcRγ, a cysteine residue (C44) at the transmembrane/cytoplasmic interface is conserved in many species (Figure 3.6). We hypothesise that this conserved site on FcRγ is involved in palmitoylation, which is potentially important for the expression and localisation of GPVI/FcRγ complex. An FcRγ C44S mutant has been generated previously in the Tomlinson lab, where serine replaced cysteine at position 44 and therefore it cannot be palmitoylated. The functional impact of FcRγ C44S mutant was tested by the NFAT-luciferase assay. WT or C44S FcRγ, together with an equal amount of GPVIa-myc, and NFAT-luciferase reporter, were transiently transfected into DT40 cells. NFAT activation induced by two different collagen concentrations, and using three different quantities of transfected GPVI/FcRγ, was not affected by C44S FcRγ mutation (Figure 3.7A), and GPVI cell surface expression was similarly unaffected by C44S FcRγ mutation (Figure 3.7B). However, it cannot be ruled out that this cysteine may be involved in GPVI/FcRγ in a platelet, given that the assay involved a non-platelet model cell line. Taken together with the earlier GPVI comparative data, it was decided to proceed with FcRγ WT and GPVIa-10x His for the cell transfection work in Chapter 4, to generate GPVI/FcRγ SMALPs from transfected HEK-293T cells.

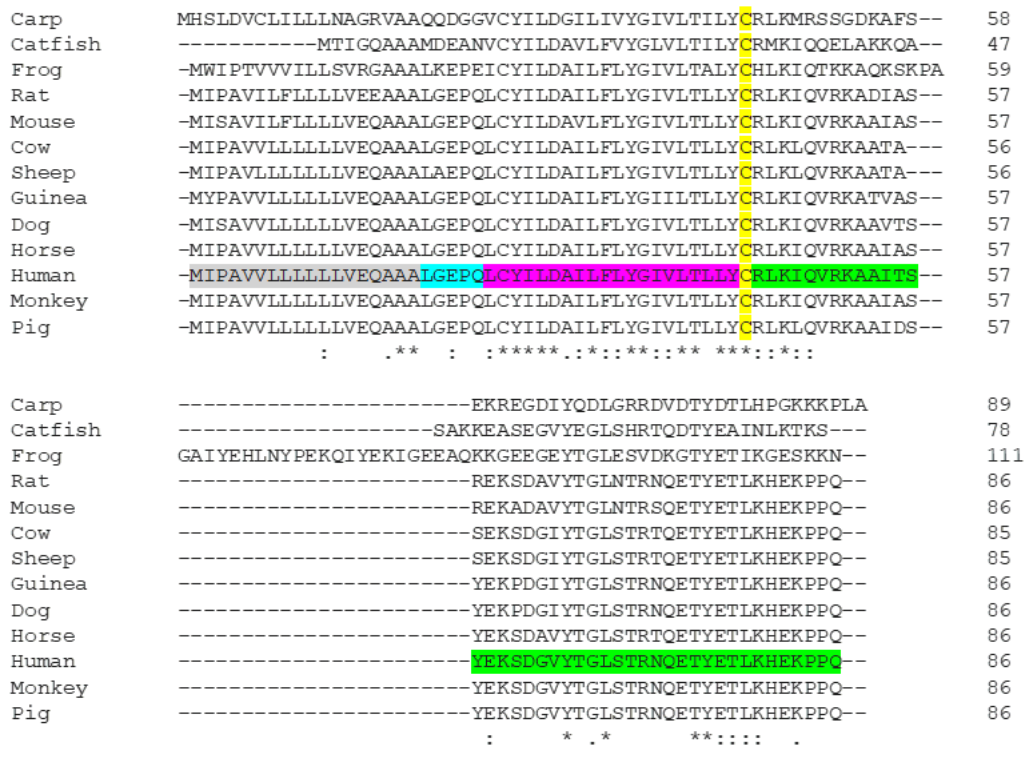


Figure 3.6 Sequence alignment of FcRγ in different species.

In the human sequence, the signal sequence is highlighted in grey, the extracellular region is highlighted in light blue, transmembrane region is highlighted in light purple and intracellular region highlighted in light green. The conserved cysteine 44 across species is highlighted in light yellow.

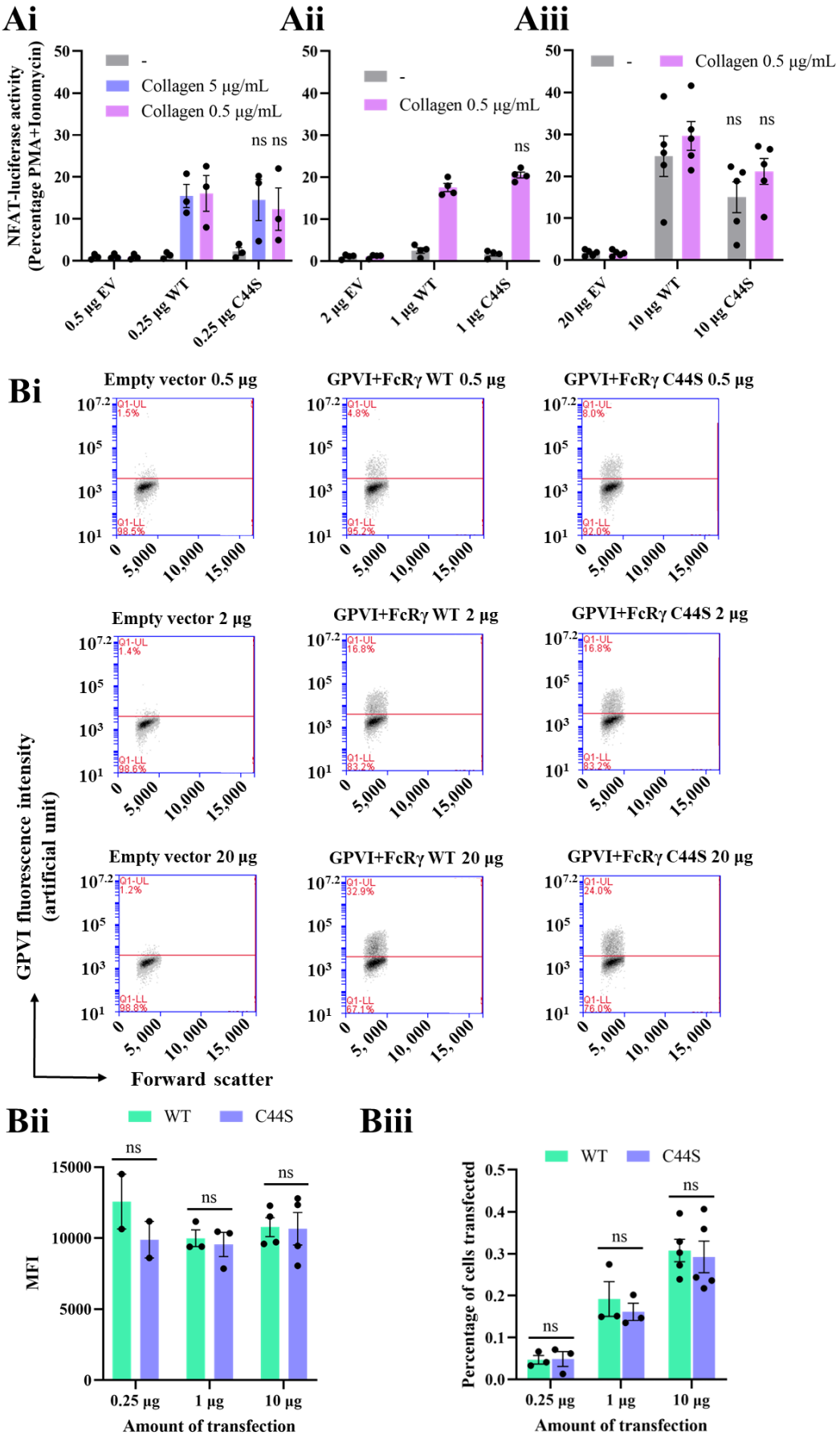

Ai
Aii
Aiii
NFAT-luciferase activity (Percentage PMA+Ionomycin)
-
Collagen 5 μg/mL
Collagen 0.5 μg/mL
ns ns
0.5 μg EV
0.25 μg WT
0.25 μg C44S
2 μg EV
1 μg WT
1 μg C44S
ns
20 μg EV
10 μg WT
10 μg C44S
Bi
Empty vector 0.5 μg
GPVI+FcRγ WT 0.5 μg
GPVI+FcRγ C44S 0.5 μg
Empty vector 2 μg
GPVI+FcRγ WT 2 μg
GPVI+FcRγ C44S 2 μg
Empty vector 20 μg
GPVI+FcRγ WT 20 μg
GPVI+FcRγ C44S 20 μg
GPVI fluorescence intensity (artificial unit)
Forward scatter
Bii
WT
C44S
MFI
0.25 μg
1 μg
10 μg
Amount of transfection
Biii
Percentage of cells transfected
Amount of transfection

Figure 3.7 Wild-type and FcRγ C44S mutant have similar GPVI signalling and surface expression levels in DT40 B cells.

(A) DT40 cells were transfected with NFAT-luciferase reporter, GPVI and FcRγ (WT or C44S) with the indicated amounts, then stimulated with the indicated concentrations of Horm collagen and subjected to NFAT-luciferase reporter assay. The luciferase activity readout of unstimulated or collagen-stimulated was presented as the percentage of that of cells stimulated with PMA and ionomycin (positive controls). Error bars represent the standard error of the mean from three to five independent experiments. (Bi) GPVI surface expression levels were measured by flow cytometry with GPVI monoclonal antibody HY101 followed by FITC-conjugated anti-mouse antibody. Representative plots from three (for 0.25 μg of transfection), four (for 1 μg of transfection), or five (for 10 μg of transfection) independent experiments were shown. The percentages indicated by the red numbers represent the percentage of GPVI/FcRγ-transfected cells (Q1-UL) or the percentage of untransfected cells (Q1-LL). (Bii) Relative GPVI expression were quantified by the median fluorescence intensity (MFI). Error bars represent the standard error of the mean from two to four independent experiments. (Biii) The transfection efficiencies were quantified. Error bars represent the standard error of the mean from three or five independent experiments. EV, empty vector. WT, wild type.

3.2.4 Characterisation of GPVI monoclonal antibodies' performance in Western blotting

To isolate GPVI from human platelets or transfected cell lines, as will be done in the next two chapters, it is important to identify useful GPVI antibodies. Apart from the commercially available mouse anti-human GPVI mAb HY101, which can be applied in immunoprecipitation (IP), and mouse anti-human GPVI mAb 11A7, which was provided by Elizabeth Gardiner (Canberra) and can be used in Western blotting, six new mouse anti-human mAbs to GPVI were received from Bernhard Nieswandt (Wurzburg), namely 313A10, 322D10, 336A9, 336E2, 338E5 and 338E7, plus JAQ1 that is commercially available. Importantly, 338E5 was shown not to be specific to GPVI, because it stained GPVI-knockout humen erythroleukaemia cells (Koo and Tomlinson, unpublished, data not shown), thus it was not examined further in this thesis. The performance of these antibodies in IP and co-IP will be further demonstrated in Chapter 5.

In Western blotting of whole cell lysates from human platelet or GPVI/FcRγ-transfected HEK-293T cells, 338E7 detected GPVI to the best extent under both reduced and non-reduced conditions (Figure 3.8). 336E2 also detected GPVI under both non-reduced and reduced conditions, but more weakly than 338E7, while 336A9 detected GPVI to a similar extent as 336E2, but only in non-reduced samples. 313A10 and 322D10 Western blotted GPVI relatively weakly and only under non-reduced conditions, whereas 338E5 and JAQ1 were not effective Western blotting antibodies. Importantly, the detected bands were specific to GPVI expression, as no bands were detected in empty vector transfected HEK-293T cells (Figure 3.8).

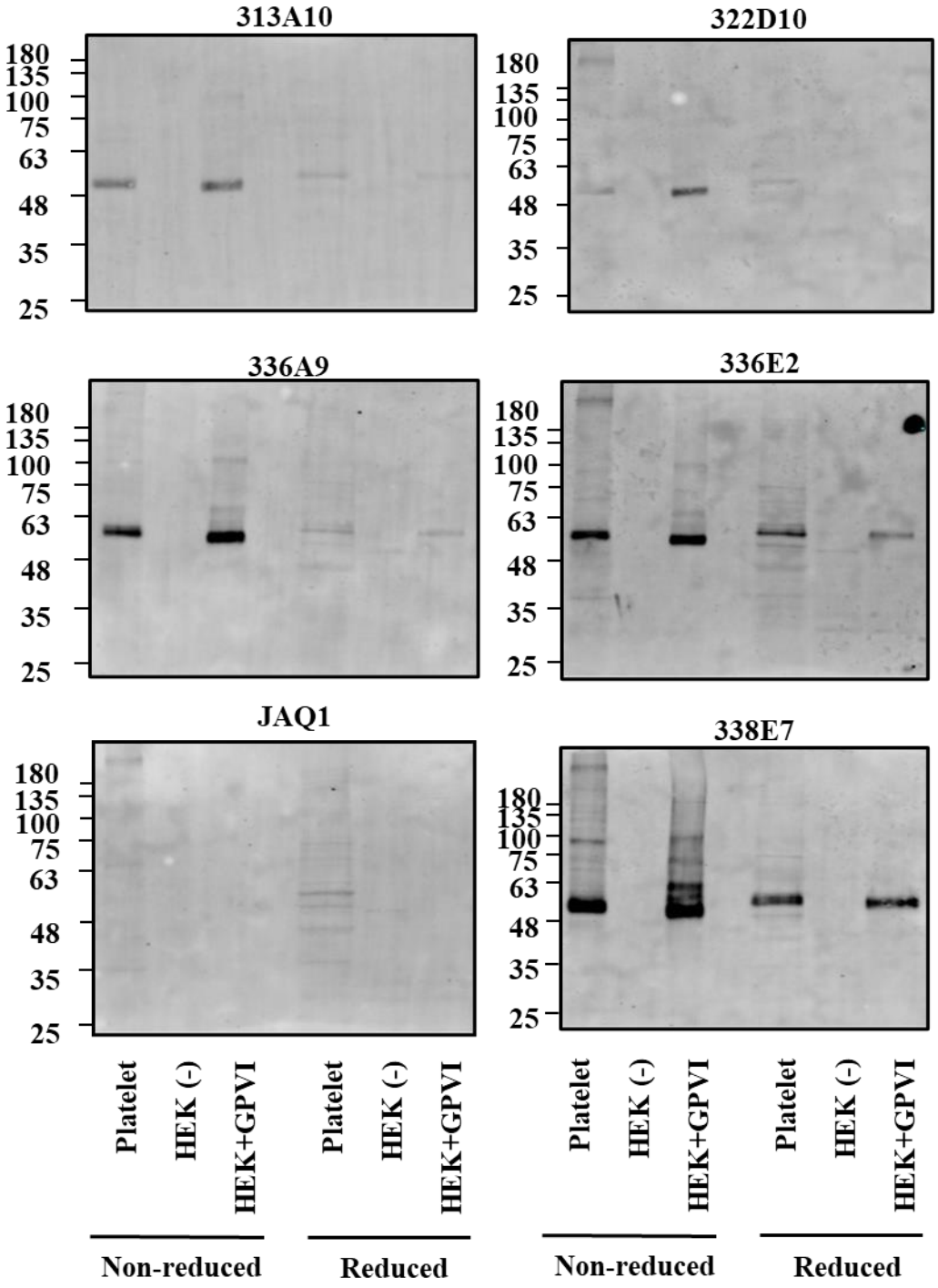


Figure 3.8 Characterisation of anti-GPVI monoclonal antibodies for Western blotting.

Human platelets, mock-transfected and GPVI/FcRγ-transfected HEK-293T cells were lysed in 1% Triton X-100 lysis buffer and Western blotting done with the indicated GPVI antibodies (0.5 µg/ml) under non-reducing and reducing conditions. Images are representative of four (non-reducing samples) or two (reduced samples) independent experiments.

3.3 Discussion

In this chapter, expression constructs for four isoforms of GPVI with a 10x His tag have been generated, including two allelic isoforms, GPVIa and GPVIb, and the alternatively spliced forms, GPVIa-Δexon5 and GPVIb-Δexon5. Their expression has been confirmed in transiently transfected HEK-293T cells, on both surface level (via flow cytometry) and whole-cell level (via western blotting on whole cell lysates). The surface and whole-cell expression levels of the four GPVI isoforms were comparable. The functionality of the four GPVI isoforms was investigated using an NFAT-luciferase assay which has been shown to efficiently detect the weak but sustained signalling events following GPVI activation by collagen in the DT40 cell line (Tomlinson et al., 2007). The four GPVI isoforms all induced signals downstream of Horm collagen binding, and no significant functional differences were detected. Using the same NFAT-luciferase assay, signalling by FcRγ WT and C44S was also investigated, with no significant GPVI signalling difference in response to Horm collagen observed. The performance of six new monoclonal antibodies to GPVI in Western blotting was also tested, with the best performing one, 338E7, identified.

The two most common GPVI haplotypes were firstly reported in 2001, when Croft et al. reported five amino acid substitutions and showed that one of them, S219P, is associated with increased risk of myocardial infarction (Croft et al., 2001). Since then, there have been a few studies in platelets revealing the phenotypic difference between donors with these two haplotypes, which were later referred to as GPVIa and GPVIb (Joutsi-Korhonen et al., 2003). The results in this chapter represent the first direct comparison of GPVIa and GPVIb in cell line model systems, and found no significant difference in surface and whole-cell expression levels, which is consistent with the findings of Trifiro et al. that GPVIa and GPVIb do not have a statistically significant difference on the expression levels in human platelets (Trifiro et al., 2009). However, our results from NFAT-luciferase assay failed to detect significant signalling

difference downstream of GPVIa and GPVIb, in response to collagen stimulation. This contradicts the downstream tyrosine phosphorylation difference between the two isoforms that Trifiro et al. reported (Trifiro et al., 2009). This may be due to the fact that the NFAT-luciferase assay is very sensitive in detecting weak but sustained Ca^{2+} concentration elevation induced by collagen stimulation in cell lines (Tomlinson et al., 2007). Furthermore, the NFAT assay measures transcriptional responses over six hours, rather than the rapid GPVI/FcRγ-proximal signalling events measured by Trifiro et al (Trifiro et al., 2009). It would have been useful to investigate GPVI-induced tyrosine phosphorylation in the DT40 model system, but this was previously shown to be relatively weak (Tomlinson et al., 2007) and so not ideal for a comparison of GPVIa and GPVIb. Ultimately, it would be interesting to compare GPVIa and GPVIb in a human GPVI knock-in mouse model system, as has already been done for GPVIa (Mangin et al., 2012; Navarro et al., 2022), but the lack of any differences detected in ths chapter would not justify such a major experiment.

GPVI-Δexon5 is a short form of GPVI, lacking part of the O-glycosylated stalk region, which can be found in sequence databases but has not previously been studied. Alternative splicing is a common and essential procedure to increase the diversity of the proteome. For example, the Ca^{2+} sensor stromal interaction molecule 2 (STIM2), which is localised to the endoplasmic reticulum and regulates store-operated Ca^{2+} entry (SOCE) downstream of GPVI/FcRγ activation, has two alternatively spliced forms, STIM2.1 and STIM2.2. These differently regulate SOCE through their interactions with the Orai1 SOCE channel and calmodulin: STIM2.1 is an inhibitor of SOCE whereas STIM2.2 is an activator (Miederer et al., 2015). GPVI has 8 exons, where exons 1-7 encode the extracellular region and exon 8 encodes the transmembrane and intracellular tail (Ezumi et al., 2000; Perrella et al., 2021). Early GPVI cloning efforts identified three alternatively spliced isoforms, including what is now regarded as the wild-type sequence, one lacking exon5 and one longer isoform which encodes 620 amino

acids without an apparent transmembrane region (Ezumi et al., 2000; Jandrot-Perrus et al., 2000). The longer isoform has a 4-base insertion in exon7, which introduces a frameshift in the following sequence. When this longer isoform was expressed in a Monkey kidney cell line, COS-7, it did not bind to CRP (Ezumi et al., 2000). Few studies that examined these alternatively spliced forms of GPVI failed to generate more information regarding their expression and function, for example, Sun et al. checked the expression of the three GPVI isoforms in human umbilical vein endothelial cells (HUVECs) and found only the normal length isoform exists (Sun et al., 2003). Exon5-7 encode the mucin-like, heavily O-glycosylated stalk region of GPVI. The result in this chapter showed no significant difference of the exon5-deleted GPVI in surface and whole-cell expression from the full-length GPVI, for both the alleles, in HEK-293T and DT40 cell lines (only surface expression level was examined in the latter). Moreover, no significant difference was observed in collagen-induced downstream signalling between normal-length and exon5-deleted GPVI, using the NFAT-luciferase assay in transfected DT40 cells. As discussed in the previous paragraph, these over-expression data in cell lines may not recapitulate the true situation in platelets. In future, it would be useful to investigate the relative expression of full-length and exon5-deleted GPVI in human platelets. Indeed, the GPVI Western blots in Figure 3.8 show some evidence of lower molecular weight forms of GPVI. However, this would need verification by mass spectrometry proteomics or generation of an exon5-specific antibody. However, the lack of any effect of exon5 deletion in this chapter would question the merit of major follow-up studies, such as assessing exon5-deleted GPVI in platelets using a knock-in mouse strategy.

It has been reported by Trifiro et al. that one of the amino acid substitutions between GPVIa and GPVIb, Q317L (Q in GPVIa and L in GPVIb), accounted for increased calmodulin binding in the less frequent haplotype, GPVIb (Trifiro et al., 2009). Calmodulin is a ubiquitous Ca^{2+}-sensing protein that has many target proteins (Clapham, 2007), with GPVI being one of them

and interacting with it via cytoplasmic residues 294 to 303 (Andrews et al., 2002; Locke et al., 2003). Trifiro et al. reported that transfected GPVIb can co-immunoprecipitate higher levels of endogenous calmodulin from Dami cells, a human megakaryocytic cell line, compared to GPVIa. They inferred that such increased calmodulin binding of GPVIb may reduce metalloproteinase shedding of GPVI, resulting in decreased levels of soluble GPVI in plasma. Since soluble GPVI may inhibit thrombosis by blocking collagen at sites of atherosclerotic plaque rupture, this provides a potential explanation for the association of GPVIb with increased risk of thrombosis (Gardiner et al., 2007; Trifiro et al., 2009). However, Matthews later reported no significant difference between the two haplotypes in GPVI shedding by ADAM10 (the major sheddase for GPVI), using an in vitro shedding assay which is based on transiently transfected HEK-293T cells (Matthews, 2018). In the future, the same type of GPVI shedding assay could be performed on HEK-293T cells transfected with exon5-deleted GPVI to further check the functional difference between exon5-deleted and normal length GPVI. However, the GPVI cleavage site is five amino acids above the plasma membrane, between the PAR and QYY sequences, which is 42 amino acids downstream of the 18 missing amino acods in exon5-deleted GPVI (see Figure 3.1), so an effect on shedding would seem unlikely.

Palmitoylation is a post-translational lipid modification (Martin et al., 2011) and plays important roles in protein-membrane interacting, protein trafficking and protein-protein interactions (Smotrys & Linder, 2004). In fact, several membrane proteins with cysteine residues near the junction of transmembrane and cytoplasmic regions have been reported to be palmitoylated and this is associated with their functions. A striking example is LAT, a central scaffold protein in the GPVI/FcRγ and T cell receptor intracellular signalling cascades; mutation of the cysteines prevents LAT association to lipid rafts and prevents T cell receptor signalling (Lin et al., 1999). Furthermore, palmitoylation and depalmitoylation of the small GTPase Ras, a critical activator of MAPK signalling downstream of GPVI/FcRγ and many

other receptors, regulates its localisation between the ER, Golgi and plasma membrane (Linder & Deschenes, 2007). In addition, palmitoylation of SARS-CoV-2 S protein plays an essential role in membrane fusion, and thus is critical for the infectivity of the virus (Wu et al., 2021). The conserved cysteine at the junction of transmembrane and cytoplasmic regions in the FcRγ intracellular tail is likely to be palmitoylated because a global proteomics study identified FcRγ as one of >1,300 palmitoylated proteins in human platelets, although it was not significantly enriched in comparison to the unlabelled control group (Dowal et al., 2011). However, our results from NFAT-luciferase assay on WT and C44S FcRγ indicated that the mutant at the proposed palmitoylation site showed no significant functional difference from WT, in both basal and collagen-stimulated conditions. However, it cannot be ruled out that C44S FcRγ may have functional effects that might be revealed via other functional assays, for example, difference in the ability to be shed by metalloproteinase ADAM10, which could be determined by the ADAM10 shedding assay that has been described previously (Noy et al., 2016). It is also possible that FcRγ is not palmitoylated, or perhaps not palmitoylated in DT40 cells but palmitoylated in other cells such as platelets, therefore an important next step would be to assess its palmitoylation which can be done using metabolic labelling with labelled palmitate (Eschenbrenner et al., 2020). Nevertheless, our results here provided no evidence that the C44S FcRγ is a promising mutant for the signalling and/or structural studies of the GPVI/FcRγ complex.

To summarise, in this chapter, four GPVI expression constructs were generated and tested, showing their similarity in expression level and ability to initiate collagen-induced downstream signalling, in transfected cell line systems. FcRγ WT and C44S were also similar in their ability to initiate collagen-induced downstream signalling. In addition, six GPVI monoclonal antibodies were characterised and the best performing one, 338E7, identified for Western Blotting. This chapter has therefore characterised essential reagents for most of the

biochemistry experiments in the next two chapters of this thesis. The most common GPVI isoform, GPVIa, and WT FcRγ will be the focus of the SMALP work in the next chapter.

CHAPTER 4

Purification and characterisation of GPVI/FcRγ SMALPs from transfected HEK-293T cells

Chapter 4 Purification and characterisation of GPVI/FcRγ SMALPs from transfected HEK-293T cells

4.1 Introduction

Platelet collagen receptor glycoprotein VI (GPVI) plays an important role in the onset and the development of thrombosis. GPVI binds collagen in the subendothelial matrix at the site of blood vessel injury, and induces downstream signalling events through the ITAMs in FcRγ, where a disulphide-linked dimer of FcRγ forms a complex with one GPVI protein. The phosphorylated ITAMs provide a docking site for Syk family kinases, and further initiates a downstream signalling cascade that activates the platelets. As mentioned in section 1.2.1, GPVI is also the receptor for fibrin(ogen), thus it is involved in the latter stages of thrombosis when firm thrombi involving multiple layers of platelets are formed. GPVI is a potentially attractive anti-thrombosis drug target, as GPVI-deficient mice are protected against lethal thromboembolism (Lockyer et al., 2006) and arterial thrombosis (Bender et al., 2011). Moreover, a human population identified in Chile with a missense mutation in the *Gp6* gene, and subsequently no GPVI expression, have platelets which fail to aggregate on collagen, yet the affected people have only mild bleeding problems (Matus et al., 2013; Nagy et al., 2020).

GPVI is a transmembrane protein with its extracellular region containing two IgSF domains (D1 and D2) that recognise all of its known ligands so far, a stalk region which is heavily O-glycosylated, a single transmembrane α-helix and cytoplasmic tail. Several crystal structures of GPVI IgSF domains have been solved so far, as mentioned in section 1.2.1. These include the original, dimeric structure of GPVI D1 and D2 domains, which shows a back-to-back dimer with the interface at the D2 domains (Horii et al., 2006). The inhibitory nanobody-bound dimeric structure, on the other hand, shows the D2 domains from two monomers exchanging β sheets with each other, and the nanobody, Nb2, binding the D1 domain (Slater et al., 2021).

A third structure is a CRP-bound dimeric structure, showing back-to-back dimers with the interface at the D2 domains, similar to the original GPVI dimer structure. CRP binds to the D1 domains, in a position close to the Nb2-binding groove, which indicates that the Nb2 inhibitory effect could be due to allosteric modulation or steric clash (Feitsma et al., 2022; Slater et al., 2021). Notably, all these solved structures involve only GPVI D1 and D2 domains, and no structures involving the glycosylated stalk, the transmembrane helix and the cytoplasmic tail have been solved. Moreover, these structural studies on GPVI did not provide a definitive answer as to how GPVI dimerises, and there is controversy in the literature over whether the GPVI dimer represents a biologically active form of the receptor, with a unique ligand-binding epitope in comparison to the monomer (Clark, Damaskinaki, et al., 2021; Clark, Neagoe, et al., 2021; Slater et al., 2018). To better understand the mechanism and functional significance of GPVI dimerisation, a full-length GPVI structure, ideally in complex with the FcRγ, would be beneficial, as the regions other than the two IgSF domains could potentially introduce steric constraints and refinement to their spatial arrangements. In addition, the structure of full-length GPVI in complex with FcRγ could help explain the mechanism of GPVI clustering upon binding agonists, thus providing insights into the downstream signalling events.

It is challenging to extract transmembrane proteins out of their native lipid bilayer environment without destroying their bioactive structures and interactions, as the detergent-micelle-encapsulated membrane proteins can easily be destabilised (Dorr et al., 2016). Moreover, the extracting procedures typically involve tedious screening of detergents and buffers (Lee et al., 2016). There has been no reported success in extracting a full-length GPVI into appropriate detergent micelles; moreover, understanding GPVI-FcRγ interaction is crucial to the interpretation of GPVI signalling events, and tackling the structural basis of this interaction is even harder to achieve, as it is mediated by the transmembrane regions.

To address the common problems in membrane protein extraction, a novel strategy utilising SMALPs, has been adopted. SMA co-polymers have been utilised to excise patches out of native membranes, generating nanodiscs directly from membrane bilayer without the involvement of detergents in any of the steps (Knowles et al., 2009; Lee et al., 2016). SMALPs are disc-shaped, containing the native arrangement of lipid bilayer and the membrane proteins embedded inside, are around ~10 nm in diameters and readily amenable to many biochemical and biophysical applications (Dorr et al., 2016; Krishnarjuna & Ramamoorthy, 2022; Lee et al., 2016). In this chapter, the SMALP technology was applied to the extraction and characterisation of the GPVI/FcRγ complex from a human cell line over-expression system, with an ultimate goal to develop materials and methodologies for the structural determination of full-length GPVI in complex with FcRγ. An ADAM10 knock-out HEK-293T cell line (Koo et al., 2020) was used, as the endogenously expressed ADAM10, a transmembrane metalloproteinase, can reduce yield by shedding GPVI (Gardiner et al., 2004; Koo et al., 2022; Noy et al., 2016).

The aims of this chapter are:

1. To extract over-expressed His-tagged GPVI and FcRγ into SMALPs, from an ADAM10-knockout HEK-293T cell line, and to purify GPVI/FcRγ SMALPs.

2. To characterise the purified GPVI/FcRγ SMALPs in terms of their purity, protein oligomerisation status, functionality, and preliminary structural determination.

4.2 Results

4.2.1 Purification of GPVI-SMALPs

The first aim of this chapter was to generate and purify GPVI SMALPs from GPVIa-His and FcRγ transfected HEK-293T cells, the latter being ADAM10 knockout to prevent the constitutive GPVI cleavage by ADAM10 that was previously demonstrated in HEK-293T cells (Gardiner et al., 2004; Koo et al., 2022; Noy et al., 2016). The protocol developed is shown in Figure 4.1. The cells were passaged into 15 cm plates in batches, transiently transfected using PEI, and harvested 48 hours later. Expression of GPVI was confirmed by flow cytometry (Figure 4.2A). Cells were stored at -80 °C immediately after harvesting until use. On the day of generating SMALPs, ~8 mL centrifuged volume of cells were defrosted on ice, membranes isolated and SMALPed using SMALP 30010P (Orbiscope). After the 1st round of SMALP generation, the un-SMALPed pellet was reincubated with SMALP 30010P to maximise SMALP generation efficiency. The SMALPs were incubated with Ni-NTA beads to capture His-tagged GPVI-SMALPs and the solution-bead mixture was then pooled together into a gravity-based affinity column. After washing, His-tagged SMALPs were eluted with imidazole. Analyses of samples from the purification procedure by SDS-PAGE demonstrated successful purification of a major protein band at the predicted molecular weight of GPVI by Coomassie and silver stain (Figure 4.2Bi-ii), and GPVI Western blotting confirmed the presence of GPVI (Figure 4.2Biii).

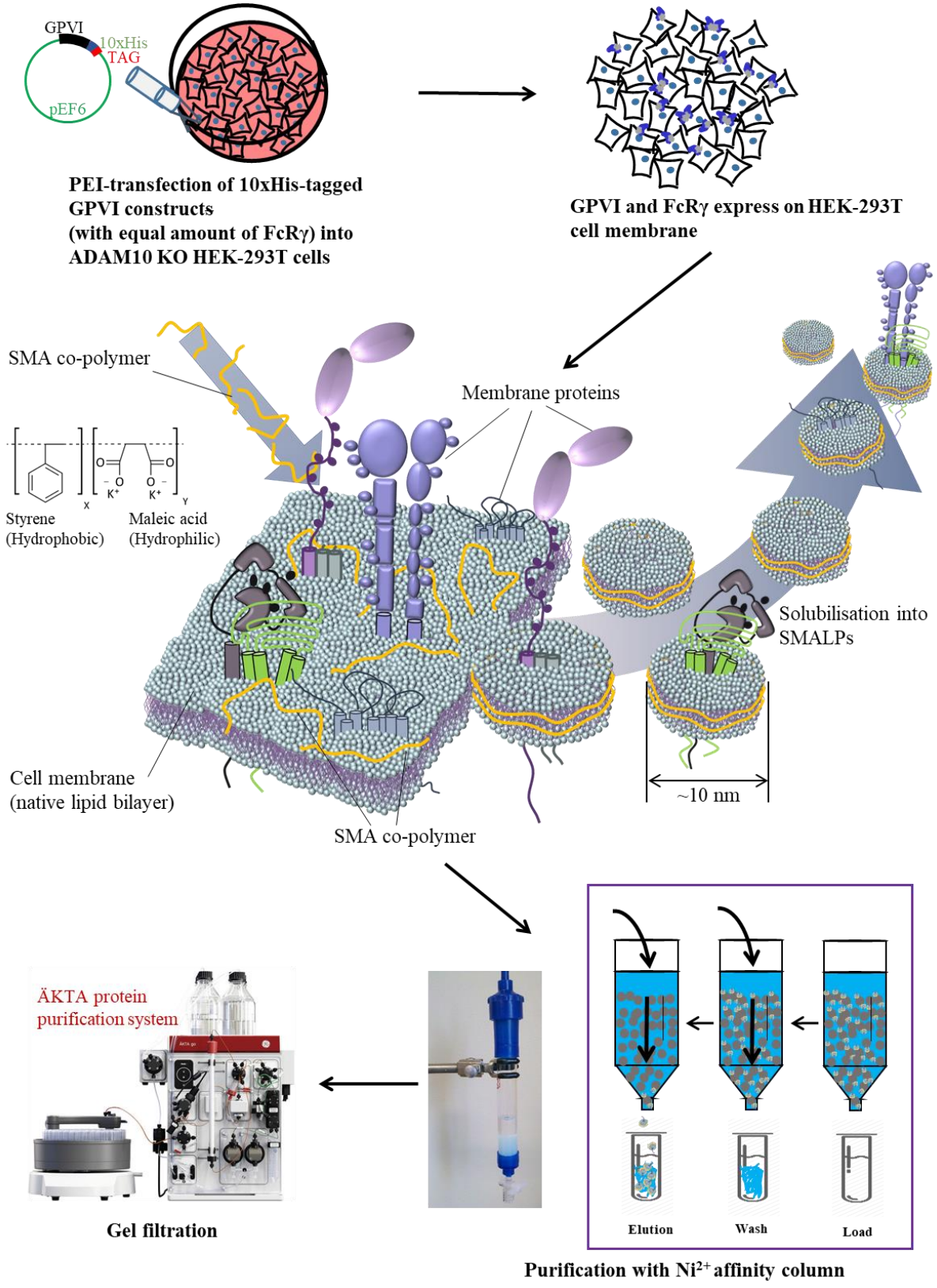
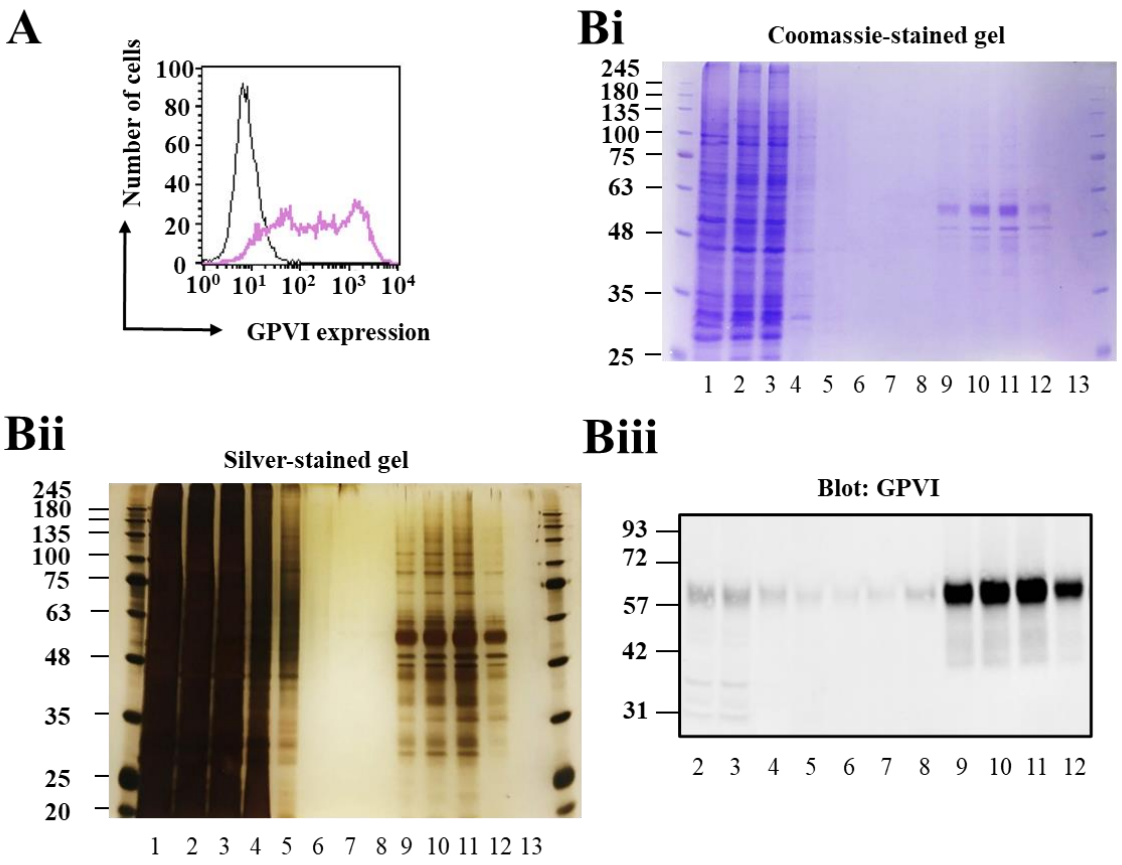


Figure 4.1 Experimental procedures for generating and purifying GPVI SMALPs from transfected HEK-293T cells.



1. SMALP supernatant, 1st round
2. Column flow through, 1st round, 2.5 mL bead slurry +~22 mL SMALPs (the first half), 0.068% loaded
3. Column flow through, 1st round, 2.5 mL bead slurry +~22 mL SMALPs (the second half), 0.068% loaded
4. Column flow through, 2nd round, 3 mL bead slurry +~22 mL SMALPs, 0.068% loaded
5. Column wash1 with SMALP solution B (30 mL), 0.05% loaded
6. Column wash2 with SMALP solution B (30 mL), 0.05% loaded
7. 10 mM imidazole wash (30 mL), 0.05% loaded
8. 20 mM imidazole (30 mL), 0.05% loaded
9. Elution1—500 mM imidazole (1.5 mL), 1% loaded
10. Elution2—500 mM imidazole (1.5 mL), 1% loaded
11. Elution3—500 mM imidazole (1.5 mL), 1% loaded
12. Elution4—500 mM imidazole (1.5 mL), 1% loaded
13. Ni beads after elution (resuspended in 2.5 mL solution B. In total ~5 mL with beads), 0.6% loaded

Figure 4.2 Purification of GPVIa-His SMALPs.

(A) ADAM10-knockout HEK-293T cells were transfected with GPVIa-His and FcRγ expression constructs, and two days later analysed by flow cytometry with GPVI mAb HY101 followed by FITC-conjugated anti-mouse secondary antibody. The purple trace represents GPVI staining and the black trace the isotype-matched MOPC-21 negative control mAb. (B) GPVIa-10xHis was transfected into and expressed in HEK-293T cells (from 100 confluent 15 cm plates) and GPVIa-His SMALPs purified as described in Figure 4.1. For maximum solubilisation efficiency, the un-SMALPed debris from the 1st round of SMALP generation was collected and incubated with SMA, and the generated SMALPs were affinity purified via a Ni-NTA gravity column. Purified SMALPs from both rounds were combined for downstream characterisation. The indicated fractions from the purification procedure were analysed by Coomassie stain (Bi), silver stain (Bii) and Western blotting with GPVI mAb 338E7 (Biii).

4.2.2 Gel filtration of GPVI/FcRγ SMALPs reveals distinct populations of GPVI oligomers

The purified SMALPs were further separated by size via gel filtration. Imidazole-eluted SMALPs were dialysed, concentrated, combined together, and separated via a Superdex 200 10/300 Increase column. SMALP solution B (50 mM Tris pH=8, 500 mM NaCl, 10% glycerol) was used throughout the gel filtration procedures. 500 µL fractions were collected. The resulting profile was a wide peak, right after the void volume (Figure 4.3A). When fractions 4-14, corresponding to the peak, were loaded onto SDS-PAGE and subjected to Western blotting, GPVI and FcRγ were observed in all these fractions, under either non-reduced or reduced conditions (Figure 4.3B). Under non-reduced conditions, a GPVI blot revealed the existence of GPVI dimers and high molecular weight species; the latter are probably GPVI oligomers within the same SMALPs or aggregation of several GPVI-containing SMALPs (Figure 4.3B). Nevertheless, the existence of the FcRγ dimer under non-reduced condition and FcRγ monomer under reduced condition (Figure 4.3B) suggests that FcRγ and GPVI express as a complex in the transiently transfected HEK-293T cells, and they can be isolated together into the same SMALPs.

Interestingly, when the same fractions were loaded onto SMA-PAGE, a native PAGE method where SMALPs are not disrupted and the encapsulated proteins not denatured (Pollock et al., 2019), followed by Western blotting against GPVI and FcRγ, each fraction showed up as a single smear, with the molecular weight span from above 720 kDa to 66 kDa, decreasing from the early fractions to the later ones (Figure 4.3C). This corresponds well with the gel filtration profile (Figure 4.3A). The early fractions consisted of large particles with several hundreds of kDa. The later fractions (fraction 9-14) are potentially purer as they were less smeared (Figure 4.3C). Moreover, the bands in each fraction overlayed on GPVI and FcRγ blots, a further confirmation that they form a complex and exist in the same SMALPs. The SMA-PAGE results

suggest that GPVI/FcRγ in SMALPs from HEK-293T cells possibly comprise different oligomeric states of the GPVI/FcRγ complexes.

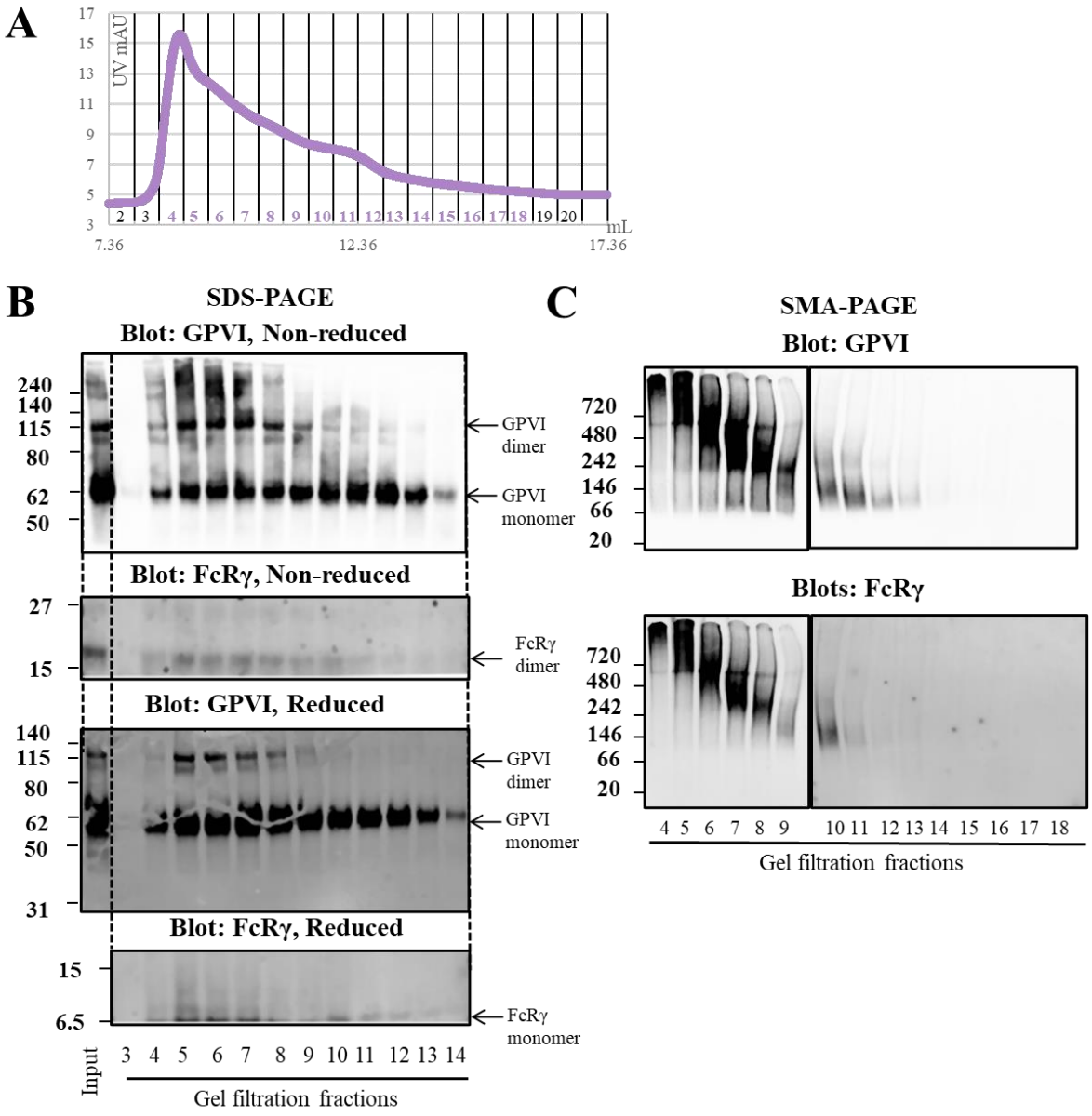


Figure 4.3 Gel filtration of GPVI/FcRγ SMALPs reveals distinct populations of GPVI oligomers.

(A) Superdex 200 10/300 Increase column gel filtration profile of the pooled, dialysed and concentrated GPVI-SMALP elutions from Ni-NTA affinity column. Numbers on the X-axis refer to the number of the fractions collected. (B) SDS-PAGE and (C) native SMA-PAGE of gel filtration fractions followed by Western blotting for GPVI and FcRγ.

4.2.3 GPVI-SMALPs bind collagen

To evaluate whether GPVI encapsulated in SMALPs remains functional, a collagen pull-down assay was performed. The gel filtration fractions from section 4.2.2 were pooled into three groups—fraction 4-6, fraction 7-9 and fraction 10-13, and pulled down by collagen-conjugated agarose beads. GPVI blot revealed efficient pull-down in all three groups (Figure 4.4). Similar quantities of input GPVI for each of the three pull-downs was confirmed by GPVI Western blotting (Figure 4.4). Together, this suggests that GPVI in SMALPs is properly folded and functional in binding collagen.

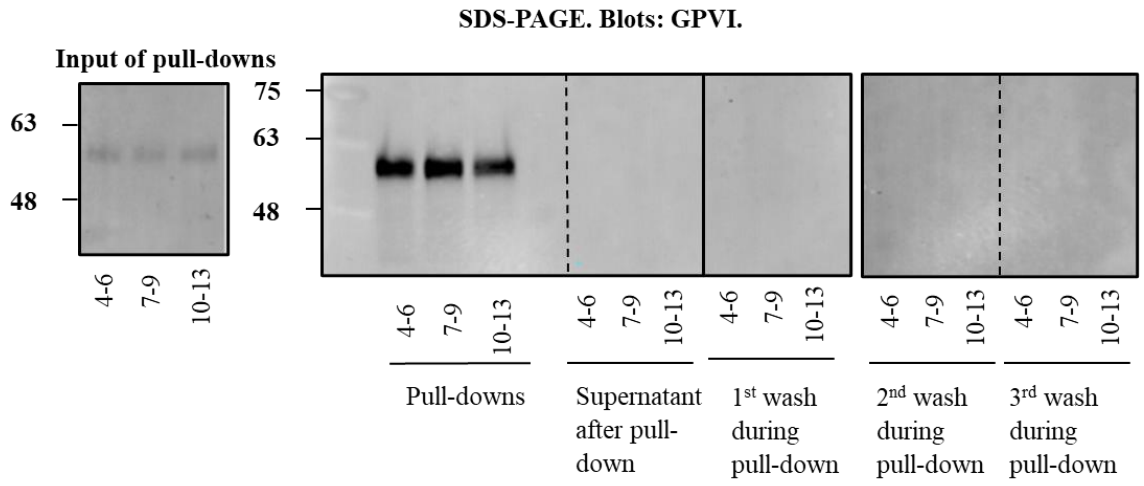


Figure 4.4 GPVI SMALPs bind collagen.

The GPVI SMALP gel filtration fractions from Fig. 4.3 were pooled as indicated, and subjected to collagen-agarose pulldown assay followed by GPVI Western blotting. Dashed lines were used to separate different parts of the blot for clarity. The solid line in the middle of the blot indicates that different parts of the same gel were grouped together on the image. Images from different gels are separately displayed.

4.2.4 The purified GPVI/FcRγ SMALPs are relatively pure

To assess the purity of the GPVI/FcRγ SMALP samples, the gel filtration fractions were run on SDS-PAGE and silver stained. Three major bands were detected at approximately 100 kDa, 57 kDa and 18 kDa (Figure 4.5). These were excised out of the silver-stained gel as indicated (Figure 4.5), and subjected to liquid chromatography followed by tandem mass spectrometry (LC-MS-MS), which was kindly performed by Dr. Norman Day and Dr. Jinglei Yu from the Advanced Mass Spectrometry Facility, University of Birmingham. The output protein lists revealed GPVI as the top hit for the ~100 kDa and the ~57 kDa bands, suggesting them being GPVI dimer and GPVI monomer, respectively, and FcRγ as the top hit for the ~18 kDa band, suggesting it being a FcRγ dimer (Supplementary Tables 1-3). As these three bands were relatively the strongest among all bands that showed up in the silver-stained gel, these results demonstrate that the purified SMALPs are relatively pure, with GPVI and FcRγ being the main protein components.

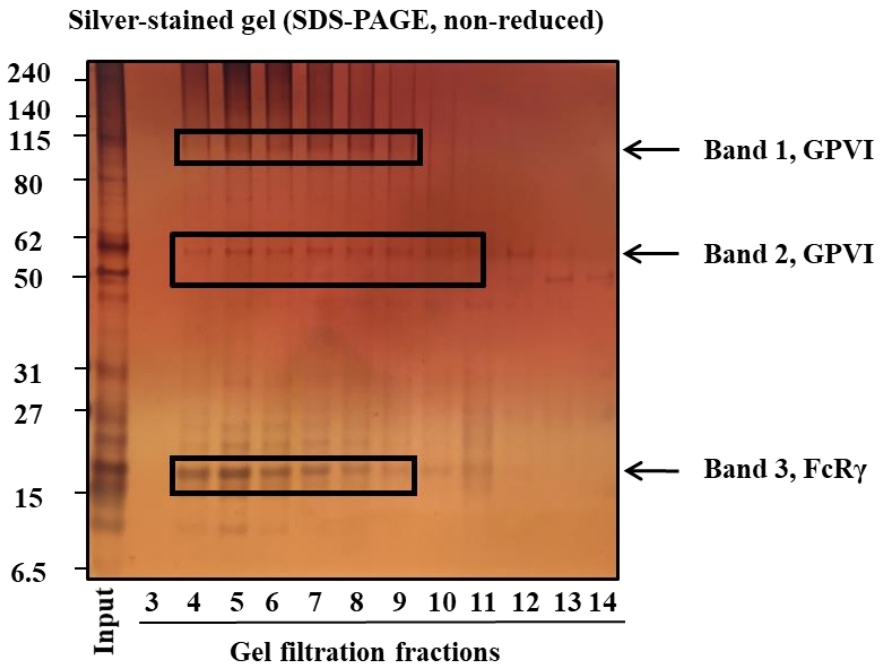


Figure 4.5 The purified GPVI/FcRγ SMALPs are relatively pure.

GPVI SMALP gel filtration fractions were analysed by SDS-PAGE followed by silver stain. The three main bands, at approximately 100 kDa, 57 kDa and 18 kDa, were excised as indicated by the black rectangles and analysed by LC-MS-MS, and the major species identified are indicated by the arrows. The filtered list of protein entries from LC-MS-MS are shown in Supplementary Tables 1-3.

4.2.5 GPVI/FcRγ SMALPs show single-dispersed particles under negative stain EM

To visualise the purified GPVI/FcRγ SMALPs, fractions 5, 7 and 10 from gel filtration, were chosen as representatives for possible high-, medium- and low-order oligomers for negative stain EM, which was kindly performed by Dr. Saskia Bakker from Advanced Bioimaging, University of Warwick. Among the images, those from fraction 7 showed clearly single-dispersed, protein-like particles (Figure 4.6A). 2D classification was performed from ~1,000 particles on the images collected from fraction 7, where 39 class averages were generated (Figure 4.6B). The averages were ranked by the number of particles in the corresponding classes with the frequencies calculated (Figure 4.6C). Visualisation of GPVI SMALPs binding collagen III on the grid was also attempted, but unfortunately the collagen fibres failed to be observed.

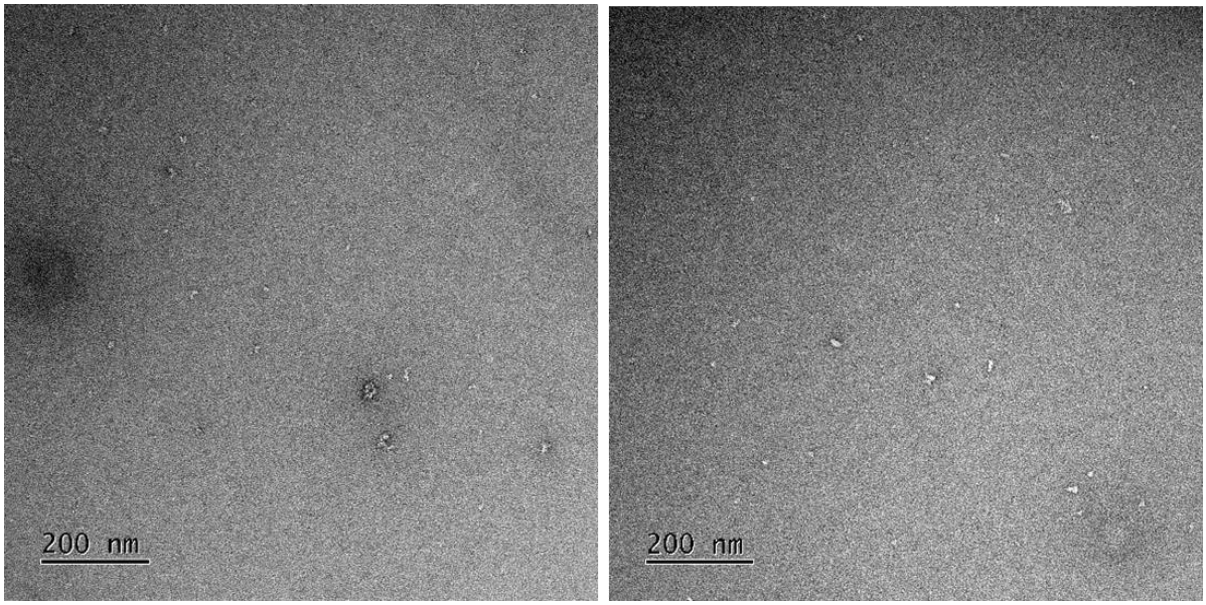


Figure 4.6 Representative negative stain electron microscopy images of GPVI SMALPs showed single-dispersed, protein-like particles.

GPVI SMALP gel filtration fraction 7 from Figure 4.3 was 10-fold diluted in solution B and subjected to negative stain electron microscopy. Two representative images are shown.

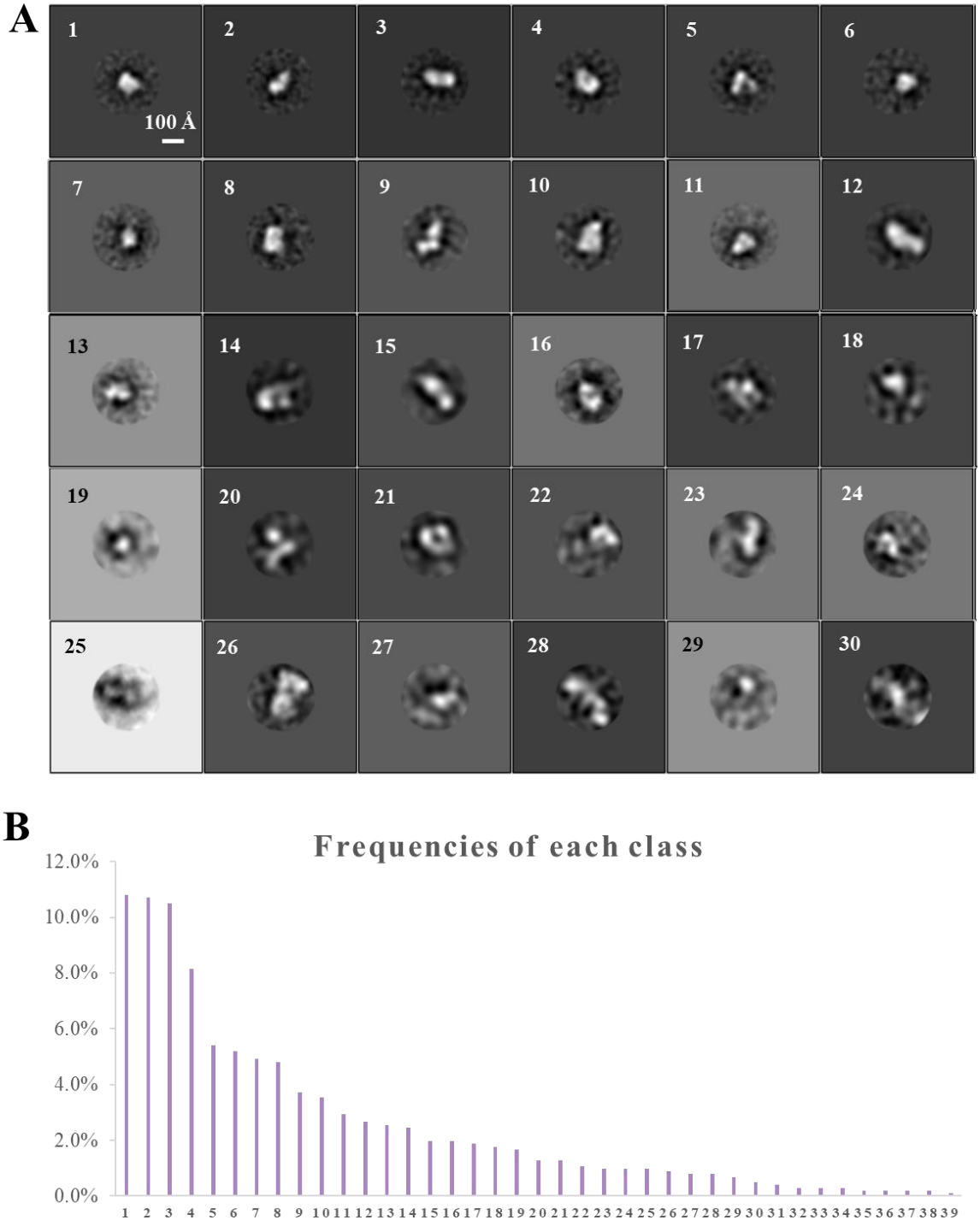


Figure 4.7 2D class averages from particles picked from negative stain electron microscope images.

(A) Negative stain images from fraction 7 in Figure 4.3 were collected, with single particles picked, aligned and grouped into 2D class averages using RELION. 50 classes were requested and 39 classes were produced; they were numbered 1-39 with descending amount of particles in their corresponding classes. The averages from the first 30 class averages are shown; the last 9 class averages are either too blurry or of an unusual shape that is unlikely to represent GPVI SMALPs. The scale bar is only shown in class 1, but it is the same for all classes. (B) Frequencies of particles in different classes.

4.3 Discussion

In this chapter, full-length GPVI in complex with FcRγ has been successfully extracted into SMALPs, from a transfected human cell line, HEK-293T. GPVI/FcRγ SMALPs purified with Ni-NTA gravity column and gel filtration showed a wide size distribution, possibly comprising the GPVI/FcRγ complex with different oligomeric states. Purified GPVI/FcRγ in SMALPs with different sizes can all bind collagen. The purified GPVI/FcRγ SMALPs are relatively pure, with GPVI and FcRγ being the major protein components, and single-dispersed particles of the purified GPVI/FcRγ SMALPs can be observed under negative stain EM. This is the first report of purifying GPVI with lipid nanodiscs.

The gel filtration profile of purified GPVI/FcRγ SMALPs comprises a wide peak right after the void volume (Figure 4.3A). This profile potentially demonstrates two major peaks, the first one right after the void volume and the second one in between fractions 11-12, which are connected by a series of middle-sized particles, represented as the slope between the two peaks (Figure 4.3A, fractions 5-10). A similar phenomenon on purified SMALPs has been observed in a recently published study where tetraspanin CD81 was expressed in *P. pastoris* yeast, extracted into SMALPs, purified and characterised (Ayub et al., 2020); the size exclusion chromatography profile comprises two peaks, one large peak right after the void volume and a second one containing a lesser amount of particles. CD81 was detected in both the peaks by Western blotting, and the circular dichroism spectra of both peaks overlapped, suggesting both peaks contains natively folded CD81; however, only the second peak, which may represent CD81 monomer, can bind to hepatitis C virus (HCV) E2 glycoprotein, which is an established CD81-binding protein (Pileri et al., 1998; Stroh et al., 2018). The authors speculated that the first peak may comprise the oligomers of CD81, or dimerised SMALP discs, and the abolished binding to HCV E2 glycoprotein of the first peak could be due to a sterically blocked binding site rather than the proteins themselves being unstructured (Ayub et al., 2020). The gel filtration

profile presented in this chapter indicates that, in addition to the two major populations which are more homogeneous, the purified GPVI/FcRγ SMALPs here may comprise additional populations with intermediate sizes. This could possibly reflect the different oligomerisation and clustering status of GPVI/FcRγ in the HEK-293T cell line. It could also be an over-expression phenomenon, such that GPVI density on the cell surface is so high that GPVI molecules cluster spontaneously in the absence of GPVI agonists. On an optimised side, given that all particles in gel filtration fractions in this report consist of properly folded GPVI which can bind collagen, the expression system may have captured a wide range of different oligomeric states of the GPVI/FcRγ complex, which could ultimately help to explain the molecular mechanisms of GPVI dimerisation and clustering.

The gel filtration elution volume profiles in this chapter are relatively consistent with the column calibration curve; however, a molecular weight bias up to 33% from the calibration curve exist (Supplementary Figure 1). This could be attributed to the fact that the column calibration was performed with soluble, globular protein standards in PBS, therefore the conformation of the standards, the charge and hydrophobicity status of the standards, and the buffer conditions are all different from the GPVI/FcRγ SMALP samples presented in this chapter. Besides, the SMA belt creates a very different interface to the aqueous solution, in comparison to the protein/buffer interfaces or detergent miselle/buffer interfaces in most other samples, and the wide range of molecular weights of the GPVI/FcRγ SMALPs here may make the molecular weight readings from a native gel less accurate. In addition, the largest size of the protein standards that were used to generate the column calibration curve is 200 kDa, which may render the calibration curve less fitted in the higher molecular weight range. However, given that the gel filtration fractions in this chapter have been characterised by GPVI/FcRγ Western blotting, the collagen-binding assay, mass spectrometry and negative stain EM, there

is enough evidence that different populations of GPVI/FcRγ SMALPs have been generated and purified.

The work here also featured the application of one relatively new native PAGE method, SMA-PAGE, which was specifically developed for SMALPs by Pollock et al (Pollock et al., 2019). SMA-PAGE utilises the unique negatively charged belt, the SMA polymer, as the driving force in PAGE, instead of the traditional SDS, thus the migration of particles on PAGE can be achieved without the addition of any other chemicals apart from the native sample buffer (0.08 mg/mL bromophenol blue, 20 mM Tris pH=8, 50% glycerol for 5x) or the need of heating, preventing the proteins from being denatured and enabling the whole SMALP to migrate in an intact way during electrophoresis. The apparatus used for SMA-PAGE is as simple as for the traditional SDS-PAGE, with all reagents affordable for general experimental usage. In addition, comparing to other native PAGE methods, such as blue native PAGE, SMA-PAGE requires no additives in either the loading samples or running buffers, and maybe more importantly, provides a relatively uniform shape of all particles, since all SMALPs retain the disc shape and similar sizes, at least in the plane of the disc. SMA-PAGE followed by anti-GPVI and anti-FcRγ Western blotting here elegantly demonstrated the molecular weight distribution of purified SMALPs, with the bands decreasing progressively from the early to later fractions, corresponding with the gel filtration peak profile. Moreover, relatively little amount of the samples (several tens of μL) is needed in SMA-PAGE, in comparison to many other biophysical characterisations such as analytical ultracentrifugation and circular dichroism. As such, SMA-PAGE has served as an efficient and promising method for identifying the size of GPVI/FcRγ SMALPs, although it needs to be further investigated whether they are oligomers encapsulated in SMALPs or SMALPs that aggregate together.

The purified GPVI/FcRγ SMALPs obtained in this chapter are functional in binding collagen, and relatively pure with GPVI and FcRγ being the main protein components. In addition,

negative stain EM has identified single-dispersed particles, with reasonable sizes and several 2D class averages generated. However, the amount of particles selected for 2D classification was only around 1,000, which was too low for 3D structure construction. To measure the quantity of purified GPVI in each fraction of gel filtration, three methods were adopted: Coomassie-stained SDS-PAGE with the samples in comparison with BSA standards, anti-GPVI Western blotting on samples in comparison with recombinant GPVI-Fc protein, and nanodrop (Supplementary Figure 2). These methods generated inconsistent results, but the measured concentrations were all at ~100 ng or below, suggesting an insufficient yield for further biophysical characterisation and structural determination. Besides, silver staining on gel filtration fractions of purified SMALPs still showed multiple visible bands which were not at the sizes of GPVI or FcRγ (Figure 4.5), and the anti-His-tag Western blot on the same fractions also showed several additional protein bands apart from the ~57 kDa GPVI monomer band and the ~110 kDa GPVI dimer band (Supplementary Figure 3). Alhough they can be separated on gel based on molecular weights, it could be difficult to distinguish GPVI/FcRγ from contaminant proteins on EM images, which obscures structure determination. Moving forward, for high-resolution structure determination, a larger amount of purer protein samples is needed, which could be achieved by the use of suspension HEK-293T cells, from which large volumes can relatively easily be grown, and strategies to improve protein purification, as will be discussed in more detail in section 6.2.

Taken together, the results in this chapter have demonstrated SMALPs and HEK-293T cells as promising tools to generate full-length GPVI in complex with FcRγ, for their characterisation towards structural determination. Optimisation of the expression system and purification strategies will be needed for the ultimate goal to solve the high-resolution structure of GPVI/FcRγ complex in SMALPs.

CHAPTER 5

Investigation of platelet membrane receptor interaction and stoichiometry using SMALPs

Chapter 5 Investigation of platelet membrane receptor interaction and stoichiometry using SMALPs

5.1 Introduction

Many major platelet membrane receptors and their signalling pathways have been identified so far, as have their roles in platelet response to agonists/antagonists, platelet activation, aggregation and thrombus formation (Clemetson & Clemetson, 2019; Poddar & Banerjee, 2020). However, there is still much to understand about the organisation and interactions of these major platelet membrane receptors with other membrane proteins on the platelet surface. Traditional membrane protein interaction mapping methods include co-immunoprecipitation (co-IP) and immunofluorescence microscopy; however, these methods have their limitations. Co-IP performed on detergent-micelle-encapsulated proteins can suffer from artefacts generated by the dynamic characteristics of detergent micelles, such that the dissociation and merging of these micelles can introduce false negative or false positive results of protein-protein interactions. Immunofluorescence microscopy can be a powerful tool for monitoring membrane protein interactions in real time and in live cells, but it requires additional labelling by either antibodies or genetically built-in tags on proteins, both of which could introduce steric hindrance and thus interfere with protein interaction; moreover, the blinking events of fluorophores can render difficulties in data interpretation (Clark, Neagoe, et al., 2021). In this chapter, the possibility of using SMALPs to map platelet membrane protein interactions and stoichiometry was explored. The hypotheses here are that SMALPs generated from native human platelets can encapsulate intact membrane protein assemblies and preserve membrane protein interactions with their extracellular or intracellular partner molecules, thus will provide useful information about platelet membrane protein interactions and stoichiometry. The SMALP generation protocol for human platelets was firstly optimised to address the relatively

low volume of platelet pellets that can be collected from one donor, and to ensure that the native protein organisation in human platelets is not changed during SMALP generation procedures. Using the optimised SMALP generation protocol, the preservation of two known protein complexes, GPVI/FcRγ and ADAM10/Tspan15, in the same SMALPs from human platelets, was examined. GPVI SMALPs from human platelets were then closely examined for the investigation of GPVI phospho-signalosome and GPVI-interacting membrane proteins, and GPVI conformational differences in detergent micelles and in SMALPs were accessed. Finally, novel biochemical assays based on cell surface biotinylation and SMA-PAGE were developed and applied to the investigation of a wide range of platelet membrane proteins.

The aims of this chapter are:

- To develop a SMALP generation protocol that can be routinely performed on freshly isolated, washed human platelets, and that doesn't interfere with the intact protein interaction from native platelets;
- To examine whether GPVI/FcRγ and ADAM10/Tspan15 complexes can be preserved in the same SMALPs from human platelets, respectively, and to compare this with detergent lysates;
- To compare the efficiency of GPVI immunoprecipitation, when GPVI is solubilised into detergent micelles or into SMALPs;
- To examine the membrane interactome and phospho-signalosome of GPVI, using human platelet SMALPs;
- To develop novel biochemical assays based on cell surface biotinylation and SMA-PAGE for the investigation of platelet membrane protein interaction and stoichiometry in native human platelets.

5.2 Results

5.2.1 Optimisation of SMALP generating methodologies for washed human platelets

The aim of this section was to develop an efficient and routine protocol to generate SMALPs from platelets and perform bench-top biochemical experiments with these platelet SMALPs. The standard protocol of generating SMALPs from intact cells was published by Lee et al. (Lee et al., 2016), where membranes are isolated from a relatively large number of cells and their total mass measured; the membranes are then homogenised, resuspended to 2.5% (wt/vol) and the suspension incubated with SMA polymer. However, to generate SMALPs from human platelets, the starting point is freshly drawn blood at the beginning of the day, from which a relatively small volume of platelet pellet is produced. Moreover, as drawing blood and preparing washed platelets from whole blood generally takes a few hours, it is not practical to go into the relatively long membrane isolation steps on the same day. As such, the SMALP generating procedure was simplified by removing the membrane isolation step and resuspending the platelets directly into SMALP solution B (50 mM Tris, 500 mM NaCl, 10% glycerol, pH=8); since platelets have no nucleus, lack many organelles and possess an intracellular membrane system, this simplification should in theory not prevent SMALP generation. The platelets were then homogenised in this buffer by a dounce homogeniser, and SMA was added. The rest of the protocol, including incubating with SMA for at least 2 h at room temperature and ultracentrifuge to remove insoluble debris, remained unchanged from the original protocol (Lee et al., 2016). To establish the effectiveness of the modified protocol, platelet SMALPs were firstly Western blotted for GPVI and αIIb (part of the major integrin αIIbβ3 complex) as two model platelet membrane proteins (Figure 5.1). Protein signals with comparable strength were detected in homogenised platelets, in platelet-SMA incubation and in the formed SMALPs, but not in the insoluble debris (Figure 5.1). This simplified platelet SMALP generation protocol was then adopted throughout this chapter.

Next, it was evaluated how well SMALPs were able to extract and represent the native state of platelets under these experimental conditions, in comparison to NP-40 detergent-solubilisation. As platelets have limited amounts of proteins, a relatively well-defined proteome as well as the pTyr profile, the anti-pTyr Western blotting serves as an excellent evaluation. Strikingly, whole cell SMALPs showed substantially higher levels of p-Tyr than NP-40 lysates (Figure 5.2). The latter showed relatively low levels of basal pTyr, and several prominent pTyr bands were induced by CRP stimulation, with major bands likely corresponding to PLCγ2, Btk, Syk, Src, LAT (Figure 5.2). This suggests that the platelets are hyper-activated during the aforementioned SMALP-generation procedure. To determine the cause of this problem, each component of SMALP solution B (50 mM Tris, 500 mM NaCl, 10% glycerol, pH=8.0) was scrutinised. The addition of 10% (vol/vol) glycerol did not change platelet p-Tyr profile (data not shown); thus, the focus was placed on NaCl concentration, Tris concentration, and the buffer pH. The pelleted platelets were resuspended in buffers containing 50 mM Tris pH=8, and NaCl with a concentration gradient from 150 mM to 500 mM (Figure 5.3A). Interestingly, as NaCl concentration increased, the amount of detected p-Tyr and the intensity of each p-Tyr signal were similarly increased (Figure 5.3A). In contrast, neither the change of buffer pH between 7.3 (the pH of modified Tyrode's buffer) and 8.0 (the pH of SMALP solution B), nor the change of Tris concentration from 10 mM to 50 mM, affected the protein band pattern on p-Tyr blots (Figure 5.3B and C). Thus, the high concentration of NaCl (500 mM) in SMALP solution B was identified as the main cause of platelet hyper-activation.

The outcome of these experiments was that further experiments in this chapter were mainly performed with the modified SMALP working solution B (50 mM Tris pH=8, **150 mM NaCl**, 10% glycerol), unless otherwise stated. With this optimised buffer condition, the band patterns on p-Tyr Western blot were comparable in whole cell SMALPs and whole cell detergent lysates from platelets, with clearly distinguished differences between resting and activated platelets

(Figure 5.4). Where indicated, NaCl was supplemented to the SMALP solution for a final concentration of 500 mM, to disrupt the unspecific aggregation among several SMALPs, which has been reported before (Postis et al., 2015) and also observed in this thesis (Supplementary Figure 4).

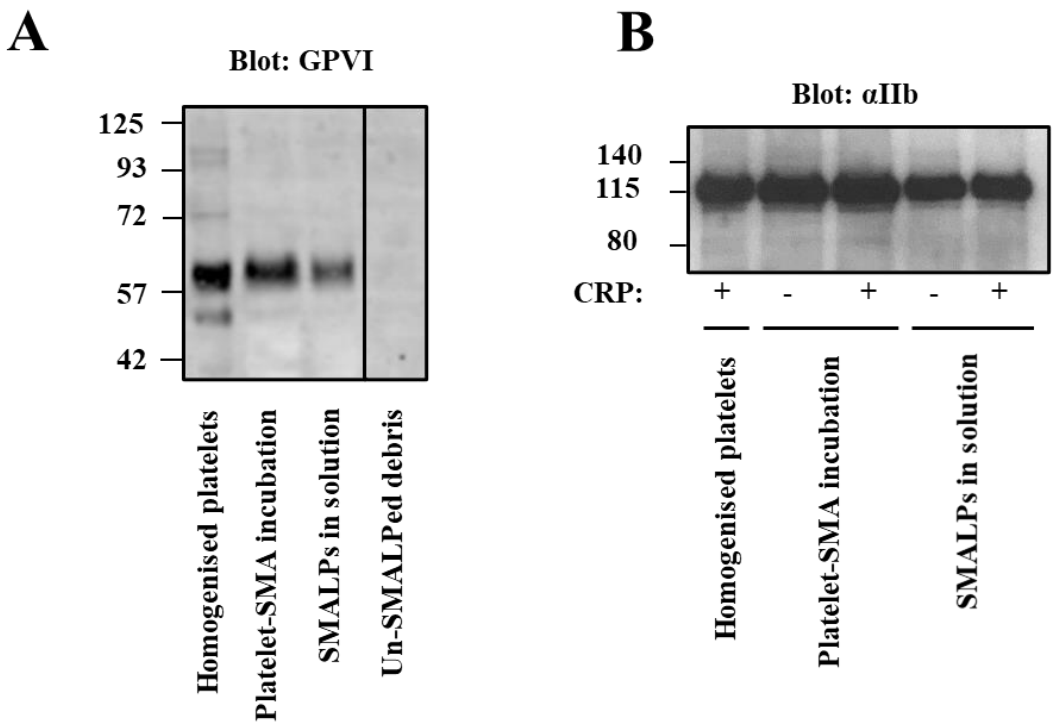


Figure 5.1 Platelet membrane proteins can be solubilised by SMALP 30010P.

Human platelets were isolated from freshly drawn blood, resuspended in optimised SMALP solution B (50 mM Tris, 150 mM NaCl, 10 % glycerol), and homogenised in a dounce homogeniser. SMA (SMALP 30010P) was added to the homogenised platelets, and the mixture incubated for 2 h at room temperature. SMALPs and un-SMALPed debris were then separated by ultracentrifugation. Un-SMALPed debris were resuspended into buffer with the same volume as the SMALP-containing supernant for comparison. (A) The products in each steps were collected and subjected to Western blotting for GPVI. (B) Platelets were stimulated with CRP or treated with an equal amount of buffer as a negative control, and the products in each steps were collected and subjected to Western blotting for αIIb.

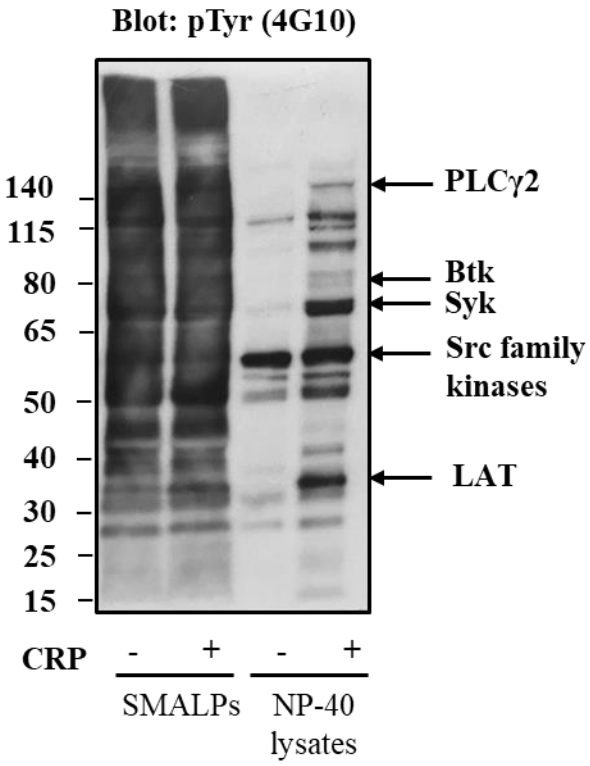


Figure 5.2 Whole cell SMALPs from human platelets yield hyper-phosphorylated proteins that are independent of CRP activation.

Washed human platelets were prepared from freshly drawn blood and activated by CRP. The activated (or resting-state control) platelets were then centrifuged at 10,000 xg for 1 min at room temperature, resuspended again into SMALP solution B (50 mM Tris diluted 1:10 from pH=8, **500 mM NaCl**, 10% glycerol) and subjected to platelet SMALP procedures (lanes 1-2), or directly lysed in 1% NP-40 lysis buffer (lanes 3-4). The samples were loaded onto a 4-12% gradient gel, subjected to SDS-PAGE and Western blotted with anti-p-Tyr antibody.

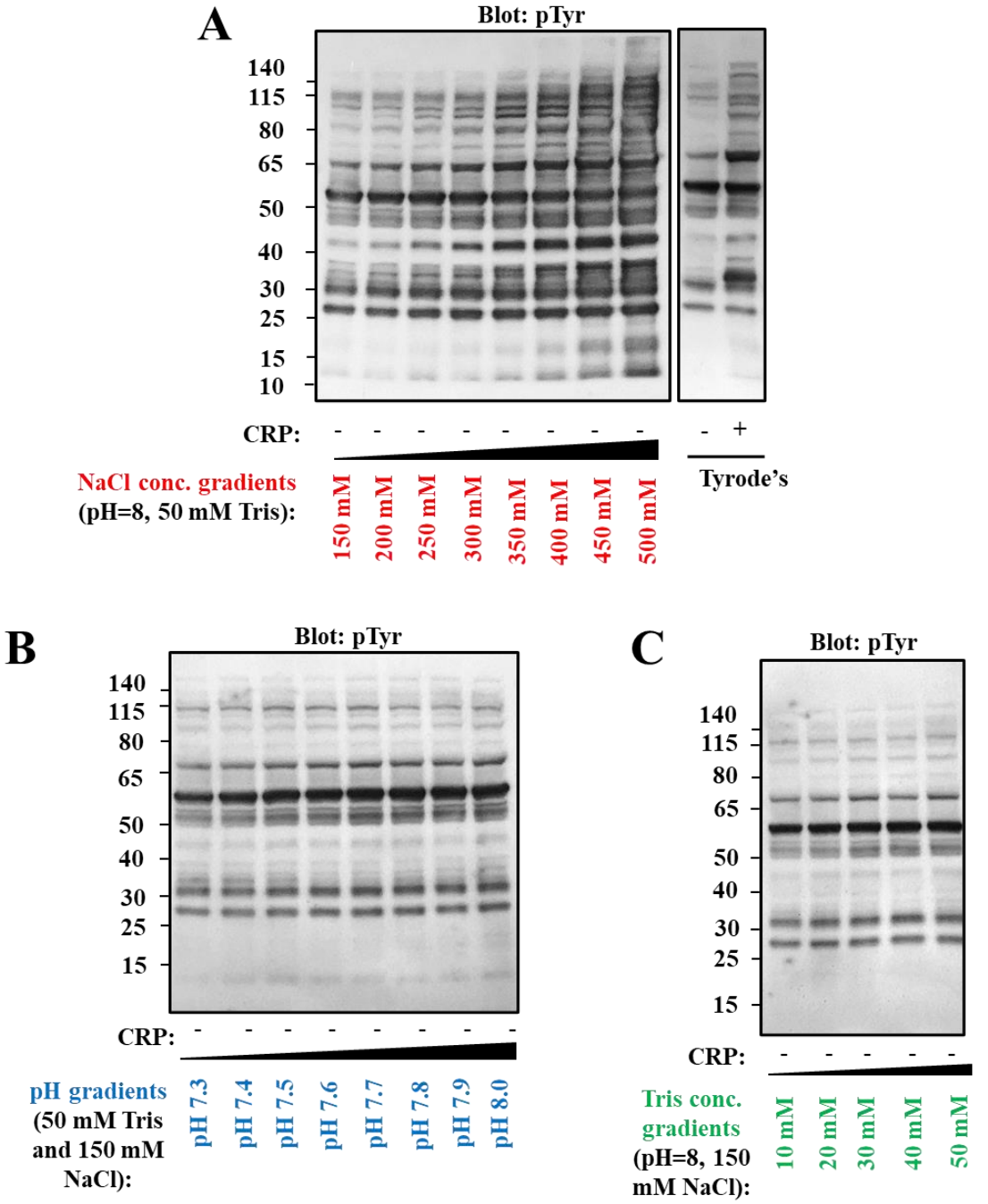


Figure 5.3 Influence of different buffer conditions on platelet protein tyrosine phosphorylation.

Human platelets were isolated from freshly drawn blood, stimulated with CRP if indicated, centrifuged down and resuspend in the indicated buffers. Samples were subjected to SDS-PAGE followed by Western blotting for pTyr. (A) Influence of NaCl concentration, with 50 mM Tris and pH=8. In the last two lanes, the same batch of washed platelets were resuspended in modified Tyrode's buffer instead of Tris-NaCl buffer, with incubation at 37 °C for 90 s with or without CRP activation, to confirm the response of platelets to the agonist. (B) Influence of pH, with 50 mM Tris and 150 mM NaCl. (C) Influence of Tris concentration, with 150 mM NaCl and pH=8.

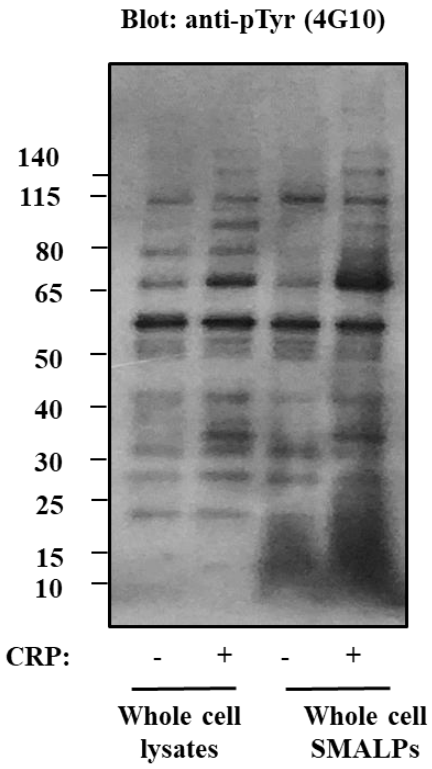


Figure 5.4 Whole cell lysates and whole cell SMALPs from human platelets presented similar band patterns on p-Tyr Western blot, when using the optimised SMALP buffer B containing 150 mM NaCl.

Human platelets were isolated from freshly drawn blood, incubated at 37 °C for 90 s with or without CRP activation, then solubilised by NP-40 detergent or into SMALPs. The generated whole cell lysates and whole cell SMALPs were loaded on SDS-PAGE and subjected to Western blotting for p-Tyr. The data is representative of three independent experiments.

5.2.2 GPVI/FcRγ and ADAM10/Tspan15 complexes can be preserved in SMALPs from human platelets

To develop SMALPs as a novel platform for the investigation of membrane protein interactions, it was firstly examined whether SMALPs can preserve known membrane protein complexes. Two pairs of proteins, GPVI/FcRγ and ADAM10/Tspan15, which are known to form complexes on the cell surface, respectively, were chosen (Koo et al., 2020; Lipper et al., 2022; Zheng et al., 2001). Resting-state platelets were solubilised into either detergent lysates or SMALPs, the samples pre-cleared and subjected to GPVI IP, ADAM10 IP or Tspan15 IP. FcRγ was detected in GPVI IPs, using a range of different GPVI antibodies, from detergent lysates or SMALPs by Western blotting (Figure 5.5A), indicating that the GPVI/FcRγ complex can be preserved in both Triton X-100 cell lysates and in SMALPs. Similarly, in platelet SMALPs, Tspan15 was detected by Western blotting in ADAM10 IPs, and vice versa (Figure 5.5B). This interaction was not preserved in Triton X-100 lysates (Figure 5.5Bi); however, it did get preserved when platelets were lysed with a milder detergent, Brij97, which is widely used in the tetraspanin field to preserve protein interactions (Hemler, 2003; Le Naour et al., 2006; Protty et al., 2009) (Figure 5.5Bii). The relatively stronger ADAM10 bands in ADAM10 IPs relative to Tspan15 IPs, and vice versa (Figure 5.5B), are most likely due to the fact that there are two other TspanC8 tetraspanins expressed in platelets that compete with Tspan15 for ADAM10 binding (Koo et al., 2022). To summarise, the two pairs of membrane protein complexes, GPVI/FcRγ and ADAM10/Tspan15, can be encapsulated together into the same SMALPs from human platelets, suggesting that this methodology may be useful for the identification of novel membrane protein interactions.

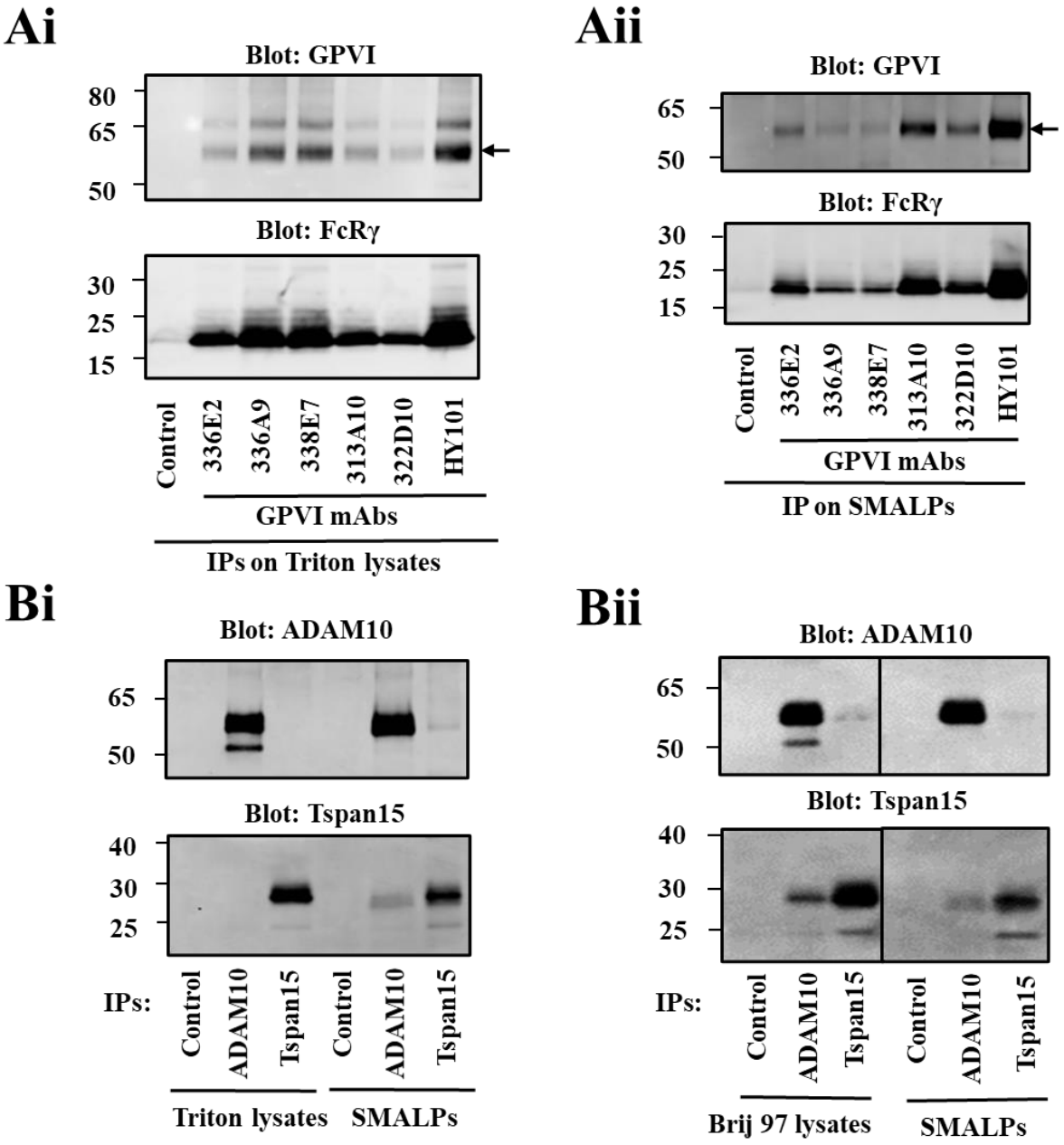


Figure 5.5 SMALPs isolated from human platelets preserve GPVI/FcRγ and ADAM10/Tspan15 complexes.

Washed human platelets were lysed in 1% Triton X-100, 1% Brij 97 or into SMALPs, as indicated, then subjected to IP with the antibodies indicated. For IPs on SMALPs, the solution was supplemented to 500 mM NaCl to disrupt the potential aggregations between different SMALPs. The IPs were eluted, then subjected to SDS-PAGE followed by Western blotting with the antibodies indicated. Arrows in panel A indicate the canonical GPVI band. GPVI and FcRγ blots are representatives of three independent experiments. ADAM10 and Tspan15 blots are representative of two independent experiments.

5.2.3 GPVI solubilised into detergent lysates and SMALPs has differential epitope accessibilities to anti-GPVI antibodies

The five new GPVI monoclonal antibodies from Bernhard Nieswandt's lab (University of Würzburg), described in Chapter 3, were used for GPVI immunoprecipitation (IP). Some striking differences were observed for particular antibodies depending on whether human platelets were lysed in 1% Triton X-100 detergent or into SMALPs (Figure 5.5A and 5.6). For example, 338E7 immunoprecipitated GPVI from detergent lysates with the highest efficiency, comparing to other antibodies, but immunoprecipitated GPVI from SMALPs with the lowest efficiency among the five antibodies (Figure 5.6). In contrast, 313A10 immunoprecipitated GPVI with relatively low efficiency from detergent lysate, but immunoprecipitated GPVI SMALPs with relatively high efficiency (Figure 5.6). These data suggest that the GPVI mAbs have distinct epitopes that have differential accessibilities in detergent micelles versus SMALPs. However, more definitive conclusions regarding the epitopes of these GPVI antibodies cannot be drawn until epitope mapping experiments for example, GPVI chimeras with mutations at the proposed epitope positions, are performed.

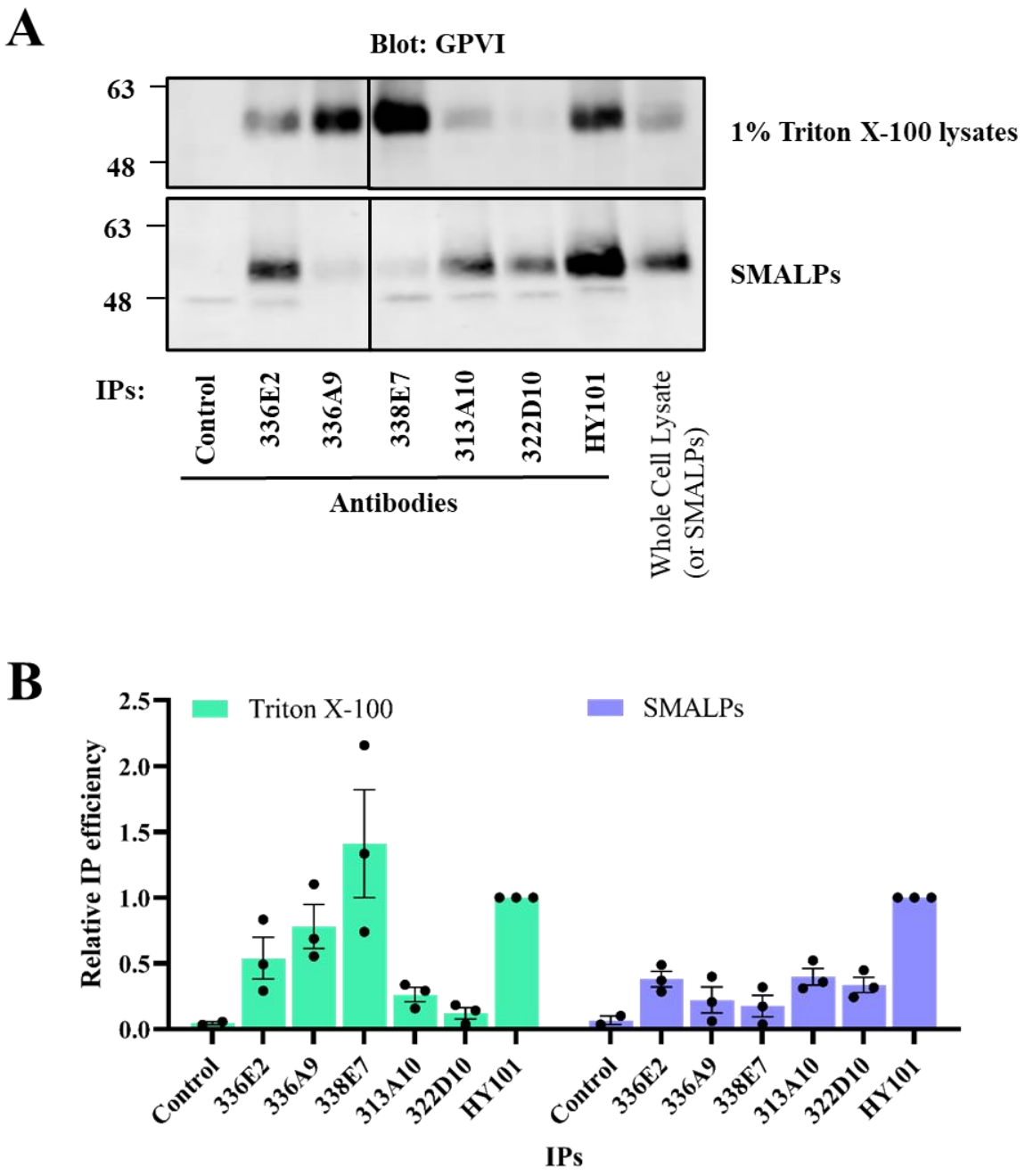


Figure 5.6 GPVI mAbs immunoprecipitate GPVI in detergent lysates and in SMALPs with different efficiencies.

(A) Washed human platelets were lysed with 1% Triton X-100 lysis buffer or solubilised into SMALPs, immunoprecipitated with the indicated mAbs and Western blotted with GPVI mAb, 338E7. The solid lanes on the image indicate that different parts of the same gel were grouped together. (B) Data were quantitated from three experiments and normalised to HY101 immunoprecipitations that were arbitrarily set at 1. Error bars represent the standard error of mean.

5.2.4 GPVI SMALPs do not reveal novel phosphorylated proteins in the GPVI signalling pathway

In this section, GPVI SMALPs were used in combination with anti-pTyr Western blotting to explore whether there are any novel phosphorylated proteins in the GPVI signalosome, and how these are changed upon GPVI agonist stimulation. As stated in section 5.2.1, the anti-pTyr Western blotting is an excellent evaluation of platelet phosphor-proteome. GPVI IPs were done with one of the GPVI mAbs, 336E2, which was shown to be capable of immunoprecipitating GPVI from both detergent micelles and SMALPs (Figure 5.6). Washed human platelets (resting or CRP-activated) were lysed by NP-40 detergent, or extracted into SMALPs, subjected to IP, then the immunoprecipitated proteins were eluted and Western blotted with GPVI, FcRγ, the GPVI signalling pathway kinase Syk, and p-Tyr (Figure 5.7). IPs were performed at 4 °C overnight; for SMALP IPs, the SMALPs were firstly generated with modified SMALP working solution B (50 mM Tris pH=8, 150 mM NaCl, 10% glycerol), then the NaCl concentration was supplemented to 500 mM. p-Tyr blot on NP-40 lysates from CRP-activated platelets showed two major strong bands at ~65 kDa and ~25 kDa, presumably Syk and phosphorylated FcRγ dimer, respectively; in contrast, pTyr blot on SMALPs from CRP-activated platelets showed only one band at a similar position to the presumed FcRγ dimer band (above 25 kDa), with the strength much weaker than that in NP-40 IP (Figure 5.7A). No strikingly novel phospho-protein was revealed on pTyr blot in the IP on GPVI SMALPs. In addition, the GPVI mAb of choice, 336E2, IPed GPVI from NP-40 lysates more efficiently than from SMALPs, as shown by the stronger bands in anti-GPVI, anti-FcRγ and anti-Syk Western blotting (Figure 5.7B), which is probably due to the difference in epitope accessibility between the two solubilisation methods. pTyr blotting of whole cell lysates demonstrated that the phospho-proteome was not affected by the different solubilisation methods in these experiments (Figure 5.7C).

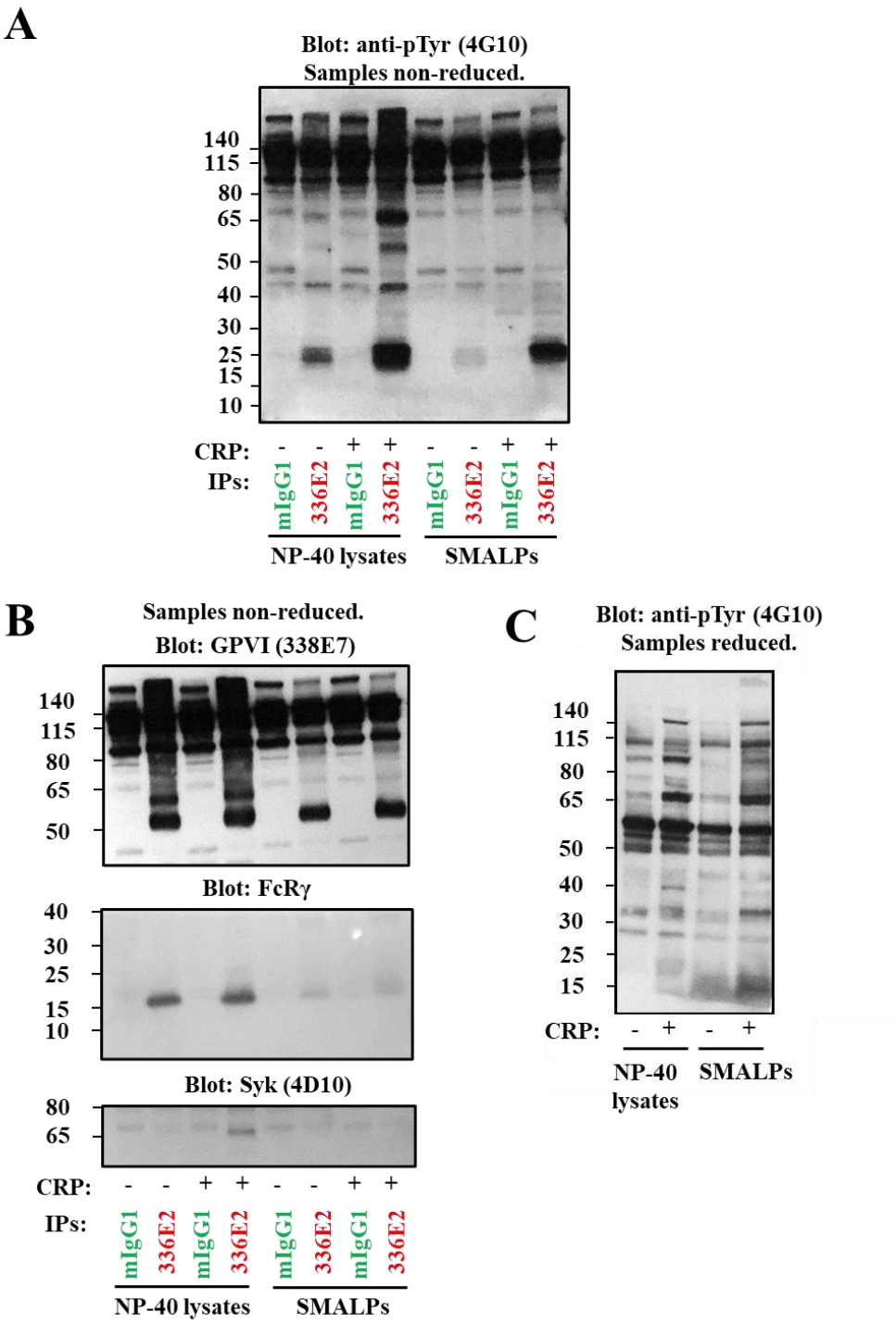


Figure 5.7 GPVI IPs on GPVI SMALPs from human platelets did not reveal novel phosphorylated proteins in the GPVI signalling pathway.

Human platelets were isolated from freshly drawn blood, stimulated with CRP, then lysed in 1% NP-40 or into SMALPs. Eluents from IPs were loaded to SDS-PAGE followed by Western blotting for p-Tyr (A), GPVI, FcRγ, and Syk (B). The whole cell lysates and whole cell SMALPs were preserved and subjected to SDS-PAGE and Western blotting for pTyr (C). Blots are representative of 4 independent experiments.

5.2.5 A novel biotinylation assay, based on co-IP, does not reveal GPVI-interacting membrane proteins, but may be useful in discovering novel membrane protein interactions

In this section, a co-IP assay, based on the strong and specific interaction between biotin and avidin, was developed for SMALPs, to explore a wide range of platelet membrane proteins and their interactions with each other (Figure 5.8). The same assay has been successfully applied to detergent lysates previously, where it was used to identify GPVI and tetraspanin Tspan9 as the components of human platelet tetraspanin microdomains, using two different detergents, Brij 97 and Triton X-100, with the former better preserving tetraspanin-tetraspanin interactions (Hemler, 2003; Le Naour et al., 2006; Protty et al., 2009). As co-IPs performed on detergent lysates have the potential for generating false positive and false negative results due to detergent artefacts, and the results are dependent on each individual detergent's capacity to solubilise membrane proteins and to preserve protein-protein interactions (Protty et al., 2009), SMALPs were adopted here for their capacity to preserve native membrane protein complexes. First, the lysines and primary amines on the extracellular side of platelet membrane proteins were labelled with biotin. This was achieved using a membrane-impermeable Sulfo-NHS-LC-Biotin reagent, where the NHS ester crosslinks primary amines. The surface-biotinylated platelets were then solubilised into SMALPs, and SMALPs subjected to IP with antibodies against a variety of membrane proteins of interest. The IPed SMALPs were eluted and applied to SDS-PAGE followed by streptavidin Western blotting. For the IPed membrane proteins, if they have partner membrane proteins, these partner proteins should be encapsulated into the same SMALPs and the whole SMALPs IPed together; thus, on streptavidin blot, each protein in IPed SMALPs should show up as a single band, and the identity of the proteins can be deduced by their molecular weights (Figure 5.8).

Using this assay, the ADAM10/Tspan15 interaction was confirmed: when IPing ADAM10 SMALPs from the surface-biotinylated platelets, one band at the size of ADAM10 (~60 kDa) showed up on streptavidin blot (Figure 5.9A and B), as well as a band just above 25 kDa which corresponds to the size of Tspan15 (Figure 5.9A); vice versa, when IPing Tspan15 SMALPs from the surface-biotinylated platelets, one band at the molecular weight of Tspan15 (above 25 kDa) as well as a band corresponding to the molecular weight of ADAM10 was present (Figure 5.9A and B). Note that the presumed Tspan15 band on streptavidin blot from ADAM10 IP had a slightly lower molecular weight than that of Tspan15 IP (Figure 5.9A), which could be because ADAM10 has an additional five other TspanC8 tetraspanin partners, of which Tspan14 and Tspan33 are expressed by platelets (Koo et al., 2022) and so likely to be present in ADAM10 SMALPs.

Another pair of membrane protein complexes, CD151 and integrin α6, where CD151 is another member of the tetraspanin superfamily and has been shown to interact with α6β1 integrin (Hemler, 2005), was also applied to this assay, and their interaction similarly confirmed in SMALPs, where integrin α6 was ~130-150 kDa and CD151 ~28 kDa (Figure 5.9A and B). Furthermore, when IPing CD9, another member of the tetraspanin superfamily that has been shown to have multiple partner membrane proteins (Reyes et al., 2018) including the scavenger receptor CD36 in platelets (Miao et al., 2001), multiple bands above the molecular weight of CD9 (~20 kDa) were observed on the streptavidin blot (Figure 5.9A); the exact identities of these proteins are unknown, but it is possible that CD9 has multiple partner membrane proteins on platelet surface, and the CD9-containing SMALPs have captured different protein complexes consisting of CD9 and its different partner proteins.

In contrast, when IPing GPVI SMALPs from surface-biotinylated human platelets with several different antibodies against GPVI, no interesting interacting protein bands were observed on streptavidin Western blot, apart from the band at the molecular weight corresponding to GPVI

itself (Figure 5.10A). No clear interacting proteins were evident either when the imaging exposure time was increased (Figure 5.10B). FcRγ did not appear on the streptavidin Western blot, possibly because it has only five amino acids in the extracellular side with only the first one being lysine, thus may not accessible to the biotin-labelling reagent here. The streptavidin blot on GPVI IPs suggests that GPVI might not have intimate membrane protein partners on platelet surface, apart from FcRγ; however, it is also possible that other GPVI interacting membrane proteins exist, but they have small extracellular regions which are not accessible to the surface biotinylation reagent in this experiment.

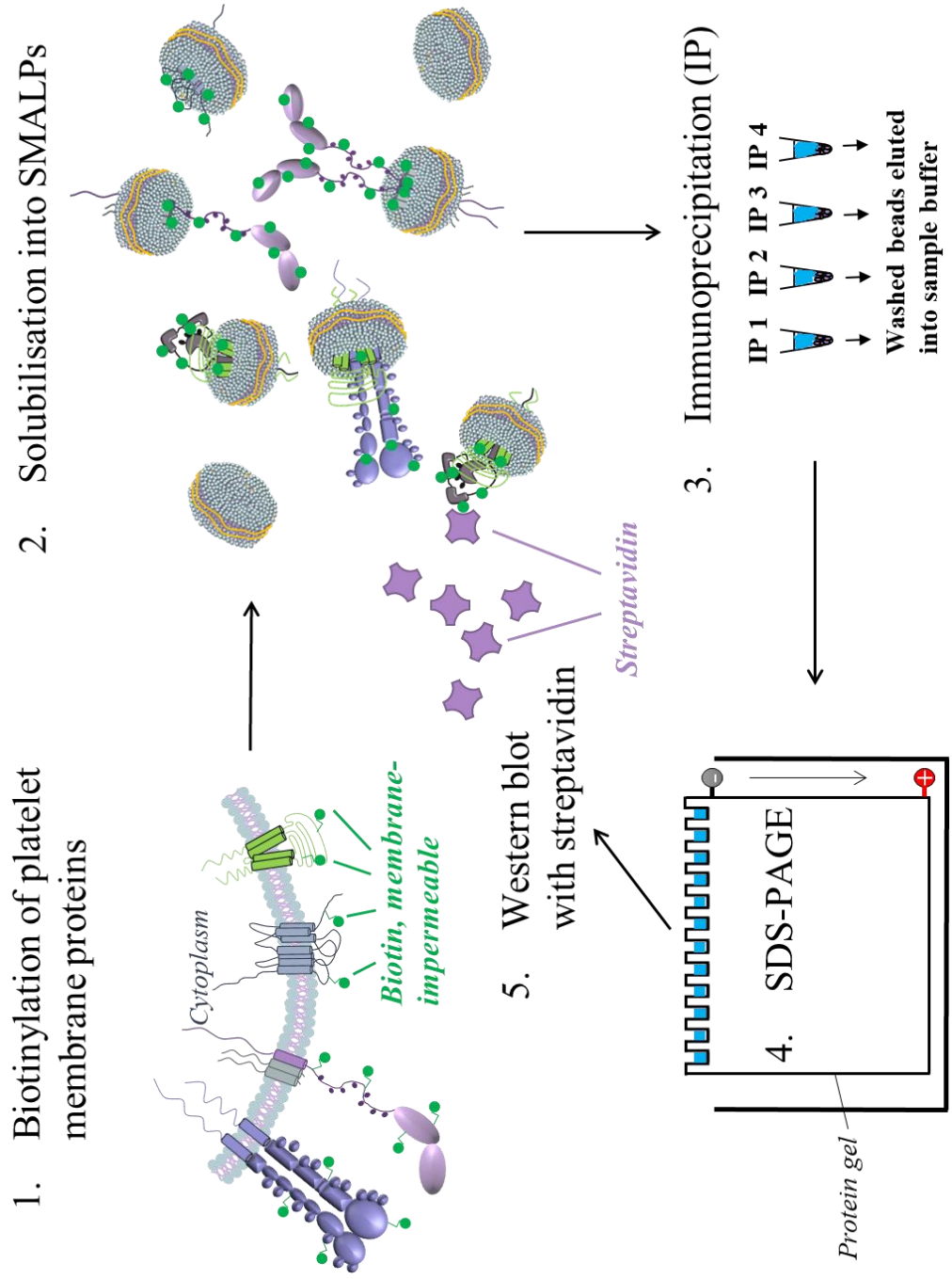


Figure 5.8 Experimental procedures of the co-IP assay on biotinylated SMALPs from human platelets.

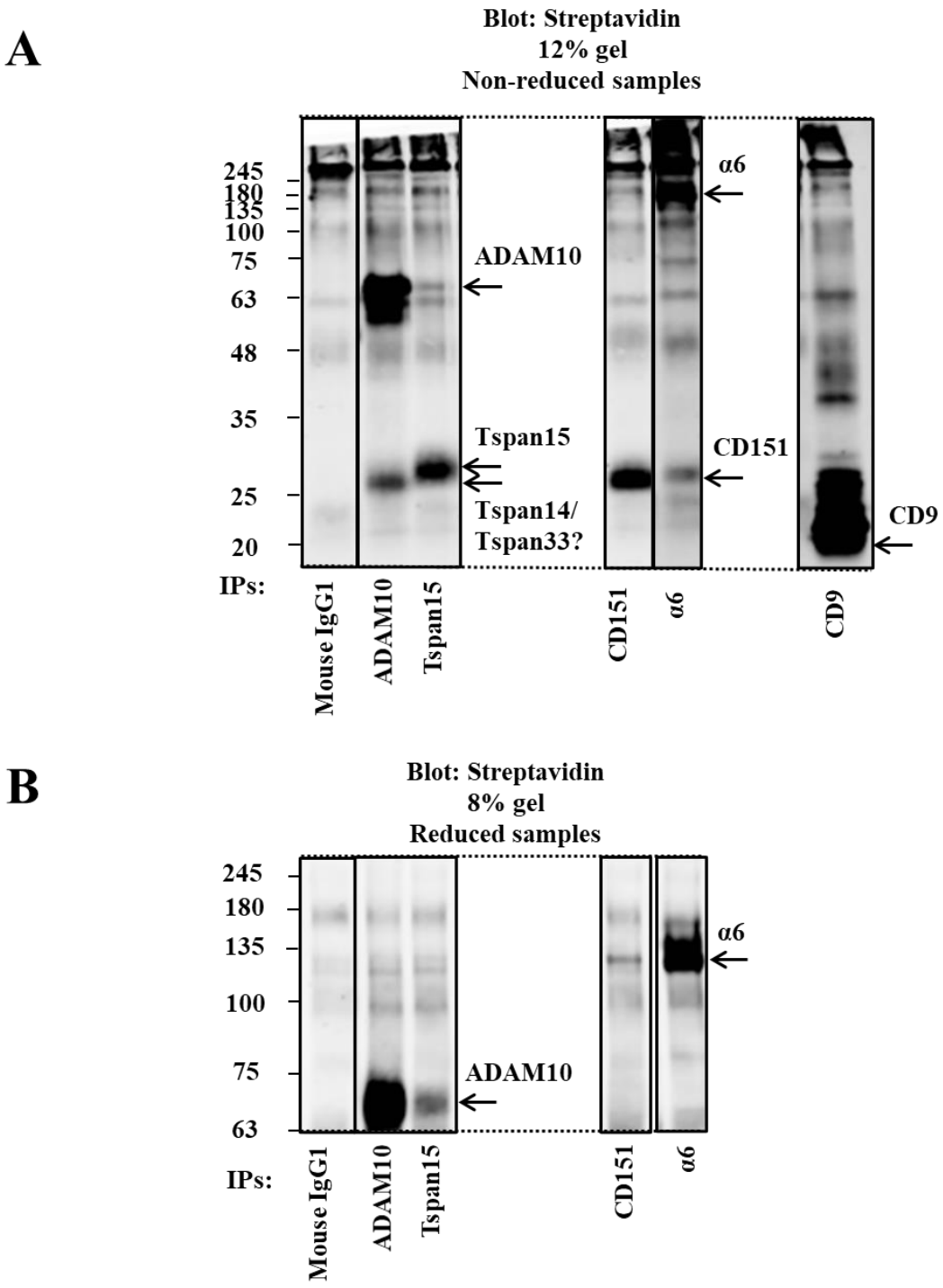


Figure 5.9 A novel co-IP assay based on biotin-streptavidin interaction is useful in confirming membrane protein interactions and for the potential discovery of novel protein interactions.

Washed platelets were surface biotinylated, solubilised into SMALPs and IPed with the indicated antibodies. The IPs were eluted into Laemmli sample buffer, and subjected to SDS-PAGE followed by Western blotting for streptavidin. Blots are representative of 3 independent experiments.

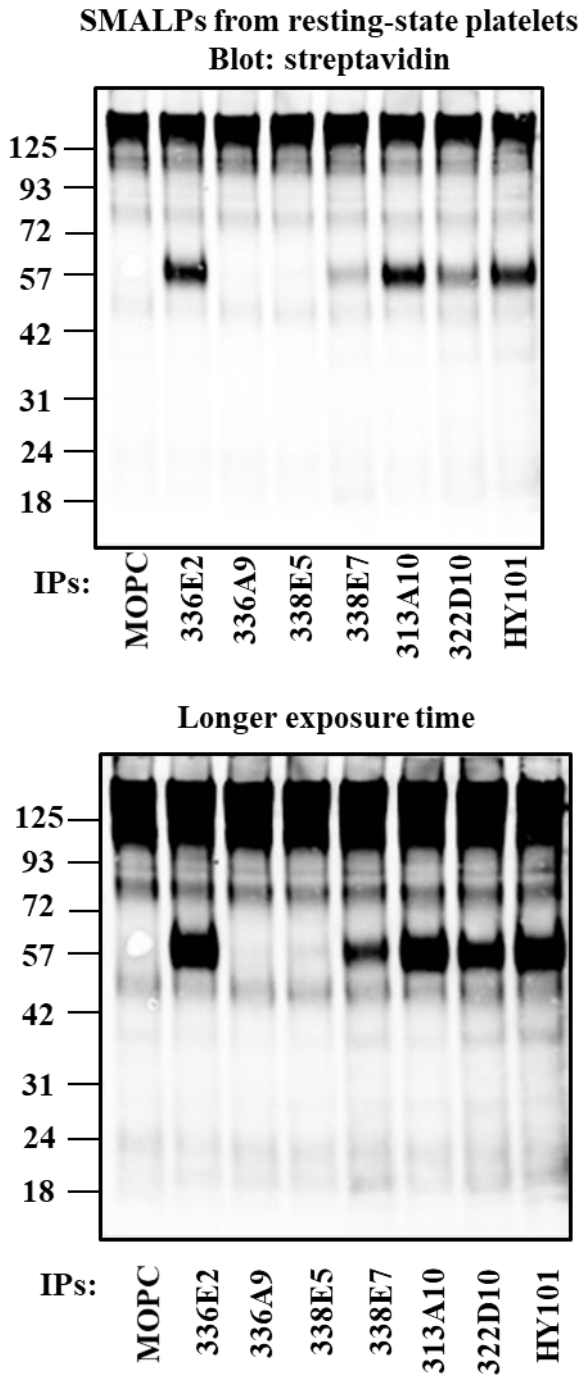


Figure 5.10 Immunoprecipitation of GPVI SMALPs from human platelets does not reveal novel GPVI-interacting membrane proteins.

Washed platelets were surface biotinylated, solubilised into SMALPs and IPed with GPVI mAbs as indicated. The IPs were eluted and subjected to SDS-PAGE followed by Western blotting for streptavidin. Blots are representative of two independent experiments.

5.2.6 A novel native PAGE method, SMA-PAGE, can be used for the investigation of platelet membrane protein interaction and stoichiometry

The aims of this section were to establish an SMA-PAGE protocol (Pollock et al., 2019) that can be performed routinely on unpurified human platelet SMALPs for a wide range of membrane proteins, and to explore whether this optimised SMA-PAGE protocol can be used to investigate human platelet membrane protein interaction and stoichiometry. In the optimised SMA-PAGE protocol, SMALPs were generated from freshly isolated human platelets with optimised SMALP solution B (50 mM Tris pH=8, 150 mM NaCl, 10% glycerol); after SMALPs were formed and separated from the unsolubilised debris, the NaCl concentration in the solution was supplemented to 500 mM to prevent the potential aggregation of SMALPs. The samples were then mixed with native sample buffer, loaded on native PAGE and Western blotted with antibodies to a variety of membrane proteins of interest. The resulting blots should show the molecular weights of protein assemblies, which are formed by the blotted membrane protein together with their interacting proteins, within the same SMALPs.

The first selected membrane protein for platelet SMA-PAGE analysis was CLEC-2, a platelet-activating receptor at 2,000-4,000 molecules per human platelet (Haining et al., 2019; Rayes et al., 2019), which is ~33-35 kDa in the monomeric form on SDS-PAGE, but has been reported to form dimers and higher order oligomers on the platelet surface and in solution (Hughes et al., 2010; Martin et al., 2021; Pollitt et al., 2014). For CLEC-2 blots on SMA-PAGE, a major band of ~48 kDa was detected, with multiple additional bands that may represent SMALPs with multimeric forms of CLEC-2 or unidentified associated proteins (Figure 5.11A). To gain insights into whether the ~48 kDa band represented monomeric CLEC-2 SMALPs, two different recombinant CLEC-2 proteins were compared to CLEC-2 SMALPs, namely CLEC-2-His (monomeric) and CLEC-2-IgFc (dimeric), although they have not been run on SMA-PAGE before and it was unclear how they would run in this gel system. CLEC-2-His showed

two major bands on SMA-PAGE at the same molecular weight of the ~48 kDa CLEC-2-SMALP band, and the higher molecular weight band of ~132 kDa which also existed in CLEC-2 SMALPs (Figure 5.11A). The higher ~132 kDa band may represent a CLEC-2 dimer formed through ectodomain interactions. The CLEC-2-IgFc, on the other hand, showed relatively high-molecular weight bands, similar to the case of 1% Brij platelet lysates (Figure 5.11A), possibly because of receptor clustering or poor separation of this soluble, recombinant protein in a native PAGE setting (i.e. without SDS). The band patterns from both resting and rhodocytin (Rho)-activated platelets were similar (Figure 5.11A), where rhodocytin is a snake venom toxin agonist for CLEC-2 (Suzuki-Inoue et al., 2006). Taken together, this suggests that CLEC-2 exists as a mixture of monomer and dimers on human platelets, with the monomer dominating. However, a definitive conclusion cannot be drawn from this data because of the complications in comparing CLEC-2-SMALPs with recombinant CLEC-2 on SMA-PAGE. It is also unclear precisely how the presence of the SMA belt and lipids would affect the mobility of the CLEC-2-SMALP, although a contribution of ~5-10 kDa was shown previously (Lee et al., 2016; Pollock et al., 2019).

The second selected protein was GPVI, with a molecular weight of ~57 kDa, which would rise to ~75 kDa considering its associated disulphide-linked FcRγ dimer of ~18 kDa. The GPVI/FcRγ SMALPs ran as a single band at ~125 kDa on SMA-PAGE, and the band patterns from resting state and CRP-activated platelets were the same (Figure 5.11B). This size was smaller than an expected dimer (~160 kDa including SMA and lipids), but larger than an expected monomer (~85 kDa including SMA and lipids), indicating that it might consist of a GPVI/FcRγ complex together with an interacting protein. This putative protein could be either a membrane protein, or a protein located intracellularly but associated with the GPVI/FcRγ complex. It does not appear to be the Src family kinase Lyn, a cytoplasmic protein previously reported to interact with GPVI tail (Ezumi et al., 1998; Suzuki-Inoue et al., 2002), because Lyn

was not detected at ~125 kDa by Western blot of SMA-PAGE (data not shown). This suggests that the association between GPVI/FcRγ complex and Lyn was not preserved during the SMALP generation and SMA-PAGE procedures described here. Follow-up studies, such as using mass spectrometry proteomics, would be needed to identify the protein components of this ~125 kDa band.

The third protein to be investigated was integrin αIIb, which forms a dimer with integrin β3, and αIIbβ3 is uniquely expressed by platelets (Bledzka et al., 2019). The αIIb blot on SMA-PAGE showed three major bands, one approximately at the size of an αIIbβ3 heterodimer (just below 242 kDa), one approximately at twice the size of an αIIbβ3 heterodimer (just below 480 kDa), and one more minor band approximately at four times the size of an αIIbβ3 heterodimer (between 720 and 1048 kDa) (Figure 5.11C). This suggests that αIIbβ3 exists predominantly as a single heterodimer or as a dimer of heterodimers, although given that αIIbβ3 is the most highly expressed platelet membrane protein, a proportion of these dimers could have been captured within a SMALP by chance, in the absence of any direct interaction. The observation of the potential dimers and tetramers of the whole complex of αIIbβ3, has not been shown elsewhere before.

The fourth protein to be studied was GPIbα, the vWF receptor on platelets that plays an important role in platelet tethering to sites of vascular injury, and is expressed at 25,000-35,000 molecules per platelet (Burkhart et al., 2012; Li, 2019; Zeiler et al., 2014). GPIbα is a ~135 kDa transmembrane protein and is a part of the large transmembrane receptor complex of GPIb-IX-V. As described in section 1.2.3, GPIb is formed by one GPIbα disulphide-linked to two GPIbβ (~26 kDa) (Luo et al., 2007), the GPIb-IX complex is formed by one GPIX (~20 kDa) disulphide-linked to one GPIb (the $\alpha\beta_2$ complex), and GPV weakly interacts with the GPIb-IX complex presumably through polar interactions (Feng et al., 2006; Li & Emsley, 2013). While the stoichiometry within the GPIb-IX complex is relatively well defined (Luo et

al., 2007), there have been controversies regarding the ratio of GPIb-IX to GPV, such as whether a GPV is associated with one or two GPIb-IX complexes (Li, 2019). In SMA-PAGE blots for GPIbα, major bands were detected at ~334 and ~518 kDa (Figure 5.11D), with a smeary appearance that is likely due to heterogenous glycosylation of GPIb-IX-V proteins and the diffusion behaviours of GPIb-IX, the later has been shown to count for the interaction of GPIb-IX with other membrane proteins than GPV (Arthur et al., 2005; Sullam et al., 1998). The bands at ~334 and ~518 kDa, could potentially represent GPIb-IX-V and $(GPIb\text{-}IX)_2$-V, respectively.

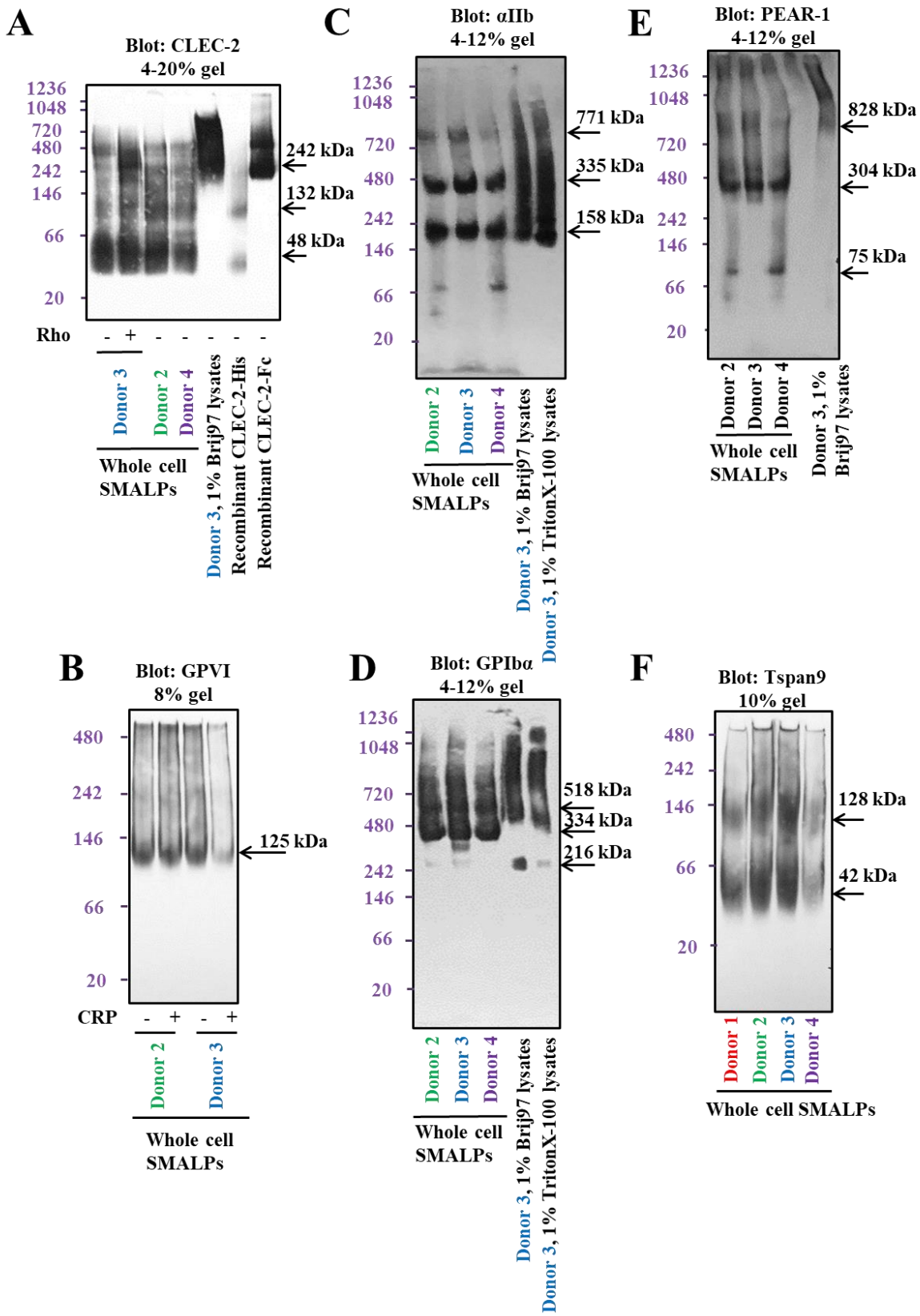
The fifth chosen protein was Platelet Endothelial Aggregation Receptor-1 (PEAR-1), a 150 kDa transmembrane protein that plays an activatory role on platelets (Kardeby et al., 2021; Nanda et al., 2005), On SMA-PAGE, PEAR-1 ran mainly as a ~300 kDa band with some minor higher molecular weight bands, as well as a ~75 kDa band in two of the three donors (Figure 5.11E), the latter possibly due to protein degradation. There was evidence that PEAR-1 tyrosine phosphorylation can be triggered by homoclustering of this receptor, induced by immune-clustering (Nanda et al., 2005); thus, the ~300 kDa band might represent a PEAR-1 homodimer.

The sixth protein to be tested by SMA-PAGE was tetraspanin Tspan9, a ~27 kDa protein that interacts with GPVI and is required for normal GPVI lateral mobility in the membrane and signalling, although there is no strong evidence for a direct interaction between Tspan9 and GPVI (Haining, Matthews, et al., 2017; Protty et al., 2009). On SMA-PAGE, Tspan9 ran as two major bands at ~128 kDa and above 42 kDa (Figure 5.11F). This suggests that Tspan9 is present as a monomer and possibly in complex with GPVI/FcRγ, given the co-migration in Figures 5.11B and 5.11F.

Tspan15 was the seventh to be investigated, and ran as 832 and 70 kDa bands (Figure 5.11G). This provided no clear evidence of the predicted heterodimer with ADAM10 at ~90 kDa, the

structure of which was recently solved using cryo-EM (Lipper et al., 2022), unless the heterodimer runs at a slightly lower molecular weight than expected. The 832 kDa band was striking but was only strongly evident in two of the three donors (Figure 5.11G). In contrast, ADAM10 ran predominantly at ~90 kDa on SMA-PAGE (Figure 5.11H), suggesting that it does indeed exist as a heterodimer with a TspanC8 such as Tspan15. This raises doubt as to the specificity of the Tspan15 antibody used in Figure 5.9G.

Finally, two additional tetraspanins, CD151 and CD9, were tested together with their potential partners on platelets, the laminin-binding integrin α6β1 (Jankovicova et al., 2020; Yang et al., 2012) and the scavenger receptor CD36 (Miao et al., 2001), respectively. The CD151 blot on SMA-PAGE showed a band of ~78 kDa, but with considerable smearing of the band to higher molecular weight forms, and an unexplained absence of signal for one of the donors (Figure 5.11I). This pattern did not correspond to the α6 blot, which showed a major band of ~269 kDa (Figure 5.11J) that is strikingly similar to the predicted ~280 kDa for α6β1. This lack of evidence for a CD151/α6β1 interaction in platelets is not consistent with successful co-IPs of these proteins in relatively stringent detergent (Protty et al., 2009), but it is possible that the CD151 antibody used was not specific to CD151. The CD9 blot on SMA-PAGE showed strong smears spreading from below 66 kDa to above 242 kDa (Figure 5.11K), possibly corresponding to the fact that this tetraspanin is the second most highly expressed membrane protein on platelets at ~50,000 molecules per platelet (Protty et al., 2009), and may have multiple partners and/or multiple proteins in sufficient proximity to co-localise with in SMALPs. CD36 blots on SMA-PAGE were also quite smeary with the bands spanning a wide molecular weight range (Figure 5.11L), thus it is not possible from these data to conclude that CD9 and CD36 exist in complex with each other.


A
Blot: CLEC-2
4-20% gel
1236
1048
720
480
242
146
66
20
242 kDa
132 kDa
48 kDa
Rho
- + - - - - -
Donor 3
Donor 2
Donor 4
Donor 3, 1% Brij97 lysates
Recombinant CLEC-2-His
Recombinant CLEC-2-Fc
Whole cell SMALPs
C
Blot: αIIb
4-12% gel
1236
1048
720
480
242
146
66
20
771 kDa
335 kDa
158 kDa
Donor 2
Donor 3
Donor 4
Donor 3, 1% Brij97 lysates
Donor 3, 1% TritonX-100 lysates
Whole cell SMALPs
E
Blot: PEAR-1
4-12% gel
1236
1048
720
480
242
146
66
20
828 kDa
304 kDa
75 kDa
Donor 2
Donor 3
Donor 4
Donor 3, 1% Brij97 lysates
Whole cell SMALPs
B
Blot: GPVI
8% gel
480
242
146
66
20
125 kDa
CRP
- + - +
Donor 2
Donor 3
Whole cell SMALPs
D
Blot: GPIbα
4-12% gel
1236
1048
720
480
242
146
66
20
518 kDa
334 kDa
216 kDa
Donor 2
Donor 3
Donor 4
Donor 3, 1% Brij97 lysates
Donor 3, 1% TritonX-100 lysates
Whole cell SMALPs
F
Blot: Tspan9
10% gel
480
242
146
66
20
128 kDa
42 kDa
Donor 1
Donor 2
Donor 3
Donor 4
Whole cell SMALPs

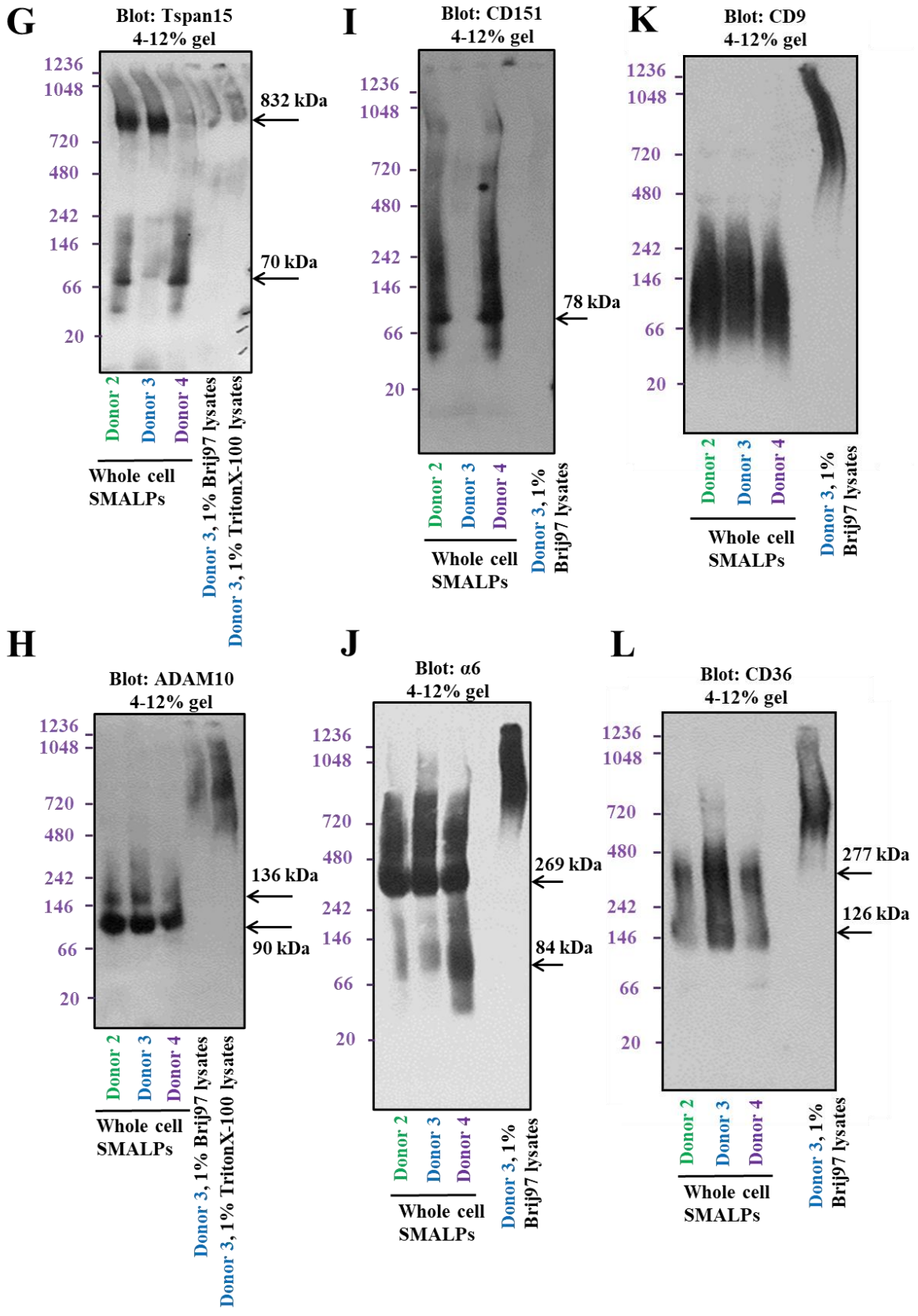

G
Blot: Tspan15
4-12% gel
1236
1048
720
480
242
146
66
20
832 kDa
70 kDa
Donor 2
Donor 3
Donor 4
Whole cell SMALPs
Donor 3, 1% Brij97 lysates
Donor 3, 1% TritonX-100 lysates
I
Blot: CD151
4-12% gel
78 kDa
Donor 3, 1% Brij97 lysates
K
Blot: CD9
4-12% gel
H
Blot: ADAM10
4-12% gel
136 kDa
90 kDa
J
Blot: α6
4-12% gel
269 kDa
84 kDa
L
Blot: CD36
4-12% gel
277 kDa
126 kDa

Figure 5.11 SMA-PAGE on human platelet SMALPs followed by Western blotting revealed the molecular weights of protein complexes.

Washed human platelets were stimulated with agonists if indicated, and then solubilised into SMALPs or with the indicated detergents. All samples loaded on SMA-PAGE were mixed with 5x native sample buffer without boiling prior to loading. The gel was then subjected to Western blotting with the indicated antibodies. The approximate molecular weight of each protein band or smear was calculated by measuring the distance that each molecular weight marker migrated on the gel, plotting against the log10 values of the molecular weight of each marker to get a regression curve, and fitting the travelling distance of the band in question into the curve.

5.3 Discussion

In this chapter, a simplified protocol of generating SMALPs from washed human platelets, for bench-top biochemical experiments to investigate platelet receptor interactions, was developed. The key differences between this new protocol and that described by Lee et al. (Lee et al., 2016) was that high pressure C3 cell homogenisation and membrane preparation steps were removed. Furthermore, the SMALP buffer was optimised by reducing the NaCl concentration from 500 mM to 150 mM, because the higher concentration was found to induce platelet activation. The resulting SMALP generation conditions successfully preserved native membrane protein complexes such as GPVI/FcRγ and ADAM10/Tspan15.

When using the five new GPVI mAbs from Bernhard Nieswandt's lab to IP GPVI from platelets, the relative IP efficiencies among mAbs were different when IPing GPVI from detergent (Triton X-100) lysates and from SMALPs. This could be due to differences in epitope accessibility when GPVI is solubilised with different strategies. SMALPs have been reported to preserve the native conformation of the encapsulated proteins, such as in the case of RhD and RhCE proteins from erythrocytes. A conformation-specific RhD antibody can IP SMALPs containing RhD from RhD^+ populations, whereas the Rh proteins solubilised into detergent micelles were unable to be detected by conformation-specific RhD antibodies, indicating that at least one important comformation of RhD epitope was preserved in SMALPs from erythrocyte membrane (Apoil et al., 1997; Desrames et al., 2020; Goossens et al., 1987). It has also been shown that membrane proteins in SMALPs are more stable than in detergent micelles, for example, $A_{2a}R$, a member of GPCR family, displayed increased thermostability and tolerance to freeze-thaw cycles when solubilised into SMALPs compared to DDM micelles (Jamshad, Charlton, et al., 2015). Thus, the epitope-recognising difference in GPVI IPs from detergent micelles and from SMALPs, may reflect a more native-like GPVI conformation in SMALPs, highlighting the potential of applying SMALP-encapsulated proteins for the

screening of small molecule agonists/inhibitors and antibodies, as stated by the aforementioned SMALP study on RhD/RhCE proteins as well (Desrames et al., 2020). On the other hand, SMALPs have been reported to trap certain conformational states of their encapsulated membrane proteins. The partial agonist-bound structure of glycine receptors (GlyR) was solved only when they were extracted into SMALPs (Yu et al., 2021). The ATP-binding cassette (ABC) transporter, Sav1866, when extracted into SMALPs, lost its capacity to hydrolyse ATP; this could be due to the conformational constraints of the transporter in SMALPs, such that it was trapped in a certain state and not as mobile as in native cell membrane, although it could also be due to SMA binding the Mg^{2+} in solution which is essential for the function of the transporter (Pollock et al., 2022). Given these previous examples, it could also be the case that SMALPs trap certain GPVI conformations or restrict its mobility, thus impacting on antibody recognition. The relatively rigid nanodisc shape and the existence of surrounding lipids in SMALPs may also provide more steric hindrance to the encapsulated GPVI for it to be recognised by certain mAbs. The epitopes of these new mAbs to GPVI will need to be mapped for further explanation of the data here.

The GPVI membrane interactome and pTyr signalosome were also explored, using IPed GPVI SMALPs from human platelets, with comparison to detergent lysates. A co-IP assay, based on biotin-labelling of surface proteins and streptavidin Western blotting, did not reveal novel membrane proteins that co-localise with GPVI in SMALPs. However, the co-IP assay here is dependent on biotinylation of membrane proteins on primary amines, thus it can miss some membrane proteins with small extracellular regions, such as FcRγ. Similarly, GPVI IP of SMALPs did not reveal novel pTyr proteins in the GPVI signalling pathway. A band corresponding to the molecular weight of FcRγ was the only major band identified. In future, mass-spectrometry based methods could be adopted on the IPed GPVI SMALPs from human platelets for the discovery of novel regulatory and signalling proteins, although such

experiments will need to be carefully controlled with detergent-isolated GPVI and whole-cell SMALPs, and the results will need to be further validated by binding and functional assays. In addition, it is not clear how well SMALPs can preserve the interaction between integral membrane proteins and their intracellular signalling partner proteins, and this could be dependent on different membrane proteins and their cytosol partners. It has been reported that in erythrocytes, when isolating the membrane by hypotonic lysis with buffers of different ionic strength, the spectrin-based skeleton can either be retained with or depleted from the generated SMALPs (Desrames et al., 2020). To further investigate whether this is also the case with GPVI and the proteins in its phosphor-signalosome, the pTyr profile of GPVI SMALPs that were generated in buffers with different ionic strength could be compared.

Although not detected by the novel, biotinylation-based co-IP assay, GPVI and FcRγ were confirmed to co-exist in the same SMALPs by GPVI IP and anti-FcRγ Western blotting. Similarly, ADAM10 and Tspan15 were confirmed to co-exist in the same SMALPs by IP of one protein and Western blotting for the other, and this membrane protein complex was also revealed by the biotinylation-based co-IP assay, confirming the capacity of this assay to detect platelet membrane protein interactions. An intimate interaction between ADAM10 and Tspan15 was previously suggested by various methods, including co-immunoprecipitation of endogenous proteins from stringent detergent lysates (Koo et al., 2020). More recently, the cryo-EM structure in detergent micelles has revealed a heterodimer in which the ADAM10 extracellular region makes two major contacts with Tspan15, with the tetraspanin appearing to control the distance of ADAM10 metalloprotease domain cleavage site from the cell membrane (Lipper et al., 2022). The established interaction of tetraspanin CD151 and integrin α6 was also potentially revealed by this co-IP assay, as shown by the existence of a ~28 kDa band on streptavidin blot in α6 IP, and the existence of a ~120 kDa band on the streptavidin blot in CD151 IP. However, specific Western blots for both CD151 and α6 will be needed for

confirmation. Evidence that this co-IP assay has the potential for the discovery of novel interactions for membrane proteins was evident from the streptavidin blot on CD9 IP, which showed multiple protein bands with unknown identities. These are potentially the membrane proteins that come into close proximity with this tetraspanin on the platelet surface, and thus their functions could be regulated by CD9. To identify these proteins, Western blotting with specific antibodies or mass-spectrometry based detection is required.

The SMA-PAGE method followed by Western blotting was also adopted to investigate membrane protein interactions and stoichiometry, and was applied to several platelet membrane proteins in this chapter. An important caveat in this method is that it relies on Western blotting antibodies being specific, so any interesting findings must be verified using other methods. For GPVI, its existence as a mixture of monomers and dimers on the cell surface in transfected cell lines, and at least partially as dimers on human platelets, has already been reported (Clark, Neagoe, et al., 2021). Following SMA-PAGE from platelets and GPVI Western blotting, there was one major band of ~125 kDa. Even estimating an SMA plus lipid contribution of ~10 kDa (Lee et al., 2016; Pollock et al., 2019), this molecular weight is greater than the currently accepted stoichiometry of GPVI monomer plus two FcRγ chains (~85 kDa), but lower than a dimer of GPVI-FcRγ complexes (~170 kDa). Therefore, the GPVI/FcRγ complex may include an additional protein. Interestingly, SMA-PAGE followed by Tspan9 blotting revealed a band of ~128 kDa and another of ~42 kDa. The latter may be monomeric Tspan9, given its molecular weight of ~27 kDa, but the larger band may represent a Tspan9/GPVI/FcRγ complex. Previous research on Tspan9 is limited, but two publications support the idea GPVI/FcRγ forms a complex with Tspan9. In the first, Tspan9 antibodies were generated and used to show that Tspan9 is expressed by platelets but not most other cell types, similar to the platelet-specific GPVI, and has a similar copy number to GPVI in human platelets (Protty et al., 2009). In the second publication, Tspan9 knockout mice were generated and

found to have partially impaired platelet activation in response to triggering of GPVI, but not other platelet receptors (Haining, Matthews, et al., 2017). Furthermore, confocal microscopy showed co-localisation of Tspan9 and GPVI in platelets, and the two proteins co-immunoprecipitated each other, albeit only in relatively low-stringency detergent (Haining, Matthews, et al., 2017). Neither methodologies proved a direct interaction. Nevertheless, single particle tracking showed GPVI lateral diffusion to be reduced by 50% in the absence of Tspan9, providing evidence for a functional interaction between the two proteins (Haining, Matthews, et al., 2017). However, the GPVI IPs from SMALPs of surface biotinylated platelets, followed by standard PAGE and streptavidin blotting, did not reveal a ~27 kDa band that could correspond to Tspan9, although this could be a sensitivity issue if Tspan9 is not efficiently biotinylated in this assay. In future, to provide more definitive evidence for the existence of a Tspan9/GPVI/FcRγ complex, GPVI IPs of SMALPs should be followed by Tspan9 Western blotting. If real, a tetrameric Tspan9/GPVI/FcRγ complex would be strikingly similar to the well-characterised FcεRI on mast cells, which functions as the high affinity receptor for IgE. This tetrameric complex comprises the FcεRIα chain, which binds IgE and has sequence and structural similarity to GPVI, the FcRγ homodimer and FcεRIβ, which has the same four-transmembrane topology as Tspan9 but is not a tetraspanin. The existence of Tspan9/GPVI/FcRγ complexes would have implications for the current clinical trials that are aiming to inhibit GPVI-induced platelet activation to treat heart attack and ischaemic stroke. Indeed, targetting Tspan9 may provide a novel way to inhibit GPVI function.

The band pattern on CLEC-2 blot on SMA-PAGE was very similar to the pattern on recombinant CLEC-2 monomers, suggesting the majority of CLEC-2 existing in monomer forms on human platelet membrane. CLEC-2 dimerisation has been shown to be essential for its downstream signalling, as the two SH2 domains of Syk are both crucial to CLEC-2 activation, and thus two CLEC-2 molecules are needed for SH2 binding, as there is only a hem-

ITAM in one CLEC-2 molecule (Fuller et al., 2007; Rayes et al., 2019). The higher band in the recombinant CLEC-2-His on SMA-PAGE may represent the homophilic interactions between different CLEC-2 molecules, as reported by Suzuki-Inoue et al. that soluble CLEC-2 can bind platelets and CLEC-2-coated surface (Suzuki-Inoue et al., 2010). This type of homophilic interaction may also exist in CLEC-2 SMALPs from human platelets, such that the CLEC-2 molecules from individual SMALPs interact with each other at their extracellular region. Moreover, as the CLEC-2 in SMALPs were embedded in lipid bilayer, the dimers and oligomers formed on membrane surface could also be encapsulated. These different types of CLEC-2 oligomers, in addition to the fact that CLEC-2 possesses different glycosylation forms on platelet surface, could be the reasons why so many bands and smears appeared on the CLEC-2 blot on SMA-PAGE (Figure 5.8A). Other platelet membrane proteins may be close to and regulate CLEC-2 function, for example, tetraspanin CD37 (de Winde et al., 2018), and these membrane proteins may be encapsulated in CLEC-2 SMALPs, contributing to the complexity of the band patterns.

To summarise, the work in this chapter has (1) optimised the SMALP generation pipeline from human platelets, (2) demonstrated that native membrane protein complexes on the platelet surface can be preserved in SMALPs, (3) shown differential recognition of GPVI in SMALPs versus detergent micelles, suggesting different GPVI conformations from the two isolation methods, and (4) optimised SMA-PAGE and developed a novel co-IP assay based on platelet surface protein biotinylation and streptavidin Western blotting to identify platelet membrane protein interactions and stoichiometry. The work in this chapter emphasises the potential of utilising SMALPs in identifying novel regulatory mechanisms and new antiplatelet drug targets for thrombotic diseases, while also highlights the versability of SMALPs.

CHAPTER 6

General discussion

Chapter 6 General discussion

6.1 Summary of results

Platelet activation crucially depends on the interaction between platelet membrane receptors and their ligands, where the ligands can be exposed to platelets at injury or plaque rupture sites. GPVI is the major collagen receptor on platelets, and it can also bind fibrin(ogen); upon binding ligands, its downstream signalling pathway is initiated through the ITAMs on the associated FcRγ. Platelets also express many other major receptors that play important roles in adhesion and/or signalling, such as integrins αIIbβ3 and α2β1, PARs, $P2Y_1$ and $P2Y_{12}$, GPIb-IX-V, CLEC-2, PEAR-1, and other membrane proteins that can regulate the functions of some of these major receptors, such as tetraspanins. Understanding the configuration of these membrane proteins, including whether and how they form dimers, oligomers and clusters, whether and how they interact with each other, and their structural details, are important for understanding of their functions and for identifying new antiplatelet drug targets to treat arterial thrombosis. However, detergent-based membrane protein extraction methods can interfere the stability, structural integrity and protein-protein interactions of the isolated proteins. In this thesis, SMALPs were adopted to extract and characterise platelet membrane receptors, and have shown promise in GPVI/FcRγ structural determination and in investigating native receptor interaction/stoichiometry on platelets. Specifically, for full-length GPVI structural determination, purified GPVI/FcRγ SMALPs from transfected HEK-293T cells showed distinct populations of GPVI oligomers, could bind collagen, and were relatively pure and single-dispersed under negative stain EM. For the investigation of receptor interaction/stoichiometry on native platelets, the SMALP-generation protocol was specifically optimised for platelets. SMALPs were shown to preserve native membrane protein complexes, and two novel biochemical assays on platelet SMALPs, based on co-IP and SMA-PAGE, were developed to discover novel membrane protein interactions and to explore protein

stoichiometry. Therefore, SMALPs have been established as a promising tool for the investigation of platelet receptor interactions, stoichiometry and structure.

6.2 The significance of utilising SMALPs for GPVI structure and stoichiometry investigations

It has been of debate whether the dimeric form of GPVI represents a unique conformation for ligand binding. Ligand binding studies, with an emphasis on collagen and fibrin(ogen) binding, have generated contradictory results. Originally, Miura et al. showed that fibrous collagen binds to the dimeric form, but not the monomeric form of GPVI, as the recombinant GPVI-Fc protein (the extracellular domain of GPVI fused with dimeric human Fc) inhibited collagen-induced platelet aggregation, but the recombinant monomeric GPVIex protein (the extracellular domain of GPVI) did not (Miura et al., 2002). Their GPVI-Fc protein also exhibited high affinity for immobilised collagen, but the dissociation constant of GPVIex was too low to be measured (Miura et al., 2002). They concluded that the GPVI dimer may possess a specific conformation for collagen binding; alternatively, the collagen binding difference between GPVI monomer and dimer could also be attributed to increased avidity. The dimer-specific conformation idea was later reinforced by several dimer-specific antibodies, namely m-Fab-F, 204-11 and 9E18. M-Fab-F and 204-11 were shown to bind specifically to dimeric, recombinant GPVI but not monomeric GPVI by ELISA, while 204-11 binding increased m-Fab-F binding, suggesting it promoted a conformational change in GPVI dimer (Jung et al., 2012; Jung et al., 2009; Moroi et al., 2003). 9E18 bound dimeric GPVI with a 200-fold higher affinity than to monomeric GPVI (Loyau et al., 2010). These findings, together with the first crystal structure of GPVI extracellular domains that shows a back-to-back dimer with the interface at the D2 domains (Horii et al., 2006), favour the idea of "active dimer".

A few more recent findings, however, disproved the "active dimer" idea, where recombinant monomeric GPVI was shown to bind immobilised collagen by SPR and ELISA, although with lower affinity than recombinant dimeric GPVI (Onselaer et al., 2017; Xu et al., 2021). In addition, there have been controversies over whether monomeric or dimeric GPVI bind

fibrin(ogen); due to the differences in the fibrinogen- and fibrin-related reagents and GPVI expression constructs by different research groups, this issue is still inconclusive (Slater et al., 2018). Moreover, the deletion of the D2 domain of GPVI, shown to be crucial for GPVI dimerisation, did not abolish GPVI signalling in a transfected B cell line (Clark, Neagoe, et al., 2021). Bioluminescence resonance energy transfer (BRET) studies showed that GPVI existed as a mixture of monomer, dimer and higher order oligomers in transfected cell lines, and at least partially dimers on resting platelets (Berlanga et al., 2007; Clark, Neagoe, et al., 2021). These findings have questioned the functional significance of GPVI dimer.

Current structural information on GPVI is limited, with the original GPVI structure (without ligand) and a recent structure (with CRP) showing back-to-back dimers, and an inhibitory nanobody-bound structure showing a domain-swapped dimer (Feitsma et al., 2022; Horii et al., 2006; Slater et al., 2021). All three structures showed the dimer interface in the D2 domain, and they are all crystal structures of the D1 and D2 domains of GPVI. Not only do they lack the structural information in other parts of GPVI, but they also generated contradictory insights into the dimeric interface. In addition, an earlier report showed GPVI can dimerise through a disulphide bond at C338 in its intracellular tail, though its functional significance was not determined and its importance questionable because this cysteine residue is not conserved in mice (Arthur et al., 2007). As this disulphide-linked GPVI dimer was observed within 10-30 s of convulxin activation, the authors suggested that GPVI dimers mediated by extracellular domain interaction are pre-existing on the platelet surface, so that the disulphide linking in their cytoplasmic domains can happen rapidly following agonist binding (Arthur et al., 2007). Therefore, this data suggests that regions of GPVI outside of the D1 and D2 domains may play a role in GPVI dimerisation and potentially clustering. In the original GPVI D1-D2 dimer crystal structure, the same construct failed to dimerise when suspended in solution; however, as stated by the authors, the missing stalk regions may help to stabilise receptor dimerisation,

as in the case of CD94, and the association affinity on the 2D cell membrane could be higher than the 3D space in solution (Boyington et al., 2000; H. Chen et al., 2002; Horii et al., 2006). Taken together, the structurally unsolved region of GPVI could play important physiological roles, and a full-length GPVI structure, ideally in complex with FcRγ, may provide essential information with regards to GPVI stoichiometry, ligand-binding mode and mechanisms of downstream signalling.

GPVI/FcRγ encapsulated in SMALPs could be a great solution for full-length GPVI structure determination. The number of membrane protein structures solved in SMALPs has increased substantially in the last few years. Moreover, for certain membrane proteins, their conformational diversity was better preserved when using SMALPs than when using other membrane protein solubilising methods. For example, the structure of glycine receptor (GlyR) in its partial agonist-binding state was resolved for the first time in SMALPs, and in the same study, SMALP-encapsulated GlyR revealed open, desensitised and expanded-open states of the receptor, while the MSP-nanodisc-encapsulated GlyR only revealed one structure in its desensitised-like state. This suggests that the MSP nanodiscs may have imposed more mobility constraints on, or shifted the conformational equilibrium of, the receptor, in comparison to SMALPs (Yu et al., 2021). A GPVI/FcRγ SMALP structure could address how regions other than the D1 and D2 domains influence GPVI stoichiometry, and how the receptor complex is configured when inserted in a lipid bilayer. In chapter 4, it was demonstrated that the canonical GPVI and FcRγ of choice, with a 10xHis-tag on GPVI, can be expressed in ADAM10-knockout HEK-293T cells and isolated into SMALPs, and GPVI/FcRγ SMALPs can be purified using a Ni-NTA gravity column and gel filtration. The purified GPVI/FcRγ SMALPs were functional in binding collagen and were mono-dispersed under negative stain EM, and their protein components were relatively pure as shown by mass spectrometry. All these results

have shown the potential of purified GPVI/FcRγ SMALPs from HEK-293T cells for the structural determination of full-length GPVI in complex with FcRγ.

In future, to generate a high-resolution, full-length GPVI structure in SMALPs, optimisation of protein expression and purification will be necessary. The SMALPs obtained in Chapter 4 of this thesis were from 100 confluent 15 cm plates of transfected HEK-293T cells, yet the amount was only sufficient for the characterisation methods adopted in this thesis, including biochemical pull-down assay, mass spectrometry and negative stain EM, but not enough for further biophysical characterisation methods such as analytical ultracentrifugation (AUC). The amount of single dispersed particles collected from negative stain EM was also too low for a 3D structure to be constructed. It will therefore be of benefit to use a suspension cell line, such as HEK-293F, instead of the current adherent HEK-293T cells, since suspension HEK-293F cells can be grown up at much higher density than on plates, and avoid the need for laborious harvesting of adherent cells by scraping. Current efforts by other members in the Tomlinson and Watson groups have involved generating an ADAM10 knockout, suspension HEK-293F cell line. Utilising GPVI/FcRγ-transfected HEK-293F cells and a shaking incubator for cell culturing, the amount of HEK cells that can be collected in one experiment has been greatly increased.

For the GPVI/FcRγ-SMALPs purified in this thesis, the gel filtration profile suggested that the particle sizes were quite diverse; although these different particles can be separated by gel filtration, the steep slope in between the two major peaks indicated that the species in each fraction could still be heterogenous in size, which was actually confirmed by the negative stain EM image of fraction 7. These different species could be different orders of oligomer of the GPVI/FcRγ complex, and solving the structures of different oligomers could provide important insights into GPVI oligomerisation. However, for high-resolution structure determination, it would be better to obtain more homogeneous samples, representing one or two oligomerisation

states, rather than a series of different order oligomers. Moving forward, it could be beneficial to "lock" the GPVI/FcRγ complex in a specific oligomerisation state by incubating the isolated membrane with multivalent GPVI ligands, for example, dimeric or tetrameric nanobodies of GPVI, which have well-defined valency in contrast to other multivalent ligands such as collagen, CRP and CVX (Cheung et al., unpublished work). Such efforts could potentially substantially increase the proportion of GPVI/FcRγ complexes in a certain oligomeric state (i.e. GPVI/FcRγ dimer for dimeric nanobodies, GPVI/FcRγ tetramer for tetrameric nanobodies), while the binding of multimeric nanobodies to the GPVI/FcRγ complex could also increase the overall size of the isolated SMALPs, which is beneficial for cryo-EM structure determination. Alternatively, elevating the relative amount of GPVI monomers could improve the homogeneity of purified SMALPs, which could be achieved by reducing the amount of transfected DNA, or using HEPES buffer instead of Tris buffer for solubilisation, purification and gel filtration, as HEPES can more effectively buffer hydrogen than Tris, thus may prevent pH-related SMALP or protein aggregation. As shown by another study where CD81 was encapsulated into SMALPs, the population of particles with smaller size can be increased by this strategy (Ayub et al., 2020). The purity of GPVI/FcRγ SMALP samples also needs to be improved, which could be achieved by introducing a second epitope tag, such as FLAG, followed by a TEV cleavage site on the GPVI expression construct. This would allow a two-step purification strategy of FLAG capture, TEV cleavage and then His-tag capture.

6.3 The significance of utilising SMALPs for the investigation of platelet membrane receptor stoichiometry and interactome

Platelet receptor dimerisation and clustering are considered to play important roles in elevating their density, thus can increase the avidity to ligands and amplify downstream signalling events. In particular, ITAM receptors rely on clustering to induce platelet activation, in contrast to GPCRs which are dependent on conformational changes for activation (Montague et al., 2021). The controversy over GPVI stoichiometry and how this affects receptor function was discussed in section 6.2. The stoichiometry of the another ITAM receptor on platelets, CLEC-2, was also investigated. A previous study by Hughes et al. showed that chemical cross-linking of CLEC-2 on platelets, followed by anti-CLEC-2 Western blotting, revealed the receptor existing as a mixture of monomer, dimer and potentially higher order oligomers in resting-state platelets, while rhodocytin-stimulated platelets possessed increased amount of CLEC-2 dimer and oligomers (Hughes et al., 2010). The same study also applied immunogold labelling of CLEC-2 followed by electron microscopy, on resting and rhodocytin-stimulated mouse platelets, which similarly showed that CLEC-2 existed as both monomers and dimers on resting-state platelets, and the ratio of dimer/monomer and oligomer/monomer increased upon rhodocytin stimulation (Hughes et al., 2010). In this thesis, the SMA-PAGE data on CLEC-2 from human platelets demonstrated similar results with the co-existence of monomer, dimer and higher order oligomers in resting-state platelets, although with no clear evidence that the amount of dimer and oligomers increases upon rhodocytin stimulation. However, the rhodocytin stimulation was only performed on one of the donors here, and future experiments should use more donors for a direct comparison between resting and stimulated platelets. In contrast to the data from Hughes et al. which used detergents to solublise CLEC-2 (Hughes et al., 2010), protein solubilisation into SMALPs, followed by SMA-PAGE and Western blotting, can preserve the native state of membrane proteins in the lipid bilayer and requires no additional

labelling of the proteins, thus should introduce less interference to the native conformation and configuration of the membrane proteins, which provides technical advantages over cross-linking-based methods.

PEAR-1 is a novel aggregation receptor which is expressed on platelets and endothelial cells (Nanda et al., 2005). On platelets, it is an activating receptor with the only known endogenous ligand being being FcεRIα, and its signalling pathway includes phosphorylation of tyrosines in the cytoplasmic tail by SFK, followed by PI3K binding and Akt activation (Kardeby et al., 2021). In a previous study, a PEAR-1 antibody targeting the extracellular EMI protein-protein interaction domain potentiated washed platelet aggregation, but the Fab of the same antibody inhibited platelet aggregation, indicating that the PEAR-1-induced platelet activation was dependent on the divalency of the antibody, and that dimerisation and clustering of the receptor plays crucial role in its activation (Kauskot et al., 2012). This was supported by the SMA-PAGE data in this thesis, where the ~300 kDa band on PEAR-1 Western blot was very likely a PEAR-1 dimer, with other bands of higher molecular weight being potentially higher order oligomers (Figure 5.11E). Similarly, SMA-PAGE also revealed the existence of integrin αIIbβ3 oligomers, in this case with clearer and more definitive bands which very likely indicate the existence of αIIbβ3 heterodimer and dimer of heterodimers (Figure 5.11C). Clustering of integrins can increase their affinity for multivalent ligands, such as vWF and fibrin, as well as the binding affinity, therefore can support platelet aggregation (Bledzka et al., 2019; Plow et al., 2014; Ye et al., 2014). This SMA-PAGE data has demonstrated its suitability for the investigation of platelet receptor stoichiometry.

The function of many major platelet receptors has been intensively studied over the years. However, how their configuration on platelet surface changes upon ligand binding, and how these configuration changes impact signal transduction, are still poorly understood. It was recently proposed that platelet glycoprotein receptors are pattern recognition receptors and can

recognise a wide range of charged particles, due to the large variety of endogenous and exogenous ligands that can interact with them (Montague et al., 2021). A rapid and convenient method to map the configuration of these receptors on the platelet surface can therefore be key to capture the transient or stable configuration states of receptors under different conditions. The optimised SMA-PAGE method developed in this thesis, can serve as a convenient, closer-to-native, and relatively high-throughput way, in comparison to other biochemical methods, to explore platelet receptor stoichiometry. The traditional methods to study the stoichiometry of platelet receptors, including chemical cross-linking, confocal and super-resolution microscopy, and *in vitro* binding experiments such as ELISA and SPR, all require artificial modification of the proteins, for example, chemical labelling or the addition of tags via genetic modification of the construct, which can interfere with the native protein interactions and generate artefacts. In addition, although the *in vitro* binding measurements can offer more detailed information on the binding affinity and kinetics, these measurements are usually performed in an environment which is very different from the physiologically relevant conditions. For example, in ELISA and SPR exeperiments, the immobilised proteins or ligands can adopt specific orientations, which can either favour or disrupt binding. The different recombinant proteins generated by different research groups can also be a problem. For example, GPVI has been shown to interact with recombinant or purified fibrin, but not the fibrins that were obtained from human plasma or from human whole blood, highlighting the crucial roles played by different reagents in such *in vitro* or *ex vivo* binding experiments (Zhang et al., 2020). SMA-PAGE circumvents these artefacts of traditional methods, providing a new way to look at receptor stoichiometry, without the need for specialised equipment. The results from the Western blots on SMA-PAGE are preliminary and require further validation of protein identities and confirmation that the Western blotting antibodies are specific. However, they are complementary to the

aforementioned biochemical or biophysical methods and can provide information on protein stoichiometry in the near-native state.

SMALPs have also been proved useful in membrane protein interaction investigation in this thesis. This was demonstrated by the co-IP and SMA-PAGE experiments on SMALPs. Excellent example membrane proteins to test this would be the tetraspanin superfamily, as they function by interacting with other membrane proteins (their so-called partner proteins) and compartmentalising them into nanodomains where binding and signalling events can be enriched (Kummer et al., 2020). Novel partner proteins of a specific tetraspanin are usually identified by co-IP experiments followed by mass spectrometry proteomics, while the mapping of interaction sites can be achieved using mutated expression constructs transfected into cell lines. As SMALPs can preserve the native environment of membrane proteins and their interactions between each other, they serve as a better platform for the co-IP experiments for the discovery of novel partner proteins of tetraspanins. The IPed SMALPs can also be subjected to mass spectrometry-based protein identification. In this thesis, the preservation of the ADAM10/Tspan15 complex and potentially α6 integrin/CD151 complex in the same SMALPs was confirmed by IP and co-IP experiments, confirming the capacity of SMALPs in capturing tetraspanin-partner protein interactions. The discovery of novel partner proteins was shown to be particularly promising in the cases of Tspan9 and CD9, with the former potentially complexing with GPVI. However, similar to using SMALPs for the investigation of platelet receptor stoichiometry, the results of co-IP on SMALPs will need to be further validated, for example using tetraspanin knockout models to test the physiological significance of tetraspanin interaction.

6.4 The widening applications of SMALPs

The majority of studies utilising SMALPs focus on structure determination and biophysical characterisation (Krishnarjuna & Ramamoorthy, 2022). Such studies usually apply over-expression systems to maximise the protein yield; while the SMALP-encapsulated membrane proteins are still embedded in the lipid bilayer environment, such lipid environments could be different from the endogenous environment. Isolation of endogenous proteins into SMALPs has been done by a few groups, where the proteins have been shown to adopt their native conformation. For example, the previously mentioned RhD-SMALPs isolated from human erythrocytes can be IPed by a conformation-dependent monoclonal anti-RhD antibody, F5, and the IPed RhD-SMALPs can be detected on Western blot by another anti-RhD antibody, LOR15C9, which is conformation-independent (Desrames et al., 2020). This data indicated that the RhD protein in SMALPs from native erythrocytes preserved at least one important native conformation, highlighting how SMALPs preserve the intact states of encapsulated proteins and potentially lipids from endogenous cells. This thesis has extended the application of SMALPs towards the discovery of novel protein-protein interactions. The results here proved the capacity of SMALPs for bench-top protein interaction studies, and the protein interactions can be studied specifically for chosen proteins, rather than in a global proteomics manner, thus opening a novel direction for the application of SMALPs and further demonstrating their versatility. The use of SMALPs for protein interaction and stoichiometry investigation relieves operators from the tedious screening of detergents which cannot always preserve native protein-protein interactions, and the merging and dissociation of detergent micelles can generate false positives or false negative results.

One issue in many biophysical applications of SMALPs, for example AUC, is that the performance of the assay is dependent on having sufficient amounts of protein. This is particularly a problem for endogenously expressed proteins. Purification of GPVI/FcRγ

SMALPs from human platelets, via His-tagged GPVI nanobodies and Ni-NTA gravity column, was tried during this thesis, yet the yield was so low that GPVI could barely be detected on silver-stained SDS-PAGE gels, although GPVI was detectable by Western blotting (data not shown). Increasing the amount of GPVI nanobodies used for purification, and mixing of different His-tagged GPVI nanobodies, did improve the amount of purified GPVI SMALPs, as shown by Western blotting, but GPVI was lost after the samples were subjected to dialysis, suggesting the yield was still too low for further applications (data not shown). Moreover, a side-by-side comparison of GPVI expression levels in human platelets and transiently transfected ADAM10-knockout HEK-293T cells showed that 3 L of human blood was needed for a comparative expression level of ten 10-cm plates of confluent transfected HEK-293T cells (Supplementary Figure 5). Therefore, it is substantially easier to generate sufficient amounts of GPVI SMALPs from over-expression in HEK-293T cells than from human platelets. In addition, the use of His-tagged nanobodies may also lower the purification efficiency if they are not of sufficiently high affinity. This protein yield issue for SMALPs with endogenous proteins highlights the difficulty of purifying sufficient SMALPs containing specific membrane proteins. This thesis adopted a different route, by designing, developing and optimising biochemical experiments on unpurified, "crude" SMALPs, which took advantage of the intactness nature of SMALPs from endogenous cells, but circumvented the purification problem. However, due to the low yield of purified GPVI SMALPs from human platelets, the structural determination work on GPVI SMALPs was performed from an over-expressed system, as was described in Chapter 4.

The standard protocols for SMALP generation are more for large-scale production and biophysical characterisation, and for bacterial expression systems, for example, the use of a C3 high pressure homogeniser to burst cell walls open (Lee et al., 2016); however, the protocols on platelet SMALPs in this thesis are for biochemistry-based techniques that generally require

much less material and “minimised” operation systems comparing to biophysical and structural studies, i.e. in 1.5 mL eppendorfs. This offers the opportunity for the development of simplified, cheaper and quicker protocols of SMALP generation and purification, which is preferable for higher-throughput screening of a larger variety of membrane proteins in our SMALP-based assays. Such attempts have to be taken with caution, though, due to our current lack of detailed understanding of SMALP formation procedures, and the outpace of SMALP-based experiments comparing to the principles of SMALP generation. The modification and/or removal of steps in the protocol may cause unexpected outcomes, for example, the tyrosine phosphorylation phenomenon indicating platelet hyper-activation and thus a very likely disorder of protein-protein interaction in high NaCl concentration (500 mM). Higher concentration of NaCl was needed for the disruption of potential SMALP aggregation, though, as demonstrated by the higher molecular weight bands on CLEC-2 Western blot of SMA-PAGE (Supplementary Figure 4). Moreover, it was shown that the removal of hand-homogenisation and the final ultracentrifugation steps (after SMALP generation, to remove un-SMALPed debris) did not interfere with the band patterns on SMA-PAGE (Supplementary Figure 4), and the removal of these steps could considerately decrease the amount of platelets needed to generate SMALPs. Nevertheless, further checks including electron microscopy will be needed to confirm that membrane proteins are still encapsulated in SMALPs. These highlight the difficulty in the protocol developing procedures, but more importantly, highlight the significance in the methodology development work, which may greatly deepen our understanding of how SMALPs are generated, how each procedure contributes to SMALP morphology, and how the SMALP generation is influenced by different conditions. All of these could potentially contribute to our understanding of SMALP formation principles, from an experimental perspective, while most of this type of studies attempt to utilise computational

simulations, for example, molecular dynamics simulation (Caparotta et al., 2021; Xue et al., 2018).

The biotinylation-based co-IP assay and SMA-PAGE assay have been developed on SMALPs, by utilising and combining commonly used biochemical techniques, with generic devices in a biochemistry lab. Both assays are relatively high-throughput in comparison to other SMALP-based studies, as neither IP or Western blotting requires a large amount of SMALP samples, thus a single platelet preparation from one donor can offer enough material for many platelet membrane proteins to be examined, especially for SMA-PAGE as only tens of μL of SMALP samples are needed per blot. These assays are simple, convenient, efficient, and offer a possible platelet membrane interaction and stoichiometry check for each individual donor, as a large set of platelet membrane proteins can be applied using these assays, and the data can be employed for the illustration of individual platelet membrane protein characteristics difference. The two assays each have their own advantages. SMA-PAGE requires less material to generate useful information, and the native gel can reveal protein distribution spanning from 20 kDa up to more than 1,000 kDa, allowing for the detection of large molecular weight protein assemblies. The biotinylation co-IP assay involves slightly more steps including platelet labelling and co-IP, where the co-IP step needs more material, but the band patterns on streptavidin blot are in general easier to interpret, as individual proteins show up separately.

A few drawbacks of SMA-PAGE are that the band patterns of several membrane proteins of choice in our studies were hard to explain, and the molecular weights of the bands can deviate from the actual molecular weight of the protein (or protein assemblies). However, the inconclusive band pattern and deviation of molecular weights are common issues in native PAGE, mostly due to the difference of intrinsic charges that each individual, intact proteins can carry and expose on their surfaces when they remain folded. The SMA-PAGE method has advantages over other widely used native PAGE methods, such as blue native PAGE and clear

native PAGE, in the sense that no additives are needed in the loading sample as the SMA belt of the nanodisc already serves as an excellent driving force for protein migration. Furthermore, the SMALPs are relatively uniformly shaped, at least in the dimension of the disc plane, which can decrease the impact of protein shape and intrinsic charges on protein migration. An additional bonus is that most of the commercial or hand-made native gels can be used directly for SMA-PAGE, and there are almost no additional steps in electrophoresis, transferring and blotting procedures, in contrast to some other native PAGE methods, for example blue native PAGE where tedious additional washing steps on the membrane have to be applied to wash away the Coomassie dye on the membrane for Western blotting. The migration performance of SMALPs and detergent lysates was compared on the SMA-PAGE gel running system in this thesis, and the Western blots for most of the chosen proteins showed different band patterns in the two samples, with the bands from detergent lysates usually ending up in much higher molecular weights that are not physiologically relevant, or being much more smeared with the individual bands hard to distinguish (Figure 5.11). This demonstrated the important role that the SMA belt plays in SMA-PAGE, while also confirming that the SMA-PAGE method is a unique way to determine the molecular weight of membrane protein assemblies, which could not be achieved without utilising SMALPs in the same PAGE system. Recombinant protein samples were used as positive controls on SMA-PAGE for CLEC-2, by loading CLEC-2-His as a monomer control and CLEC-2-Fc as a dimer control. Although the band pattern from platelet SMALPs resembled the one from monomeric CLEC-2-His (Figure 5.11A), these recombinant proteins are not the best controls to use, as they are not in SMALPs and therefore the migration depends more on their intrinsic surface charges, and the molecular weight does not contain the contribution from SMA belt and the encapsulated lipids. For proteins with hard-to-interpret band patterns on SMA-PAGE, it will be hard to find an appropriate positive control to facilitate the interpretation of the result.

Another drawback, in common for these two assays, is that they can only serve as an initial checking step or a final confirmation for protein-protein interactions identified by other technologies, since no biological conclusion can be drawn without the combination with other technologies. In the biotinylation assay, the streptavidin blot cannot indicate the exact identity of the protein bands; a quick way to confirm the band component would be Western blotting against specific proteins, but this only applies to the situations where the band identity is almost definitive according to previous knowledge about the possible interactions. Similarly, in SMA-PAGE, it is only the molecular weight of the protein assemblies containing the proteins of interest that can be shown, but not the protein components in the assemblies. As western blotting on SMA-PAGE in this study was done on whole-cell SMALPs, it is not feasible to stain the gel and cut out the corresponding bands for mass spectrometry analyses; potentially, to further check the protein identities in the bands, the crude SMALPs need to be IPed and sent for mass spectrometry.

Several groups have applied mass spectrometry to examine the protein and lipid components in SMALPs, and this type of study has drawn increasing attention over the last few years. The reported studies in this field were mainly aiming for an overview of whole-membrane protein extraction in SMALPs, for a specific cell type, or an overview of the lipid comparison for the investigation of lipid enrichment or depletion around certain proteins (Esmaili et al., 2020; Laursen et al., 2016; Pollock et al., 2019; Teo et al., 2019). There was also an attempt to apply native mass spectrometry methods to explore the stoichiometry of proteins encapsulated in SMALPs (Hellwig et al., 2018). The assays in this thesis present a different way to look at SMA-extracted proteomes and protein-protein interactions, focusing on the selected, specific proteins (or pairs of proteins) of interest, instead of the whole set of membrane proteins, thus providing a novel way of using SMALPs for identifying novel protein interactions. In future.

using mass spectrometry to demonstrate the full list of proteins in the specific SMALPs containing the proteins of interest may be particularly useful.

6.5 Final conclusions and future remarks

In this thesis, SMALPs were demonstrated as a promising tool for determining the structure of GPVI/FcRγ complex in a near-native lipid bilayer environment, for isolating native membrane protein complexes from human platelets, and for the investigation of platelet receptor interactions and stoichiometry. The established GPVI/FcRγ SMALP generation protocol, from transfected HEK-293T cells, can be repeated with further optimisation for higher protein amount, purer samples and more homogenous sizes of particles, for the final goal of solving the high-resolution structure of GPVI/FcRγ in a native nanodisc environment. The optimised SMALP generation protocol on human platelets, have taken into account the propensity of platelets to be activated by the environment, and taken advantage of the anucleate and membrane-richnature of platelets. Further optimisation and simplification of the protocol is still worth exploring, with more evaluation methods to be adopted, such as negative stain EM to check the morphology of SMALPs. The co-IP and SMA-PAGE assays that were developed on human platelet SMALPs, have demonstrated their usability in exploring platelet receptor stoichiometry and discovering novel membrane protein interactions, and can be readily applied to a wider range of membrane proteins. Taken together, the results in this thesis have paved the way for several interesting and practical future directions, to utilise SMALPs for platelet receptor structure, stoichiometry and interaction investigations, while also widening the application of SMALPs.

Appendix

Supplementary Table 1 List of proteins identified in the ~100 kDa band (Band 1 in Figure 4.5).

The ~100 kDa band from silver-stained SDS-PAGE gel loaded with gel filtration fractions was excised from fractions 4-9, pooled together, and subjected to trypsin digestion followed by liquid chromatography and tandem mass spectrometry. Only proteins which had a FDR (false discovery rate) >1, are not contaminants e.g. keratin, and are located in the membrane, are included, and they are ranked by the number of peptides identified for each protein. GPVI and FcRγ are highlighted in purple in the table. Number of peptides (#peptides) refers to the total number of distinct peptide sequences identified from all included searches, while number of unique peptides (#unique peptides) refers to the total number of distinct peptide sequences unique to the protein. PSM refers to peptide score matches. GPVI and FcRγ were highlighted in purple.

Accession	Description	Coverage [%]	# Peptides	# PSMs	# Unique Peptides	Molecular weight [kDa]	Score Sequest HT:
Q9HCN6	Platelet glycoprotein VI OS=Homo sapiens OX=9606 GN=GP6 PE=1 SV=4	21	7	17	7	36.8	35.18
P04843	Dolichyl-diphosphooligosaccharide--protein glycosyltransferase subunit 1 OS=Homo sapiens OX=9606 GN=RPN1 PE=1 SV=1	7	3	3	3	68.5	0
Q9Y6M5	Zinc transporter 1 OS=Homo sapiens OX=9606 GN=SLC30A1 PE=1 SV=3	5	2	2	2	55.3	2.31
Q9ULF5	Zinc transporter ZIP10 OS=Homo sapiens OX=9606 GN=SLC39A10 PE=1 SV=2	2	2	2	2	94.1	0
P30273	High affinity immunoglobulin epsilon receptor subunit gamma OS=Homo sapiens OX=9606 GN=FCER1G PE=1 SV=1	23	2	2	2	9.7	3.83
A0A140VKC4	Methyl-CpG-binding protein 2 OS=Homo sapiens OX=9606 GN=MECP2 PE=2 SV=1	8	2	2	2	53.3	0
Q4VCS5	Angiomotin OS=Homo sapiens OX=9606 GN=AMOT PE=1 SV=1	1	2	2	2	118	0
P27824	Calnexin OS=Homo sapiens OX=9606 GN=CANX PE=1 SV=2	2	1	1	1	67.5	0

L0R5A1	Alternative protein CSF2RB OS=Homo sapiens OX=9606 GN=CSF2RB PE=4 SV=1	7	1	1	1	11.6	0
Q13433	Zinc transporter ZIP6 OS=Homo sapiens OX=9606 GN=SLC39A6 PE=1 SV=3	1	1	1	1	85	1.92
Q8NEW0	Zinc transporter 7 OS=Homo sapiens OX=9606 GN=SLC30A7 PE=2 SV=1	4	1	1	1	41.6	0

Supplementary Table 2 List of proteins identified in the ~57 kDa band (Band 2 in Figure 4.5)

The ~57 kDa band from silver-stained SDS-PAGE gel loaded with gel filtration fractions was excised from fractions 4-11, pooled together, and subjected to trypsin digestion followed by liquid chromatography and tandem mass spectrometry. Protein inclusion criteria and the meaning of each column are the same as those in Supplementary Table 1. GPVI and FcRγ are highlighted in purple.

Accession	Description	Coverage [%]	# Peptides	# PSMs	# Unique Peptides	Molecular weight [kDa]	Score Sequest HT
Q9HCN6	Platelet glycoprotein VI OS=Homo sapiens OX=9606 GN=GP6 PE=1 SV=4	21	6	9	6	36.8	21.28
P25705	ATP synthase subunit alpha, mitochondrial OS=Homo sapiens OX=9606 GN=ATP5F1A PE=1 SV=1	8	4	4	4	59.7	1.89
P30273	High affinity immunoglobulin epsilon receptor subunit gamma OS=Homo sapiens OX=9606 GN=FCER1G PE=1 SV=1	23	2	2	2	9.7	3.69
L0R5A1	Alternative protein CSF2RB OS=Homo sapiens OX=9606 GN=CSF2RB PE=4 SV=1	7	1	1	1	11.6	0

A8K8G8	cDNA FLJ75219 OS=Homo sapiens OX=9606 PE=2 SV=1	3	1	1	1	48.2	0
V9HW31	ATP synthase subunit beta OS=Homo sapiens OX=9606 GN=HEL-S-271 PE=1 SV=1	4	1	1	1	56.5	2.14
P08670	Vimentin OS=Homo sapiens OX=9606 GN=VIM PE=1 SV=4	2	1	1	1	53.6	1.61
F8WAR4	MICOS complex subunit OS=Homo sapiens OX=9606 GN=CHCHD3 PE=1 SV=1	3	1	1	1	27.7	0
Q8NEW0	Zinc transporter 7 OS=Homo sapiens OX=9606 GN=SLC30A7 PE=2 SV=1	3	1	1	1	41.6	1.87

Supplementary Table 3 List of proteins identified in the bands at ~18 kDa (Band 3 in Figure 4.5).

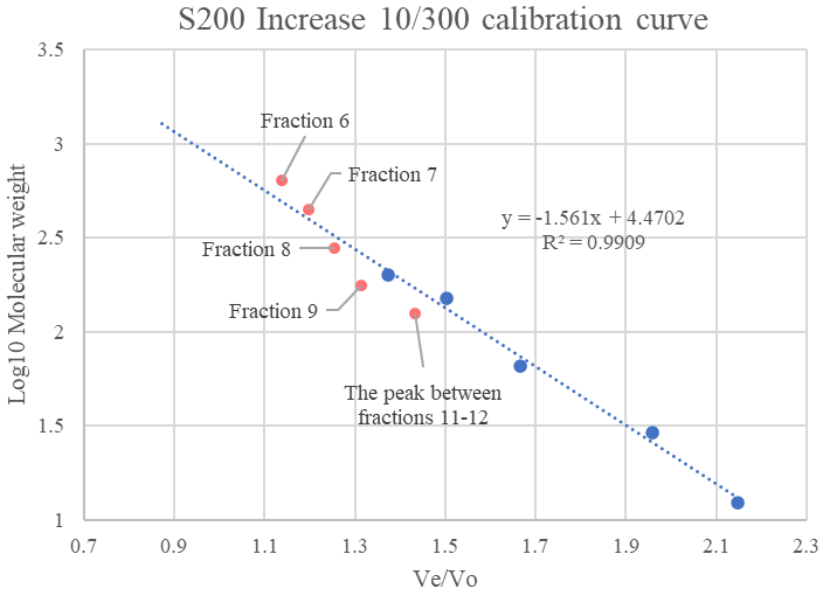
The ~18 kDa band from silver-stained SDS-PAGE gel loaded with gel filtration fractions was excised from fractions 4-9, pooled together, and subjected to trypsin digestion followed by liquid chromatography and tandem mass spectrometry. Protein inclusion criteria and the meaning of each column are the same as those in Supplementary Table 1. FcRγ is highlighted in purple.

Accession	Description	Coverage [%]	# Peptides	# PSMs	# Unique Peptides	Molecular weight [kDa]	Score Sequest HT
P30273	High affinity immunoglobulin epsilon receptor subunit gamma OS=Homo sapiens OX=9606 GN=FCER1G PE=1 SV=1	41	6	9	6	9.7	21.17
A0A075B6Z2	T cell receptor alpha joining 56 (Fragment) OS=Homo sapiens OX=9606 GN=TRAJ56 PE=4 SV=1	38	1	1	1	2.2	0
B2R9T9	cDNA, FLJ94551 OS=Homo sapiens OX=9606 PE=2 SV=1	5	1	1	1	26.2	0

A

Standard proteins	Vo or Ve	Vo or Ve values	Ve/Vo	Molecular weight (kDa)	Log10 Molecular weight
Blue Dextran	Vo	8.45		2000	
B amylase	Ve	11.6	1.4	200	2.3
Alcohol Dehydrogenase	Ve	12.7	1.5	150	2.2
Albumin	Ve	14.1	1.7	66	1.8
Carbonic Anhydrase	Ve	16.5	2.0	29	1.5
Cytochrome C	Ve	18.1	2.1	12.4	1.1

B



C

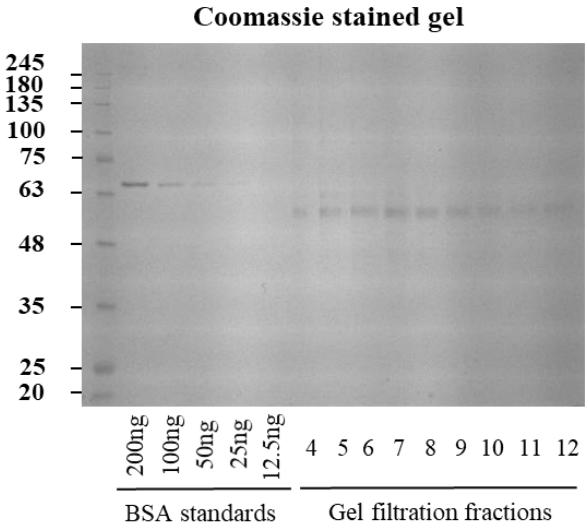
Gel filtration fractions	Ve values (mL)	Ve/Vo	Molecular weight on Western Blot (kDa)	Molecular weight calculated by the calibration curve (kDa)	Bias from the calibration curve
Fraction 6	9.6	1.1	634.9	495.3	28%
Fraction 7	10.1	1.2	444.6	400.4	11%
Fraction 8	10.6	1.3	279.7	323.7	-14%
Fraction 9	11.1	1.3	176.0	261.7	-33%
The peak between fractions 11-12	12.1	1.4	124.2	170.5	-27%

Supplementary Figure 1 Calibration of the S200 Increase 10/300 column, and fitting of GPVI/FcRγ SMALP gel filtration fractions and peaks into the calibration curve.

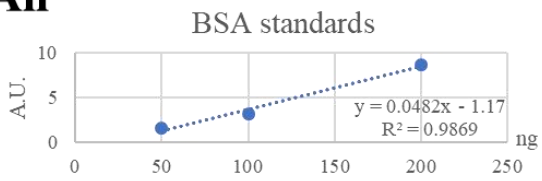
(A) Five molecular weight markers (B amylase, Alcohol dehydrogenase, Albumin, Carbonic Anhydrase and Cytochrome C) solubilised in PBS were passed through the S200 Increase 10/300 column, with their corresponding elution volumes (Ve) recorded. The void volume (Vo) was determined by passing Blue dextran, 2,000 kDa, through the same column. The data was kindly provided by Dr. Alexandre Slater, University of Birmingham. (B) Log10 values of the molecular weight of each marker protein in (A) were calculated and plotted against Ve/Vo. A linear trendline was fitted to the marker protein data points (blue). Data points from GPVI/FcRγ SMALP gel filtration in (C) were also plotted (pink). (C) In the gel filtration experiment on GPVI/FcRγ SMALPs (Section

4.2.2), the positions in the middle of each fraction (Figure 4.3A) were recorded as the Ve values for fractions 6, 7, 8, 9, respectively, while the Ve of the second peak (Figure 4.3A, positioned between fractions 11-12) was also recorded. The molecular weight of proteins in each fraction was calculated from the GPVI blot on SMA-PAGE (Figure 4.3C), by fitting the travelling distance of the protein band into the regression curve of the blot, as described in Figure 5.11; if the protein band of a fraction is smeary, the molecular weight in the middle of smear was used. The molecular weight of proteins in each fraction was also calculated from their Ve/Vo values using the column calibration curve in (B). The bias was calculated by subtracting the molecular weight calculated in the calibration curve from the molecular weight on Western blot, and then dividing this value by the molecular weight calculated in the calibration curve. A positive value indicates that the actual molecular weight on the Western blot is higher than the molecular weight calculated from the calibration curve, while a negative value indicates that the actual molecular weight on the Western blot is lower than the molecular weight calculated from the calibration curve. The data of the first peak (Figure 4.3A, positioned between fractions 4-5) was not shown here, because the sample run higher than the largest marker, 720 kDa, on SMA-PAGE (Figure 4.3C), and therefore it is not possible to read the molecular weight of the proteins in this peak.

Ai



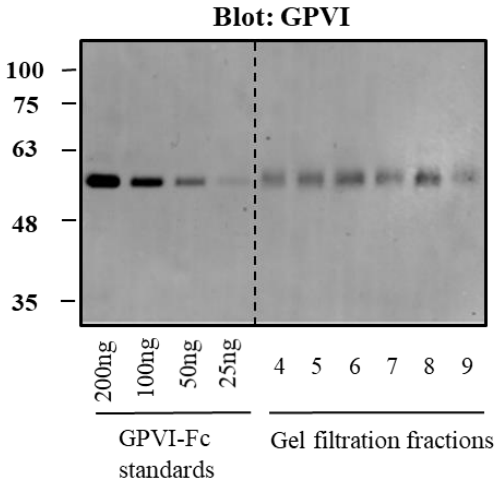
Aii



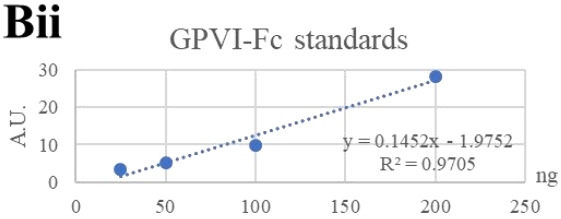
Aiii

GF fractions	Predicted amount per lane (ng), undiluted	Predicted conc. (mg/mL)
4	135.68	0.0081
5	134.65	0.0081
6	135.16	0.0081
7	171.78	0.0103
8	153.11	0.0092
9	165.98	0.0100
10	119.5	0.0072

Bi



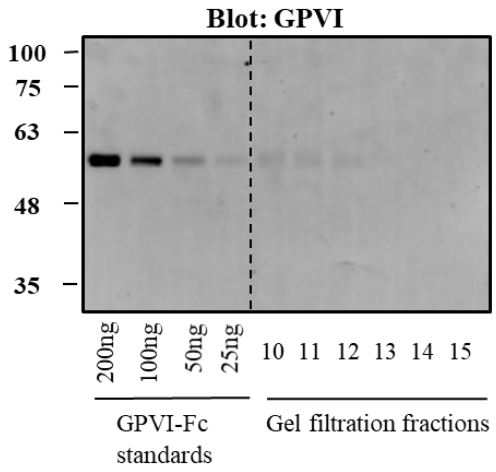
Bii



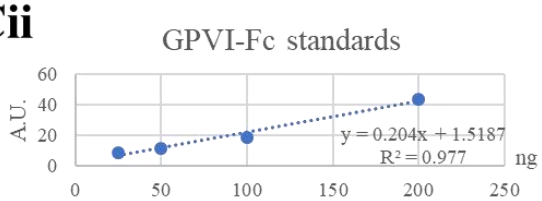
Biii

Gel filtration fractions	Predicted amount per lane (ng), 1:40 dilution	Predicted conc. (mg/mL)
4	44.46	0.0889
5	48.38	0.0968
6	51.96	0.1039
7	35.3	0.0706
8	36.81	0.0736
9	28.96	0.0579

Ci



Cii



Ciii

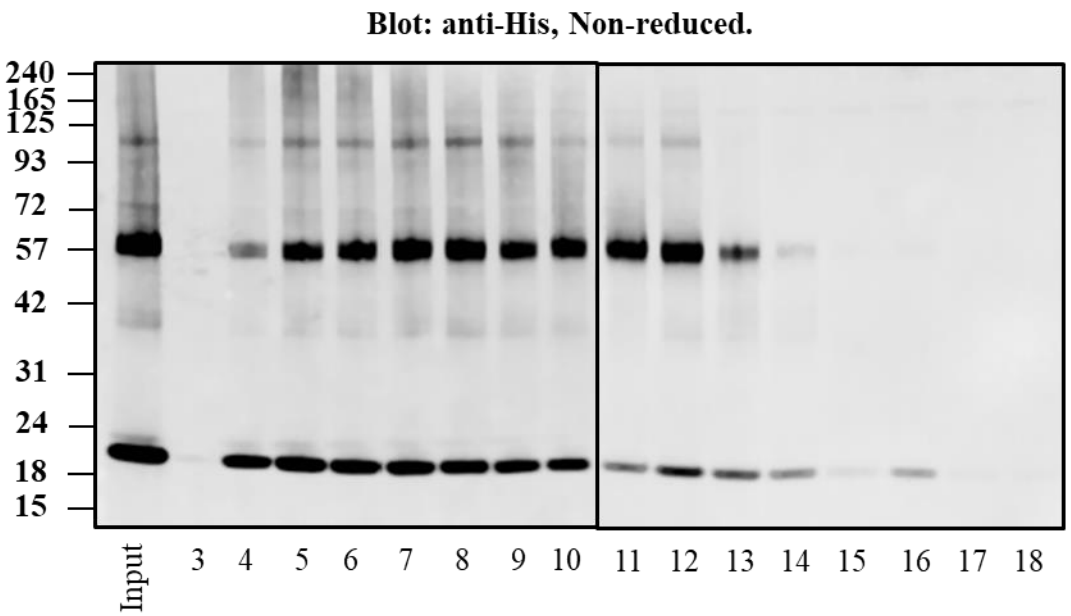
Gel filtration fractions	Predicted amount per lane (ng), 1:40 dilution	Predicted conc. (mg/mL)
10	38.29	0.0766
11	33.78	0.0676
12	31.62	0.0632

D

Gel filtration fractions	Concentration (mg/mL)	A260/A280
4	0.046	2.587
5	0.046	2.391
6	0.056	2.107
7	0.025	2.966
8	0.025	2.64
9	0.043	2.419
10	0.061	2.131
11	0.061	2.213
12	0.042	2.56
13	0.055	2.309
14	0.066	2.045
15	0.056	2.036
16	0.084	1.893
17	0.057	2.193
18	0.051	2.157

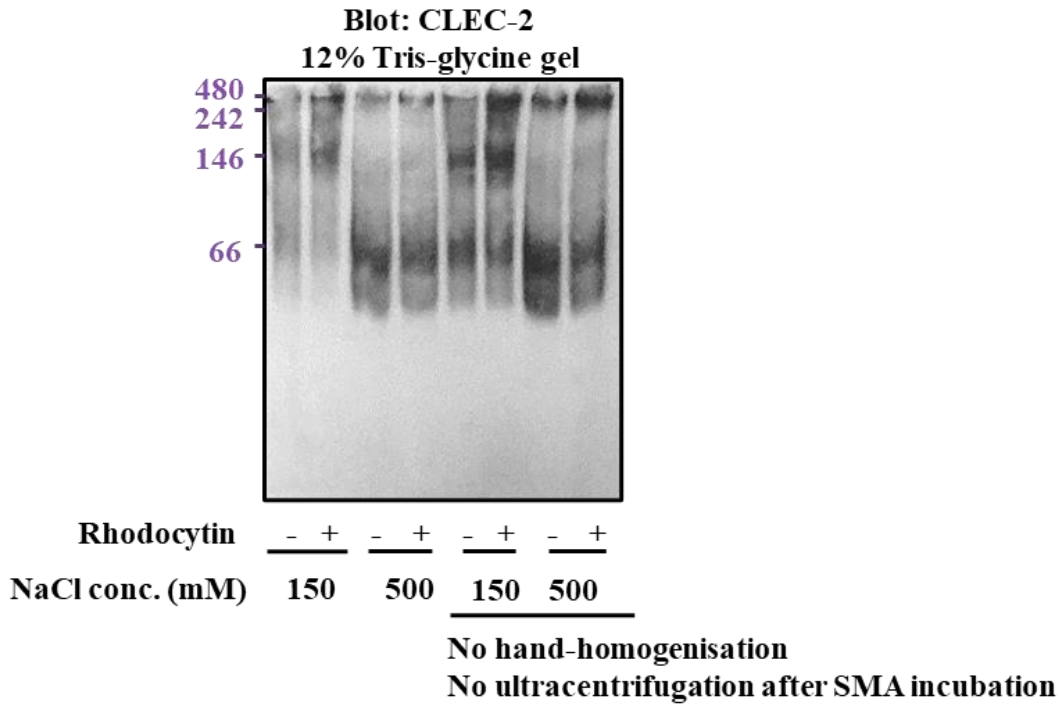
Supplementary Figure 2 Concentration measurement of the gel filtration fractions via BSA standards, recombinant GPVI-Fc standards and nanodrop generated different results, but the results are in the range of 0.02-0.1 mg/mL in most cases.

(A) BSA standards were loaded with indicated amount per lane. For gel filtration fractions, 20 μL samples with 4 μL 6x Laemmli sample buffer were heated at 75 °C for 10 min, then 20 μL was loaded onto the gel. After SDS-PAGE, the gel was subjected to Coomassie staining (Ai), and the stained gel imaged and quantified using the Odyssey Imaging System. A BSA standard curve was generated by plotting the band strength against the amount of protein per lane (Aii). The predicted amount of proteins for each lane and the calculated concentration of the gel filtration fractions are detailed in Aiii. The samples were run under reduced conditions. (B) Recombinant GPVI-Fc fusion protein were loaded with the indicated amount per lane; for each lane, 10 μL of GPVI-Fc solution was mixed with 2x Laemmli sample buffer and heated at 75 °C for 10 min. For gel filtration fractions (4-9), 20 μL was loaded per lane, containing 10 μL of 2x Laemmli sample buffer, 9.5 μL of PBS and 0.5 μL of gel filtration fraction sample, heated at 75 °C for 10 min before loading to the gel. After SDS-PAGE, the gel was subjected to GPVI blot (Bi), and the membrane imaged and quantified using the Odyssey Imaging System. The GPVI-Fc standards were quantified and a standard curve generated by plotting the band strength against the amount of protein per lane (Bii). The predicted amount of proteins for each lane and the calculated concentration of the gel filtration fractions are detailed in Biii. The samples were run under reduced conditions. (C) The experiment was conducted similarly to panel B, but with different gel filtration fractions (10-15). No visible bands were detected from the diluted samples of fractions 13-15, thus their predicted concentrations could not be calculated. (D) The nanodrop readings of the concentrations of fractions 4-18. The device was blanked with SMALP solution B.



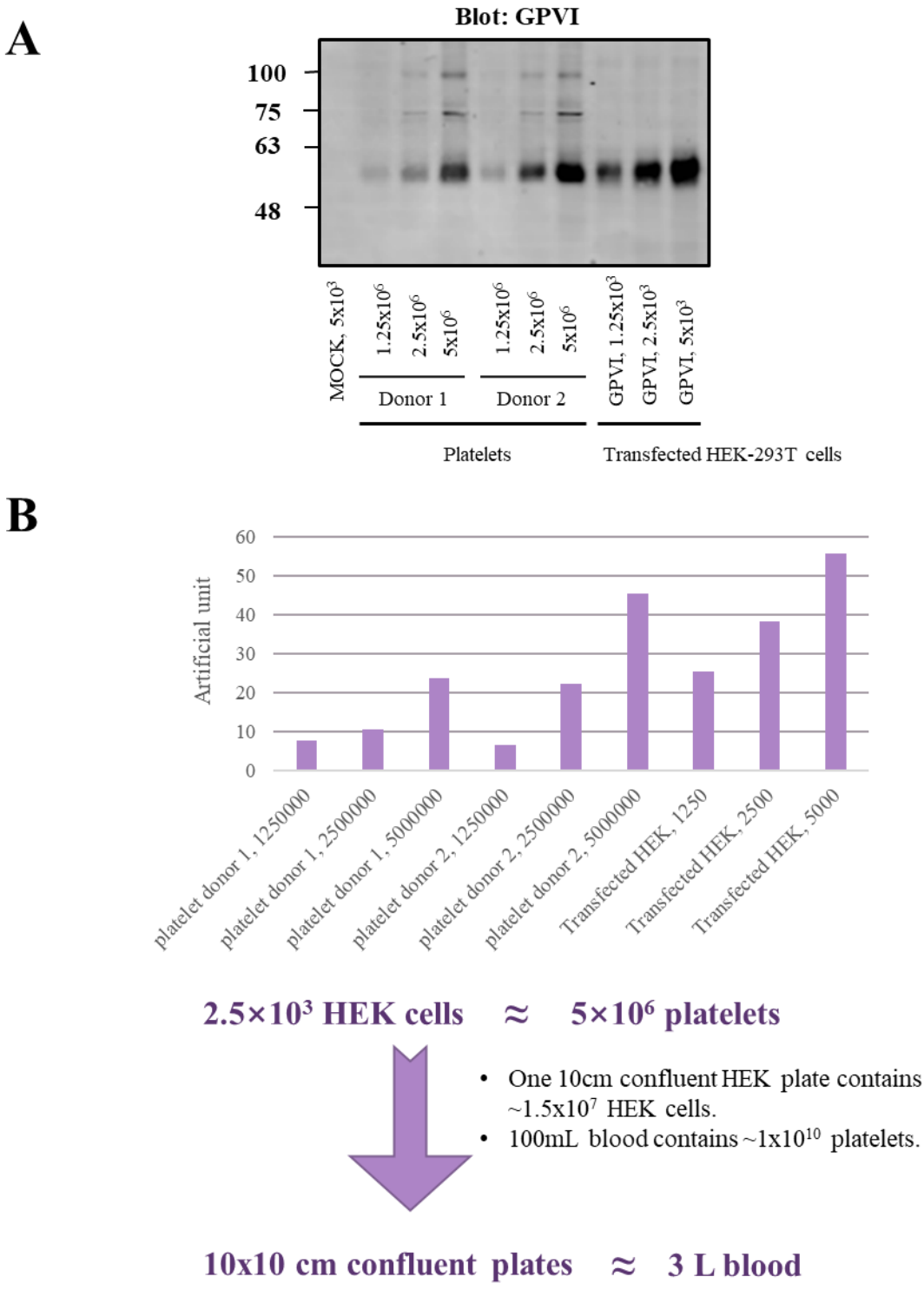
Supplementary Figure 3 The purified GPVI/FcRγ SMALPs are relatively pure.

GPVI SMALP gel filtration fractions were analysed by SDS-PAGE followed by anti-His-tag Western blotting.



Supplementary Figure 4 NaCl concentration in the final SMALP solution affects the ratio of high order oligomers of CLEC-2 on SMA-PAGE.

Human platelets were prepared from freshly drawn blood and activated with 200 nM rhodocytin as described in section 2.4.2, then SMALPs were generated using optimised SMALP solution B (50 mM Tris diluted 1:10 from pH=8, **150 mM NaCl**, 10% glycerol). For lanes 1-4, the standard SMALP generation protocol was used. The final solution, containing SMALPs, was either directly mixed with 5x native sample buffer and loaded on the gel (lanes 1-2), or supplemented to a final NaCl concentration of 500 mM before mixing with native sample buffer and loaded on the gel (lanes 3-4). For lanes 5-8, the SMALP generation protocol was simplified, with the manual homogenisation and ultracentrifugation after SMA incubation omitted, as indicated. The final solution, containing SMALPs, was either directly mixed with 5x native sample buffer and loaded on the gel (lanes 5-6), or supplemented to a final NaCl concentration of 500 mM before mixing with native sample buffer and loaded on the gel (lanes 7-8). The samples were loaded onto SMA-PAGE and Western blotted with CLEC-2 antibody (AYP1).



Supplementary Figure 5 Comparison of the amount of GPVI that can be collected from transfected ADAM10-knckout HEK-293T cells and from freshly isolated human platelets.

Human platelets were isolated from freshly drawn blood, from two healthy donors, and lysed in 1% Triton X-100. For ADAM10-knockout HEK-293T cells, they were transfected with GPVI and FcRγ expression constructs and then lysed in 1% Triton X-100 lysis buffer. (A) Western blotting with anti-GPVI antibody was done and quantified (B), and the relative amount of transfected HEK-293T cells and human platelets expressing similar amount of GPVI (on whole cell level) was calculated.

References

Acton, S. E., Farrugia, A. J., Astarita, J. L., Mourao-Sa, D., Jenkins, R. P., Nye, E., Hooper, S., van Blijswijk, J., Rogers, N. C., Snelgrove, K. J., Rosewell, I., Moita, L. F., Stamp, G., Turley, S. J., Sahai, E., & Reis e Sousa, C. (2014). Dendritic cells control fibroblastic reticular network tension and lymph node expansion. *Nature*, *514*(7523), 498-502. https://doi.org/10.1038/nature13814

Aggrey, A. A., Srivastava, K., Ture, S., Field, D. J., & Morrell, C. N. (2013). Platelet induction of the acute-phase response is protective in murine experimental cerebral malaria. *J Immunol*, *190*(9), 4685-4691. https://doi.org/10.4049/jimmunol.1202672

Agrawal, S., Ganguly, S., Hajian, P., Cao, J. N., & Agrawal, A. (2015). PDGF upregulates CLEC-2 to induce T regulatory cells. *Oncotarget*, *6*(30), 28621-28632. https://doi.org/10.18632/oncotarget.5765

Ahn, V. E., Faull, K. F., Whitelegge, J. P., Fluharty, A. L., & Prive, G. G. (2003). Crystal structure of saposin B reveals a dimeric shell for lipid binding. *Proc Natl Acad Sci U S A*, *100*(1), 38-43. https://doi.org/10.1073/pnas.0136947100

Al-Tamimi, M., Mu, F. T., Arthur, J. F., Shen, Y., Moroi, M., Berndt, M. C., Andrews, R. K., & Gardiner, E. E. (2009). Anti-glycoprotein VI monoclonal antibodies directly aggregate platelets independently of FcgammaRIIa and induce GPVI ectodomain shedding. *Platelets*, *20*(2), 75-82. https://doi.org/10.1080/09537100802645029

Alfrey, T., & Lavin, E. (1945). The Copolymerization of Styrene and Maleic Anhydride. *Journal of the American Chemical Society*, *67*(11), 2044-2045. https://doi.org/DOI 10.1021/ja01227a502

Ali, R. A., Wuescher, L. M., & Worth, R. G. (2015). Platelets: essential components of the immune system. *Curr Trends Immunol*, *16*, 65-78. https://www.ncbi.nlm.nih.gov/pubmed/27818580

Andonegui, G., Kerfoot, S. M., McNagny, K., Ebbert, K. V., Patel, K. D., & Kubes, P. (2005). Platelets express functional Toll-like receptor-4. *Blood*, *106*(7), 2417-2423. https://doi.org/10.1182/blood-2005-03-0916

Andrews, R. K., Gardiner, E. E., Shen, Y., Whisstock, J. C., & Berndt, M. C. (2003). Glycoprotein Ib-IX-V. *Int J Biochem Cell Biol*, *35*(8), 1170-1174. https://doi.org/10.1016/s1357-2725(02)00280-7

Andrews, R. K., Munday, A. D., Mitchell, C. A., & Berndt, M. C. (2001). Interaction of calmodulin with the cytoplasmic domain of the platelet membrane glycoprotein Ib-IX-V complex. *Blood*, *98*(3), 681-687. https://doi.org/10.1182/blood.v98.3.681

Andrews, R. K., Suzuki-Inoue, K., Shen, Y., Tulasne, D., Watson, S. P., & Berndt, M. C. (2002). Interaction of calmodulin with the cytoplasmic domain of platelet glycoprotein VI. *Blood*, *99*(11), 4219-4221. https://doi.org/10.1182/blood-2001-11-0008

Antl, M., von Bruhl, M. L., Eiglsperger, C., Werner, M., Konrad, I., Kocher, T., Wilm, M., Hofmann, F., Massberg, S., & Schlossmann, J. (2007). IRAG mediates NO/cGMP-dependent inhibition of platelet aggregation and thrombus formation. *Blood*, *109*(2), 552-559. https://doi.org/10.1182/blood-2005-10-026294

Apoil, P. A., Reid, M. E., Halverson, G., Mouro, I., Colin, Y., Roubinet, F., Cartron, J. P., & Blancher, A. (1997). A human monoclonal anti-D antibody which detects a nonconformation-dependent epitope on the RhD protein by immunoblot. *Br J Haematol*, *98*(2), 365-374. https://doi.org/10.1046/j.1365-2141.1997.2183041.x

Arachea, B. T., Sun, Z., Potente, N., Malik, R., Isailovic, D., & Viola, R. E. (2012). Detergent selection for enhanced extraction of membrane proteins. *Protein Expr Purif*, *86*(1), 12-20. https://doi.org/10.1016/j.pep.2012.08.016

Arachiche, A., Mumaw, M. M., de la Fuente, M., & Nieman, M. T. (2013). Protease-activated receptor 1 (PAR1) and PAR4 heterodimers are required for PAR1-enhanced cleavage of PAR4 by alpha-thrombin. *J Biol Chem*, *288*(45), 32553-32562. https://doi.org/10.1074/jbc.M113.472373

Arthur, J. F., Gardiner, E. E., Matzaris, M., Taylor, S. G., Wijeyewickrema, L., Ozaki, Y., Kahn, M. L., Andrews, R. K., & Berndt, M. C. (2005). Glycoprotein VI is associated with GPIb-IX-V on the membrane of resting and activated platelets. *Thromb Haemost*, *93*(4), 716-723. https://doi.org/10.1160/TH04-09-0584

Arthur, J. F., Shen, Y., Kahn, M. L., Berndt, M. C., Andrews, R. K., & Gardiner, E. E. (2007). Ligand binding rapidly induces disulfide-dependent dimerization of glycoprotein VI on the platelet plasma membrane. *J Biol Chem*, *282*(42), 30434-30441. https://doi.org/10.1074/jbc.M701330200

Asazuma, N., Wilde, J. I., Berlanga, O., Leduc, M., Leo, A., Schweighoffer, E., Tybulewicz, V., Bon, C., Liu, S. K., McGlade, C. J., Schraven, B., & Watson, S. P. (2000). Interaction of linker for activation of T cells with multiple adapter proteins in platelets activated by the glycoprotein VI-selective ligand, convulxin. *J Biol Chem*, *275*(43), 33427-33434. https://doi.org/10.1074/jbc.M001439200

Aslam, R., Speck, E. R., Kim, M., Crow, A. R., Bang, K. W., Nestel, F. P., Ni, H., Lazarus, A. H., Freedman, J., & Semple, J. W. (2006). Platelet Toll-like receptor expression modulates lipopolysaccharide-induced thrombocytopenia and tumor necrosis factor-alpha production in vivo. *Blood*, *107*(2), 637-641. https://doi.org/10.1182/blood-2005-06-2202

Asselin, J., Gibbins, J. M., Achison, M., Lee, Y. H., Morton, L. F., Farndale, R. W., Barnes, M. J., & Watson, S. P. (1997). A collagen-like peptide stimulates tyrosine phosphorylation of syk and phospholipase C gamma2 in platelets independent of the integrin alpha2beta1. *Blood*, *89*(4), 1235-1242. https://www.ncbi.nlm.nih.gov/pubmed/9028946

Astarita, J. L., Acton, S. E., & Turley, S. J. (2012). Podoplanin: emerging functions in development, the immune system, and cancer. *Front Immunol*, *3*, 283. https://doi.org/10.3389/fimmu.2012.00283

Ayub, H., Clare, M., Milic, I., Chmel, N. P., Boning, H., Devitt, A., Krey, T., Bill, R. M., & Rothnie, A. J. (2020). CD81 extracted in SMALP nanodiscs comprises two distinct protein populations within a lipid environment enriched with negatively charged headgroups. *Biochim Biophys Acta Biomembr*, *1862*(11), 183419. https://doi.org/10.1016/j.bbamem.2020.183419

Badimon, L., Padro, T., & Vilahur, G. (2012). Atherosclerosis, platelets and thrombosis in acute ischaemic heart disease. *Eur Heart J Acute Cardiovasc Care*, *1*(1), 60-74. https://doi.org/10.1177/2048872612441582

Baker, N. C., Lipinski, M. J., Lhermusier, T., & Waksman, R. (2014). Overview of the 2014 Food and Drug Administration Cardiovascular and Renal Drugs Advisory Committee meeting about vorapaxar. *Circulation*, *130*(15), 1287-1294. https://doi.org/10.1161/CIRCULATIONAHA.114.011471

Ball, L. E., Riley, L. J., Hadasha, W., Pfukwa, R., Smith, C. J. I., Dafforn, T. R., & Klumperman, B. (2021). Influence of DIBMA Polymer Length on Lipid Nanodisc Formation and Membrane Protein Extraction. *Biomacromolecules*, *22*(2), 763-772. https://doi.org/10.1021/acs.biomac.0c01538

Ballerini, P., Dovizio, M., Bruno, A., Tacconelli, S., & Patrignani, P. (2018). P2Y12 Receptors in Tumorigenesis and Metastasis. *Front Pharmacol*, *9*, 66. https://doi.org/10.3389/fphar.2018.00066

Banerjee, S., Pal, T. K., & Guha, S. K. (2012). Probing molecular interactions of poly(styrene-co-maleic acid) with lipid matrix models to interpret the therapeutic potential of the co-polymer. *Biochim Biophys Acta*, *1818*(3), 537-550. https://doi.org/10.1016/j.bbamem.2011.12.010

Barniol-Xicota, M., & Verhelst, S. H. L. (2020). Isolation of intramembrane proteases in membrane-like environments. *Biochim Biophys Acta Biomembr*, *1862*(4), 183193. https://doi.org/10.1016/j.bbamem.2020.183193

Bartley, T. D., Bogenberger, J., Hunt, P., Li, Y. S., Lu, H. S., Martin, F., Chang, M. S., Samal, B., Nichol, J. L., Swift, S., & et al. (1994). Identification and cloning of a megakaryocyte growth and development factor that is a ligand for the cytokine receptor Mpl. *Cell*, *77*(7), 1117-1124. https://doi.org/10.1016/0092-8674(94)90450-2

Bayburt, T. H., Grinkova, Y. V., & Sligar, S. G. (2002). Self-assembly of discoidal phospholipid bilayer nanoparticles with membrane scaffold proteins. *Nano Letters*, *2*(8), 853-856. https://doi.org/10.1021/nl025623k

Beck, F., Geiger, J., Gambaryan, S., Veit, J., Vaudel, M., Nollau, P., Kohlbacher, O., Martens, L., Walter, U., Sickmann, A., & Zahedi, R. P. (2014). Time-resolved characterization of cAMP/PKA-dependent signaling reveals that platelet inhibition is a concerted process involving multiple signaling pathways. *Blood*, *123*(5), e1-e10. https://doi.org/10.1182/blood-2013-07-512384

Beer, J. H., Buchi, L., & Steiner, B. (1994). Glycocalicin: a new assay--the normal plasma levels and its potential usefulness in selected diseases. *Blood*, *83*(3), 691-702. https://www.ncbi.nlm.nih.gov/pubmed/8298132

Bender, M., Hagedorn, I., & Nieswandt, B. (2011). Genetic and antibody-induced glycoprotein VI deficiency equally protects mice from mechanically and FeCl(3) -induced thrombosis. *J Thromb Haemost*, *9*(7), 1423-1426. https://doi.org/10.1111/j.1538-7836.2011.04328.x

Bender, M., Hofmann, S., Stegner, D., Chalaris, A., Bosl, M., Braun, A., Scheller, J., Rose-John, S., & Nieswandt, B. (2010). Differentially regulated GPVI ectodomain shedding by multiple platelet-expressed proteinases. *Blood*, *116*(17), 3347-3355. https://doi.org/10.1182/blood-2010-06-289108

Bender, M., Thon, J. N., Ehrlicher, A. J., Wu, S., Mazutis, L., Deschmann, E., Sola-Visner, M., Italiano, J. E., & Hartwig, J. H. (2015). Microtubule sliding drives proplatelet elongation and is dependent on cytoplasmic dynein. *Blood*, *125*(5), 860-868. https://doi.org/10.1182/blood-2014-09-600858

Bennett, J. S., Chan, C., Vilaire, G., Mousa, S. A., & DeGrado, W. F. (1997). Agonist-activated alphavbeta3 on platelets and lymphocytes binds to the matrix protein osteopontin. *J Biol Chem*, *272*(13), 8137-8140. https://doi.org/10.1074/jbc.272.13.8137

Berditchevski, F., Zutter, M. M., & Hemler, M. E. (1996). Characterization of novel complexes on the cell surface between integrins and proteins with 4 transmembrane domains (TM4 proteins). *Mol Biol Cell*, *7*(2), 193-207. https://doi.org/10.1091/mbc.7.2.193

Bergmeier, W., Piffath, C. L., Cheng, G., Dole, V. S., Zhang, Y., von Andrian, U. H., & Wagner, D. D. (2004). Tumor necrosis factor-alpha-converting enzyme (ADAM17) mediates GPIbalpha shedding from platelets in vitro and in vivo. *Circ Res*, *95*(7), 677-683. https://doi.org/10.1161/01.RES.0000143899.73453.11

Berlanga, O., Bori-Sanz, T., James, J. R., Frampton, J., Davis, S. J., Tomlinson, M. G., & Watson, S. P. (2007). Glycoprotein VI oligomerization in cell lines and platelets. *J Thromb Haemost*, *5*(5), 1026-1033. https://doi.org/10.1111/j.1538-7836.2007.02449.x

Berndt, M. C., Gregory, C., Kabral, A., Zola, H., Fournier, D., & Castaldi, P. A. (1985). Purification and preliminary characterization of the glycoprotein Ib complex in the

human platelet membrane. *Eur J Biochem*, *151*(3), 637-649. https://doi.org/10.1111/j.1432-1033.1985.tb09152.x

Bjornestad, V. A., Orwick-Rydmark, M., & Lund, R. (2021). Understanding the Structural Pathways for Lipid Nanodisc Formation: How Styrene Maleic Acid Copolymers Induce Membrane Fracture and Disc Formation. *Langmuir*, *37*(20), 6178-6188. https://doi.org/10.1021/acs.langmuir.1c00304

Bledzka, K., Qin, J., & Plow, E. F. (2019). 12 - Integrin αIIbβ3. In A. D. Michelson (Ed.), *Platelets (Fourth Edition)* (pp. 227-241). Academic Press. https://doi.org/https://doi.org/10.1016/B978-0-12-813456-6.00012-6

Boucheix, C., Benoit, P., Frachet, P., Billard, M., Worthington, R. E., Gagnon, J., & Uzan, G. (1991). Molecular cloning of the CD9 antigen. A new family of cell surface proteins. *J Biol Chem*, *266*(1), 117-122. https://www.ncbi.nlm.nih.gov/pubmed/1840589

Bourne, J. H., Colicchia, M., Di, Y., Martin, E., Slater, A., Roumenina, L. T., Dimitrov, J. D., Watson, S. P., & Rayes, J. (2021). Heme induces human and mouse platelet activation through C-type-lectin-like receptor-2. *Haematologica*, *106*(2), 626-629. https://doi.org/10.3324/haematol.2020.246488

Boyington, J. C., Raiz, A. N., Brooks, A. G., Patamawenu, A., & Sun, P. D. (2000). Reconstitution of bacterial expressed human CD94: the importance of the stem region for dimer formation. *Protein Expr Purif*, *18*(2), 235-241. https://doi.org/10.1006/prep.1999.1188

Brady, N. G., Qian, S., & Bruce, B. D. (2019). Analysis of styrene maleic acid alternating copolymer supramolecular assemblies in solution by small angle X-ray scattering. *European Polymer Journal*, *111*, 178-184. https://doi.org/10.1016/j.eurpolymj.2018.11.034

Brass, L. F., Tomaiuolo, M., Welsh, J., Poventud-Fuentes, I., Zhu, L., Diamond, S. L., & Stalker, T. J. (2019). 20 - Hemostatic Thrombus Formation in Flowing Blood. In A. D. Michelson (Ed.), *Platelets (Fourth Edition)* (pp. 371-391). Academic Press. https://doi.org/https://doi.org/10.1016/B978-0-12-813456-6.00020-5

Broecker, J., Eger, B. T., & Ernst, O. P. (2017). Crystallogenesis of Membrane Proteins Mediated by Polymer-Bounded Lipid Nanodiscs. *Structure*, *25*(2), 384-392. https://doi.org/10.1016/j.str.2016.12.004

Brown, R. A., Masters, A. J., Price, C., & Yuan, X. F. (1989). 6 - Chain Segregation in Block Copolymers. In G. Allen & J. C. Bevington (Eds.), *Comprehensive Polymer Science and Supplements* (pp. 155-198). Pergamon. https://doi.org/https://doi.org/10.1016/B978-0-08-096701-1.00043-4

Bruhn, H. (2005). A short guided tour through functional and structural features of saposin-like proteins. *Biochem J*, *389*(Pt 2), 249-257. https://doi.org/10.1042/BJ20050051

Bultmann, A., Li, Z., Wagner, S., Peluso, M., Schonberger, T., Weis, C., Konrad, I., Stellos, K., Massberg, S., Nieswandt, B., Gawaz, M., Ungerer, M., & Munch, G. (2010). Impact of glycoprotein VI and platelet adhesion on atherosclerosis--a possible role of fibronectin. *J Mol Cell Cardiol*, *49*(3), 532-542. https://doi.org/10.1016/j.yjmcc.2010.04.009

Burkhart, J. M., Vaudel, M., Gambaryan, S., Radau, S., Walter, U., Martens, L., Geiger, J., Sickmann, A., & Zahedi, R. P. (2012). The first comprehensive and quantitative analysis of human platelet protein composition allows the comparative analysis of structural and functional pathways. *Blood*, *120*(15), e73-82. https://doi.org/10.1182/blood-2012-04-416594

Cao, Y., Fang, J., Shi, Y., Wang, H., Chen, X., Liu, Y., Zhu, Z., Cao, Y., Hong, Z., & Chai, Y. (2022). Screening potential P-glycoprotein inhibitors by combination of a detergent-

free membrane protein extraction with surface plasmon resonance biosensor. *Acta Pharm Sin B*, *12*(7), 3113-3123. https://doi.org/10.1016/j.apsb.2022.03.016

Caparotta, M., Puiatti, M., & Masone, D. (2021). Artificial stabilization of the fusion pore by intra-organelle styrene-maleic acid copolymers. *Soft Matter*, *17*(36), 8314-8321. https://doi.org/10.1039/d1sm00978h

Carlson, M. L., Young, J. W., Zhao, Z., Fabre, L., Jun, D., Li, J., Li, J., Dhupar, H. S., Wason, I., Mills, A. T., Beatty, J. T., Klassen, J. S., Rouiller, I., & Duong, F. (2018). The Peptidisc, a simple method for stabilizing membrane proteins in detergent-free solution. *Elife*, *7*. https://doi.org/10.7554/eLife.34085

Cattaneo, M. (2003). Inherited platelet-based bleeding disorders. *J Thromb Haemost*, *1*(7), 1628-1636. https://doi.org/10.1046/j.1538-7836.2003.00266.x

Cattaneo, M. (2005). The P2 receptors and congenital platelet function defects. *Semin Thromb Hemost*, *31*(2), 168-173. https://doi.org/10.1055/s-2005-869522

Cattaneo, M. (2019a). 14 - The Platelet P2 Receptors. In A. D. Michelson (Ed.), *Platelets (Fourth Edition)* (pp. 259-277). Academic Press. https://doi.org/https://doi.org/10.1016/B978-0-12-813456-6.00014-X

Cattaneo, M. (2019b). 48 - Inherited Disorders of Platelet Function. In A. D. Michelson (Ed.), *Platelets (Fourth Edition)* (pp. 877-904). Academic Press. https://doi.org/https://doi.org/10.1016/B978-0-12-813456-6.00048-5

Cattaneo, M., Bettega, D., Lombardi, R., Lecchi, A., & Mannucci, P. M. (1992). Sustained correction of the bleeding time in an afibrinogenaemic patient after infusion of fresh frozen plasma. *Br J Haematol*, *82*(2), 388-390. https://doi.org/10.1111/j.1365-2141.1992.tb06434.x

Cattaneo, M., Canciani, M. T., Lecchi, A., Kinlough-Rathbone, R. L., Packham, M. A., Mannucci, P. M., & Mustard, J. F. (1990). Released adenosine diphosphate stabilizes thrombin-induced human platelet aggregates. *Blood*, *75*(5), 1081-1086. https://www.ncbi.nlm.nih.gov/pubmed/2137716

Chapman, L. M., Aggrey, A. A., Field, D. J., Srivastava, K., Ture, S., Yui, K., Topham, D. J., Baldwin, W. M., 3rd, & Morrell, C. N. (2012). Platelets present antigen in the context of MHC class I. *J Immunol*, *189*(2), 916-923. https://doi.org/10.4049/jimmunol.1200580

Charrin, S., Jouannet, S., Boucheix, C., & Rubinstein, E. (2014). Tetraspanins at a glance. *Journal of Cell Science*, *127*(17), 3641-3648. https://doi.org/10.1242/jcs.154906

Chen, H., Locke, D., Liu, Y., Liu, C., & Kahn, M. L. (2002). The platelet receptor GPVI mediates both adhesion and signaling responses to collagen in a receptor density-dependent fashion. *J Biol Chem*, *277*(4), 3011-3019. https://doi.org/10.1074/jbc.M109714200

Chen, J., Diacovo, T. G., Grenache, D. G., Santoro, S. A., & Zutter, M. M. (2002). The alpha(2) integrin subunit-deficient mouse: a multifaceted phenotype including defects of branching morphogenesis and hemostasis. *Am J Pathol*, *161*(1), 337-344. https://doi.org/10.1016/s0002-9440(10)64185-5

Chien, C. H., Helfinger, L. R., Bostock, M. J., Solt, A., Tan, Y. L., & Nietlispach, D. (2017). An Adaptable Phospholipid Membrane Mimetic System for Solution NMR Studies of Membrane Proteins. *J Am Chem Soc*, *139*(42), 14829-14832. https://doi.org/10.1021/jacs.7b06730

Chipot, C., Dehez, F., Schnell, J. R., Zitzmann, N., Pebay-Peyroula, E., Catoire, L. J., Miroux, B., Kunji, E. R. S., Veglia, G., Cross, T. A., & Schanda, P. (2018). Perturbations of Native Membrane Protein Structure in Alkyl Phosphocholine Detergents: A Critical Assessment of NMR and Biophysical Studies. *Chem Rev*, *118*(7), 3559-3607. https://doi.org/10.1021/acs.chemrev.7b00570

Clapham, D. E. (2007). Calcium signaling. *Cell*, *131*(6), 1047-1058. https://doi.org/10.1016/j.cell.2007.11.028

Clark, J. C. (2020). *The role of dimerisation in the activation of platelets by the collagen receptor GPVI* University of Birmingham]. Birmingham. https://etheses.bham.ac.uk/

Clark, J. C., Damaskinaki, F. N., Cheung, Y. F. H., Slater, A., & Watson, S. P. (2021). Structure-function relationship of the platelet glycoprotein VI (GPVI) receptor: does it matter if it is a dimer or monomer? *Platelets*, *32*(6), 724-732. https://doi.org/10.1080/09537104.2021.1887469

Clark, J. C., Neagoe, R. A. I., Zuidscherwoude, M., Kavanagh, D. M., Slater, A., Martin, E. M., Soave, M., Stegner, D., Nieswandt, B., Poulter, N. S., Hummert, J., Herten, D. P., Tomlinson, M. G., Hill, S. J., & Watson, S. P. (2021). Evidence that GPVI is Expressed as a Mixture of Monomers and Dimers, and that the D2 Domain is not Essential for GPVI Activation. *Thromb Haemost*, *121*(11), 1435-1447. https://doi.org/10.1055/a-1401-5014

Clark, S. R., Ma, A. C., Tavener, S. A., McDonald, B., Goodarzi, Z., Kelly, M. M., Patel, K. D., Chakrabarti, S., McAvoy, E., Sinclair, G. D., Keys, E. M., Allen-Vercoe, E., Devinney, R., Doig, C. J., Green, F. H., & Kubes, P. (2007). Platelet TLR4 activates neutrophil extracellular traps to ensnare bacteria in septic blood. *Nat Med*, *13*(4), 463-469. https://doi.org/10.1038/nm1565

Clemetson, J. M., Polgar, J., Magnenat, E., Wells, T. N. C., & Clemetson, K. J. (1999). The platelet collagen receptor GPVI is an immunoglobulin superfamily member closely related to Fc alpha R and natural killer receptors. *Blood*, *94*(10), 619a-619a. <Go to ISI>://WOS:000083790302801

Clemetson, K. J. (2012). Platelets and primary haemostasis. *Thromb Res*, *129*(3), 220-224. https://doi.org/10.1016/j.thromres.2011.11.036

Clemetson, K. J., & Clemetson, J. M. (2019). 9 - Platelet Receptors. In A. D. Michelson (Ed.), *Platelets (Fourth Edition)* (pp. 169-192). Academic Press. https://doi.org/https://doi.org/10.1016/B978-0-12-813456-6.00009-6

Clemetson, K. J., Clemetson, J. M., Proudfoot, A. E., Power, C. A., Baggiolini, M., & Wells, T. N. (2000). Functional expression of CCR1, CCR3, CCR4, and CXCR4 chemokine receptors on human platelets. *Blood*, *96*(13), 4046-4054. https://www.ncbi.nlm.nih.gov/pubmed/11110672

Cocco, E., Varughese, J., Buza, N., Bellone, S., Glasgow, M., Bellone, M., Todeschini, P., Carrara, L., Silasi, D. A., Azodi, M., Schwartz, P. E., Rutherford, T. J., Pecorelli, S., Lockwood, C. J., & Santin, A. D. (2011). Expression of tissue factor in adenocarcinoma and squamous cell carcinoma of the uterine cervix: implications for immunotherapy with hI-con1, a factor VII-IgGFc chimeric protein targeting tissue factor. *BMC Cancer*, *11*, 263. https://doi.org/10.1186/1471-2407-11-263

Colbasevici, A., Voskoboynikova, N., Orekhov, P. S., Bozdaganyan, M. E., Karlova, M. G., Sokolova, O. S., Klare, J. P., Mulkidjanian, A. Y., Shaitan, K. V., & Steinhoff, H. J. (2020). Lipid dynamics in nanoparticles formed by maleic acid-containing copolymers: EPR spectroscopy and molecular dynamics simulations. *Biochim Biophys Acta Biomembr*, *1862*(5), 183207. https://doi.org/10.1016/j.bbamem.2020.183207

Colman, R. W. (2006). Are hemostasis and thrombosis two sides of the same coin? *J Exp Med*, *203*(3), 493-495. https://doi.org/10.1084/jem.20060217

Corin, K., Baaske, P., Ravel, D. B., Song, J., Brown, E., Wang, X., Wienken, C. J., Jerabek-Willemsen, M., Duhr, S., Luo, Y., Braun, D., & Zhang, S. (2011). Designer lipid-like peptides: a class of detergents for studying functional olfactory receptors using commercial cell-free systems. *PLoS One*, *6*(11), e25067. https://doi.org/10.1371/journal.pone.0025067

Craig, A. F., Clark, E. E., Sahu, I. D., Zhang, R., Frantz, N. D., Al-Abdul-Wahid, M. S., Dabney-Smith, C., Konkolewicz, D., & Lorigan, G. A. (2016). Tuning the size of styrene-maleic acid copolymer-lipid nanoparticles (SMALPs) using RAFT polymerization for biophysical studies. *Biochim Biophys Acta*, *1858*(11), 2931-2939. https://doi.org/10.1016/j.bbamem.2016.08.004

Crittenden, J. R., Bergmeier, W., Zhang, Y., Piffath, C. L., Liang, Y., Wagner, D. D., Housman, D. E., & Graybiel, A. M. (2004). CalDAG-GEFI integrates signaling for platelet aggregation and thrombus formation. *Nat Med*, *10*(9), 982-986. https://doi.org/10.1038/nm1098

Croft, S. A., Samani, N. J., Teare, M. D., Hampton, K. K., Steeds, R. P., Channer, K. S., & Daly, M. E. (2001). Novel platelet membrane glycoprotein VI dimorphism is a risk factor for myocardial infarction. *Circulation*, *104*(13), 1459-1463. https://doi.org/10.1161/hc3801.096397

Cuevas Arenas, R., Danielczak, B., Martel, A., Porcar, L., Breyton, C., Ebel, C., & Keller, S. (2017). Fast Collisional Lipid Transfer Among Polymer-Bounded Nanodiscs. *Sci Rep*, *7*, 45875. https://doi.org/10.1038/srep45875

da Silva Ferreira, N. C., Alves, L. A., & Soares-Bezerra, R. J. (2019). Potential Therapeutic Applications of P2 Receptor Antagonists: From Bench to Clinical Trials. *Curr Drug Targets*, *20*(9), 919-937. https://doi.org/10.2174/1389450120666190213095923

Dahmane, T., Damian, M., Mary, S., Popot, J. L., & Baneres, J. L. (2009). Amphipol-assisted in vitro folding of G protein-coupled receptors. *Biochemistry*, *48*(27), 6516-6521. https://doi.org/10.1021/bi801729z

Daly, M. E. (2011). Determinants of platelet count in humans. *Haematologica*, *96*(1), 10-13. https://doi.org/10.3324/haematol.2010.035287

Dangelmaier, C., Jin, J., Smith, J. B., & Kunapuli, S. P. (2001). Potentiation of thromboxane A2-induced platelet secretion by Gi signaling through the phosphoinositide-3 kinase pathway. *Thromb Haemost*, *85*(2), 341-348. https://www.ncbi.nlm.nih.gov/pubmed/11246558

Daruwalla, J., Nikfarjam, M., Greish, K., Malcontenti-Wilson, C., Muralidharan, V., Christophi, C., & Maeda, H. (2010). In vitro and in vivo evaluation of tumor targeting styrene-maleic acid copolymer-pirarubicin micelles: Survival improvement and inhibition of liver metastases. *Cancer Sci*, *101*(8), 1866-1874. https://doi.org/10.1111/j.1349-7006.2010.01619.x

Das, M., Ithychanda, S., Qin, J., & Plow, E. F. (2014). Mechanisms of talin-dependent integrin signaling and crosstalk. *Biochim Biophys Acta*, *1838*(2), 579-588. https://doi.org/10.1016/j.bbamem.2013.07.017

Dawaliby, R., Trubbia, C., Delporte, C., Masureel, M., Van Antwerpen, P., Kobilka, B. K., & Govaerts, C. (2016). Allosteric regulation of G protein-coupled receptor activity by phospholipids. *Nat Chem Biol*, *12*(1), 35-39. https://doi.org/10.1038/nchembio.1960

De Candia, E., Hall, S. W., Rutella, S., Landolfi, R., Andrews, R. K., & De Cristofaro, R. (2001). Binding of thrombin to glycoprotein Ib accelerates the hydrolysis of Par-1 on intact platelets. *J Biol Chem*, *276*(7), 4692-4698. https://doi.org/10.1074/jbc.M008160200

de la Fuente, M., Noble, D. N., Verma, S., & Nieman, M. T. (2012). Mapping human protease-activated receptor 4 (PAR4) homodimer interface to transmembrane helix 4. *J Biol Chem*, *287*(13), 10414-10423. https://doi.org/10.1074/jbc.M112.341438

De Luca, G., Savonitto, S., van't Hof, A. W., & Suryapranata, H. (2015). Platelet GP IIb-IIIa Receptor Antagonists in Primary Angioplasty: Back to the Future. *Drugs*, *75*(11), 1229-1253. https://doi.org/10.1007/s40265-015-0425-7

de Sauvage, F. J., Hass, P. E., Spencer, S. D., Malloy, B. E., Gurney, A. L., Spencer, S. A., Darbonne, W. C., Henzel, W. J., Wong, S. C., Kuang, W. J., & et al. (1994). Stimulation of megakaryocytopoiesis and thrombopoiesis by the c-Mpl ligand. *Nature*, *369*(6481), 533-538. https://doi.org/10.1038/369533a0

de Winde, C. M., Matthews, A. L., van Deventer, S., van der Schaaf, A., Tomlinson, N. D., Jansen, E., Eble, J. A., Nieswandt, B., McGettrick, H. M., Figdor, C. G., Tomlinson, M. G., Acton, S. E., & van Spriel, A. B. (2018). C-type lectin-like receptor 2 (CLEC-2)-dependent dendritic cell migration is controlled by tetraspanin CD37. *Journal of Cell Science*, *131*(19). https://doi.org/10.1242/jcs.214551

Degrauwe, S., Pilgrim, T., Aminian, A., Noble, S., Meier, P., & Iglesias, J. F. (2017). Dual antiplatelet therapy for secondary prevention of coronary artery disease. *Open Heart*, *4*(2), e000651. https://doi.org/10.1136/openhrt-2017-000651

Desrames, A., Genetet, S., Delcourt, M. P., Goossens, D., & Mouro-Chanteloup, I. (2020). Detergent-free isolation of native red blood cell membrane complexes. *Biochim Biophys Acta Biomembr*, *1862*(2), 183126. https://doi.org/10.1016/j.bbamem.2019.183126

Dominguez Pardo, J. J., van Walree, C. A., Egmond, M. R., Koorengevel, M. C., & Killian, J. A. (2019). Nanodiscs bounded by styrene-maleic acid allow trans-cis isomerization of enclosed photoswitches of azobenzene labeled lipids. *Chem Phys Lipids*, *220*, 1-5. https://doi.org/10.1016/j.chemphyslip.2019.02.002

Dorr, J. M., Koorengevel, M. C., Schafer, M., Prokofyev, A. V., Scheidelaar, S., van der Cruijsen, E. A., Dafforn, T. R., Baldus, M., & Killian, J. A. (2014). Detergent-free isolation, characterization, and functional reconstitution of a tetrameric K+ channel: the power of native nanodiscs. *Proc Natl Acad Sci U S A*, *111*(52), 18607-18612. https://doi.org/10.1073/pnas.1416205112

Dorr, J. M., Scheidelaar, S., Koorengevel, M. C., Dominguez, J. J., Schafer, M., van Walree, C. A., & Killian, J. A. (2016). The styrene-maleic acid copolymer: a versatile tool in membrane research. *Eur Biophys J*, *45*(1), 3-21. https://doi.org/10.1007/s00249-015-1093-y

Dowal, L., Yang, W., Freeman, M. R., Steen, H., & Flaumenhaft, R. (2011). Proteomic analysis of palmitoylated platelet proteins. *Blood*, *118*(13), e62-73. https://doi.org/10.1182/blood-2011-05-353078

Drulyte, I., Gutgsell, A. R., Lloris-Garcera, P., Liss, M., Geschwindner, S., Radjainia, M., Frauenfeld, J., & Loving, R. (2023). Direct cell extraction of membrane proteins for structure-function analysis. *Sci Rep*, *13*(1), 1420. https://doi.org/10.1038/s41598-023-28455-w

Du, X., Beutler, L., Ruan, C., Castaldi, P. A., & Berndt, M. C. (1987). Glycoprotein Ib and glycoprotein IX are fully complexed in the intact platelet membrane. *Blood*, *69*(5), 1524-1527. https://www.ncbi.nlm.nih.gov/pubmed/2436691

Du, X., Harris, S. J., Tetaz, T. J., Ginsberg, M. H., & Berndt, M. C. (1994). Association of a phospholipase A2 (14-3-3 protein) with the platelet glycoprotein Ib-IX complex. *J Biol Chem*, *269*(28), 18287-18290. https://www.ncbi.nlm.nih.gov/pubmed/8034572

Durr, U. H., Soong, R., & Ramamoorthy, A. (2013). When detergent meets bilayer: birth and coming of age of lipid bicelles. *Prog Nucl Magn Reson Spectrosc*, *69*, 1-22. https://doi.org/10.1016/j.pnmrs.2013.01.001

Durrant, T. N., van den Bosch, M. T., & Hers, I. (2017). Integrin alphaIIbbeta3 outside-in signaling. *Blood*, *130*(14), 1607-1619. https://doi.org/10.1182/blood-2017-03-773614

Ebrahim, M., Jamasbi, J., Adler, K., Megens, R. T. A., M'Bengue, Y., Blanchet, X., Uhland, K., Ungerer, M., Brandl, R., Weber, C., Elia, N., Lorenz, R., Munch, G., & Siess, W.

(2018). Dimeric Glycoprotein VI Binds to Collagen but Not to Fibrin. *Thromb Haemost*, *118*(2), 351-361. https://doi.org/10.1160/TH17-04-0302

Eckly, A., Heijnen, H., Pertuy, F., Geerts, W., Proamer, F., Rinckel, J. Y., Leon, C., Lanza, F., & Gachet, C. (2014). Biogenesis of the demarcation membrane system (DMS) in megakaryocytes. *Blood*, *123*(6), 921-930. https://doi.org/10.1182/blood-2013-03-492330

Edelstein, L. C., Simon, L. M., Lindsay, C. R., Kong, X., Teruel-Montoya, R., Tourdot, B. E., Chen, E. S., Ma, L., Coughlin, S., Nieman, M., Holinstat, M., Shaw, C. A., & Bray, P. F. (2014). Common variants in the human platelet PAR4 thrombin receptor alter platelet function and differ by race. *Blood*, *124*(23), 3450-3458. https://doi.org/10.1182/blood-2014-04-572479

Egan, K., Cooke, N., & Kenny, D. (2014). Living in shear: platelets protect cancer cells from shear induced damage. *Clin Exp Metastasis*, *31*(6), 697-704. https://doi.org/10.1007/s10585-014-9660-7

Elzey, B. D., Tian, J., Jensen, R. J., Swanson, A. K., Lees, J. R., Lentz, S. R., Stein, C. S., Nieswandt, B., Wang, Y., Davidson, B. L., & Ratliff, T. L. (2003). Platelet-mediated modulation of adaptive immunity. A communication link between innate and adaptive immune compartments. *Immunity*, *19*(1), 9-19. https://doi.org/10.1016/s1074-7613(03)00177-8

Eschenbrenner, E., Jouannet, S., Clay, D., Chaker, J., Boucheix, C., Brou, C., Tomlinson, M. G., Charrin, S., & Rubinstein, E. (2020). TspanC8 tetraspanins differentially regulate ADAM10 endocytosis and half-life. *Life Sci Alliance*, *3*(1). https://doi.org/10.26508/lsa.201900444

Esmaili, M., Tancowny, B. P., Wang, X., Moses, A., Cortez, L. M., Sim, V. L., Wille, H., & Overduin, M. (2020). Native nanodiscs formed by styrene maleic acid copolymer derivatives help recover infectious prion multimers bound to brain-derived lipids. *J Biol Chem*, *295*(25), 8460-8469. https://doi.org/10.1074/jbc.RA119.012348

Eto, K., Murphy, R., Kerrigan, S. W., Bertoni, A., Stuhlmann, H., Nakano, T., Leavitt, A. D., & Shattil, S. J. (2002). Megakaryocytes derived from embryonic stem cells implicate CalDAG-GEFI in integrin signaling. *Proc Natl Acad Sci U S A*, *99*(20), 12819-12824. https://doi.org/10.1073/pnas.202380099

Ezumi, Y., Shindoh, K., Tsuji, M., & Takayama, H. (1998). Physical and functional association of the Src family kinases Fyn and Lyn with the collagen receptor glycoprotein VI-Fc receptor gamma chain complex on human platelets. *J Exp Med*, *188*(2), 267-276. https://doi.org/10.1084/jem.188.2.267

Ezumi, Y., Uchiyama, T., & Takayama, H. (2000). Molecular cloning, genomic structure, chromosomal localization, and alternative splice forms of the platelet collagen receptor glycoprotein VI. *Biochem Biophys Res Commun*, *277*(1), 27-36. https://doi.org/10.1006/bbrc.2000.3624

Fabre, J. E., Nguyen, M., Latour, A., Keifer, J. A., Audoly, L. P., Coffman, T. M., & Koller, B. H. (1999). Decreased platelet aggregation, increased bleeding time and resistance to thromboembolism in P2Y1-deficient mice. *Nat Med*, *5*(10), 1199-1202. https://doi.org/10.1038/13522

Feitsma, L. J., Brondijk, H. C., Jarvis, G. E., Hagemans, D., Bihan, D., Jerah, N., Versteeg, M., Farndale, R. W., & Huizinga, E. G. (2022). Structural insights into collagen binding by platelet receptor glycoprotein VI. *Blood*, *139*(20), 3087-3098. https://doi.org/10.1182/blood.2021013614

Feng, J., Call, M. E., & Wucherpfennig, K. W. (2006). The assembly of diverse immune receptors is focused on a polar membrane-embedded interaction site. *PLoS Biol*, *4*(5), e142. https://doi.org/10.1371/journal.pbio.0040142

Fitter, S., Tetaz, T. J., Berndt, M. C., & Ashman, L. K. (1995). Molecular cloning of cDNA encoding a novel platelet-endothelial cell tetra-span antigen, PETA-3. *Blood*, *86*(4), 1348-1355. https://www.ncbi.nlm.nih.gov/pubmed/7632941

Flaumenhaft, R., & Sharda, A. (2019). 19 - Platelet Secretion. In A. D. Michelson (Ed.), *Platelets (Fourth Edition)* (pp. 349-370). Academic Press. https://doi.org/https://doi.org/10.1016/B978-0-12-813456-6.00019-9

Fox, J. E. (1994). Shedding of adhesion receptors from the surface of activated platelets. *Blood Coagul Fibrinolysis*, *5*(2), 291-304. https://doi.org/10.1097/00001721-199404000-00020

Frauenfeld, J., Loving, R., Armache, J. P., Sonnen, A. F., Guettou, F., Moberg, P., Zhu, L., Jegerschold, C., Flayhan, A., Briggs, J. A., Garoff, H., Low, C., Cheng, Y., & Nordlund, P. (2016). A saposin-lipoprotein nanoparticle system for membrane proteins. *Nat Methods*, *13*(4), 345-351. https://doi.org/10.1038/nmeth.3801

Fuller, G. L., Williams, J. A., Tomlinson, M. G., Eble, J. A., Hanna, S. L., Pohlmann, S., Suzuki-Inoue, K., Ozaki, Y., Watson, S. P., & Pearce, A. C. (2007). The C-type lectin receptors CLEC-2 and Dectin-1, but not DC-SIGN, signal via a novel YXXL-dependent signaling cascade. *J Biol Chem*, *282*(17), 12397-12409. https://doi.org/10.1074/jbc.M609558200

Garavito, R. M., & Ferguson-Miller, S. (2001). Detergents as tools in membrane biochemistry. *J Biol Chem*, *276*(35), 32403-32406. https://doi.org/10.1074/jbc.R100031200

Garcia-Nafria, J., Nehme, R., Edwards, P. C., & Tate, C. G. (2018). Cryo-EM structure of the serotonin 5-HT1B receptor coupled to heterotrimeric Go. *Nature*, *558*(7711), 620-623. https://doi.org/10.1038/s41586-018-0241-9

Gardiner, E. E., Arthur, J. F., Kahn, M. L., Berndt, M. C., & Andrews, R. K. (2004). Regulation of platelet membrane levels of glycoprotein VI by a platelet-derived metalloproteinase. *Blood*, *104*(12), 3611-3617. https://doi.org/10.1182/blood-2004-04-1549

Gardiner, E. E., Karunakaran, D., Shen, Y., Arthur, J. F., Andrews, R. K., & Berndt, M. C. (2007). Controlled shedding of platelet glycoprotein (GP)VI and GPIb-IX-V by ADAM family metalloproteinases. *J Thromb Haemost*, *5*(7), 1530-1537. https://doi.org/10.1111/j.1538-7836.2007.02590.x

Gawaz, M. (2018). Novel Ligands for Platelet Glycoprotein VI. *Thromb Haemost*, *118*(3), 435-436. https://doi.org/10.1055/s-0038-1635080

Gear, A. R., & Camerini, D. (2003). Platelet chemokines and chemokine receptors: linking hemostasis, inflammation, and host defense. *Microcirculation*, *10*(3-4), 335-350. https://doi.org/10.1038/sj.mn.7800198

Gharpure, A., Teng, J., Zhuang, Y., Noviello, C. M., Walsh, R. M., Jr., Cabuco, R., Howard, R. J., Zaveri, N. T., Lindahl, E., & Hibbs, R. E. (2019). Agonist Selectivity and Ion Permeation in the alpha3beta4 Ganglionic Nicotinic Receptor. *Neuron*, *104*(3), 501-511 e506. https://doi.org/10.1016/j.neuron.2019.07.030

Gilio, K., Harper, M. T., Cosemans, J. M., Konopatskaya, O., Munnix, I. C., Prinzen, L., Leitges, M., Liu, Q., Molkentin, J. D., Heemskerk, J. W., & Poole, A. W. (2010). Functional divergence of platelet protein kinase C (PKC) isoforms in thrombus formation on collagen. *J Biol Chem*, *285*(30), 23410-23419. https://doi.org/10.1074/jbc.M110.136176

Gitz, E., Pollitt, A. Y., Gitz-Francois, J. J., Alshehri, O., Mori, J., Montague, S., Nash, G. B., Douglas, M. R., Gardiner, E. E., Andrews, R. K., Buckley, C. D., Harrison, P., & Watson, S. P. (2014). CLEC-2 expression is maintained on activated platelets and on platelet microparticles. *Blood*, *124*(14), 2262-2270. https://doi.org/10.1182/blood-2014-05-572818

Golebiewska, E. M., & Poole, A. W. (2015). Platelet secretion: From haemostasis to wound healing and beyond. *Blood Rev*, *29*(3), 153-162. https://doi.org/10.1016/j.blre.2014.10.003

Goossens, D., Champomier, F., Rouger, P., & Salmon, C. (1987). Human monoclonal antibodies against blood group antigens. Preparation of a series of stable EBV immortalized B clones producing high levels of antibody of different isotypes and specificities. *J Immunol Methods*, *101*(2), 193-200. https://doi.org/10.1016/0022-1759(87)90150-5

Greish, K., Sawa, T., Fang, J., Akaike, T., & Maeda, H. (2004). SMA-doxorubicin, a new polymeric micellar drug for effective targeting to solid tumours. *J Control Release*, *97*(2), 219-230. https://doi.org/10.1016/j.jconrel.2004.03.027

Grenache, D. G., Coleman, T., Semenkovich, C. F., Santoro, S. A., & Zutter, M. M. (2003). Alpha2beta1 integrin and development of atherosclerosis in a mouse model: assessment of risk. *Arterioscler Thromb Vasc Biol*, *23*(11), 2104-2109. https://doi.org/10.1161/01.ATV.0000097282.22923.EF

Grime, R. L., Goulding, J., Uddin, R., Stoddart, L. A., Hill, S. J., Poyner, D. R., Briddon, S. J., & Wheatley, M. (2020). Single molecule binding of a ligand to a G-protein-coupled receptor in real time using fluorescence correlation spectroscopy, rendered possible by nano-encapsulation in styrene maleic acid lipid particles. *Nanoscale*, *12*(21), 11518-11525. https://doi.org/10.1039/d0nr01060j

Grime, R. L., Logan, R. T., Nestorow, S. A., Sridhar, P., Edwards, P. C., Tate, C. G., Klumperman, B., Dafforn, T. R., Poyner, D. R., Reeves, P. J., & Wheatley, M. (2021). Differences in SMA-like polymer architecture dictate the conformational changes exhibited by the membrane protein rhodopsin encapsulated in lipid nano-particles. *Nanoscale*, *13*(31), 13519-13528. https://doi.org/10.1039/d1nr02419a

Guidetti, G. F., Bernardi, B., Consonni, A., Rizzo, P., Gruppi, C., Balduini, C., & Torti, M. (2009). Integrin alpha2beta1 induces phosphorylation-dependent and phosphorylation-independent activation of phospholipase Cgamma2 in platelets: role of Src kinase and Rac GTPase. *J Thromb Haemost*, *7*(7), 1200-1206. https://doi.org/10.1111/j.1538-7836.2009.03444.x

Gulamhussein, A. A., Uddin, R., Tighe, B. J., Poyner, D. R., & Rothnie, A. J. (2020). A comparison of SMA (styrene maleic acid) and DIBMA (di-isobutylene maleic acid) for membrane protein purification. *Biochim Biophys Acta Biomembr*, *1862*(7), 183281. https://doi.org/10.1016/j.bbamem.2020.183281

Gunsel, U., & Hagn, F. (2022). Lipid Nanodiscs for High-Resolution NMR Studies of Membrane Proteins. *Chem Rev*, *122*(10), 9395-9421. https://doi.org/10.1021/acs.chemrev.1c00702

Guo, J., & Piguet, P. F. (1998). Stimulation of thrombocytopoiesis decreases platelet beta2 but not beta1 or beta3 integrins. *Br J Haematol*, *100*(4), 712-719. https://doi.org/10.1046/j.1365-2141.1998.00618.x

Gutmann, D. A., Mizohata, E., Newstead, S., Ferrandon, S., Postis, V., Xia, X., Henderson, P. J., van Veen, H. W., & Byrne, B. (2007). A high-throughput method for membrane protein solubility screening: the ultracentrifugation dispersity sedimentation assay. *Protein Sci*, *16*(7), 1422-1428. https://doi.org/10.1110/ps.072759907

Haberstock-Debic, H., Andre, P., Mills, S., Phillips, D. R., & Conley, P. B. (2011). A clopidogrel-insensitive inducible pool of P2Y12 receptors contributes to thrombus formation: inhibition by elinogrel, a direct-acting, reversible P2Y12 antagonist. *J Pharmacol Exp Ther*, *339*(1), 54-61. https://doi.org/10.1124/jpet.111.184143

Haining, E. J., Cherpokova, D., Wolf, K., Becker, I. C., Beck, S., Eble, J. A., Stegner, D., Watson, S. P., & Nieswandt, B. (2017). CLEC-2 contributes to hemostasis

independently of classical hemITAM signaling in mice. *Blood*, *130*(20), 2224-2228. https://doi.org/10.1182/blood-2017-03-771907

Haining, E. J., Matthews, A. L., Noy, P. J., Romanska, H. M., Harris, H. J., Pike, J., Morowski, M., Gavin, R. L., Yang, J., Milhiet, P. E., Berditchevski, F., Nieswandt, B., Poulter, N. S., Watson, S. P., & Tomlinson, M. G. (2017). Tetraspanin Tspan9 regulates platelet collagen receptor GPVI lateral diffusion and activation. *Platelets*, *28*(7), 629-642. https://doi.org/10.1080/09537104.2016.1254175

Haining, E. J., Nicolson, P. L. R., Onselaer, M.-B., Poulter, N. S., Rayes, J., Thomas, M. R., & Watson, S. P. (2019). 11 - GPVI and CLEC-2. In A. D. Michelson (Ed.), *Platelets (Fourth Edition)* (pp. 213-226). Academic Press. https://doi.org/https://doi.org/10.1016/B978-0-12-813456-6.00011-4

Hall, S. C. L., Tognoloni, C., Charlton, J., Bragginton, E. C., Rothnie, A. J., Sridhar, P., Wheatley, M., Knowles, T. J., Arnold, T., Edler, K. J., & Dafforn, T. R. (2018). An acid-compatible co-polymer for the solubilization of membranes and proteins into lipid bilayer-containing nanoparticles. *Nanoscale*, *10*(22), 10609-10619. https://doi.org/10.1039/c8nr01322e

Han, X., Bouck, E. G., Zunica, E. R., Arachiche, A., & Nieman, M. T. (2019). 13 - Protease-Activated Receptors. In A. D. Michelson (Ed.), *Platelets (Fourth Edition)* (pp. 243-257). Academic Press. https://doi.org/https://doi.org/10.1016/B978-0-12-813456-6.00013-8

Han, X., Guo, B., Li, Y., & Zhu, B. (2014). Tissue factor in tumor microenvironment: a systematic review. *J Hematol Oncol*, *7*, 54. https://doi.org/10.1186/s13045-014-0054-8

Han, X., & Nieman, M. T. (2018). PAR4 (Protease-Activated Receptor 4): PARticularly Important 4 Antiplatelet Therapy. *Arterioscler Thromb Vasc Biol*, *38*(2), 287-289. https://doi.org/10.1161/ATVBAHA.117.310550

Harbi, M. H., Smith, C. W., Nicolson, P. L. R., Watson, S. P., & Thomas, M. R. (2021). Novel antiplatelet strategies targeting GPVI, CLEC-2 and tyrosine kinases. *Platelets*, *32*(1), 29-41. https://doi.org/10.1080/09537104.2020.1849600

Harding, B. D., Dixit, G., Burridge, K. M., Sahu, I. D., Dabney-Smith, C., Edelmann, R. E., Konkolewicz, D., & Lorigan, G. A. (2019). Characterizing the structure of styrene-maleic acid copolymer-lipid nanoparticles (SMALPs) using RAFT polymerization for membrane protein spectroscopic studies. *Chem Phys Lipids*, *218*, 65-72. https://doi.org/10.1016/j.chemphyslip.2018.12.002

Hardy, D., Desuzinges Mandon, E., Rothnie, A. J., & Jawhari, A. (2018). The yin and yang of solubilization and stabilization for wild-type and full-length membrane protein. *Methods*, *147*, 118-125. https://doi.org/10.1016/j.ymeth.2018.02.017

Harrison, N., Koo, C. Z., & Tomlinson, M. G. (2021). Regulation of ADAM10 by the TspanC8 Family of Tetraspanins and Their Therapeutic Potential. *Int J Mol Sci*, *22*(13). https://doi.org/10.3390/ijms22136707

Harrison, P., Wilbourn, B., Debili, N., Vainchenker, W., Breton-Gorius, J., Lawrie, A. S., Masse, J. M., Savidge, G. F., & Cramer, E. M. (1989). Uptake of plasma fibrinogen into the alpha granules of human megakaryocytes and platelets. *J Clin Invest*, *84*(4), 1320-1324. https://doi.org/10.1172/JCI114300

Hartmann, D., de Strooper, B., Serneels, L., Craessaerts, K., Herreman, A., Annaert, W., Umans, L., Lubke, T., Lena Illert, A., von Figura, K., & Saftig, P. (2002). The disintegrin/metalloprotease ADAM 10 is essential for Notch signalling but not for alpha-secretase activity in fibroblasts. *Hum Mol Genet*, *11*(21), 2615-2624. https://doi.org/10.1093/hmg/11.21.2615

Hartwig, J. H. (2013). Chapter 8 - The Platelet Cytoskeleton. In A. D. Michelson (Ed.), *Platelets (Third Edition)* (pp. 145-168). Academic Press. https://doi.org/https://doi.org/10.1016/B978-0-12-387837-3.00008-0

Heemskerk, J. W., Willems, G. M., Rook, M. B., & Sage, S. O. (2001). Ragged spiking of free calcium in ADP-stimulated human platelets: regulation of puff-like calcium signals in vitro and ex vivo. *J Physiol*, *535*(Pt 3), 625-635. https://doi.org/10.1111/j.1469-7793.2001.00625.x

Helenius, A., & Simons, K. (1975). Solubilization of membranes by detergents. *Biochim Biophys Acta*, *415*(1), 29-79. https://doi.org/10.1016/0304-4157(75)90016-7

Hellwig, N., Peetz, O., Ahdash, Z., Tascon, I., Booth, P. J., Mikusevic, V., Diskowski, M., Politis, A., Hellmich, Y., Hanelt, I., Reading, E., & Morgner, N. (2018). Native mass spectrometry goes more native: investigation of membrane protein complexes directly from SMALPs. *Chem Commun (Camb)*, *54*(97), 13702-13705. https://doi.org/10.1039/c8cc06284f

Hemler, M. E. (2003). Tetraspanin proteins mediate cellular penetration, invasion, and fusion events and define a novel type of membrane microdomain. *Annu Rev Cell Dev Biol*, *19*, 397-422. https://doi.org/10.1146/annurev.cellbio.19.111301.153609

Hemler, M. E. (2005). Tetraspanin functions and associated microdomains. *Nat Rev Mol Cell Biol*, *6*(10), 801-811. https://doi.org/10.1038/nrm1736

Henn, V., Slupsky, J. R., Grafe, M., Anagnostopoulos, I., Forster, R., Muller-Berghaus, G., & Kroczek, R. A. (1998). CD40 ligand on activated platelets triggers an inflammatory reaction of endothelial cells. *Nature*, *391*(6667), 591-594. https://doi.org/10.1038/35393

Hill, D. J. T., Odonnell, J. H., & Osullivan, P. W. (1985). Analysis of the Mechanism of Copolymerization of Styrene and Maleic-Anhydride. *Macromolecules*, *18*(1), 9-17. https://doi.org/DOI 10.1021/ma00143a002

Hitchcock, I. S., & Kaushansky, K. (2014). Thrombopoietin from beginning to end. *Br J Haematol*, *165*(2), 259-268. https://doi.org/10.1111/bjh.12772

Hitchcock, J. R., Cook, C. N., Bobat, S., Ross, E. A., Flores-Langarica, A., Lowe, K. L., Khan, M., Dominguez-Medina, C. C., Lax, S., Carvalho-Gaspar, M., Hubscher, S., Rainger, G. E., Cobbold, M., Buckley, C. D., Mitchell, T. J., Mitchell, A., Jones, N. D., Van Rooijen, N., Kirchhofer, D., . . . Cunningham, A. F. (2015). Inflammation drives thrombosis after Salmonella infection via CLEC-2 on platelets. *J Clin Invest*, *125*(12), 4429-4446. https://doi.org/10.1172/JCI79070

Hoffmann, M., Eisermann, J., Schoffmann, F. A., Das, M., Vargas, C., Keller, S., & Hinderberger, D. (2021). Influence of different polymer belts on lipid properties in nanodiscs characterized by CW EPR spectroscopy. *Biochim Biophys Acta Biomembr*, *1863*(10), 183681. https://doi.org/10.1016/j.bbamem.2021.183681

Horii, K., Brooks, M. T., & Herr, A. B. (2009). Convulxin forms a dimer in solution and can bind eight copies of glycoprotein VI: implications for platelet activation. *Biochemistry*, *48*(13), 2907-2914. https://doi.org/10.1021/bi801820q

Horii, K., Kahn, M. L., & Herr, A. B. (2006). Structural basis for platelet collagen responses by the immune-type receptor glycoprotein VI. *Blood*, *108*(3), 936-942. https://doi.org/10.1182/blood-2006-01-010215

Hou, Y., Carrim, N., Wang, Y., Gallant, R. C., Marshall, A., & Ni, H. (2015). Platelets in hemostasis and thrombosis: Novel mechanisms of fibrinogen-independent platelet aggregation and fibronectin-mediated protein wave of hemostasis. *J Biomed Res*, *29*. https://doi.org/10.7555/JBR.29.20150121

Huang, J., Li, X., Shi, X., Zhu, M., Wang, J., Huang, S., Huang, X., Wang, H., Li, L., Deng, H., Zhou, Y., Mao, J., Long, Z., Ma, Z., Ye, W., Pan, J., Xi, X., & Jin, J. (2019). Platelet

integrin alphaIIbbeta3: signal transduction, regulation, and its therapeutic targeting. *J Hematol Oncol*, *12*(1), 26. https://doi.org/10.1186/s13045-019-0709-6

Hughes, C. E., Pollitt, A. Y., Mori, J., Eble, J. A., Tomlinson, M. G., Hartwig, J. H., O'Callaghan, C. A., Futterer, K., & Watson, S. P. (2010). CLEC-2 activates Syk through dimerization. *Blood*, *115*(14), 2947-2955. https://doi.org/10.1182/blood-2009-08-237834

Inoue, O., Suzuki-Inoue, K., McCarty, O. J., Moroi, M., Ruggeri, Z. M., Kunicki, T. J., Ozaki, Y., & Watson, S. P. (2006). Laminin stimulates spreading of platelets through integrin alpha6beta1-dependent activation of GPVI. *Blood*, *107*(4), 1405-1412. https://doi.org/10.1182/blood-2005-06-2406

Iric, K. (2020). *Assembly of DNA-encapsulated lipid bilayers and their application to studies of GPCRs* Technische Universität Dresden]. Dresden. urn:nbn:de:bsz:14-qucosa2-729711

Iric, K., Subramanian, M., Oertel, J., Agarwal, N. P., Matthies, M., Periole, X., Sakmar, T. P., Huber, T., Fahmy, K., & Schmidt, T. L. (2018). DNA-encircled lipid bilayers. *Nanoscale*, *10*(39), 18463-18467. https://doi.org/10.1039/c8nr06505e

Italiano, J. E., Jr., Lecine, P., Shivdasani, R. A., & Hartwig, J. H. (1999). Blood platelets are assembled principally at the ends of proplatelet processes produced by differentiated megakaryocytes. *J Cell Biol*, *147*(6), 1299-1312. https://doi.org/10.1083/jcb.147.6.1299

Jacobson, K. A., Deflorian, F., Mishra, S., & Costanzi, S. (2011). Pharmacochemistry of the platelet purinergic receptors. *Purinergic Signal*, *7*(3), 305-324. https://doi.org/10.1007/s11302-011-9216-0

Jain, S., Russell, S., & Ware, J. (2009). Platelet glycoprotein VI facilitates experimental lung metastasis in syngenic mouse models. *J Thromb Haemost*, *7*(10), 1713-1717. https://doi.org/10.1111/j.1538-7836.2009.03559.x

Jamshad, M., Charlton, J., Lin, Y. P., Routledge, S. J., Bawa, Z., Knowles, T. J., Overduin, M., Dekker, N., Dafforn, T. R., Bill, R. M., Poyner, D. R., & Wheatley, M. (2015). G-protein coupled receptor solubilization and purification for biophysical analysis and functional studies, in the total absence of detergent. *Biosci Rep*, *35*(2). https://doi.org/10.1042/BSR20140171

Jamshad, M., Grimard, V., Idini, I., Knowles, T. J., Dowle, M. R., Schofield, N., Sridhar, P., Lin, Y. P., Finka, R., Wheatley, M., Thomas, O. R., Palmer, R. E., Overduin, M., Govaerts, C., Ruysschaert, J. M., Edler, K. J., & Dafforn, T. R. (2015). Structural analysis of a nanoparticle containing a lipid bilayer used for detergent-free extraction of membrane proteins. *Nano Res*, *8*(3), 774-789. https://doi.org/10.1007/s12274-014-0560-6

Jandrot-Perrus, M., Busfield, S., Lagrue, A. H., Xiong, X., Debili, N., Chickering, T., Le Couedic, J. P., Goodearl, A., Dussault, B., Fraser, C., Vainchenker, W., & Villeval, J. L. (2000). Cloning, characterization, and functional studies of human and mouse glycoprotein VI: a platelet-specific collagen receptor from the immunoglobulin superfamily. *Blood*, *96*(5), 1798-1807. https://www.ncbi.nlm.nih.gov/pubmed/10961879

Jankovicova, J., Frolikova, M., Palenikova, V., Valaskova, E., Cerny, J., Secova, P., Bartokova, M., Horovska, L., Manaskova-Postlerova, P., Antalikova, J., & Komrskova, K. (2020). Expression and distribution of CD151 as a partner of alpha6 integrin in male germ cells. *Sci Rep*, *10*(1), 4374. https://doi.org/10.1038/s41598-020-61334-2

Jenkins, C. S., Phillips, D. R., Clemetson, K. J., Meyer, D., Larrieu, M. J., & Luscher, E. F. (1976). Platelet membrane glycoproteins implicated in ristocetin-induced aggregation. Studies of the proteins on platelets from patients with Bernard-Soulier syndrome and

von Willebrand's disease. *J Clin Invest*, *57*(1), 112-124. https://doi.org/10.1172/JCI108251

Jones, C. I., Garner, S. F., Angenent, W., Bernard, A., Berzuini, C., Burns, P., Farndale, R. W., Hogwood, J., Rankin, A., Stephens, J. C., Tom, B. D., Walton, J., Dudbridge, F., Ouwehand, W. H., Goodall, A. H., & Bloodomics, C. (2007). Mapping the platelet profile for functional genomic studies and demonstration of the effect size of the GP6 locus. *J Thromb Haemost*, *5*(8), 1756-1765. https://doi.org/10.1111/j.1538-7836.2007.02632.x

Jouannet, S., Saint-Pol, J., Fernandez, L., Nguyen, V., Charrin, S., Boucheix, C., Brou, C., Milhiet, P. E., & Rubinstein, E. (2016). TspanC8 tetraspanins differentially regulate the cleavage of ADAM10 substrates, Notch activation and ADAM10 membrane compartmentalization. *Cell Mol Life Sci*, *73*(9), 1895-1915. https://doi.org/10.1007/s00018-015-2111-z

Joutsi-Korhonen, L., Smethurst, P. A., Rankin, A., Gray, E., M, I. J., Onley, C. M., Watkins, N. A., Williamson, L. M., Goodall, A. H., de Groot, P. G., Farndale, R. W., & Ouwehand, W. H. (2003). The low-frequency allele of the platelet collagen signaling receptor glycoprotein VI is associated with reduced functional responses and expression. *Blood*, *101*(11), 4372-4379. https://doi.org/10.1182/blood-2002-08-2591

Jung, S. M., Moroi, M., Soejima, K., Nakagaki, T., Miura, Y., Berndt, M. C., Gardiner, E. E., Howes, J. M., Pugh, N., Bihan, D., Watson, S. P., & Farndale, R. W. (2012). Constitutive dimerization of glycoprotein VI (GPVI) in resting platelets is essential for binding to collagen and activation in flowing blood. *J Biol Chem*, *287*(35), 30000-30013. https://doi.org/10.1074/jbc.M112.359125

Jung, S. M., Tsuji, K., & Moroi, M. (2009). Glycoprotein (GP) VI dimer as a major collagen-binding site of native platelets: direct evidence obtained with dimeric GPVI-specific Fabs. *J Thromb Haemost*, *7*(8), 1347-1355. https://doi.org/10.1111/j.1538-7836.2009.03496.x

Kaneider, N. C., Kaser, A., Tilg, H., Ricevuti, G., & Wiedermann, C. J. (2003). CD40 ligand-dependent maturation of human monocyte-derived dendritic cells by activated platelets. *Int J Immunopathol Pharmacol*, *16*(3), 225-231. https://doi.org/10.1177/039463200301600307

Kannan, M., Ahmad, F., Yadav, B. K., Kumar, R., Choudhry, V. P., & Saxena, R. (2009). Molecular defects in ITGA2B and ITGB3 genes in patients with Glanzmann thrombasthenia. *J Thromb Haemost*, *7*(11), 1878-1885. https://doi.org/10.1111/j.1538-7836.2009.03579.x

Karamatic Crew, V., Burton, N., Kagan, A., Green, C. A., Levene, C., Flinter, F., Brady, R. L., Daniels, G., & Anstee, D. J. (2004). CD151, the first member of the tetraspanin (TM4) superfamily detected on erythrocytes, is essential for the correct assembly of human basement membranes in kidney and skin. *Blood*, *104*(8), 2217-2223. https://doi.org/10.1182/blood-2004-04-1512

Kardeby, C., Damaskinaki, F. N., Sun, Y., & Watson, S. P. (2021). Is the endogenous ligand for PEAR1 a proteoglycan: clues from the sea. *Platelets*, *32*(6), 779-785. https://doi.org/10.1080/09537104.2020.1863938

Kato, K., Kanaji, T., Russell, S., Kunicki, T. J., Furihata, K., Kanaji, S., Marchese, P., Reininger, A., Ruggeri, Z. M., & Ware, J. (2003). The contribution of glycoprotein VI to stable platelet adhesion and thrombus formation illustrated by targeted gene deletion. *Blood*, *102*(5), 1701-1707. https://doi.org/10.1182/blood-2003-03-0717

Kato, T., Ogami, K., Shimada, Y., Iwamatsu, A., Sohma, Y., Akahori, H., Horie, K., Kokubo, A., Kudo, Y., & Maeda, E. (1995). Purification and characterization of thrombopoietin. *J Biochem*, *118*(1), 229-236. https://doi.org/10.1093/oxfordjournals.jbchem.a124883

Kauskot, A., Di Michele, M., Loyen, S., Freson, K., Verhamme, P., & Hoylaerts, M. F. (2012). A novel mechanism of sustained platelet alphaIIbbeta3 activation via PEAR1. *Blood*, *119*(17), 4056-4065. https://doi.org/10.1182/blood-2011-11-392787

Keane, C., Tilley, D., Cunningham, A., Smolenski, A., Kadioglu, A., Cox, D., Jenkinson, H. F., & Kerrigan, S. W. (2010). Invasive Streptococcus pneumoniae trigger platelet activation via Toll-like receptor 2. *J Thromb Haemost*, *8*(12), 2757-2765. https://doi.org/10.1111/j.1538-7836.2010.04093.x

Kelemen, E., Cserhati, I., & Tanos, B. (1958). Demonstration and some properties of human thrombopoietin in thrombocythaemic sera. *Acta Haematol*, *20*(6), 350-355. https://doi.org/10.1159/000205503

Khan, A., Li, D., Ibrahim, S., Smyth, E., & Woulfe, D. S. (2014). The physical association of the P2Y12 receptor with PAR4 regulates arrestin-mediated Akt activation. *Mol Pharmacol*, *86*(1), 1-11. https://doi.org/10.1124/mol.114.091595

Kim, O. V., Litvinov, R. I., Alber, M. S., & Weisel, J. W. (2017). Quantitative structural mechanobiology of platelet-driven blood clot contraction. *Nat Commun*, *8*(1), 1274. https://doi.org/10.1038/s41467-017-00885-x

Kim, S., Foster, C., Lecchi, A., Quinton, T. M., Prosser, D. M., Jin, J., Cattaneo, M., & Kunapuli, S. P. (2002). Protease-activated receptors 1 and 4 do not stimulate G(i) signaling pathways in the absence of secreted ADP and cause human platelet aggregation independently of G(i) signaling. *Blood*, *99*(10), 3629-3636. https://doi.org/10.1182/blood.v99.10.3629

Kimmerlin, Q., Moog, S., Ravanat, C., Strassel, C., & Lanza, F. (2022). Glycoprotein V : the unsolved GPV puzzle. *Platelets*, *33*(6), 833-840. https://doi.org/10.1080/09537104.2021.2022114

Kleinschmidt, J. H., Wiener, M. C., & Tamm, L. K. (1999). Outer membrane protein A of E. coli folds into detergent micelles, but not in the presence of monomeric detergent. *Protein Sci*, *8*(10), 2065-2071. https://doi.org/10.1110/ps.8.10.2065

Klumperman, B. (2010). Mechanistic considerations on styrene-maleic anhydride copolymerization reactions. *Polymer Chemistry*, *1*(5), 558-562. https://doi.org/10.1039/b9py00341j

Knight, C. G., Morton, L. F., Onley, D. J., Peachey, A. R., Ichinohe, T., Okuma, M., Farndale, R. W., & Barnes, M. J. (1999). Collagen-platelet interaction: Gly-Pro-Hyp is uniquely specific for platelet Gp VI and mediates platelet activation by collagen. *Cardiovasc Res*, *41*(2), 450-457. https://doi.org/10.1016/s0008-6363(98)00306-x

Knowles, T. J., Finka, R., Smith, C., Lin, Y. P., Dafforn, T., & Overduin, M. (2009). Membrane proteins solubilized intact in lipid containing nanoparticles bounded by styrene maleic acid copolymer. *J Am Chem Soc*, *131*(22), 7484-7485. https://doi.org/10.1021/ja810046q

Komar, J., Alvira, S., Schulze, R. J., Martin, R., Lycklama, A. N. J. A., Lee, S. C., Dafforn, T. R., Deckers-Hebestreit, G., Berger, I., Schaffitzel, C., & Collinson, I. (2016). Membrane protein insertion and assembly by the bacterial holo-translocon SecYEG-SecDF-YajC-YidC. *Biochem J*, *473*(19), 3341-3354. https://doi.org/10.1042/BCJ20160545

Konopatskaya, O., Gilio, K., Harper, M. T., Zhao, Y., Cosemans, J. M., Karim, Z. A., Whiteheart, S. W., Molkentin, J. D., Verkade, P., Watson, S. P., Heemskerk, J. W., & Poole, A. W. (2009). PKCalpha regulates platelet granule secretion and thrombus formation in mice. *J Clin Invest*, *119*(2), 399-407. https://doi.org/10.1172/JCI34665

Koo, C. Z., Harrison, N., Noy, P. J., Szyroka, J., Matthews, A. L., Hsia, H. E., Muller, S. A., Tushaus, J., Goulding, J., Willis, K., Apicella, C., Cragoe, B., Davis, E., Keles, M., Malinova, A., McFarlane, T. A., Morrison, P. R., Nguyen, H. T. H., Sykes, M. C., . . .

Tomlinson, M. G. (2020). The tetraspanin Tspan15 is an essential subunit of an ADAM10 scissor complex. *J Biol Chem*, *295*(36), 12822-12839. https://doi.org/10.1074/jbc.RA120.012601

Koo, C. Z., Matthews, A. L., Harrison, N., Szyroka, J., Nieswandt, B., Gardiner, E. E., Poulter, N. S., & Tomlinson, M. G. (2022). The Platelet Collagen Receptor GPVI Is Cleaved by Tspan15/ADAM10 and Tspan33/ADAM10 Molecular Scissors. *Int J Mol Sci*, *23*(5). https://doi.org/10.3390/ijms23052440

Koupenova, M., Kehrel, B. E., Corkrey, H. A., & Freedman, J. E. (2017). Thrombosis and platelets: an update. *Eur Heart J*, *38*(11), 785-791. https://doi.org/10.1093/eurheartj/ehw550

Krishnarjuna, B., & Ramamoorthy, A. (2022). Detergent-Free Isolation of Membrane Proteins and Strategies to Study Them in a Near-Native Membrane Environment. *Biomolecules*, *12*(8). https://doi.org/10.3390/biom12081076

Kumar, P., Cymes, G. D., & Grosman, C. (2021). Structure and function at the lipid-protein interface of a pentameric ligand-gated ion channel. *Proc Natl Acad Sci U S A*, *118*(23). https://doi.org/10.1073/pnas.2100164118

Kummer, D., Steinbacher, T., Schwietzer, M. F., Tholmann, S., & Ebnet, K. (2020). Tetraspanins: integrating cell surface receptors to functional microdomains in homeostasis and disease. *Med Microbiol Immunol*, *209*(4), 397-405. https://doi.org/10.1007/s00430-020-00673-3

Kunicki, T. J., Federici, A. B., Salomon, D. R., Koziol, J. A., Head, S. R., Mondala, T. S., Chismar, J. D., Baronciani, L., Canciani, M. T., & Peake, I. R. (2004). An association of candidate gene haplotypes and bleeding severity in von Willebrand disease (VWD) type 1 pedigrees. *Blood*, *104*(8), 2359-2367. https://doi.org/10.1182/blood-2004-01-0349

Kuter, D. J. (2019). 61 - Thrombopoietin Receptor Agonists. In A. D. Michelson (Ed.), *Platelets (Fourth Edition)* (pp. 1085-1110). Academic Press. https://doi.org/https://doi.org/10.1016/B978-0-12-813456-6.00061-8

Kuter, D. J., Beeler, D. L., & Rosenberg, R. D. (1994). The purification of megapoietin: a physiological regulator of megakaryocyte growth and platelet production. *Proc Natl Acad Sci U S A*, *91*(23), 11104-11108. https://doi.org/10.1073/pnas.91.23.11104

Lam, W. A., Chaudhuri, O., Crow, A., Webster, K. D., Li, T. D., Kita, A., Huang, J., & Fletcher, D. A. (2011). Mechanics and contraction dynamics of single platelets and implications for clot stiffening. *Nat Mater*, *10*(1), 61-66. https://doi.org/10.1038/nmat2903

Larsen, A. N., Sorensen, K. K., Johansen, N. T., Martel, A., Kirkensgaard, J. J., Jensen, K. J., Arleth, L., & Midtgaard, S. R. (2016). Dimeric peptides with three different linkers self-assemble with phospholipids to form peptide nanodiscs that stabilize membrane proteins. *Soft Matter*, *12*(27), 5937-5949. https://doi.org/10.1039/c6sm00495d

Lau, L. M., Wee, J. L., Wright, M. D., Moseley, G. W., Hogarth, P. M., Ashman, L. K., & Jackson, D. E. (2004). The tetraspanin superfamily member CD151 regulates outside-in integrin alphaIIbbeta3 signaling and platelet function. *Blood*, *104*(8), 2368-2375. https://doi.org/10.1182/blood-2003-12-4430

Laursen, T., Borch, J., Knudsen, C., Bavishi, K., Torta, F., Martens, H. J., Silvestro, D., Hatzakis, N. S., Wenk, M. R., Dafforn, T. R., Olsen, C. E., Motawia, M. S., Hamberger, B., Moller, B. L., & Bassard, J. E. (2016). Characterization of a dynamic metabolon producing the defense compound dhurrin in sorghum. *Science*, *354*(6314), 890-893. https://doi.org/10.1126/science.aag2347

Lavington, S., & Watts, A. (2020). Lipid nanoparticle technologies for the study of G protein-coupled receptors in lipid environments. *Biophys Rev*. https://doi.org/10.1007/s12551-020-00775-5

Lavington, S., & Watts, A. (2021). Detergent-free solubilisation & purification of a G protein coupled receptor using a polymethacrylate polymer. *Biochim Biophys Acta Biomembr*, *1863*(1), 183441. https://doi.org/10.1016/j.bbamem.2020.183441

Law, D. A., DeGuzman, F. R., Heiser, P., Ministri-Madrid, K., Killeen, N., & Phillips, D. R. (1999). Integrin cytoplasmic tyrosine motif is required for outside-in alphaIIbbeta3 signalling and platelet function. *Nature*, *401*(6755), 808-811. https://doi.org/10.1038/44599

le Maire, M., Champeil, P., & Moller, J. V. (2000). Interaction of membrane proteins and lipids with solubilizing detergents. *Biochim Biophys Acta*, *1508*(1-2), 86-111. https://doi.org/10.1016/s0304-4157(00)00010-1

Le Maire, M., Kwee, S., Andersen, J. P., & Moller, J. V. (1983). Mode of interaction of polyoxyethyleneglycol detergents with membrane proteins. *Eur J Biochem*, *129*(3), 525-532. https://doi.org/10.1111/j.1432-1033.1983.tb07080.x

Le Naour, F., Andre, M., Boucheix, C., & Rubinstein, E. (2006). Membrane microdomains and proteomics: lessons from tetraspanin microdomains and comparison with lipid rafts. *Proteomics*, *6*(24), 6447-6454. https://doi.org/10.1002/pmic.200600282

Lebozec, K., Jandrot-Perrus, M., Avenard, G., Favre-Bulle, O., & Billiald, P. (2017). Design, development and characterization of ACT017, a humanized Fab that blocks platelet's glycoprotein VI function without causing bleeding risks. *MAbs*, *9*(6), 945-958. https://doi.org/10.1080/19420862.2017.1336592

Lee, A. G. (2003). Lipid-protein interactions in biological membranes: a structural perspective. *Biochim Biophys Acta*, *1612*(1), 1-40. https://doi.org/10.1016/s0005-2736(03)00056-7

Lee, R. H., Stefanini, L., & Bergmeier, W. (2019). 18 - Platelet Signal Transduction. In A. D. Michelson (Ed.), *Platelets (Fourth Edition)* (pp. 329-348). Academic Press. https://doi.org/https://doi.org/10.1016/B978-0-12-813456-6.00018-7

Lee, S. C., Knowles, T. J., Postis, V. L., Jamshad, M., Parslow, R. A., Lin, Y. P., Goldman, A., Sridhar, P., Overduin, M., Muench, S. P., & Dafforn, T. R. (2016). A method for detergent-free isolation of membrane proteins in their local lipid environment. *Nat Protoc*, *11*(7), 1149-1162. https://doi.org/10.1038/nprot.2016.070

Leger, A. J., Jacques, S. L., Badar, J., Kaneider, N. C., Derian, C. K., Andrade-Gordon, P., Covic, L., & Kuliopulos, A. (2006). Blocking the protease-activated receptor 1-4 heterodimer in platelet-mediated thrombosis. *Circulation*, *113*(9), 1244-1254. https://doi.org/10.1161/CIRCULATIONAHA.105.587758

Leitz, A. J., Bayburt, T. H., Barnakov, A. N., Springer, B. A., & Sligar, S. G. (2006). Functional reconstitution of Beta2-adrenergic receptors utilizing self-assembling Nanodisc technology. *Biotechniques*, *40*(5), 601-602, 604, 606, passim. https://doi.org/10.2144/000112169

Leon, C., Hechler, B., Vial, C., Leray, C., Cazenave, J. P., & Gachet, C. (1997). The P2Y1 receptor is an ADP receptor antagonized by ATP and expressed in platelets and megakaryoblastic cells. *FEBS Lett*, *403*(1), 26-30. https://doi.org/10.1016/s0014-5793(97)00022-7

Leoncikas, V., Wu, H., Ward, L. T., Kierzek, A. M., & Plant, N. J. (2016). Generation of 2,000 breast cancer metabolic landscapes reveals a poor prognosis group with active serotonin production. *Sci Rep*, *6*, 19771. https://doi.org/10.1038/srep19771

Lewandrowski, U., Wortelkamp, S., Lohrig, K., Zahedi, R. P., Wolters, D. A., Walter, U., & Sickmann, A. (2009). Platelet membrane proteomics: a novel repository for functional research. *Blood*, *114*(1), e10-19. https://doi.org/10.1182/blood-2009-02-203828

Li, C., Li, J., Li, Y., Lang, S., Yougbare, I., Zhu, G., Chen, P., & Ni, H. (2012). Crosstalk between Platelets and the Immune System: Old Systems with New Discoveries. *Adv Hematol*, *2012*, 384685. https://doi.org/10.1155/2012/384685

Li, C. Q., Dong, J. F., Lanza, F., Sanan, D. A., Sae-Tung, G., & Lopez, J. A. (1995). Expression of platelet glycoprotein (GP) V in heterologous cells and evidence for its association with GP Ib alpha in forming a GP Ib-IX-V complex on the cell surface. *J Biol Chem*, *270*(27), 16302-16307. https://doi.org/10.1074/jbc.270.27.16302

Li, J., Vootukuri, S., Shang, Y., Negri, A., Jiang, J. K., Nedelman, M., Diacovo, T. G., Filizola, M., Thomas, C. J., & Coller, B. S. (2014). RUC-4: a novel alphaIIbbeta3 antagonist for prehospital therapy of myocardial infarction. *Arterioscler Thromb Vasc Biol*, *34*(10), 2321-2329. https://doi.org/10.1161/ATVBAHA.114.303724

Li, R. (2019). 10 - The Glycoprotein Ib-IX-V Complex. In A. D. Michelson (Ed.), *Platelets (Fourth Edition)* (pp. 193-211). Academic Press. https://doi.org/https://doi.org/10.1016/B978-0-12-813456-6.00010-2

Li, R., & Emsley, J. (2013). The organizing principle of the platelet glycoprotein Ib-IX-V complex. *J Thromb Haemost*, *11*(4), 605-614. https://doi.org/10.1111/jth.12144

Li, W. H., Qiu, Y., Zhang, H. Q., Liu, Y., You, J. F., Tian, X. X., & Fang, W. G. (2013). P2Y2 receptor promotes cell invasion and metastasis in prostate cancer cells. *Br J Cancer*, *109*(6), 1666-1675. https://doi.org/10.1038/bjc.2013.484

Lian, L., Wang, Y., Draznin, J., Eslin, D., Bennett, J. S., Poncz, M., Wu, D., & Abrams, C. S. (2005). The relative role of PLCbeta and PI3Kgamma in platelet activation. *Blood*, *106*(1), 110-117. https://doi.org/10.1182/blood-2004-05-2005

Lin, J., Weiss, A., & Finco, T. S. (1999). Localization of LAT in glycolipid-enriched microdomains is required for T cell activation. *J Biol Chem*, *274*(41), 28861-28864. https://doi.org/10.1074/jbc.274.41.28861

Linder, M. E., & Deschenes, R. J. (2007). Palmitoylation: policing protein stability and traffic. *Nat Rev Mol Cell Biol*, *8*(1), 74-84. https://doi.org/10.1038/nrm2084

Lipper, C. H., Egan, E. D., Gabriel, K.-H., & Blacklow, S. C. (2022). Structural Basis for Selective Proteolysis of ADAM10 Substrates at Membrane-Proximal Sites. *bioRxiv*, 2022.2010.2022.513345. https://doi.org/10.1101/2022.10.22.513345

Liu, C. Y., Battaglia, M., Lee, S. H., Sun, Q. H., Aster, R. H., & Visentin, G. P. (2005). Platelet factor 4 differentially modulates CD4+CD25+ (regulatory) versus CD4+CD25- (nonregulatory) T cells. *J Immunol*, *174*(5), 2680-2686. https://doi.org/10.4049/jimmunol.174.5.2680

Liu, J., Pestina, T. I., Berndt, M. C., Jackson, C. W., & Gartner, T. K. (2005). Botrocetin/VWF-induced signaling through GPIb-IX-V produces TxA2 in an alphaIIbbeta3- and aggregation-independent manner. *Blood*, *106*(8), 2750-2756. https://doi.org/10.1182/blood-2005-04-1667

Liu, T. D., Ren, S. H., Ding, X., Xie, Z. L., & Kong, Y. (2018). A Short Half-Life alphaIIbbeta(3) Antagonist ANTP266 Reduces Thrombus Formation. *Int J Mol Sci*, *19*(8). https://doi.org/10.3390/ijms19082306

Lloris-Garcera, P., Klinter, S., Chen, L., Skynner, M. J., Loving, R., & Frauenfeld, J. (2020). DirectMX - One-Step Reconstitution of Membrane Proteins From Crude Cell Membranes Into Salipro Nanoparticles. *Front Bioeng Biotechnol*, *8*, 215. https://doi.org/10.3389/fbioe.2020.00215

Locke, D., Liu, C., Peng, X., Chen, H., & Kahn, M. L. (2003). Fc Rgamma -independent signaling by the platelet collagen receptor glycoprotein VI. *J Biol Chem*, *278*(17), 15441-15448. https://doi.org/10.1074/jbc.M212338200

Lockyer, S., Okuyama, K., Begum, S., Le, S., Sun, B., Watanabe, T., Matsumoto, Y., Yoshitake, M., Kambayashi, J., & Tandon, N. N. (2006). GPVI-deficient mice lack collagen responses and are protected against experimentally induced pulmonary thromboembolism. *Thromb Res*, *118*(3), 371-380. https://doi.org/10.1016/j.thromres.2005.08.001

Loyau, S., Dumont, B., Ajzenberg, N., & Jandrot-Perrus, M. (2010). Platelet Glycoprotein VI Dimerisation Is An Active Process and Enables the Receptor to Be Competent. *Blood*, *116*(21), 1312-1312. <Go to ISI>://WOS:000289662203525

Loyau, S., Dumont, B., Ollivier, V., Boulaftali, Y., Feldman, L., Ajzenberg, N., & Jandrot-Perrus, M. (2012). Platelet glycoprotein VI dimerization, an active process inducing receptor competence, is an indicator of platelet reactivity. *Arterioscler Thromb Vasc Biol*, *32*(3), 778-785. https://doi.org/10.1161/ATVBAHA.111.241067

Luna, V. M., Vazir, M., Vaish, A., Chong, S., Chen, I., & Yamane, H. K. (2018). Generation of membrane proteins in polymer-based lipoparticles as flow cytometry antigens. *European Polymer Journal*, *109*, 483-488. https://doi.org/10.1016/j.eurpolymj.2018.10.017

Luo, S. Z., & Li, R. (2008). Specific heteromeric association of four transmembrane peptides derived from platelet glycoprotein Ib-IX complex. *J Mol Biol*, *382*(2), 448-457. https://doi.org/10.1016/j.jmb.2008.07.037

Luo, S. Z., Mo, X., Afshar-Kharghan, V., Srinivasan, S., Lopez, J. A., & Li, R. (2007). Glycoprotein Ibalpha forms disulfide bonds with 2 glycoprotein Ibbeta subunits in the resting platelet. *Blood*, *109*(2), 603-609. https://doi.org/10.1182/blood-2006-05-024091

Machlus, K. R., & Italiano, J. E. (2019). 2 - Megakaryocyte Development and Platelet Formation. In A. D. Michelson (Ed.), *Platelets (Fourth Edition)* (pp. 25-46). Academic Press. https://doi.org/https://doi.org/10.1016/B978-0-12-813456-6.00002-3

Machlus, K. R., & Italiano, J. E., Jr. (2013). The incredible journey: From megakaryocyte development to platelet formation. *J Cell Biol*, *201*(6), 785-796. https://doi.org/10.1083/jcb.201304054

Mackman, N. (2004). Role of tissue factor in hemostasis, thrombosis, and vascular development. *Arterioscler Thromb Vasc Biol*, *24*(6), 1015-1022. https://doi.org/10.1161/01.ATV.0000130465.23430.74

Mackman, N. (2012). New insights into the mechanisms of venous thrombosis. *J Clin Invest*, *122*(7), 2331-2336. https://doi.org/10.1172/JCI60229

Malia, T. J., & Wagner, G. (2007). NMR structural investigation of the mitochondrial outer membrane protein VDAC and its interaction with antiapoptotic Bcl-xL. *Biochemistry*, *46*(2), 514-525. https://doi.org/10.1021/bi061577h

Malinin, N. L., Zhang, L., Choi, J., Ciocea, A., Razorenova, O., Ma, Y. Q., Podrez, E. A., Tosi, M., Lennon, D. P., Caplan, A. I., Shurin, S. B., Plow, E. F., & Byzova, T. V. (2009). A point mutation in KINDLIN3 ablates activation of three integrin subfamilies in humans. *Nat Med*, *15*(3), 313-318. https://doi.org/10.1038/nm.1917

Mammadova-Bach, E., Gil-Pulido, J., Sarukhanyan, E., Burkard, P., Shityakov, S., Schonhart, C., Stegner, D., Remer, K., Nurden, P., Nurden, A. T., Dandekar, T., Nehez, L., Dank, M., Braun, A., Mezzano, D., Abrams, S. I., & Nieswandt, B. (2020). Platelet glycoprotein VI promotes metastasis through interaction with cancer cell-derived galectin-3. *Blood*, *135*(14), 1146-1160. https://doi.org/10.1182/blood.2019002649

Mammadova-Bach, E., Ollivier, V., Loyau, S., Schaff, M., Dumont, B., Favier, R., Freyburger, G., Latger-Cannard, V., Nieswandt, B., Gachet, C., Mangin, P. H., & Jandrot-Perrus, M. (2015). Platelet glycoprotein VI binds to polymerized fibrin and promotes thrombin generation. *Blood*, *126*(5), 683-691. https://doi.org/10.1182/blood-2015-02-629717

Mangin, P. H., Kleitz, L., Boucheix, C., Gachet, C., & Lanza, F. (2009). CD9 negatively regulates integrin alphaIIbbeta3 activation and could thus prevent excessive platelet recruitment at sites of vascular injury. *J Thromb Haemost*, *7*(5), 900-902. https://doi.org/10.1111/j.1538-7836.2009.03322.x

Mangin, P. H., Onselaer, M. B., Receveur, N., Le Lay, N., Hardy, A. T., Wilson, C., Sanchez, X., Loyau, S., Dupuis, A., Babar, A. K., Miller, J. L., Philippou, H., Hughes, C. E., Herr, A. B., Ariens, R. A., Mezzano, D., Jandrot-Perrus, M., Gachet, C., & Watson, S. P. (2018). Immobilized fibrinogen activates human platelets through glycoprotein VI. *Haematologica*, *103*(5), 898-907. https://doi.org/10.3324/haematol.2017.182972

Mangin, P. H., Tang, C., Bourdon, C., Loyau, S., Freund, M., Hechler, B., Gachet, C., & Jandrot-Perrus, M. (2012). A humanized glycoprotein VI (GPVI) mouse model to assess the antithrombotic efficacies of anti-GPVI agents. *J Pharmacol Exp Ther*, *341*(1), 156-163. https://doi.org/10.1124/jpet.111.189050

Martin, B. R., Wang, C., Adibekian, A., Tully, S. E., & Cravatt, B. F. (2011). Global profiling of dynamic protein palmitoylation. *Nat Methods*, *9*(1), 84-89. https://doi.org/10.1038/nmeth.1769

Martin, E. M., Zuidscherwoude, M., Moran, L. A., Di, Y., Garcia, A., & Watson, S. P. (2021). The structure of CLEC-2: mechanisms of dimerization and higher-order clustering. *Platelets*, *32*(6), 733-743. https://doi.org/10.1080/09537104.2021.1906407

Matthews, A. L. (2018). *Regulation of the major platelet collagen and fibrin receptor gpvi by adam10 and tspanc8 tetraspanins* University of Birmingham]. University of Birmingham eTheses repository. Birmingham.

Matthews, A. L., Koo, C. Z., Szyroka, J., Harrison, N., Kanhere, A., & Tomlinson, M. G. (2018). Regulation of Leukocytes by TspanC8 Tetraspanins and the "Molecular Scissor" ADAM10. *Front Immunol*, *9*, 1451. https://doi.org/10.3389/fimmu.2018.01451

Matthews, A. L., Szyroka, J., Collier, R., Noy, P. J., & Tomlinson, M. G. (2017). Scissor sisters: regulation of ADAM10 by the TspanC8 tetraspanins. *Biochem Soc Trans*, *45*(3), 719-730. https://doi.org/10.1042/BST20160290

Matus, V., Valenzuela, G., Saez, C. G., Hidalgo, P., Lagos, M., Aranda, E., Panes, O., Pereira, J., Pillois, X., Nurden, A. T., & Mezzano, D. (2013). An adenine insertion in exon 6 of human GP6 generates a truncated protein associated with a bleeding disorder in four Chilean families. *J Thromb Haemost*, *11*(9), 1751-1759. https://doi.org/10.1111/jth.12334

May, F., Hagedorn, I., Pleines, I., Bender, M., Vogtle, T., Eble, J., Elvers, M., & Nieswandt, B. (2009). CLEC-2 is an essential platelet-activating receptor in hemostasis and thrombosis. *Blood*, *114*(16), 3464-3472. https://doi.org/10.1182/blood-2009-05-222273

McArthur, K., Chappaz, S., & Kile, B. T. (2018). Apoptosis in megakaryocytes and platelets: the life and death of a lineage. *Blood*, *131*(6), 605-610. https://doi.org/10.1182/blood-2017-11-742684

Menter, D. G., Tucker, S. C., Kopetz, S., Sood, A. K., Crissman, J. D., & Honn, K. V. (2014). Platelets and cancer: a casual or causal relationship: revisited. *Cancer Metastasis Rev*, *33*(1), 231-269. https://doi.org/10.1007/s10555-014-9498-0

Mezu-Ndubuisi, O. J., & Maheshwari, A. (2021). The role of integrins in inflammation and angiogenesis. *Pediatr Res*, *89*(7), 1619-1626. https://doi.org/10.1038/s41390-020-01177-9

Miao, W. M., Vasile, E., Lane, W. S., & Lawler, J. (2001). CD36 associates with CD9 and integrins on human blood platelets. *Blood*, *97*(6), 1689-1696. https://doi.org/10.1182/blood.v97.6.1689

Michael, J. V., Wurtzel, J. G. T., Mao, G. F., Rao, A. K., Kolpakov, M. A., Sabri, A., Hoffman, N. E., Rajan, S., Tomar, D., Madesh, M., Nieman, M. T., Yu, J., Edelstein, L. C., Rowley, J. W., Weyrich, A. S., & Goldfinger, L. E. (2017). Platelet microparticles

infiltrating solid tumors transfer miRNAs that suppress tumor growth. *Blood*, *130*(5), 567-580. https://doi.org/10.1182/blood-2016-11-751099

Miederer, A. M., Alansary, D., Schwar, G., Lee, P. H., Jung, M., Helms, V., & Niemeyer, B. A. (2015). A STIM2 splice variant negatively regulates store-operated calcium entry. *Nat Commun*, *6*, 6899. https://doi.org/10.1038/ncomms7899

Mills, D. C. (1996). ADP receptors on platelets. *Thromb Haemost*, *76*(6), 835-856. https://www.ncbi.nlm.nih.gov/pubmed/8971999

Miura, Y., Takahashi, T., Jung, S. M., & Moroi, M. (2002). Analysis of the interaction of platelet collagen receptor glycoprotein VI (GPVI) with collagen. A dimeric form of GPVI, but not the monomeric form, shows affinity to fibrous collagen. *J Biol Chem*, *277*(48), 46197-46204. https://doi.org/10.1074/jbc.M204029200

Mo, X., Liu, L., Lopez, J. A., & Li, R. (2012). Transmembrane domains are critical to the interaction between platelet glycoprotein V and glycoprotein Ib-IX complex. *J Thromb Haemost*, *10*(9), 1875-1886. https://doi.org/10.1111/j.1538-7836.2012.04841.x

Moller, J. V., & le Maire, M. (1993). Detergent binding as a measure of hydrophobic surface area of integral membrane proteins. *J Biol Chem*, *268*(25), 18659-18672. https://www.ncbi.nlm.nih.gov/pubmed/8395515

Montague, S. J., Patel, P., Martin, E. M., Slater, A., Quintanilla, L. G., Perrella, G., Kardeby, C., Nagy, M., Mezzano, D., Mendes, P. M., & Watson, S. P. (2021). Platelet activation by charged ligands and nanoparticles: platelet glycoprotein receptors as pattern recognition receptors. *Platelets*, *32*(8), 1018-1030. https://doi.org/10.1080/09537104.2021.1945571

Moraes, I., Evans, G., Sanchez-Weatherby, J., Newstead, S., & Stewart, P. D. (2014). Membrane protein structure determination - the next generation. *Biochim Biophys Acta*, *1838*(1 Pt A), 78-87. https://doi.org/10.1016/j.bbamem.2013.07.010

Moroi, M., Mizuguchi, J., Kawashima, S., Nagamatsu, M., Miura, Y., Nakagaki, T., Ito, K., & Jung, S. M. (2003). A new monoclonal antibody, mAb 204-11, that influences the binding of platelet GPVI to fibrous collagen. *Thromb Haemost*, *89*(6), 996-1003. https://www.ncbi.nlm.nih.gov/pubmed/12783112

Morrell, C. N., Aggrey, A. A., Chapman, L. M., & Modjeski, K. L. (2014). Emerging roles for platelets as immune and inflammatory cells. *Blood*, *123*(18), 2759-2767. https://doi.org/10.1182/blood-2013-11-462432

Morrison, K. A., Akram, A., Mathews, A., Khan, Z. A., Patel, J. H., Zhou, C., Hardy, D. J., Moore-Kelly, C., Patel, R., Odiba, V., Knowles, T. J., Javed, M. U., Chmel, N. P., Dafforn, T. R., & Rothnie, A. J. (2016). Membrane protein extraction and purification using styrene-maleic acid (SMA) copolymer: effect of variations in polymer structure. *Biochem J*, *473*(23), 4349-4360. https://doi.org/10.1042/BCJ20160723

Morrow, D. A., Alberts, M. J., Mohr, J. P., Ameriso, S. F., Bonaca, M. P., Goto, S., Hankey, G. J., Murphy, S. A., Scirica, B. M., Braunwald, E., Thrombin Receptor Antagonist in Secondary Prevention of Atherothrombotic Ischemic Events, T. S. C., & Investigators. (2013). Efficacy and safety of vorapaxar in patients with prior ischemic stroke. *Stroke*, *44*(3), 691-698. https://doi.org/10.1161/STROKEAHA.111.000433

Morton, L. F., Hargreaves, P. G., Farndale, R. W., Young, R. D., & Barnes, M. J. (1995). Integrin alpha 2 beta 1-independent activation of platelets by simple collagen-like peptides: collagen tertiary (triple-helical) and quaternary (polymeric) structures are sufficient alone for alpha 2 beta 1-independent platelet reactivity. *Biochem J*, *306 (Pt 2)*, 337-344. https://doi.org/10.1042/bj3060337

Nagae, M., Morita-Matsumoto, K., Kato, M., Kaneko, M. K., Kato, Y., & Yamaguchi, Y. (2014). A platform of C-type lectin-like receptor CLEC-2 for binding O-glycosylated

podoplanin and nonglycosylated rhodocytin. *Structure*, *22*(12), 1711-1721. https://doi.org/10.1016/j.str.2014.09.009

Nagy, M., Perrella, G., Dalby, A., Becerra, M. F., Garcia Quintanilla, L., Pike, J. A., Morgan, N. V., Gardiner, E. E., Heemskerk, J. W. M., Azocar, L., Miquel, J. F., Mezzano, D., & Watson, S. P. (2020). Flow studies on human GPVI-deficient blood under coagulating and noncoagulating conditions. *Blood Adv*, *4*(13), 2953-2961. https://doi.org/10.1182/bloodadvances.2020001761

Nakamura, F., Pudas, R., Heikkinen, O., Permi, P., Kilpelainen, I., Munday, A. D., Hartwig, J. H., Stossel, T. P., & Ylanne, J. (2006). The structure of the GPIb-filamin A complex. *Blood*, *107*(5), 1925-1932. https://doi.org/10.1182/blood-2005-10-3964

Nanda, N., Bao, M., Lin, H., Clauser, K., Komuves, L., Quertermous, T., Conley, P. B., Phillips, D. R., & Hart, M. J. (2005). Platelet endothelial aggregation receptor 1 (PEAR1), a novel epidermal growth factor repeat-containing transmembrane receptor, participates in platelet contact-induced activation. *J Biol Chem*, *280*(26), 24680-24689. https://doi.org/10.1074/jbc.M413411200

Nasarre, C., Roth, M., Jacob, L., Roth, L., Koncina, E., Thien, A., Labourdette, G., Poulet, P., Hubert, P., Cremel, G., Roussel, G., Aunis, D., & Bagnard, D. (2010). Peptide-based interference of the transmembrane domain of neuropilin-1 inhibits glioma growth in vivo. *Oncogene*, *29*(16), 2381-2392. https://doi.org/10.1038/onc.2010.9

Nath, A., Atkins, W. M., & Sligar, S. G. (2007). Applications of phospholipid bilayer nanodiscs in the study of membranes and membrane proteins. *Biochemistry*, *46*(8), 2059-2069. https://doi.org/10.1021/bi602371n

Nath, A., Grinkova, Y. V., Sligar, S. G., & Atkins, W. M. (2007). Ligand binding to cytochrome P450 3A4 in phospholipid bilayer nanodiscs: the effect of model membranes. *J Biol Chem*, *282*(39), 28309-28320. https://doi.org/10.1074/jbc.M703568200

Navarro, S., Starke, A., Heemskerk, J. W. M., Kuijpers, M. J. E., Stegner, D., & Nieswandt, B. (2022). Targeting of a Conserved Epitope in Mouse and Human GPVI Differently Affects Receptor Function. *Int J Mol Sci*, *23*(15). https://doi.org/10.3390/ijms23158610

Niedergang, F., Alcover, A., Knight, C. G., Farndale, R. W., Barnes, M. J., Francischetti, I. M., Bon, C., & Leduc, M. (2000). Convulxin binding to platelet receptor GPVI: competition with collagen related peptides. *Biochem Biophys Res Commun*, *273*(1), 246-250. https://doi.org/10.1006/bbrc.2000.2940

Nieman, M. T. (2008). Protease-activated receptor 4 uses anionic residues to interact with alpha-thrombin in the absence or presence of protease-activated receptor 1. *Biochemistry*, *47*(50), 13279-13286. https://doi.org/10.1021/bi801334s

Nieswandt, B., Bergmeier, W., Schulte, V., Rackebrandt, K., Gessner, J. E., & Zirngibl, H. (2000). Expression and function of the mouse collagen receptor glycoprotein VI is strictly dependent on its association with the FcRgamma chain. *J Biol Chem*, *275*(31), 23998-24002. https://doi.org/10.1074/jbc.M003803200

Nieswandt, B., Brakebusch, C., Bergmeier, W., Schulte, V., Bouvard, D., Mokhtari-Nejad, R., Lindhout, T., Heemskerk, J. W., Zirngibl, H., & Fassler, R. (2001). Glycoprotein VI but not alpha2beta1 integrin is essential for platelet interaction with collagen. *EMBO J*, *20*(9), 2120-2130. https://doi.org/10.1093/emboj/20.9.2120

Nieswandt, B., Hafner, M., Echtenacher, B., & Mannel, D. N. (1999). Lysis of tumor cells by natural killer cells in mice is impeded by platelets. *Cancer Res*, *59*(6), 1295-1300. https://www.ncbi.nlm.nih.gov/pubmed/10096562

Nieswandt, B., Schulte, V., Bergmeier, W., Mokhtari-Nejad, R., Rackebrandt, K., Cazenave, J. P., Ohlmann, P., Gachet, C., & Zirngibl, H. (2001). Long-term antithrombotic

protection by in vivo depletion of platelet glycoprotein VI in mice. *J Exp Med*, *193*(4), 459-469. https://doi.org/10.1084/jem.193.4.459

Noy, P. J., Yang, J., Reyat, J. S., Matthews, A. L., Charlton, A. E., Furmston, J., Rogers, D. A., Rainger, G. E., & Tomlinson, M. G. (2016). TspanC8 Tetraspanins and A Disintegrin and Metalloprotease 10 (ADAM10) Interact via Their Extracellular Regions: EVIDENCE FOR DISTINCT BINDING MECHANISMS FOR DIFFERENT TspanC8 PROTEINS. *J Biol Chem*, *291*(7), 3145-3157. https://doi.org/10.1074/jbc.M115.703058

Nurden, A. T. (2019). Clinical significance of altered collagen-receptor functioning in platelets with emphasis on glycoprotein VI. *Blood Rev*, *38*, 100592. https://doi.org/10.1016/j.blre.2019.100592

Nurden, A. T., & Caen, J. P. (1975). Specific roles for platelet surface glycoproteins in platelet function. *Nature*, *255*(5511), 720-722. https://doi.org/10.1038/255720a0

Nurden, P., Poujol, C., Winckler, J., Combrie, R., Pousseau, N., Conley, P. B., Levy-Toledano, S., Habib, A., & Nurden, A. T. (2003). Immunolocalization of P2Y1 and TPalpha receptors in platelets showed a major pool associated with the membranes of alpha -granules and the open canalicular system. *Blood*, *101*(4), 1400-1408. https://doi.org/10.1182/blood-2002-02-0642

Offermanns, S. (2006). Activation of platelet function through G protein-coupled receptors. *Circ Res*, *99*(12), 1293-1304. https://doi.org/10.1161/01.RES.0000251742.71301.16

Offermanns, S., Laugwitz, K. L., Spicher, K., & Schultz, G. (1994). G proteins of the G12 family are activated via thromboxane A2 and thrombin receptors in human platelets. *Proc Natl Acad Sci U S A*, *91*(2), 504-508. https://doi.org/10.1073/pnas.91.2.504

Olmeda, B., Garcia-Alvarez, B., & Perez-Gil, J. (2013). Structure-function correlations of pulmonary surfactant protein SP-B and the saposin-like family of proteins. *Eur Biophys J*, *42*(2-3), 209-222. https://doi.org/10.1007/s00249-012-0858-9

Olsson, A. K., & Cedervall, J. (2018). The pro-inflammatory role of platelets in cancer. *Platelets*, *29*(6), 569-573. https://doi.org/10.1080/09537104.2018.1453059

Onselaer, M. B., Hardy, A. T., Wilson, C., Sanchez, X., Babar, A. K., Miller, J. L. C., Watson, C. N., Watson, S. K., Bonna, A., Philippou, H., Herr, A. B., Mezzano, D., Ariens, R. A. S., & Watson, S. P. (2017). Fibrin and D-dimer bind to monomeric GPVI. *Blood Adv*, *1*(19), 1495-1504. https://doi.org/10.1182/bloodadvances.2017007732

Orekhov, P. S., Bozdaganyan, M. E., Voskoboynikova, N., Mulkidjanian, A. Y., Karlova, M. G., Yudenko, A., Remeeva, A., Ryzhykau, Y. L., Gushchin, I., Gordeliy, V. I., Sokolova, O. S., Steinhoff, H. J., Kirpichnikov, M. P., & Shaitan, K. V. (2022). Mechanisms of Formation, Structure, and Dynamics of Lipoprotein Discs Stabilized by Amphiphilic Copolymers: A Comprehensive Review. *Nanomaterials (Basel)*, *12*(3). https://doi.org/10.3390/nano12030361

Orekhov, P. S., Bozdaganyan, M. E., Voskoboynikova, N., Mulkidjanian, A. Y., Steinhoff, H. J., & Shaitan, K. V. (2019). Styrene/Maleic Acid Copolymers Form SMALPs by Pulling Lipid Patches out of the Lipid Bilayer. *Langmuir*, *35*(10), 3748-3758. https://doi.org/10.1021/acs.langmuir.8b03978

Orwick Rydmark, M., Christensen, M. K., Koksal, E. S., Kantarci, I., Kustanovich, K., Yantchev, V., Jesorka, A., & Gozen, I. (2019). Styrene maleic acid copolymer induces pores in biomembranes. *Soft Matter*, *15*(39), 7934-7944. https://doi.org/10.1039/c9sm01407a

Palacios-Acedo, A. L., Mege, D., Crescence, L., Dignat-George, F., Dubois, C., & Panicot-Dubois, L. (2019). Platelets, Thrombo-Inflammation, and Cancer: Collaborating With the Enemy. *Front Immunol*, *10*, 1805. https://doi.org/10.3389/fimmu.2019.01805

Pallini, C., Pike, J. A., O'Shea, C., Andrews, R. K., Gardiner, E. E., Watson, S. P., & Poulter, N. S. (2021). Immobilized collagen prevents shedding and induces sustained GPVI clustering and signaling in platelets. *Platelets*, *32*(1), 59-73. https://doi.org/10.1080/09537104.2020.1849607

Park, S. H., Wu, J., Yao, Y., Singh, C., Tian, Y., Marassi, F. M., & Opella, S. J. (2020). Membrane proteins in magnetically aligned phospholipid polymer discs for solid-state NMR spectroscopy. *Biochim Biophys Acta Biomembr*, *1862*(9), 183333. https://doi.org/10.1016/j.bbamem.2020.183333

Patrono, C. (2019). 50 - Aspirin. In A. D. Michelson (Ed.), *Platelets (Fourth Edition)* (pp. 921-936). Academic Press. https://doi.org/https://doi.org/10.1016/B978-0-12-813456-6.00050-3

Perrella, G., Nagy, M., Watson, S. P., & Heemskerk, J. W. M. (2021). Platelet GPVI (Glycoprotein VI) and Thrombotic Complications in the Venous System. *Arterioscler Thromb Vasc Biol*, *41*(11), 2681-2692. https://doi.org/10.1161/ATVBAHA.121.316108

Phillips, D. R., & Agin, P. P. (1977). Platelet plasma membrane glycoproteins. Evidence for the presence of nonequivalent disulfide bonds using nonreduced-reduced two-dimensional gel electrophoresis. *J Biol Chem*, *252*(6), 2121-2126. https://www.ncbi.nlm.nih.gov/pubmed/845165

Phillips, D. R., Charo, I. F., Parise, L. V., & Fitzgerald, L. A. (1988). The platelet membrane glycoprotein IIb-IIIa complex. *Blood*, *71*(4), 831-843. https://www.ncbi.nlm.nih.gov/pubmed/2833328

Pileri, P., Uematsu, Y., Campagnoli, S., Galli, G., Falugi, F., Petracca, R., Weiner, A. J., Houghton, M., Rosa, D., Grandi, G., & Abrignani, S. (1998). Binding of hepatitis C virus to CD81. *Science*, *282*(5390), 938-941. https://doi.org/10.1126/science.282.5390.938

Piotrowicz, R. S., Orchekowski, R. P., Nugent, D. J., Yamada, K. Y., & Kunicki, T. J. (1988). Glycoprotein Ic-IIa functions as an activation-independent fibronectin receptor on human platelets. *J Cell Biol*, *106*(4), 1359-1364. https://doi.org/10.1083/jcb.106.4.1359

Plow, E. F., Haas, T. A., Zhang, L., Loftus, J., & Smith, J. W. (2000). Ligand binding to integrins. *J Biol Chem*, *275*(29), 21785-21788. https://doi.org/10.1074/jbc.R000003200

Plow, E. F., Meller, J., & Byzova, T. V. (2014). Integrin function in vascular biology: a view from 2013. *Curr Opin Hematol*, *21*(3), 241-247. https://doi.org/10.1097/MOH.0000000000000042

Poddar, M., & Banerjee, S. (2020). Molecular Aspects of Pathophysiology of Platelet Receptors. In *Platelets*. https://doi.org/10.5772/intechopen.92856

Pollitt, A. Y., Grygielska, B., Leblond, B., Desire, L., Eble, J. A., & Watson, S. P. (2010). Phosphorylation of CLEC-2 is dependent on lipid rafts, actin polymerization, secondary mediators, and Rac. *Blood*, *115*(14), 2938-2946. https://doi.org/10.1182/blood-2009-12-257212

Pollitt, A. Y., Poulter, N. S., Gitz, E., Navarro-Nunez, L., Wang, Y. J., Hughes, C. E., Thomas, S. G., Nieswandt, B., Douglas, M. R., Owen, D. M., Jackson, D. G., Dustin, M. L., & Watson, S. P. (2014). Syk and Src family kinases regulate C-type lectin receptor 2 (CLEC-2)-mediated clustering of podoplanin and platelet adhesion to lymphatic endothelial cells. *J Biol Chem*, *289*(52), 35695-35710. https://doi.org/10.1074/jbc.M114.584284

Pollock, N. L., Lee, S. C., Patel, J. H., Gulamhussein, A. A., & Rothnie, A. J. (2018). Structure and function of membrane proteins encapsulated in a polymer-bound lipid bilayer.

Biochim Biophys Acta Biomembr, *1860*(4), 809-817. https://doi.org/10.1016/j.bbamem.2017.08.012

Pollock, N. L., Lloyd, J., Montinaro, C., Rai, M., & Dafforn, T. R. (2022). Conformational trapping of an ABC transporter in polymer lipid nanoparticles. *Biochem J*, *479*(2), 145-159. https://doi.org/10.1042/BCJ20210312

Pollock, N. L., Rai, M., Simon, K. S., Hesketh, S. J., Teo, A. C. K., Parmar, M., Sridhar, P., Collins, R., Lee, S. C., Stroud, Z. N., Bakker, S. E., Muench, S. P., Barton, C. H., Hurlbut, G., Roper, D. I., Smith, C. J. I., Knowles, T. J., Spickett, C. M., East, J. M., . . . Dafforn, T. R. (2019). SMA-PAGE: A new method to examine complexes of membrane proteins using SMALP nano-encapsulation and native gel electrophoresis. *Biochim Biophys Acta Biomembr*, *1861*(8), 1437-1445. https://doi.org/10.1016/j.bbamem.2019.05.011

Poole, A., Gibbins, J. M., Turner, M., van Vugt, M. J., van de Winkel, J. G., Saito, T., Tybulewicz, V. L., & Watson, S. P. (1997). The Fc receptor gamma-chain and the tyrosine kinase Syk are essential for activation of mouse platelets by collagen. *EMBO J*, *16*(9), 2333-2341. https://doi.org/10.1093/emboj/16.9.2333

Popot, J. L., Althoff, T., Bagnard, D., Baneres, J. L., Bazzacco, P., Billon-Denis, E., Catoire, L. J., Champeil, P., Charvolin, D., Cocco, M. J., Cremel, G., Dahmane, T., de la Maza, L. M., Ebel, C., Gabel, F., Giusti, F., Gohon, Y., Goormaghtigh, E., Guittet, E., . . . Zoonens, M. (2011). Amphipols From A to Z. *Annual Review of Biophysics, Vol 40*, *40*, 379-+. https://doi.org/10.1146/annurev-biophys-042910-155219

Popot, J. L., Berry, E. A., Charvolin, D., Creuzenet, C., Ebel, C., Engelman, D. M., Flotenmeyer, M., Giusti, F., Gohon, Y., Hong, Q., Lakey, J. H., Leonard, K., Shuman, H. A., Timmins, P., Warschawski, D. E., Zito, F., Zoonens, M., Pucci, B., & Tribet, C. (2003). Amphipols: polymeric surfactants for membrane biology research. *Cell Mol Life Sci*, *60*(8), 1559-1574. https://doi.org/10.1007/s00018-003-3169-6

Popovic, K., Holyoake, J., Pomes, R., & Prive, G. G. (2012). Structure of saposin A lipoprotein discs. *Proc Natl Acad Sci U S A*, *109*(8), 2908-2912. https://doi.org/10.1073/pnas.1115743109

Postina, R., Schroeder, A., Dewachter, I., Bohl, J., Schmitt, U., Kojro, E., Prinzen, C., Endres, K., Hiemke, C., Blessing, M., Flamez, P., Dequenne, A., Godaux, E., van Leuven, F., & Fahrenholz, F. (2004). A disintegrin-metalloproteinase prevents amyloid plaque formation and hippocampal defects in an Alzheimer disease mouse model. *J Clin Invest*, *113*(10), 1456-1464. https://doi.org/10.1172/JCI20864

Postis, V., Rawson, S., Mitchell, J. K., Lee, S. C., Parslow, R. A., Dafforn, T. R., Baldwin, S. A., & Muench, S. P. (2015). The use of SMALPs as a novel membrane protein scaffold for structure study by negative stain electron microscopy. *Biochim Biophys Acta*, *1848*(2), 496-501. https://doi.org/10.1016/j.bbamem.2014.10.018

Poulter, N. S., Pollitt, A. Y., Owen, D. M., Gardiner, E. E., Andrews, R. K., Shimizu, H., Ishikawa, D., Bihan, D., Farndale, R. W., Moroi, M., Watson, S. P., & Jung, S. M. (2017). Clustering of glycoprotein VI (GPVI) dimers upon adhesion to collagen as a mechanism to regulate GPVI signaling in platelets. *J Thromb Haemost*, *15*(3), 549-564. https://doi.org/10.1111/jth.13613

Previtali, E., Bucciarelli, P., Passamonti, S. M., & Martinelli, I. (2011). Risk factors for venous and arterial thrombosis. *Blood Transfus*, *9*(2), 120-138. https://doi.org/10.2450/2010.0066-10

Prive, G. G. (2009). Lipopeptide detergents for membrane protein studies. *Curr Opin Struct Biol*, *19*(4), 379-385. https://doi.org/10.1016/j.sbi.2009.07.008

Prosser, R. S., Hwang, J. S., & Vold, R. R. (1998). Magnetically aligned phospholipid bilayers with positive ordering: a new model membrane system. *Biophys J*, *74*(5), 2405-2418. https://doi.org/10.1016/S0006-3495(98)77949-4

Protty, M. B., Watkins, N. A., Colombo, D., Thomas, S. G., Heath, V. L., Herbert, J. M., Bicknell, R., Senis, Y. A., Ashman, L. K., Berditchevski, F., Ouwehand, W. H., Watson, S. P., & Tomlinson, M. G. (2009). Identification of Tspan9 as a novel platelet tetraspanin and the collagen receptor GPVI as a component of tetraspanin microdomains. *Biochem J*, *417*(1), 391-400. https://doi.org/10.1042/BJ20081126

Proverbio, D., Roos, C., Beyermann, M., Orban, E., Dotsch, V., & Bernhard, F. (2013). Functional properties of cell-free expressed human endothelin A and endothelin B receptors in artificial membrane environments. *Biochim Biophys Acta*, *1828*(9), 2182-2192. https://doi.org/10.1016/j.bbamem.2013.05.031

Pytela, R., Pierschbacher, M. D., & Ruoslahti, E. (1985). A 125/115-kDa cell surface receptor specific for vitronectin interacts with the arginine-glycine-aspartic acid adhesion sequence derived from fibronectin. *Proc Natl Acad Sci U S A*, *82*(17), 5766-5770. https://doi.org/10.1073/pnas.82.17.5766

Qiu, W., Fu, Z., Xu, G. G., Grassucci, R. A., Zhang, Y., Frank, J., Hendrickson, W. A., & Guo, Y. (2018). Structure and activity of lipid bilayer within a membrane-protein transporter. *Proc Natl Acad Sci U S A*, *115*(51), 12985-12990. https://doi.org/10.1073/pnas.1812526115

Quach, M. E., Chen, W., & Li, R. (2018). Mechanisms of platelet clearance and translation to improve platelet storage. *Blood*, *131*(14), 1512-1521. https://doi.org/10.1182/blood-2017-08-743229

Raborn, J., Wang, W., & Luo, B. H. (2011). Regulation of integrin alphaIIbbeta3 ligand binding and signaling by the metal ion binding sites in the beta I domain. *Biochemistry*, *50*(12), 2084-2091. https://doi.org/10.1021/bi2000092

Radoicic, J., Park, S. H., & Opella, S. J. (2018). Macrodiscs Comprising SMALPs for Oriented Sample Solid-State NMR Spectroscopy of Membrane Proteins. *Biophys J*, *115*(1), 22-25. https://doi.org/10.1016/j.bpj.2018.05.024

Rahman, M. M., Basta, T., Teng, J., Lee, M., Worrell, B. T., Stowell, M. H. B., & Hibbs, R. E. (2022). Structural mechanism of muscle nicotinic receptor desensitization and block by curare. *Nat Struct Mol Biol*, *29*(4), 386-394. https://doi.org/10.1038/s41594-022-00737-3

Ram, P., & Prestegard, J. H. (1988). Magnetic field induced ordering of bile salt/phospholipid micelles: new media for NMR structural investigations. *Biochim Biophys Acta*, *940*(2), 289-294. https://doi.org/10.1016/0005-2736(88)90203-9

Ramakrishnan, V., DeGuzman, F., Bao, M., Hall, S. W., Leung, L. L., & Phillips, D. R. (2001). A thrombin receptor function for platelet glycoprotein Ib-IX unmasked by cleavage of glycoprotein V. *Proc Natl Acad Sci U S A*, *98*(4), 1823-1828. https://doi.org/10.1073/pnas.98.4.1823

Ravula, T., Hardin, N. Z., Ramadugu, S. K., Cox, S. J., & Ramamoorthy, A. (2018). Formation of pH-Resistant Monodispersed Polymer-Lipid Nanodiscs. *Angew Chem Int Ed Engl*, *57*(5), 1342-1345. https://doi.org/10.1002/anie.201712017

Ravula, T., Hardin, N. Z., Ramadugu, S. K., & Ramamoorthy, A. (2017). pH Tunable and Divalent Metal Ion Tolerant Polymer Lipid Nanodiscs. *Langmuir*, *33*(40), 10655-10662. https://doi.org/10.1021/acs.langmuir.7b02887

Ravula, T., Ramadugu, S. K., Di Mauro, G., & Ramamoorthy, A. (2017). Bioinspired, Size-Tunable Self-Assembly of Polymer-Lipid Bilayer Nanodiscs. *Angew Chem Int Ed Engl*, *56*(38), 11466-11470. https://doi.org/10.1002/anie.201705569

Rayes, J., Watson, S. P., & Nieswandt, B. (2019). Functional significance of the platelet immune receptors GPVI and CLEC-2. *J Clin Invest*, *129*(1), 12-23. https://doi.org/10.1172/JCI122955

Reth, M. (1989). Antigen receptor tail clue. *Nature*, *338*(6214), 383-384. https://doi.org/10.1038/338383b0

Revacept in Symptomatic Carotid Stenosis. In: https://ClinicalTrials.gov/show/NCT01645306.

Reyat, J. S., Chimen, M., Noy, P. J., Szyroka, J., Rainger, G. E., & Tomlinson, M. G. (2017). ADAM10-Interacting Tetraspanins Tspan5 and Tspan17 Regulate VE-Cadherin Expression and Promote T Lymphocyte Transmigration. *J Immunol*, *199*(2), 666-676. https://doi.org/10.4049/jimmunol.1600713

Reyes, R., Cardenes, B., Machado-Pineda, Y., & Cabanas, C. (2018). Tetraspanin CD9: A Key Regulator of Cell Adhesion in the Immune System. *Front Immunol*, *9*, 863. https://doi.org/10.3389/fimmu.2018.00863

Richardson, J. L., Shivdasani, R. A., Boers, C., Hartwig, J. H., & Italiano, J. E., Jr. (2005). Mechanisms of organelle transport and capture along proplatelets during platelet production. *Blood*, *106*(13), 4066-4075. https://doi.org/10.1182/blood-2005-06-2206

Rossmann, M., Schultz-Heienbrok, R., Behlke, J., Remmel, N., Alings, C., Sandhoff, K., Saenger, W., & Maier, T. (2008). Crystal structures of human saposins C andD: implications for lipid recognition and membrane interactions. *Structure*, *16*(5), 809-817. https://doi.org/10.1016/j.str.2008.02.016

Santoro, S. A., Walsh, J. J., Staatz, W. D., & Baranski, K. J. (1991). Distinct determinants on collagen support alpha 2 beta 1 integrin-mediated platelet adhesion and platelet activation. *Cell Regul*, *2*(11), 905-913. https://doi.org/10.1091/mbc.2.11.905

Sasaki, T., Shirai, T., Tsukiji, N., Otake, S., Tamura, S., Ichikawa, J., Osada, M., Satoh, K., Ozaki, Y., & Suzuki-Inoue, K. (2018). Functional characterization of recombinant snake venom rhodocytin: rhodocytin mutant blocks CLEC-2/podoplanin-dependent platelet aggregation and lung metastasis. *J Thromb Haemost*, *16*(5), 960-972. https://doi.org/10.1111/jth.13987

Schaff, M., Tang, C., Maurer, E., Bourdon, C., Receveur, N., Eckly, A., Hechler, B., Arnold, C., de Arcangelis, A., Nieswandt, B., Denis, C. V., Lefebvre, O., Georges-Labouesse, E., Gachet, C., Lanza, F., & Mangin, P. H. (2013). Integrin alpha6beta1 is the main receptor for vascular laminins and plays a role in platelet adhesion, activation, and arterial thrombosis. *Circulation*, *128*(5), 541-552. https://doi.org/10.1161/CIRCULATIONAHA.112.000799

Scheidelaar, S., Koorengevel, M. C., Pardo, J. D., Meeldijk, J. D., Breukink, E., & Killian, J. A. (2015). Molecular model for the solubilization of membranes into nanodisks by styrene maleic Acid copolymers. *Biophys J*, *108*(2), 279-290. https://doi.org/10.1016/j.bpj.2014.11.3464

Scheidelaar, S., Koorengevel, M. C., van Walree, C. A., Dominguez, J. J., Dorr, J. M., & Killian, J. A. (2016). Effect of Polymer Composition and pH on Membrane Solubilization by Styrene-Maleic Acid Copolymers. *Biophys J*, *111*(9), 1974-1986. https://doi.org/10.1016/j.bpj.2016.09.025

Schlesinger, M. (2018). Role of platelets and platelet receptors in cancer metastasis. *J Hematol Oncol*, *11*(1), 125. https://doi.org/10.1186/s13045-018-0669-2

Schlesinger, M. J., Magee, A. I., & Schmidt, M. F. (1980). Fatty acid acylation of proteins in cultured cells. *J Biol Chem*, *255*(21), 10021-10024. https://www.ncbi.nlm.nih.gov/pubmed/7430112

Schonberger, T., Ziegler, M., Borst, O., Konrad, I., Nieswandt, B., Massberg, S., Ochmann, C., Jurgens, T., Seizer, P., Langer, H., Munch, G., Ungerer, M., Preissner, K. T., Elvers, M., & Gawaz, M. (2012). The dimeric platelet collagen receptor GPVI-Fc reduces

platelet adhesion to activated endothelium and preserves myocardial function after transient ischemia in mice. *Am J Physiol Cell Physiol*, *303*(7), C757-766. https://doi.org/10.1152/ajpcell.00060.2012

Schroder, J., Lullmann-Rauch, R., Himmerkus, N., Pleines, I., Nieswandt, B., Orinska, Z., Koch-Nolte, F., Schroder, B., Bleich, M., & Saftig, P. (2009). Deficiency of the tetraspanin CD63 associated with kidney pathology but normal lysosomal function. *Mol Cell Biol*, *29*(4), 1083-1094. https://doi.org/10.1128/MCB.01163-08

Schror, K. (1997). Aspirin and platelets: the antiplatelet action of aspirin and its role in thrombosis treatment and prophylaxis. *Semin Thromb Hemost*, *23*(4), 349-356. https://doi.org/10.1055/s-2007-996108

Schulze, H., Korpal, M., Hurov, J., Kim, S. W., Zhang, J., Cantley, L. C., Graf, T., & Shivdasani, R. A. (2006). Characterization of the megakaryocyte demarcation membrane system and its role in thrombopoiesis. *Blood*, *107*(10), 3868-3875. https://doi.org/10.1182/blood-2005-07-2755

Schumacher, D., Strilic, B., Sivaraj, K. K., Wettschureck, N., & Offermanns, S. (2013). Platelet-derived nucleotides promote tumor-cell transendothelial migration and metastasis via P2Y2 receptor. *Cancer Cell*, *24*(1), 130-137. https://doi.org/10.1016/j.ccr.2013.05.008

Schupke, S., Hein-Rothweiler, R., Mayer, K., Janisch, M., Sibbing, D., Ndrepepa, G., Hilz, R., Laugwitz, K. L., Bernlochner, I., Gschwendtner, S., Kupka, D., Gori, T., Zeiher, A. M., Schunkert, H., Massberg, S., Kastrati, A., & Investigators, I. S.-P.-T. (2019). Revacept, a Novel Inhibitor of Platelet Adhesion, in Patients Undergoing Elective PCI-Design and Rationale of the Randomized ISAR-PLASTER Trial. *Thromb Haemost*, *119*(9), 1539-1545. https://doi.org/10.1055/s-0039-1692423

Seigneuret, M., Delaguillaumie, A., Lagaudriere-Gesbert, C., & Conjeaud, H. (2001). Structure of the tetraspanin main extracellular domain. A partially conserved fold with a structurally variable domain insertion. *J Biol Chem*, *276*(43), 40055-40064. https://doi.org/10.1074/jbc.M105557200

Selvadurai, M. V., & Hamilton, J. R. (2018). Structure and function of the open canalicular system - the platelet's specialized internal membrane network. *Platelets*, *29*(4), 319-325. https://doi.org/10.1080/09537104.2018.1431388

Senis, Y. A., Mazharian, A., & Mori, J. (2014). Src family kinases: at the forefront of platelet activation. *Blood*, *124*(13), 2013-2024. https://doi.org/10.1182/blood-2014-01-453134

Shattil, S. J., Kim, C., & Ginsberg, M. H. (2010). The final steps of integrin activation: the end game. *Nat Rev Mol Cell Biol*, *11*(4), 288-300. https://doi.org/10.1038/nrm2871

Shenker, A., Goldsmith, P., Unson, C. G., & Spiegel, A. M. (1991). The G protein coupled to the thromboxane A2 receptor in human platelets is a member of the novel Gq family. *J Biol Chem*, *266*(14), 9309-9313. https://www.ncbi.nlm.nih.gov/pubmed/1851174

Siddiq, S., Clark, A., & Mumford, A. (2011). A systematic review of the management and outcomes of pregnancy in Glanzmann thrombasthenia. *Haemophilia*, *17*(5), e858-869. https://doi.org/10.1111/j.1365-2516.2011.02516.x

Siegel, R. S., Rae, J. L., Barth, S., Coleman, R. E., Reba, R. C., Kurlander, R., & Rosse, W. F. (1989). Platelet survival and turnover: important factors in predicting response to splenectomy in immune thrombocytopenic purpura. *Am J Hematol*, *30*(4), 206-212. https://doi.org/10.1002/ajh.2830300404

Simic, D., Bogdan, N., Teng, F., & Otieno, M. (2017). Blocking alpha5beta1 Integrin Attenuates sCD40L-Mediated Platelet Activation. *Clin Appl Thromb Hemost*, *23*(6), 607-614. https://doi.org/10.1177/1076029615624549

Simon, K. S., Pollock, N. L., & Lee, S. C. (2018). Membrane protein nanoparticles: the shape of things to come. *Biochem Soc Trans*, *46*(6), 1495-1504. https://doi.org/10.1042/BST20180139

Sincock, P. M., Mayrhofer, G., & Ashman, L. K. (1997). Localization of the transmembrane 4 superfamily (TM4SF) member PETA-3 (CD151) in normal human tissues: comparison with CD9, CD63, and alpha5beta1 integrin. *J Histochem Cytochem*, *45*(4), 515-525. https://doi.org/10.1177/002215549704500404

Sjostrand, D., Diamanti, R., Lundgren, C. A. K., Wiseman, B., & Hogbom, M. (2017). A rapid expression and purification condition screening protocol for membrane protein structural biology. *Protein Sci*, *26*(8), 1653-1666. https://doi.org/10.1002/pro.3196

Skaar, K., Korza, H. J., Tarry, M., Sekyrova, P., & Hogbom, M. (2015). Expression and Subcellular Distribution of GFP-Tagged Human Tetraspanin Proteins in Saccharomyces cerevisiae. *PLoS One*, *10*(7), e0134041. https://doi.org/10.1371/journal.pone.0134041

Slater, A., Di, Y., Clark, J. C., Jooss, N. J., Martin, E. M., Alenazy, F., Thomas, M. R., Ariens, R. A. S., Herr, A. B., Poulter, N. S., Emsley, J., & Watson, S. P. (2021). Structural characterization of a novel GPVI-nanobody complex reveals a biologically active domain-swapped GPVI dimer. *Blood*, *137*(24), 3443-3453. https://doi.org/10.1182/blood.2020009440

Slater, A., Perrella, G., Onselaer, M. B., Martin, E. M., Gauer, J. S., Xu, R. G., Heemskerk, J. W., Ariens, R. A. S., & Watson, S. P. (2018). Does fibrin(ogen) bind to monomeric or dimeric GPVI, or not at all? *Platelets*, 1-9. https://doi.org/10.1080/09537104.2018.1508649

Smith, C. W. (2018). *Regulation of platelet production and function by ITIM-containing receptors* [Doctoral dissertation, University of Birmingham]. University of Birmingham eTheses repository. Birmingham.

Smith, S. A., & Morrissey, J. H. (2019). 21 - Interactions Between Platelets and the Coagulation System. In A. D. Michelson (Ed.), *Platelets (Fourth Edition)* (pp. 393-400). Academic Press. https://doi.org/https://doi.org/10.1016/B978-0-12-813456-6.00021-7

Smotrys, J. E., & Linder, M. E. (2004). Palmitoylation of intracellular signaling proteins: regulation and function. *Annu Rev Biochem*, *73*, 559-587. https://doi.org/10.1146/annurev.biochem.73.011303.073954

Stefanini, L., Paul, D. S., Robledo, R. F., Chan, E. R., Getz, T. M., Campbell, R. A., Kechele, D. O., Casari, C., Piatt, R., Caron, K. M., Mackman, N., Weyrich, A. S., Parrott, M. C., Boulaftali, Y., Adams, M. D., Peters, L. L., & Bergmeier, W. (2015). RASA3 is a critical inhibitor of RAP1-dependent platelet activation. *J Clin Invest*, *125*(4), 1419-1432. https://doi.org/10.1172/JCI77993

Stefanini, L., Roden, R. C., & Bergmeier, W. (2009). CalDAG-GEFI is at the nexus of calcium-dependent platelet activation. *Blood*, *114*(12), 2506-2514. https://doi.org/10.1182/blood-2009-04-218768

Stegner, D., vanEeuwijk, J. M. M., Angay, O., Gorelashvili, M. G., Semeniak, D., Pinnecker, J., Schmithausen, P., Meyer, I., Friedrich, M., Dutting, S., Brede, C., Beilhack, A., Schulze, H., Nieswandt, B., & Heinze, K. G. (2017). Thrombopoiesis is spatially regulated by the bone marrow vasculature. *Nat Commun*, *8*(1), 127. https://doi.org/10.1038/s41467-017-00201-7

Stoffer, B., Reddy, Shah. (2022). *Abciximab* https://www.ncbi.nlm.nih.gov/books/NBK482195/

Stouffer, G. A., & Smyth, S. S. (2003). Effects of thrombin on interactions between beta3-integrins and extracellular matrix in platelets and vascular cells. *Arterioscler Thromb Vasc Biol*, *23*(11), 1971-1978. https://doi.org/10.1161/01.ATV.0000093470.51580.0F

Stroh, L. J., Nagarathinam, K., & Krey, T. (2018). Conformational Flexibility in the CD81-Binding Site of the Hepatitis C Virus Glycoprotein E2. *Front Immunol*, *9*, 1396. https://doi.org/10.3389/fimmu.2018.01396

Su, C. C., Li, M., Gu, R., Takatsuka, Y., McDermott, G., Nikaido, H., & Yu, E. W. (2006). Conformation of the AcrB multidrug efflux pump in mutants of the putative proton relay pathway. *J Bacteriol*, *188*(20), 7290-7296. https://doi.org/10.1128/JB.00684-06

Sullam, P. M., Hyun, W. C., Szollosi, J., Dong, J., Foss, W. M., & Lopez, J. A. (1998). Physical proximity and functional interplay of the glycoprotein Ib-IX-V complex and the Fc receptor FcgammaRIIA on the platelet plasma membrane. *J Biol Chem*, *273*(9), 5331-5336. https://doi.org/10.1074/jbc.273.9.5331

Sun, B., Tao, L., Lin, S., Calingasan, N. Y., Li, J., Tandon, N. N., Yoshitake, M., & Kambayashi, J. I. (2003). Expression of glycoprotein VI in vascular endothelial cells. *Platelets*, *14*(4), 225-232. https://doi.org/10.1080/0953710031000118858

Sun, C., Benlekbir, S., Venkatakrishnan, P., Wang, Y., Hong, S., Hosler, J., Tajkhorshid, E., Rubinstein, J. L., & Gennis, R. B. (2018). Structure of the alternative complex III in a supercomplex with cytochrome oxidase. *Nature*, *557*(7703), 123-126. https://doi.org/10.1038/s41586-018-0061-y

Sun, C., & Gennis, R. B. (2019). Single-particle cryo-EM studies of transmembrane proteins in SMA copolymer nanodiscs. *Chem Phys Lipids*, *221*, 114-119. https://doi.org/10.1016/j.chemphyslip.2019.03.007

Susa, K. J., Rawson, S., Kruse, A. C., & Blacklow, S. C. (2021). Cryo-EM structure of the B cell co-receptor CD19 bound to the tetraspanin CD81. *Science*, *371*(6526), 300-305. https://doi.org/10.1126/science.abd9836

Suzuki-Inoue, K., Fuller, G. L., Garcia, A., Eble, J. A., Pohlmann, S., Inoue, O., Gartner, T. K., Hughan, S. C., Pearce, A. C., Laing, G. D., Theakston, R. D., Schweighoffer, E., Zitzmann, N., Morita, T., Tybulewicz, V. L., Ozaki, Y., & Watson, S. P. (2006). A novel Syk-dependent mechanism of platelet activation by the C-type lectin receptor CLEC-2. *Blood*, *107*(2), 542-549. https://doi.org/10.1182/blood-2005-05-1994

Suzuki-Inoue, K., Inoue, O., Ding, G., Nishimura, S., Hokamura, K., Eto, K., Kashiwagi, H., Tomiyama, Y., Yatomi, Y., Umemura, K., Shin, Y., Hirashima, M., & Ozaki, Y. (2010). Essential in vivo roles of the C-type lectin receptor CLEC-2: embryonic/neonatal lethality of CLEC-2-deficient mice by blood/lymphatic misconnections and impaired thrombus formation of CLEC-2-deficient platelets. *J Biol Chem*, *285*(32), 24494-24507. https://doi.org/10.1074/jbc.M110.130575

Suzuki-Inoue, K., Inoue, O., Frampton, J., & Watson, S. P. (2003). Murine GPVI stimulates weak integrin activation in PLCgamma2-/- platelets: involvement of PLCgamma1 and PI3-kinase. *Blood*, *102*(4), 1367-1373. https://doi.org/10.1182/blood-2003-01-0029

Suzuki-Inoue, K., Tulasne, D., Shen, Y., Bori-Sanz, T., Inoue, O., Jung, S. M., Moroi, M., Andrews, R. K., Berndt, M. C., & Watson, S. P. (2002). Association of Fyn and Lyn with the proline-rich domain of glycoprotein VI regulates intracellular signaling. *J Biol Chem*, *277*(24), 21561-21566. https://doi.org/10.1074/jbc.M201012200

Szundi, I., Pitch, S. G., Chen, E., Farrens, D. L., & Kliger, D. S. (2021). Styrene-maleic acid copolymer effects on the function of the GPCR rhodopsin in lipid nanoparticles. *Biophys J*, *120*(20), 4337-4348. https://doi.org/10.1016/j.bpj.2021.09.012

Takada, Y., Ye, X., & Simon, S. (2007). The integrins. *Genome Biol*, *8*(5), 215. https://doi.org/10.1186/gb-2007-8-5-215

Tanenbaum, M. E., Vale, R. D., & McKenney, R. J. (2013). Cytoplasmic dynein crosslinks and slides anti-parallel microtubules using its two motor domains. *Elife*, *2*, e00943. https://doi.org/10.7554/eLife.00943

Tantry, U. S., Bliden, K. P., Chaudhary, R., Novakovic, M., Rout, A., & Gurbel, P. A. (2020). Vorapaxar in the treatment of cardiovascular diseases. *Future Cardiol*, *16*(5), 373-384. https://doi.org/10.2217/fca-2019-0090

Tao, H., Lee, S. C., Moeller, A., Roy, R. S., Siu, F. Y., Zimmermann, J., Stevens, R. C., Potter, C. S., Carragher, B., & Zhang, Q. (2013). Engineered nanostructured beta-sheet peptides protect membrane proteins. *Nat Methods*, *10*(8), 759-761. https://doi.org/10.1038/nmeth.2533

Tavassoli, M., & Aoki, M. (1989). Localization of megakaryocytes in the bone marrow. *Blood Cells*, *15*(1), 3-14. https://www.ncbi.nlm.nih.gov/pubmed/2649185

Telser, A. (2002). Molecular Biology of the Cell, 4th Edition. *Shock*, *18*(3). https://journals.lww.com/shockjournal/Fulltext/2002/09000/Molecular_Biology_of_the_Cell,_4th_Edition.15.aspx

Teo, A. C. K., Lee, S. C., Pollock, N. L., Stroud, Z., Hall, S., Thakker, A., Pitt, A. R., Dafforn, T. R., Spickett, C. M., & Roper, D. I. (2019). Analysis of SMALP co-extracted phospholipids shows distinct membrane environments for three classes of bacterial membrane protein. *Sci Rep*, *9*(1), 1813. https://doi.org/10.1038/s41598-018-37962-0

Termini, C. M., & Gillette, J. M. (2017). Tetraspanins Function as Regulators of Cellular Signaling. *Frontiers in Cell and Developmental Biology*, *5*. https://doi.org/ARTN 34

10.3389/fcell.2017.00034

Tertyshnikova, S., Yan, X., & Fein, A. (1998). cGMP inhibits IP3-induced Ca2+ release in intact rat megakaryocytes via cGMP- and cAMP-dependent protein kinases. *J Physiol*, *512 (Pt 1)*, 89-96. https://doi.org/10.1111/j.1469-7793.1998.089bf.x

Thaler, J., Ay, C., Mackman, N., Metz-Schimmerl, S., Stift, J., Kaider, A., Mullauer, L., Gnant, M., Scheithauer, W., & Pabinger, I. (2013). Microparticle-associated tissue factor activity in patients with pancreatic cancer: correlation with clinicopathological features. *Eur J Clin Invest*, *43*(3), 277-285. https://doi.org/10.1111/eci.12042

Thomas, S. G. (2019). 3 - The Structure of Resting and Activated Platelets. In A. D. Michelson (Ed.), *Platelets (Fourth Edition)* (pp. 47-77). Academic Press. https://doi.org/https://doi.org/10.1016/B978-0-12-813456-6.00003-5

Thon, J. N., Montalvo, A., Patel-Hett, S., Devine, M. T., Richardson, J. L., Ehrlicher, A., Larson, M. K., Hoffmeister, K., Hartwig, J. H., & Italiano, J. E., Jr. (2010). Cytoskeletal mechanics of proplatelet maturation and platelet release. *J Cell Biol*, *191*(4), 861-874. https://doi.org/10.1083/jcb.201006102

Thornton, P., McColl, B. W., Greenhalgh, A., Denes, A., Allan, S. M., & Rothwell, N. J. (2010). Platelet interleukin-1alpha drives cerebrovascular inflammation. *Blood*, *115*(17), 3632-3639. https://doi.org/10.1182/blood-2009-11-252643

Tomlinson, M. G., Calaminus, S. D., Berlanga, O., Auger, J. M., Bori-Sanz, T., Meyaard, L., & Watson, S. P. (2007). Collagen promotes sustained glycoprotein VI signaling in platelets and cell lines. *J Thromb Haemost*, *5*(11), 2274-2283. https://doi.org/10.1111/j.1538-7836.2007.02746.x

Tomlinson, M. G., Kane, L. P., Su, J., Kadlecek, T. A., Mollenauer, M. N., & Weiss, A. (2004). Expression and function of Tec, Itk, and Btk in lymphocytes: evidence for a unique role for Tec. *Mol Cell Biol*, *24*(6), 2455-2466. https://doi.org/10.1128/MCB.24.6.2455-2466.2004

Tonge, S. R., & Tighe, B. J. (2001). Responsive hydrophobically associating polymers: a review of structure and properties. *Adv Drug Deliv Rev*, *53*(1), 109-122. https://doi.org/10.1016/s0169-409x(01)00223-x

Tribet, C., Audebert, R., & Popot, J. L. (1996). Amphipols: polymers that keep membrane proteins soluble in aqueous solutions. *Proc Natl Acad Sci U S A*, *93*(26), 15047-15050. https://doi.org/10.1073/pnas.93.26.15047

Trifiro, E., Williams, S. A., Cheli, Y., Furihata, K., Pulcinelli, F. M., Nugent, D. J., & Kunicki, T. J. (2009). The low-frequency isoform of platelet glycoprotein VIb attenuates ligand-mediated signal transduction but not receptor expression or ligand binding. *Blood*, *114*(9), 1893-1899. https://doi.org/10.1182/blood-2009-03-209510

Trumel, C., Payrastre, B., Plantavid, M., Hechler, B., Viala, C., Presek, P., Martinson, E. A., Cazenave, J. P., Chap, H., & Gachet, C. (1999). A key role of adenosine diphosphate in the irreversible platelet aggregation induced by the PAR1-activating peptide through the late activation of phosphoinositide 3-kinase. *Blood*, *94*(12), 4156-4165. https://www.ncbi.nlm.nih.gov/pubmed/10590060

Tsukiji, N., Inoue, O., Morimoto, M., Tatsumi, N., Nagatomo, H., Ueta, K., Shirai, T., Sasaki, T., Otake, S., Tamura, S., Tachibana, T., Okabe, M., Hirashima, M., Ozaki, Y., & Suzuki-Inoue, K. (2018). Platelets play an essential role in murine lung development through Clec-2/podoplanin interaction. *Blood*, *132*(11), 1167-1179. https://doi.org/10.1182/blood-2017-12-823369

Turner, N. A., Moake, J. L., & McIntire, L. V. (2001). Blockade of adenosine diphosphate receptors P2Y(12) and P2Y(1) is required to inhibit platelet aggregation in whole blood under flow. *Blood*, *98*(12), 3340-3345. https://doi.org/10.1182/blood.v98.12.3340

Uhrin, P., Zaujec, J., Breuss, J. M., Olcaydu, D., Chrenek, P., Stockinger, H., Fuertbauer, E., Moser, M., Haiko, P., Fassler, R., Alitalo, K., Binder, B. R., & Kerjaschki, D. (2010). Novel function for blood platelets and podoplanin in developmental separation of blood and lymphatic circulation. *Blood*, *115*(19), 3997-4005. https://doi.org/10.1182/blood-2009-04-216069

van den Brink-van der Laan, E., Chupin, V., Killian, J. A., & de Kruijff, B. (2004). Stability of KcsA tetramer depends on membrane lateral pressure. *Biochemistry*, *43*(14), 4240-4250. https://doi.org/10.1021/bi036129d

van der Meijden, P. E. J., & Heemskerk, J. W. M. (2019). Platelet biology and functions: new concepts and clinical perspectives. *Nat Rev Cardiol*, *16*(3), 166-179. https://doi.org/10.1038/s41569-018-0110-0

Varga-Szabo, D., Pleines, I., & Nieswandt, B. (2008). Cell adhesion mechanisms in platelets. *Arterioscler Thromb Vasc Biol*, *28*(3), 403-412. https://doi.org/10.1161/ATVBAHA.107.150474

Voors-Pette, C., Lebozec, K., Dogterom, P., Jullien, L., Billiald, P., Ferlan, P., Renaud, L., Favre-Bulle, O., Avenard, G., Machacek, M., Pletan, Y., & Jandrot-Perrus, M. (2019). Safety and Tolerability, Pharmacokinetics, and Pharmacodynamics of ACT017, an Antiplatelet GPVI (Glycoprotein VI) Fab. *Arterioscler Thromb Vasc Biol*, *39*(5), 956-964. https://doi.org/10.1161/ATVBAHA.118.312314

Vorobjeva, N. V., & Chernyak, B. V. (2020). NETosis: Molecular Mechanisms, Role in Physiology and Pathology. *Biochemistry (Mosc)*, *85*(10), 1178-1190. https://doi.org/10.1134/S0006297920100065

Vu, T. K., Hung, D. T., Wheaton, V. I., & Coughlin, S. R. (1991). Molecular cloning of a functional thrombin receptor reveals a novel proteolytic mechanism of receptor activation. *Cell*, *64*(6), 1057-1068. https://doi.org/10.1016/0092-8674(91)90261-v

Wang, C., Polovitskaya, M. M., Delgado, B. D., Jentsch, T. J., & Long, S. B. (2022). Gating choreography and mechanism of the human proton-activated chloride channel ASOR. *Sci Adv*, *8*(5), eabm3942. https://doi.org/10.1126/sciadv.abm3942

Watkins, N. A., O'Connor, M. N., Rankin, A., Jennings, N., Wilson, E., Harmer, I. J., Davies, L., Smethurst, P. A., Dudbridge, F., Farndale, R. W., & Ouwehand, W. H. (2006).

Definition of novel GP6 polymorphisms and major difference in haplotype frequencies between populations by a combination of in-depth exon resequencing and genotyping with tag single nucleotide polymorphisms. *J Thromb Haemost*, *4*(6), 1197-1205. https://doi.org/10.1111/j.1538-7836.2006.01937.x

Watson, A. A., Brown, J., Harlos, K., Eble, J. A., Walter, T. S., & O'Callaghan, C. A. (2007). The crystal structure and mutational binding analysis of the extracellular domain of the platelet-activating receptor CLEC-2. *J Biol Chem*, *282*(5), 3165-3172. https://doi.org/10.1074/jbc.M610383200

Watson, A. A., & O'Callaghan, C. A. (2005). Crystallization and X-ray diffraction analysis of human CLEC-2. *Acta Crystallogr Sect F Struct Biol Cryst Commun*, *61*(Pt 12), 1094-1096. https://doi.org/10.1107/S1744309105037991

Wheatley, M., Charlton, J., Jamshad, M., Routledge, S. J., Bailey, S., La-Borde, P. J., Azam, M. T., Logan, R. T., Bill, R. M., Dafforn, T. R., & Poyner, D. R. (2016). GPCR-styrene maleic acid lipid particles (GPCR-SMALPs): their nature and potential. *Biochem Soc Trans*, *44*(2), 619-623. https://doi.org/10.1042/BST20150284

Wicki, A., & Christofori, G. (2007). The potential role of podoplanin in tumour invasion. *Br J Cancer*, *96*(1), 1-5. https://doi.org/10.1038/sj.bjc.6603518

Wilson, S. J., Ismat, F. A., Wang, Z., Cerra, M., Narayan, H., Raftis, J., Gray, T. J., Connell, S., Garonzik, S., Ma, X., Yang, J., & Newby, D. E. (2018). PAR4 (Protease-Activated Receptor 4) Antagonism With BMS-986120 Inhibits Human Ex Vivo Thrombus Formation. *Arterioscler Thromb Vasc Biol*, *38*(2), 448-456. https://doi.org/10.1161/ATVBAHA.117.310104

Wong, P. C., Seiffert, D., Bird, J. E., Watson, C. A., Bostwick, J. S., Giancarli, M., Allegretto, N., Hua, J., Harden, D., Guay, J., Callejo, M., Miller, M. M., Lawrence, R. M., Banville, J., Guy, J., Maxwell, B. D., Priestley, E. S., Marinier, A., Wexler, R. R., . . . Yang, J. (2017). Blockade of protease-activated receptor-4 (PAR4) provides robust antithrombotic activity with low bleeding. *Sci Transl Med*, *9*(371). https://doi.org/10.1126/scitranslmed.aaf5294

Wu, Z., Zhang, Z., Wang, X., Zhang, J., Ren, C., Li, Y., Gao, L., Liang, X., Wang, P., & Ma, C. (2021). Palmitoylation of SARS-CoV-2 S protein is essential for viral infectivity. *Signal Transduct Target Ther*, *6*(1), 231. https://doi.org/10.1038/s41392-021-00651-y

Xiao, T., Takagi, J., Coller, B. S., Wang, J. H., & Springer, T. A. (2004). Structural basis for allostery in integrins and binding to fibrinogen-mimetic therapeutics. *Nature*, *432*(7013), 59-67. https://doi.org/10.1038/nature02976

Xiong, J. P., Stehle, T., Diefenbach, B., Zhang, R., Dunker, R., Scott, D. L., Joachimiak, A., Goodman, S. L., & Arnaout, M. A. (2001). Crystal structure of the extracellular segment of integrin alpha Vbeta3. *Science*, *294*(5541), 339-345. https://doi.org/10.1126/science.1064535

Xu, R. G., Gauer, J. S., Baker, S. R., Slater, A., Martin, E. M., McPherson, H. R., Duval, C., Manfield, I. W., Bonna, A. M., Watson, S. P., & Ariens, R. A. S. (2021). GPVI (Glycoprotein VI) Interaction With Fibrinogen Is Mediated by Avidity and the Fibrinogen alphaC-Region. *Arterioscler Thromb Vasc Biol*, *41*(3), 1092-1104. https://doi.org/10.1161/ATVBAHA.120.315030

Xu, X. R., Carrim, N., Neves, M. A., McKeown, T., Stratton, T. W., Coelho, R. M., Lei, X., Chen, P., Xu, J., Dai, X., Li, B. X., & Ni, H. (2016). Platelets and platelet adhesion molecules: novel mechanisms of thrombosis and anti-thrombotic therapies. *Thromb J*, *14*(Suppl 1), 29. https://doi.org/10.1186/s12959-016-0100-6

Xue, M., Cheng, L., Faustino, I., Guo, W., & Marrink, S. J. (2018). Molecular Mechanism of Lipid Nanodisk Formation by Styrene-Maleic Acid Copolymers. *Biophys J*, *115*(3), 494-502. https://doi.org/10.1016/j.bpj.2018.06.018

Yang, X. H., Mirchev, R., Deng, X., Yacono, P., Yang, H. L., Golan, D. E., & Hemler, M. E. (2012). CD151 restricts the alpha6 integrin diffusion mode. *Journal of Cell Science*, *125*(Pt 6), 1478-1487. https://doi.org/10.1242/jcs.093963

Yasuhara, K., Arakida, J., Ravula, T., Ramadugu, S. K., Sahoo, B., Kikuchi, J. I., & Ramamoorthy, A. (2017). Spontaneous Lipid Nanodisc Fomation by Amphiphilic Polymethacrylate Copolymers. *J Am Chem Soc*, *139*(51), 18657-18663. https://doi.org/10.1021/jacs.7b10591

Ye, F., Kim, S. J., & Kim, C. (2014). Intermolecular transmembrane domain interactions activate integrin alphaIIbbeta3. *J Biol Chem*, *289*(26), 18507-18513. https://doi.org/10.1074/jbc.M113.541888

Yin, H., Liu, J., Li, Z., Berndt, M. C., Lowell, C. A., & Du, X. (2008). Src family tyrosine kinase Lyn mediates VWF/GPIb-IX-induced platelet activation via the cGMP signaling pathway. *Blood*, *112*(4), 1139-1146. https://doi.org/10.1182/blood-2008-02-140970

Yin, H., Stojanovic, A., Hay, N., & Du, X. (2008). The role of Akt in the signaling pathway of the glycoprotein Ib-IX induced platelet activation. *Blood*, *111*(2), 658-665. https://doi.org/10.1182/blood-2007-04-085514

Yu, J., Zhu, H., Lape, R., Greiner, T., Du, J., Lu, W., Sivilotti, L., & Gouaux, E. (2021). Mechanism of gating and partial agonist action in the glycine receptor. *Cell*, *184*(4), 957-968 e921. https://doi.org/10.1016/j.cell.2021.01.026

Yun, S. H., Sim, E. H., Goh, R. Y., Park, J. I., & Han, J. Y. (2016). Platelet Activation: The Mechanisms and Potential Biomarkers. *Biomed Res Int*, *2016*, 9060143. https://doi.org/10.1155/2016/9060143

Zarpellon, A., Celikel, R., Roberts, J. R., McClintock, R. A., Mendolicchio, G. L., Moore, K. L., Jing, H., Varughese, K. I., & Ruggeri, Z. M. (2011). Binding of alpha-thrombin to surface-anchored platelet glycoprotein Ib(alpha) sulfotyrosines through a two-site mechanism involving exosite I. *Proc Natl Acad Sci U S A*, *108*(21), 8628-8633. https://doi.org/10.1073/pnas.1017042108

Zeiler, M., Moser, M., & Mann, M. (2014). Copy number analysis of the murine platelet proteome spanning the complete abundance range. *Mol Cell Proteomics*, *13*(12), 3435-3445. https://doi.org/10.1074/mcp.M114.038513

Zelensky, A. N., & Gready, J. E. (2005). The C-type lectin-like domain superfamily. *FEBS J*, *272*(24), 6179-6217. https://doi.org/10.1111/j.1742-4658.2005.05031.x

Zhang, D., Ebrahim, M., Adler, K., Blanchet, X., Jamasbi, J., Megens, R. T. A., Uhland, K., Ungerer, M., Munch, G., Deckmyn, H., Weber, C., Elia, N., Lorenz, R., & Siess, W. (2020). Glycoprotein VI is not a Functional Platelet Receptor for Fibrin Formed in Plasma or Blood. *Thromb Haemost*, *120*(6), 977-993. https://doi.org/10.1055/s-0040-1710012

Zhao, Y., Zhang, D., Wang, S., Tao, L., Wang, A., Chen, W., Zhu, Z., Zheng, S., Gao, X., & Lu, Y. (2013). Holothurian glycosaminoglycan inhibits metastasis and thrombosis via targeting of nuclear factor-kappaB/tissue factor/Factor Xa pathway in melanoma B16F10 cells. *PLoS One*, *8*(2), e56557. https://doi.org/10.1371/journal.pone.0056557

Zheng, Y. M., Liu, C., Chen, H., Locke, D., Ryan, J. C., & Kahn, M. L. (2001). Expression of the platelet receptor GPVI confers signaling via the Fc receptor gamma -chain in response to the snake venom convulxin but not to collagen. *J Biol Chem*, *276*(16), 12999-13006. https://doi.org/10.1074/jbc.M009344200

Zimmerman, B., Kelly, B., McMillan, B. J., Seegar, T. C. M., Dror, R. O., Kruse, A. C., & Blacklow, S. C. (2016). Crystal Structure of a Full-Length Human Tetraspanin Reveals a Cholesterol-Binding Pocket. *Cell*, *167*(4), 1041-1051 e1011. https://doi.org/10.1016/j.cell.2016.09.056

Zivanov, J., Nakane, T., Forsberg, B. O., Kimanius, D., Hagen, W. J., Lindahl, E., & Scheres, S. H. (2018). New tools for automated high-resolution cryo-EM structure determination in RELION-3. *Elife*, *7*. https://doi.org/10.7554/eLife.42166

Zoghbi, M. E., Cooper, R. S., & Altenberg, G. A. (2016). The Lipid Bilayer Modulates the Structure and Function of an ATP-binding Cassette Exporter. *J Biol Chem*, *291*(9), 4453-4461. https://doi.org/10.1074/jbc.M115.698498

Zwaal, R. F., Comfurius, P., & Bevers, E. M. (1998). Lipid-protein interactions in blood coagulation. *Biochim Biophys Acta*, *1376*(3), 433-453. https://doi.org/10.1016/s0304-4157(98)00018-5